COMPARISON OF THE PHYSICO-CHEMICAL PROPERTIES OF BIOCHAR WITH THEIR UTILITY FOR WATER REMEDIATION AND FERTILISATION

By

NGUYEN VAN HIEN

A thesis submitted to The University of Birmingham

for the degree of

Doctor of Philosophy

School of Geography, Earth and Environmental Sciences

College of Life and Environmental Sciences

The University of Birmingham

September 2018

Abstract

Three biochars (BC) were produced from Vietnamese biomass (acacia wood chip, rice husk, and bamboo) using Top Lid Up-draft Drum (TLUD) technology. The resulting biochars were characterized using a suite of state-of-the-art methods to understand their surface area, morphology, cation exchange capacity, and surface chemistry as a basis for determining their utility for application in agriculture in Vietnam. Adsorption experiments for ammonium (NH_4^+-N) and heavy metal (Zn^{2+}) in artificial aqueous solutions were conducted to assess the adsorption capacity of the various biochars. The mechanism of adsorption was assessed via the isotherm models (Langmuir, Freundlich, Temkin), the kinetic models (Lagergren-first order and pseudo-second order models) and the intraparticle diffusion model. Then, a real wastewater (landfill leachate) with various pollutants was used to test the adsorption capacity of the biochar under environmental conditions. Biochar surface areas (measured by BET) decreased in the order wood BC (479.34 m^2/g) > bamboo BC (434.53 m^2/g) > rice husk BC (3.29 m^2/g). Meanwhile, cation exchange capacity (CEC) followed the opposite trend, being rice husk BC (26.70 Cmol/kg) > bamboo BC (20.7 Cmol/kg) > wood BC (13.53 Cmol/kg) indicating a correlation between surface are and absorption capactiy. The morphology, as shown in SEM images corresponds with the area, showing a rough surface with pores for wood BC, a hollow honeycomb-like structure for bamboo BC, and smooth surface for rice husk BC. All three biochars produced were alkaline, with pH values around 10. The surface chemistry, measured by FTIR, indicated that carboxyl and hydroxyl groups or CO_3^{2-} group were observed for all three biochars, but PO_4^{3-} and SiO_2 groups were only present in rice husk and wood BCs. The surface function groups played an important role for the adsorption of the biochars.

The differences in physicochemical properties resulted to various adsorption capacities among the biochars. For example, the adsorption capacity for NH_4^+-N was in the order rice

husk BC > bamboo BC > wood BC, and the adsorption process was governed by surface functional groups, cation exchange, and intraparticle diffusion. In comparison, the adsorption for Zn^{2+} was in the order bamboo BC > rice husk BC ≥ wood BC, and the the organic groups (carboxyl and hydroxyl groups), and inorganic groups (CO_3^{2-}, PO_4^{2-}) mainly controlled the adsorption (rather than ion exchange). There was a strong increase in adsorption for NH_4^+-N with increasing adsorbate concentrations (20-320 mg/L), while the Zn^{2+} adsorption was slowly enhanced at adsorbate concentrations higher than 60 mg/L. However, the adsorption of both the adsorbates onto the three biochar occurred via the mechanism described as multilayer formation on a heterogeneous surface.

The findings of the experiments for the wastewater (landfill leachate with concentration of NH_4^+-N up to 1790.18 mg/L) indicated that the single biochars had an excellent adsorption for NH_4^+-N with an order as for rice husk BC (44.06 ± 1.55 mg/g) > bamboo BC (40.41 ± 0.95 mg/g) ~ wood BC (38.90 ± 1.78 mg/g). Interestingly, the binary and ternary biochars also showed a good adsorption for NH_4^+-N, but not significant difference ($p > 0.05$) among them with the adsorption fluctuating between 39.89 and 43.10 mg/g. In addition, the ternary biochar (1:1:1) used for column test showed to be effective for NH_4^+-N removal with 43.69 ± 2.15 % removed after the leachate gone through the filter four times with flow rate 1 mL/min. However, the adsorption capacity of the single biochars was still lower than the theoretical maximum adsorption for NH_4^+-N due to the adsorption competitions of other cations (Ca^{2+}, Mg^+, Na^+) in the leachate. In particular, all the biochars (including binary and ternary biochars) did not adsorb K^+ ions in the leachate, while K^+ ions from the biochar surface were observed to exchange into the exited solvent to participate in the cation exchange process for the adsorption. Hence, the three biochars demonstrated to have good adsorption for NH_4^+-N (especially rice husk BC), while bamboo BC was identified as the best choice for Zn^{2+} removal.

The information presented in this thesis will be shared with local farmers in Vietnam to help them select the most efficient biochar to use for their specific needs in water purification and/or soil fertilization utilizing existing local biomass and local production methods.

Acknowledgments

Abbreviations

ASTM	American Society for Testing and Materials
AD	Anno Domini
BBC	Bamboo biochar
BET	Brunauer, Emmett, and Teller
BC*	Before Christ
BC	Biochar
BOD	Biochemical oxygen demand
BP	Before present
COD	Chemical oxygen demand
CEC	Cation exchange capacity
C	Carbon
CR	Cotton residues
DI	Distilled
EDTA	Ethylendiaminetetraacetic acid
FTIR	Fourier-transform infrared (FTIR) spectroscopy
OC	Organic carbon
PM	Pig manure
PL	Poultry litter
PH	Peanut hull
PC	Pine chip
RBC	Rice husk biochar
rpm	Round per minute
SEM	Scanning electron microscopy
SD	Standard deviation
SP	Sewage sludge mixed with pine bark
TLUD	Top – Lid Updraft Drum

UoB   University of Birmingham

UK   Uninited Kingdom

WBC   Wood biochar

Table of Contents

List of Figures

Figure1. Shematic of the geometry of the cations (NH_4^+ and Zn^{2+}) adsorbed onto a biochar particle.

List of Tables

Chapter 1. Introduction

1.1. Historical use and definition of biochar

Soils containing high black carbon content, such as from biochar, have long been of interest to researchers investigating its benefits for soil fertility. The historical use of black carbon for soil enrichment to enhance agricultural cultivation has been observed in several regions around the world. The anthropogenic soil known as Terra Preta de Indio (Glaser et al, 2001) is a famous example, which occupied about 50,000 ha in Central Amazonia in Brazil (Smith, 1980) and has been aged as 8,000 years old (Wiedner and Glaser, 2015). These black carbon soils are more fertile, measured as containing higher carbon content (44.9 gC/kg), higher pH (pH = 5.5), and higher Cation Exchange Capacity (CEC =150 mmol/kg) compared with the nearby Oxisols (Glaser et al., 2000). The carbon black containing-soils also contain higher microbial populations than those of surrounding soils (O'neill et al., 2009). Figure 1.1 shows an example soil profile, illustrating the organic rich and black-carbon loadedk nature of the Terra Preta de Indio soil compared to the surrounding soils.

Figure 1.1: The profiles of fertile Terra Preta (left) and nutrient poor Oxisol (right) (Glaser et al., 2001).

Similar soils were found in Australia, which were named Terra Preta Australis by Downie et al. (2011). These soils had charcoal present as a thick layer and the total carbon content (4.7%) was observed to be higher than that of adjacent soils (only 0.7%). This trend was also found for the contents of other nutrient elements such as nitrogen, phosphorus, potassium, and calcium. Particularly, the C from charcoal in the soils was mainly aromatic and has been dated between 650 and 1609 years before present (BP) (Downie et al., 2011). In Europe, the study of Gerlach et al. (2006) indicated the ages of charcoal and black carbon related to human activities in the soils of the Lower Rhine Basin in Northwest Germany as being from the Mesolithic (9500–5500 BC[*]) to the Medieval Ages (500–1500 AD). In Asian countries, the carbon age of charred residues in paddy soil in China formed by the farming method known as Fire–Flooding used by former farmers to remove weeds and rice residues was dated to about 5,900 BP (Hu et al., 2009). The black carbon from rice husk was also used for rice cultivation in Japan and other countries for several thousand years (Ogawa and Okimori, 2010). Thus, the presence of the ancient black carbon in the soil up to the present day means that it plays a key role in the formation of carbon sinks. However, the charred materials used historically were mainly produced by open-fire processes without oxygen control. The traditional technologies of charcoal production, such as pits, earth mounds, brick and metal kilns (Duku et al., 2011) were crucial innovations in the controlled use of fire and the early development of pyrolysis (Brown et al., 2015). Pyrolysis relates to the degradation of biomass materials by thermochemical conversion processes without oxygen supply (Bridgwater, 1994).

During pyrolysis, the components of biomass, such as cellulose, hemicellulose and lignin, undergo various reactions, including cross-linking, depolymerisation, and fragmentation (Duku et al., 2011). The products of pyrolysis include syngas, liquid (oil or bio-oil or bio-crude oil), and a complex solid known as "biochar" (Bridgwater, 1994, Spokas et al., 2012a). Hence,

biochar is the carbon-rich solid product formed from biomass materials by thermochemical process under limited or no oxygen supply (Lehmann and Joseph, 2015, Joseph et al., 2010, Mukherjee and Zimmerman, 2013b, Paethanom and Yoshikawa, 2012). Unlike charcoal and other black carbon, the formation of biochar and it's application is intended to provide soil enrichment and environmental management (Lehmann and Joseph, 2015). In particular, biochar is recalcitrant to decomposition due to it's condensed aromatic structure (Joseph et al., 2010). Various thermochemical technologies, such as carbonization, pyrolysis, gasification, and hydrothermal processing have been adopted to convert biomass into fuel (Boateng et al., 2015, Kumar and Gupta, 2009), and a residual product in all these processes is biochar (Regmi et al., 2012).

Table 1.1. Pyrolysis technologies and products of pyrolysis conversion.

Thermochemical	Other parameters	Gas %	Liquid %	Solid %	Main products
Carbonization (300-1200 °C)	Air tightness, residence time	60-75	3-5	10-35	Charcoal and gas
Pyrolysis for bio-oil (400-600 °C)	Heating rates, residence time, gas flow rates	20–40	40–70	10–25	Bio-oil
Pyrolysis for biochar (300-700 °C)	Residence time, heating rates	40–75	0–15	20–50	Biochar
Gasification (500-1500 °C)	Oxidizing media, equivalence ratio	85–95	0–5	5–15	Syngas

Source: Boateng et al. (2015)

Among these technologies, pyrolysis is normally used to produce biochar (Aller, 2016). By strict control of the production conditions, an advanced conversion system can regulate the physicochemical properties of the biochar resulting from various feedstocks to meet specific requirements (Spokas et al., 2012a). In addition, the biochar properties also are linked with the characteristics of the original feedstock, and are affected by post-processing steps, such as formation of biochar nanoparticles (Wang et al., 2013a), biochar/γ-Fe_2O_3 composite (Zhang et al., 2013), and biochar/AlOOH nanocomposites (Zhang and Gao, 2013).

1.2 Physicochemical characterization of biochar

Biochar (BC) can be produced from various feedstocks and under a variety of pyrolysis conditions (temperature, residence time, and heating rate). Feedstock characteristics and pyrolysis parameters impact on the physicochemical properties of the resulting biochar. Different feedstocks have been used to produce biochar, such as grass (Brewer et al., 2009), agricultural residues such as soybean stover and peanut husk (Ahmad et al., 2012), corncob (Budai et al., 2014), and biochars have also been derived from biowastes including sewage sludge (Lu et al., 2013, Hossain et al., 2011, Méndez et al., 2013c), manure (Park et al., 2011, Kołodyńska et al., 2012), and compost (Pellera et al., 2012). The biochars derived from grass biomass were shown to have low BET surface area and nutrient elements, but different types of grass gave various values of these parameters. For instance, BET surface area of giant reed biochars (produced at temperatures between 300 - 500 °C) fluctuated between 2.58 m^2/g and 3.04 m^2/g (Zheng et al., 2013), while witchgrass biochars produced by slow pyrolysis, fast pyrolysis, and gasification at 500 °C ranged from 21.6 m^2/g to 50.2 m^2/g (Brewer et al., 2009). However, a low content of nitrogen (N) was observed (below 1.0%) for all these biochars. Biochars produced from agricultural residues were also reported to have low BET surface area. In fact, the values were observed to range from 0.8 m^2/g to 27.1 m^2/g for sugarcane bagasse

and peanut hull BCs produced at temperatures between 300-600 $^{\circ}$C (Yao et al., 2012), and 4.59 - 4.82 m^2/g for wheat straw BCs made at temperatures between 300-500 $^{\circ}$C (Tatarková et al., 2013, Song et al., 2012). The same trend (of about 10-fold variation in surface area) was observed for biochars formed from manure and sewage waste. For example, BET surface area of the biochars produced from poultry and turkey litter (Cantrell et al., 2012, Park et al., 2011) and pig and cow manure (Kołodyńska et al., 2012) fluctuated from 2.46 to 66.7 m^2/g. In comparison, sewage sludge biochars (300-700 $^{\circ}$C) were in range between 4.10 m^2/g and 54.05 m^2/g (Méndez et al., 2013a, Yuan et al., 2013, Zielińska and Oleszczuk, 2015, Waqas et al., 2014). In contrast, biochars created from bamboo and wood biomass normally have higher BET surface areas. According to Sun et al. (2014), the values of BET surface areas of bamboo and wood BCs (600 $^{\circ}$C) were 375.5 m^2/g and 401 m^2/g, respectively. Similar values were observed for 600 $^{\circ}$C bamboo BC by Ding et al. (2010), while a higher value (517.28 m^2/g) was reported by Yang et al. (2014) for bamboo BC pyrolyzed at 1000 $^{\circ}$C. The ash content of biochars also depends on the initial feedstocks. Thus, the properties of biochar depend not only on the biomass sources, but are also influenced by the pyrolysis temperature.

The effect of pyrolysis parameters on biochar properties was reported by several previous studies. The pyrolysis products are greatly affected by temperature and residence time. For example, increasing the pyrolysis temperature from 300 to 500°C reduced the yield of pine wood biochar from 60.7% to 14.4%, but increased the content of carbon from 63.9% to 90.5% (Kim et al., 2012). Increased carbon content was also reported by Gaskin et al. (2008a) and Sun et al. (2014) for bamboo BCs. In contrast, there was a decrease of carbon content (C) for sludge biochars produced at increasing temperatures (Yuan et al., 2013, Méndez et al., 2013a, Lu et al., 2013, Hossain et al., 2011). A similar trend was observed by Cantrell et al. (2012) and Kołodyńska et al. (2012) for manure biochars. The decrease of C content in these cases may be attributed to the feedstocks having high content of volatile compounds (Zornoza et al.,

5

2016) which are easily lost during the pyrolysis process. The reduction of hydrogen (H) and oxygen (O) content of biochars resulting from higher production temperatures was supported by (Kim et al., 2012). For instance, more than 62% of H and 85 % of O were volatized from the original manure feedstocks during a pyrolysis process at 700 ^{o}C (Cantrell et al., 2012). The loss of these elements was attributed to the cleavage and cracking of weak bonds present in the biochar structure (Demirbas, 2004), which indicated that the carbon content of biochar increased with increasing pyrolysis temperature (Chen et al., 2012). Thus, the molar ratios of H/C and O/C are normally used to access the degree of aromaticity and polarity of a biochar (Gai et al., 2014). In fact, the decrease of H/C from 1.05 (in pine wood) to 0.08 (in the biochar) during pyrolysis at 700 ^{o}C indicates an increase of the aromatic content with increasing temperature (Ahmad et al., 2013). In contrast, the increase of the O/C ratio of wheat BCs from 0.29 (300 ^{o}C) to 0.05 (700 ^{o}C) was attributed to the wheat surface having a low affinity for water (Chun et al., 2004). In particular, a recent study has also used the molar O/C ratio to predict biochar stability in soil (Spokas, 2010). According to Spokas (2010), when the molar O/C ratio is higher than 0.6 the biochar will have a half-life of less than 100 years. Half-lives of between 100 – 1000 years correspond to biochars having a molar O/C ratio between 0.2 and 0.6, whereas a half-life of longer than 1000 years is classified for biochars having the O/C ratio under 0.2.

Another parameter especially affected by pyrolysis temperatures is the BET surface area. In fact, the surface area of biochars produced from poultry and turkey litters increased from 2.60 to 66.70 m^2/g when the pyrolysis temperature was increased from 350°C to 700 ^{o}C (Cantrell et al., 2012). Similar extremely high increases in surface area were seen for several biochars derived from agricultural residues such as soybean stover and peanut shell BCs increased from 3 m^2/g (300 ^{o}C) to 448 m^2/g at 700 ^{o}C (Ahmad et al., 2012). However, a decrease of BET surface

areas with increasing pyrolysis temperature was reported for safflower seed BCs above 600 °C (Onay, 2007), sugarcane bagasse BC produced at temperatures higher than 450 °C (Yao et al., 2011), and maize stalk, rice and cotton straw BCs produced above 900 °C (Fu et al., 2011). This trend is the result of structure ordering, and a decrease in micropores and increase in macropores due to volatile bubble development (Onay, 2007). The ash and pH values of biochars have been seen to increase with increasing formation temperature (Zornoza et al., 2016, Yuan et al., 2011). A low ash content was observed for biochars produced from wood (Kim et al., 2012) and bamboo (Hernandez-Mena et al., 2014) as compared to biochars derived from sludge which have an ash content in the range 52.28 - 88.07 % (Hossain et al., 2011, Chen et al., 2014). A similar trend was seen for biochars derived from agricultural residues such as rice husk BC (Claoston et al., 2014, Paethanom and Yoshikawa, 2012) and corn stover BC (Lee et al., 2010). Neutral or alkaline values of biochar pH are reported for most studies. For instance, pH values were in the range of 6.66 – 8.88 for rice husk BCs produced at 350-650 °C (Claoston et al., 2014) or 7.7 – 11.32 for soybean stover at 300 – 700 °C (Ahmad et al., 2012).

Cation exchange capacity (CEC) is an important parameter for biochar functionality, and is connected to its ability to sequester nutrients and pollutants. This parameter indicates the adsorption capacity of biochar for plant nutrients such as NH_4^+-N (Gai et al., 2014) or heavy metal pollutants such as Pb (Ding et al., 2014). However, CEC values fo

 a range of biochars were reported to decrease with increasing pyrolysis temperature (Claoston et al., 2014, Song and Guo, 2012, Gaskin et al., 2008a, Budai et al., 2014, Gai et al., 2014). According to Gai et al. (2014), CEC values were 4.0 – 5.1, 38.3 – 68.6, and 7.2 – 8.5 Cmol/kg, respectively for biochars derived from wheat straw, corn straw, and peanut shell where all were produced at 400 - 500 °C, and which was higher than that of biochars of similar compositions produced at 600 -700 °C. Higher CEC values were also seen for both corncob

7

and miscanthus (BCs 350 – 475 $^\circ$C) compared to those pyrolyzed above 470 $^\circ$C (Budai et al., 2014). The reduction of CEC with increasing temperature is caused by the increased loss of surface acidic functional groups such as phenolic, carboxylic, and lactonic acids at higher temperatures (Wang et al., 2013b). A similar decrease of acidic functional groups with increasing temperature was observed by Zornoza et al. (2016). However, Chen et al. (2014) found that the CEC of biochar formed from sewage sludge at 800-900 $^\circ$C (CEC = 126.62 - 247.51 Cmol/kg and O/C = 0.115 – 0.119) was higher than for those produced at 500-700 $^\circ$C (CEC = 30.81 - 76.75 Cmol/kg and O/C = 0.300 – 0.449). This finding contradicts the report of Lee et al. (2010) who showed a correlation between O/C and CEC of the biochar.

1.3 Biochar for soil enrichment

Investigation of the physicochemical properties of biochar is important in order to assess its applicability for soil enrichment. The addition of biochar was shown to increase the pH for several soils. According to Yuan et al, soil pH of an acidic Ultisols (pH = 4.3) soil incubated with biochar derived from leguminous straws (soybean, peanut, faba (fava) bean, and mung bean) increased from 0.59 to 1.05 pH units, while non – leguminous straw (canola, corn, wheat, rice straw, and rice husk) BC resulted in pH increases from 0.18 to 0.66 pH units. The increase of soil pH by addition of biochar was reported by Yamato et al. (2006) for garden and grass farm soils in Indonesia, by Liu et al. (2014) for paddy soil in China, and by Van Zwieten et al. (2010) for Ferrosol soil in Australia. In particular, strong pH increases were observed for Norfolk acidic soil (from 5.9 to alkaline pH region) when six biochars derived from peanut hull, pecan cell, poultry litter, and switchgrass were applied (Novak et al., 2009). The soil acidity is mainly caused by exchangeable Al^{3+} and H^+ in the soil. Thus, improvement of soil pH values (reduction of acidity) is due to the functional groups (hydroxyl, carboxyl, and carbonyl groups) on the biochar surface binding strongly with Al^{3+} (Lee et al., 2010) to form complexation cations. In

8

addition, alkaline cations (Ca^{2+}, Mg^{2+}, K^+, Na^+) are released from biochar to neutralize soil acidity (H^+) as a result of the binding of Al^{3+}, thus soil pH increases (Yuan and Xu, 2011). For instance, the concentration of exchangeable Al^{3+} was reduced from 2 Cmol/kg to below the limit of detection in Ferrosol soil enriched with paper mill waste biochars (Van Zwieten et al., 2010), while the exchangeable H^+ content of acidic Ultisol soil was reduced from 5.95 to 2.62 Cmol/kg after mung bean straw biochar was applied (Yuan and Xu, 2011). The pH decrease lead to an improvement in the available nutrients for plants grown in the soil, particularly phosphate (P). According to Yamato et al. (2006), the content of available P increased from 22.0 mg/kg (control) to 80.2 mg/kg when using Acacia wood waste - derived biochar combined with chemical fertilizer compounds (15N-15P-15K) was applied to soil used to grow maize. In addition, the nutrients (P, K, Ca, Mg, Na and micronutrients) of biochar are themselves an important nutrient source to increase the available nutrients in soil. The nutrients were reported by Zornoza et al. (2016) for pig manure (PM) and cotton residues (CR) BCs, by Gaskin et al. (2008a) for poultry litter (PL), peanut hull (PH), and pine chip (PC) BCs, and Chen et al. (2014) for municipal sewage sludge mixed with pine bark (SP) BC, which is presented in Table 1.2. The contents of the plant nutrient elements are varied and depend on the feedstocks. The biochars produced from pig manure, poultry litter, and sludge had higher contents of the nutrient elements than those from cotton crop residues and peanut hull. Although Cu and Zn are known as heavy metals, their contents are still in the range of allowed thresholds of biochar standards (IBI, 2015).

Table 1.2. The total elemental content of a range of biochars pyrolyzed at 400 °C and 500 °C with all other conditions being equal. PM = Pig manure; CR = Cotton residues; PL = poultry litter; PH = peanut hull; PC = pine chip and SP = sludge mixed with pine bark.

Sample	P mg/kg	Ca mg/kg	Mg mg/kg	K mg/kg	Cu mg/kg	Zn mg/kg
PM-400	44.53	97.7	18.66	22.14	79.35	604.9
PM-500	46.45	100.0	20.43	24.13	95.37	554.5
CR-400	7.30	76.7	18.75	63.33	14.13	59.1
CR-500	7.09	77.7	18.88	65.25	12.47	65.7
PL-400	30.1	42.7	10.07	51.1	805.0	628.0
PL-500	35.9	52.4	12.90	58.6	1034.0	752.0
PH-400	1.83	4.62	2.19	15.2	16.0	35.0
PH-500	1.97	5.12	2.50	16.4	19.0	37.0
PC-400	0.15	1.71	0.60	1.45	25.0	15.0
PC-500	0.14	1.85	0.59	1.45	9.0	18.0
SP-500	18185.58	59286.90	14736.07	8518.52	202.44	-

Biochar amendment of soil not only improves soil fertility, but also sequesters the soil carbon. Zimmerman (2010) indicated that the carbon loss (degradation) rate from soil enriched with biochars (400 °C, C = 58.6–78.6 %) produced from oak, pine, cedar, bubinga, gamma grass, and sugarcane were calculated to range from 7 to 27 % C after 100 years, and the half-life of these biochars was estimated to span from 370 – 23,800 years. The presence of biochar in soil affects the soil biogeochemistry as a result tof the natural oxidation of biochar. The oxidation of biochar leads to the formation of O-containing functional groups (e.g. acids) and thus increases the surface negativity (Cheng et al., 2008), which also results in an increase in soil CEC. The soil CEC increase reported by Nigussie et al. (2012) was from 27.22 Cmol/kg (soil without biochar) to 31.61 Cmol/kg (soil + 5 tons corn stalk BC/hectare (ha) and 33.69 Cmol/kg

(soil + 10 ton corn stalk BC/ha). The same trend, but lower values, was also reported by Ndor et al. (2015), Cornelissen et al. (2013), and Jien and Wang (2013).

Table 1.3. Improvement of soil properties resulting from biochar application. OC = ratio of O/C; CEC = Cation exchange concentration.

Biochar	pH	OC	P	K	CEC	Reference
Greenwaste BC - 450 °C	✓	✓	✓	✓	✓	Chan et al. (2008b)
Poultry litter BC - 450 °C	✓	✓	✓	✓	✓	Chan et al. (2008a)
Reed BC - 500 °C	x	✓	x	✓	-	Dai et al. (2013)
Sow manure BC- 500 °C	✓	✓	✓	✓	✓	
Pineapple peel - 500 °C	✓	✓	✓	✓	✓	
Maize stalk BC - 500 °C	✓	✓	✓	X	✓	Nigussie et al. (2012)
Wood BC – 700 °C	✓	✓	-	-	✓	Jien and Wang (2013)
Wood BC - 450 °C	✓	✓	x	x	-	Jones et al. (2012)
Cow manure BC - 500 °C	✓	✓	✓	✓	✓	Uzoma et al. (2011)
Cassava stem BC	✓	✓	✓	✓	-	Yang et al. (2015)

Thus, the improvement of pH, surface negativity, and CEC of soil following addition of biochar plays an important role in conferring soil with increased ability for heavy metal immobilization and nutrient retention. Further understanding of the specific mechanisms of action, and correlation of structure and activity will support the selection of optimal biochar parameters to address specific needs.

1.4 Effect of biochar on nutrient retention and heavy metal remediation.

The effect of biochar on nutrient retention was reported by several previous studies. Assessment has mainly focused on the adsorption capacity of biochar for ammonium (NH_4^+-N) which is known to be unstable in soil due to the ability of *Nitrosomonas* bacteria in soil to transform it into nitrite (NO_2^-) and then nitrate (NO_3^-) by Nitrobacter and Nitrosolobus bacteria respectively (Trenkel, 2010). The goal when using biochar as an adsorbent is to keep N in the ammonium form for longer and thereby to reduce the loss of N via NO_3^-, which is easily leached, or the production of nitrous oxide (N_2O) a known as a greenhouse gas, by nitrification. In fact, the adsorption of NH_4^+-N by biochar depends on the type of biochar, and the concentration of NH_4^+-N in the solution. For example, Takaya et al. (2016) found that municipal waste biochar produced at $400 - 450\,^oC$ had adsorption capacity up to 137.3 mg/g for NH_4-N from a solution containing 1000 mg NH_4^+-N/L, while presscake waste BC produced at the same temperatures had NH_4^+-N adsorption capacities in the range 128.3 – 146.4 mg/g. Much lower adsorption (2.45 – 3.50 mg/g) was observed for corncob biochar (produced at $400\,^oC$) added to $20 - 60$mg NH_4^+-N/L solution (Vu et al., 2017). The same trend was reported for twelve biochars ($400 - 700\,^oC$) produced from agricultural residues (corn straw, wheat straw and peanut shell), which showed higher adsorption by corn straw BC (1.6 - 2.3 mg/g) than wheat straw BC (0.6 – 0.9 mg/g) and peanut shell BC (0.6 - 1.2 mg/g) at 50 mgNH_4^+-N solution (Gai et al., 2014). In contrast, the findings of Gao et al. (2015) were in the range 15.8 – 17.4 mg/g for corncob and peanut shell BCs ($300 - 600\,^oC$) from a 50 mgNH_4^+-N solution.

The effect of the initial concentration of adsorbate (NH_4^+-N) on the adsorption capacity of adsorbent (biochar) was proven by the findings of Zhou et al. (2015), which indicated that the adsorption capacity of bamboo biochar increased from 0.50 to 1.68 mg/g when the initial NH_4^+-N concentration was increased from 2 to 60 mg/L. The increased adsorption capacity at

higher available adsorbate concentrations is also supported by the study of Kizito et al. (2015) who assessed the NH_4^+-N adsorption capacity of wood BC and rice husk BC using an artificial solution (NH_4Cl) and leachate from a biogas plant where the initial NH_4^+-N concentration ranged from 250 to 1,400 mg/L. The results indicated that the adsorption capacity of the biochars for the artificial solution was higher than for the leachate, and wood BC exhibited better adsorption than rice husk BC. In fact, the NH_4^+-N adsorption capacity of wood BC increased from 11.35 to 54.86 mg/g with increasing concentration of NH_4Cl in the artificial solution and from 9.73 to 42.02 mg/g with increasing concentration of NH_4^+-N in the leachate, while rice husk BC increased from 10.51 to 47.14 mg/g and 9.17 to 37.63 mg/g in the artificial solution and leachate, respectively with similar increases in NH_4^+-N concentration (Kizito et al., 2015).

In contrast, however, Yu et al. (2016) found that the biochars derived from biogas residues (pig manure and straw) had higher NH_4^+-N adsorption capacity (19.16 – 26.82 mg/g) for biogas leachate compared to the artificial solution (11.36 – 13.66 mg/g). These findings were also supported by Sarkhot et al. (2013) for the mixed hard wood BC. According to Sarkhot et al. (2013), these findings show that the cations (Ca^{2+}, Mg^{2+}, K^+, Na^+) and dissolved organic matter in the leachate helped to increase the NH_4^+-N adsorption. Biochar can retain 78 to 91 % of the adsorbed NH_4^+-N during desorption in DI water, which indicates that the adsorbent is a perfect potential precursor material to recover nutrient ions from leachate (Sarkhot et al., 2013).

Table 1.4. NH$_4^+$-N adsorbed by various biochars and initial NH$_4^+$-N concentration.

Biochar	Adsorption (mg/g)		Initial NH$_4^+$-N concentration mg/L	Reference
	q_e	q_{max}		
Corn cob - 400 °C	1.09	15.3	1000 mg/L	Zhang et al. (2014)
Corn cob - 600 °C	0.90	12.8	1000 mg/L	
Corn cob - 300 °C	130	217.4	500 mg/L	Gao et al. (2015)
Cotton stalk - 300 °C	110	202.5	500 mg/L	
Corn straw - 450 °C	0.75	1.53	40 mg/L	Liu et al. (2013)
Corn straw - 500 °C	2.12	12.04	50 mg/L	Gai et al. (2014)
Peanut shell - 300 °C	130	243.3	500 mg/L	Gao et al. (2015)
Peanut shell - 450 °C	1.00	1.58	40 mg/L	Liu et al. (2013)
Peanut shell - 500 °C	0.73	9.92	50 mg/L	Gai et al. (2014)
Oak wood -600-650 °C	123.5	-	1000 mg/L	Takaya et al. (2016)
Presscake waste 600-650 °C	163.2	-	1000 mg/L	
Municipal waste 600-650 °C	128.3	-	1000 mg/L	
Giant reed - 300 °C	1.35	2.10	200 mg/L	Zheng et al. (2013)
Giant reed - 350 °C	0.90	1.43	200 mg/L	
Giant reed - 400 °C	0.62	1.04	200 mg/L	
Wheat straw - 500 °C	0.63	4.68	50 mg/L	Gai et al. (2014)
Mixed hardwood -300 °C	2.80	-	1000 mg/L	Sarkhot et al. (2013)
Mixed hardwood -300 °C	5.3	-	1000 mg/L[*]	

*NH$_4^+$-N in diary manure effluent

Exploiting the adsorption capacity for NH$_4^+$-N in aqueous solution, biochar has been used to assess the nutrient retention ability of soil. According to Ding et al. (2010), addition of 0.5% bamboo BC to a surface soil layer (20 cm) decreased the loss of NH$_4^+$-N via leaching by 15.2%, while the reduction was 11.% for wood BC (Laird et al., 2010). The results of Huang et al. (2014a) indicated that cassava stem BC added into soil increased N fertilizer uptake by rice, which lead to the reduction of NH$_4^+$-N loss (9-10 %). The increase in N uptake by plants was also observed by Taghizadeh-Toosi et al. (2012) by applying pine wood chip BC to soil.
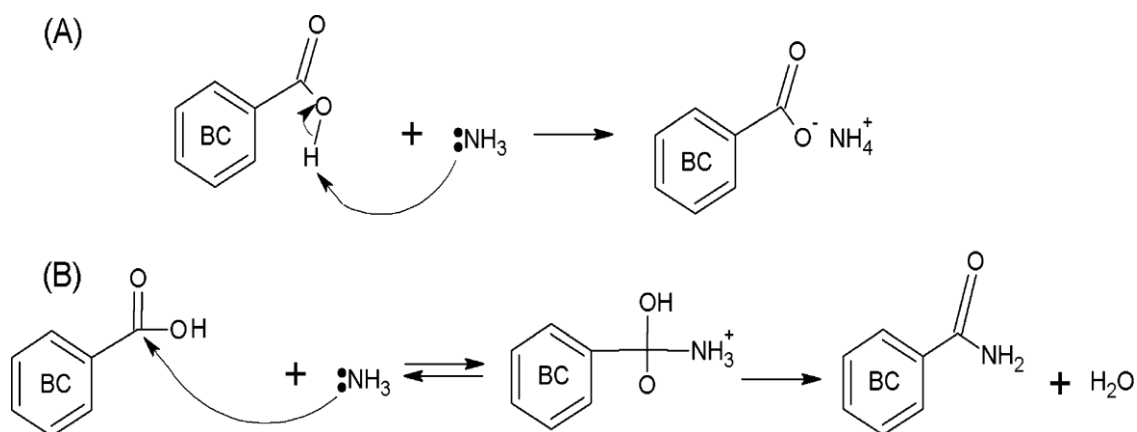
Figure 1.2. Example reactions of a carboxyl group located on a biochar surface with ammonia (NH_3) (Spokas et al., 2012b).

The adsorption of NH_4^+-N onto biochar is governed by chemical adsorption via CEC (Gai et al., 2014) supported by cations (Ca^{2+}, Mg^{2+}, Na^+, and K^+) on the surface of the biochar, or via exchange of electrons between ammonia and carboxyl groups (shown schematically in Figure 1.2) to form an ammonium salt or amide (Spokas et al., 2012b).

The adsorption capacity of different biochars towards a range of heavy metals has been assessed. In general, biochar produced from manure had higher adsorption capacity for heavy metals than biochar from other biomass (see Table 1.5). For example, Chen et al. (2011) found that the adsorption capacity of wood BC and corn straw BC was 11.0 and 4.54 mg/g for Zn^{2+}, and 12.52 and 6.79 mg/g for Cu^{2+}, respectively. In contrast, Kołodyńska et al. (2012) reported that the adsorption of pig manure BC (produced at 600 °C) was 80.88 mg/g for Zn^{2+} and 94.71 mg/g for Cu^{2+}.

In addition, Xu et al. (2013a) observed that dairy manure BC had much higher adsorption (in the range 32.24 – 54.43 mg/g) for Zn^{2+}, Cu^{2+}, and Cd^{2+} compared to rice husk BC which was in range 4.19 – 7.78 mg/g for these heavy metals. Low adsorption for Zn^{2+} and Cu^{2+} was also described by Chen et al. (2011) for other agricultural waste such as corn straw BC (11.0 and

12.52 mg/g) and hard wood BC (4.45 and 6.79 mg/g), respectively. Similar results for wood BCs were reported by Frišták et al. (2015), Ding et al. (2016), and Han et al. (2013). However, other agricultural waste-derived biochars, such as sesame straw (Park et al., 2016), wheat straw (Bogusz et al., 2015), and buffalo weed (Yakkala et al., 2013) were observed to have good adsorption capacities for heavy metals, especially buffalo weed BC (see Table 1.5).

Table 1.5. Adsorption capacity of heavy metals onto various biochars.

Biochar	Adsorption capacity (mg/g)				Reference
	Cu^{2+}	Zn^{2+}	Cd^{2+}	Pb^{2+}	
1. Biochars produced from manure					
Pig manure 400 ºC	75.49	64.96	106.01	175.29	Kołodyńska et al. (2012)
Pig manure 600 ºC	97.71	80.88	116.71	229.98	
Cow manure 400 ºC	74.95	62.43	113.50	212.95	
Cow manure 600 ºC	81.92	64.01	122.11	227.95	
Diary manure 200 ºC	-	-	-	132.69	Cao et al. (2009)
Diary manure 350 ºC	-	-	-	93.56	
Diary manure 350 ºC	35.52	32.24	54.43	-	Xu et al. (2013a)
2. Biochars produced from weed and agricultural residues					
Buffalo weed 700 ºC	-	-	11.63	333.33	Yakkala et al. (2013)
Rice husk 350 ºC	4.19	6.57	7.78	28.98	Xu et al. (2013a)
Sesame straw 700 ºC	55	34	86	102	Park et al. (2016)
Wheat straw 700 ºC	25.51	40.18	30.88	-	Bogusz et al. (2015)
Corn straw 600 ºC	12.52	11.0	-	-	Chen et al. (2011)
3. Biochars produced from wood and bamboo					
Hard wood 450 ºC	6.79	4.54	-	-	Chen et al. (2011)
Wood chips 500 ºC	2.50	0.97	1.99	-	Frišták et al. (2015)
Hickory wood 600 ºC	2.64	0.71	0.20	3.32	Ding et al. (2016)
Hard wood 500 ºC	0.38	0.07	-	-	Han et al. (2013)
Bamboo 500 ºC	-	14.42	8.04	-	Alamin and Kaewsichan (2015)

Although, there were different adsorption capacities for the different heavy metals among the biochars tested, most biochars indicated a preference to adsorb Pb^{2+} over other heavy metals. According to Park et al. (2016), the adsorption preference of Pb^{2+} over Zn^{2+}, Cu^{2+}, and Cd^{2+} was due to Pb^{2+} having a higher hydrolysis constant and atomic weight, a smaller hydrated radius, and bigger Misono softness value than the other heavy metal ions. The small hydrated radius of Pb^{2+} (4.01 Å) compared to Cd^{2+} (4.26 Å) or Zn^{2+} (4.30 Å), and the fact that Pb^{2+} is known as a hard Lewis acid (while Cd^{2+} is a soft Lewis acid) leads to Pb^{2+} having a higher affinity for the functional groups such as carboxylic and phenol groups (hard Lewis bases) on the surface of biochar (Park et al., 2016). In addition, the pK_H value (negative log of hydrolysis constant) of Pb^{2+} (7.71) was lower than that of Cd^{2+} (10.1) and Zn^{2+} (9.0), which demonstrated that Pb^{2+} was more preferable in terms of adsorption, forming inner sphere surface complexation, than the others. In addition, the higher electronegativity value of Pb^{2+}(2.33) compared to Cd^{2+} (1.69) resulted in Pb^{2+} having a higher adsorption affinity than Cd^{2+} for biochar (Yakkala et al., 2013).

Despite the different feedstocks, the biochars preferentially adsorbed Pb^{2+} from aqueous solution rather than the other metals (Cu^{2+}, Zn^{2+}, and Cd^{2+}). However, there were various adsorption mechanisms for these metals onto the biochars pyrolyzed from different biomasses. According to Xu et al. (2013a), the adsorption of Cu^{2+}, Zn^{2+}, Cd^{2+} and Pb^{2+} onto rice husk BC was mainly via complexation of metals by phenolic groups on the biochar surface, and did not occur via precipitation with PO_4^{3-}, except for Pb^{2+}(< 6.7%). In contrast, 70 - 100 % of these metals adsorbed onto diary manure BC was observed to be involved in metal – phosphate (PO_4^{3-}) precipitation.

Utilizing their strong adsorption capability, the effectiveness of different biochars to remediate soils contaminated with heavy metals was evaluated. The effect of biochar on heavy metal bioavailablity depends on the biochar type as well as the metals present in the

soil or water. In fact, the reduction of bioavailable Zn, Cd, and Pb was 87, 71, and 92%, respectively for soil amended with miscanthus BC (Houben et al., 2013) or 31.9 % for Cu and 66% for Zn following bamboo BC application to soil (Yang et al., 2016b). The reduction of soluble Zn^{2+}, Cd^{2+} and Pb^{2+} was also observed for rice husk, rice straw, and bran biochars (Zheng et al., 2012) and following application of hard wood BC onto contaminated soils by Beesley et al. (2010). Similar to the findings in aqueous solution, the preferential adsorption of Pb to biochar compared to both Zn and Cu was also exhibited in biochar – amended soil (Houben et al., 2013). This preference might be related to the higher affinity of Pb for surface functional groups (carboxylic and phenolic) of aged biochar (Houben et al., 2013). Therefore, Pb showed the least mobilization compared to Zn and Cd in mining soil amended with sugarcane straw BCs (Puga et al., 2016), or the decrease in bioavailable Cu and Pb was greater than that of bioavailable Zn and Cd for contaminated soil to which bamboo and rice straw BCs were applied (Yang et al., 2016b). The reduction in the mobilization and availability of heavy metals as a result of adsorption to BC leads to the reduction of heavy metal uptake to plants. The observation of Namgay et al. (2010) indicated that the application wood BC onto the soil significantly decreased the availability of heavy metals (As < Zn < Cd < Cu < Pb) to maize plants. The same trend was observed for corn plants cultivated on mining soil to which conorcapus biochar was added (Al-Wabel et al., 2015). In fact, the concentration of heavy metals in shoots of maize decreased to 28% for Zn, 60% for Cu, 53.2 % for Cd, and 51.3% for 5% (w:w) the biochar applied into the soil compared to the soil without biochar (Al-Wabel et al., 2015).

1.5 Context and objective of this thesis

Vietnam is known as an agricultural country with tropical weather. The biomass residues remaining after harvesting of crops (rice straw, corncob, corn straw etc.) or from processing plants (wood chips, rice husk, bamboo, coffee husk, coconut peel and shell etc.) are currently used for cooking, are burnt or are left to decompose on the field rather than being turned into novel low cost products like biochar for soil enrichment, water purification, anodes for batteries or others. The tropical weather in Vietnam causes rapid decomposition of organic matter in soil and loss of numerous nutrients (particularly N) via runoff, leaching, and emission. In soil, N nutrient mainly incorporates with soil organic matter (humic and fulvic acids), thereby the rapid decomposition leads to N loss from soil. Consequently, the use effectiveness of N fertilizer do not ecceed 50% (pulished in Vietnamese). In addition, due to limited management and treatment technology, some regions of the country face a highly polluted environment by wastewater and landfill leachate containting high contaminants (NH_4^+-N and heavy metal) which leads to pollute water and agricultural soils. Thus, turning the residues from agriculture and waste treatment into low cost novel products is necessary to solve the constraints and prevent further pollution.

Biochar was proved as a novel product for NH_4^+-N and heavy metal adsorptions. These role were reported by several studies which were on the literature review. However, the adsorption mechanisms for these adsorbates are still on debate, particularly the adsorption occurred by homogenous or heterogenous surface on mono and/or multilayer and by physical and/or chemical dasorption. Thus, this thesis aimed to systematically explore the utility of various Vietnamese biomass residues to produce biochar for nutrient capture to reduce the nutrient loss and create soil carbon sink due to slow decomposition, and use for water purification. The overall objective is thus to understand the connection between their physicochemical properties for fertiliser efficiencies in terms of ammonia adsorption capacity,

and/or water purification capabilities as determined by retention of heavy metal (Zn) and other pollutants, in order to design optimal biochar properties for use in fertilization as direct amendment to capture nutrient (NH_4^+-N) or coating to control the nutrient release and loss, and for mitigation of environmental pollution for water and soil. The working hypothesis for the thesis was that specific characteristics of the biochar would correlate with specific adsorption behaviours allowing for optimization of the biochar selection for maximal effect.

1.6 Thesis organization

There are 7 chapters in this thesis, organized as shown in Figure 1.3). Several important questions are addressed to determine the optimal biochar type, sourced using the locally available top drum down draft method, and local feedstuffs, for application in fertilization capture and water purification.
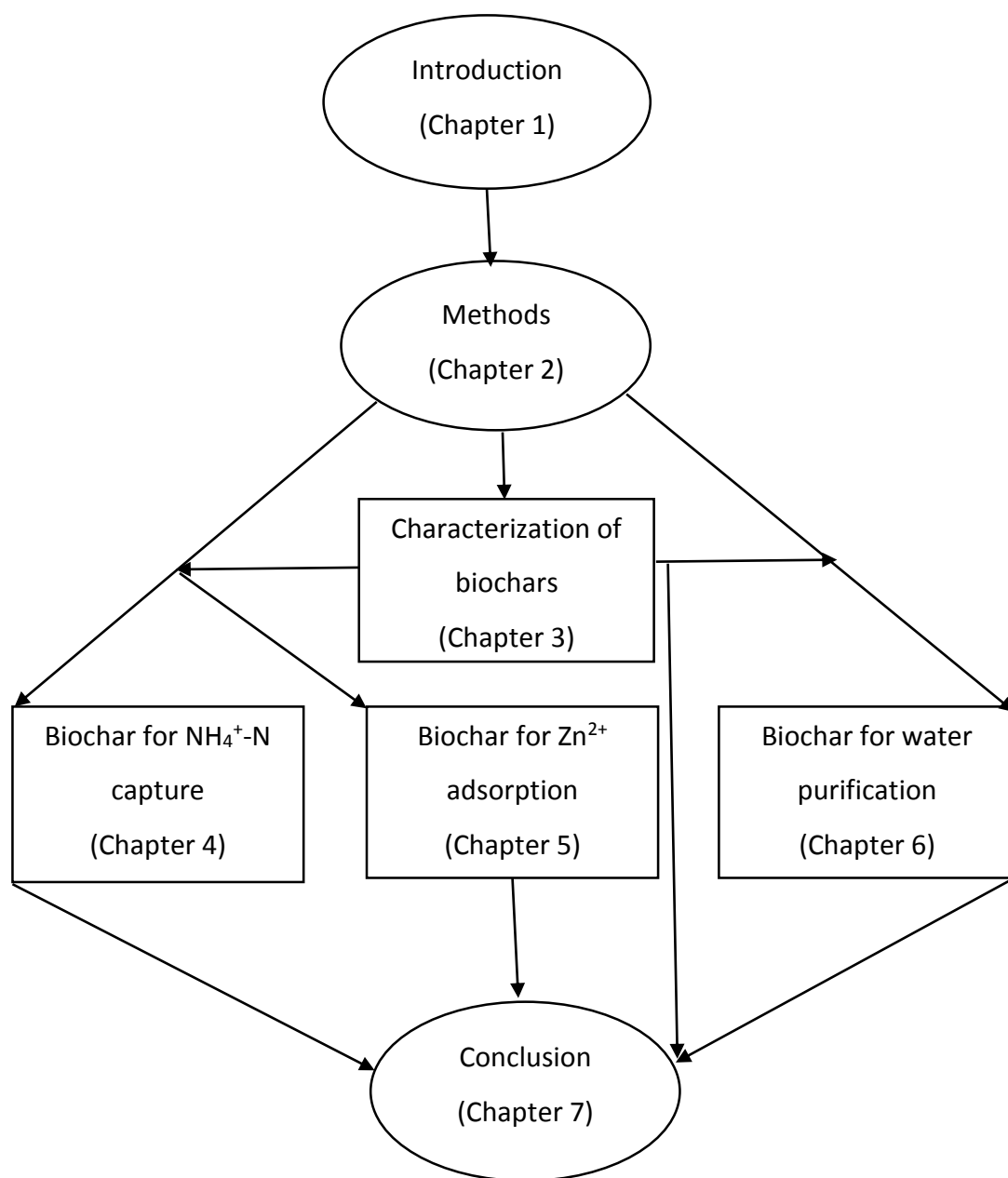
Figure 1.3. Illustrated diagram of the thesis chapters and their interrelationships.

The assessment tools include the physicochemical characterizations of biochars (**Chapter 3**), elucidation of the connection between the biochar properties and their functionalities for fertilizer (NH_4^+-N) capture (**Chapter 4**) and heavy metal (Zn^{2+}) adsorption (**Chapter 5**), and application for water purification (**Chapter 6**). The four results chapters are designed and

presented in the format of publications, and have been compiled to form the body of this thesis. The inter-relationships between the thesis chapters are illustrated in Figure 1.1.

The first paper, **Chapter 3** of the thesis, titled "Physicochemical Characterization of Biomass Residue–Derived Biochars in Vietnam", was submitted to the MDPI journal "Soil Systems". This chapter describes in detail the physicochemical properties of the three biochars produced from the different feedstocks (wood, rice husk and bamboo) that are utilised throughout the thesis. The aims of **Chapters 4 and 5** are to understand the connection between the biochar properties and their functionality for plant nutrient capture and heavy metal pollution remediation. **Chapter 4** is formatted as the second paper entitled "Adsorption of ammonium nitrogen (NH_4^+-N) ions onto various Vietnamese Biomass Residue–derived Biochars (wood, rice husk and bamboo)". **Chapter 5** presents the third paper named "Removal of Zinc (Zn^{2+}) by various Vietnamese Biomass Residue–derived Biochars (wood, rice husk and bamboo) from Aqueous Solution". The main objectives of both these chapters are to identify the adsorption capacities of the biochars and their adsorption mechanisms for NH_4^+-N and Zn^{2+}, respectively.

The findings of Chapters 4 & 5 provide basic knowledge for using the individual biochars and a mixture of biochars together for water purification (landfill leachate), which is demonstrated in **Chapter 6.** This chapter also has a paper format and is entitled "Pollutant Removal from Landfill Leachate by various Vietnamese Biomass Residue–derived Biochars (wood, rice husk and bamboo): Bath and Column Study". All methodologies utilised in the thesis are described in **Chapter 2**. A concluding chapter (**Chapter 7**) has been formed to connect the key findings of each paper/chapter into a comprehensive framework and conclusion. The integrated results represent a significant contribution towards understanding the utility of each of the biochars for the different potential applications, and the factors to consider when selecting a

biochar for a particular purpose. The conclusions also provide some suggestions for further investigation of the applicability of the biochars in real or field scenarios.

References

AHMAD, M., LEE, S. S., DOU, X., MOHAN, D., SUNG, J.-K., YANG, J. E. & OK, Y. S. 2012. Effects of pyrolysis temperature on soybean stover-and peanut shell-derived biochar properties and TCE adsorption in water. *Bioresource technology,* 118**,** 536-544.

AHMAD, M., LEE, S. S., RAJAPAKSHA, A. U., VITHANAGE, M., ZHANG, M., CHO, J. S., LEE, S.-E. & OK, Y. S. 2013. Trichloroethylene adsorption by pine needle biochars produced at various pyrolysis temperatures. *Bioresource technology,* 143**,** 615-622.

L-WABEL, M. I., USMAN, A. R., EL-NAGGAR, A. H., ALY, A. A., IBRAHIM, H. M., ELMAGHRABY, S. & AL-OMRAN, A. 2015. Conocarpus biochar as a soil amendment for reducing heavy metal availability and uptake by maize plants. *Saudi journal of biological sciences,* 22**,** 503-511.

ALAMIN, A. H. & KAEWSICHAN, L. 2015. Adsorption of Zn (II) and Cd (II) ions from aqueous solutions by Bamboo biochar cooperation with Hydroxyapatite and Calcium Sulphate. *International Journal of ChemTech Research,* 7**,** 2159-2170.

ALLER, M. F. 2016. Biochar properties: Transport, fate, and impact. *Critical Reviews in Environmental Science and Technology,* 46**,** 1183-1296.

BEESLEY, L., MORENO-JIMÉNEZ, E. & GOMEZ-EYLES, J. L. 2010. Effects of biochar and greenwaste compost amendments on mobility, bioavailability and toxicity of inorganic and organic contaminants in a multi-element polluted soil. *Environmental pollution,* 158**,** 2282-2287.

BOATENG, A. A., GARCIA-PEREZ, M., MASEK, O., BROWN, R. & DEL CAMPO, B. 2015. Biochar production technology. *Biochar for Environmental Management: Science, Technology and Implementation,* 2.

BOGUSZ, A., OLESZCZUK, P. & DOBROWOLSKI, R. 2015. Application of laboratory prepared and commercially available biochars to adsorption of cadmium, copper and zinc ions from water. *Bioresource technology,* 196**,** 540-549.

BREWER, C. E., SCHMIDT-ROHR, K., SATRIO, J. A. & BROWN, R. C. 2009. Characterization of biochar from fast pyrolysis and gasification systems. *Environmental Progress & Sustainable Energy,* 28**,** 386-396.

BRIDGWATER, A. 1994. Catalysis in thermal biomass conversion. *Applied Catalysis A: General,* 116**,** 5-47.

BROWN, R., CAMPO, B. D., BOATENG, A. A., GARCIA-PEREZ, M. & MASEK, O. 2015. Fundamentals of biochar production. *Biochar for Environmental Management. Routledge, London***,** 39-62.

BUDAI, A., WANG, L., GRONLI, M., STRAND, L. T., ANTAL JR, M. J., ABIVEN, S., DIEGUEZ-ALONSO, A., ANCA-COUCE, A. & RASSE, D. P. 2014. Surface properties and chemical composition of corncob and Miscanthus biochars: effects of production temperature and method. *Journal of agricultural and food chemistry,* 62**,** 3791-3799.

CANTRELL, K. B., HUNT, P. G., UCHIMIYA, M., NOVAK, J. M. & RO, K. S. 2012. Impact of pyrolysis temperature and manure source on physicochemical characteristics of biochar. *Bioresource technology,* 107**,** 419-428.

CAO, X., MA, L., GAO, B. & HARRIS, W. 2009. Dairy-manure derived biochar effectively sorbs lead and atrazine. *Environmental science & technology,* 43**,** 3285-3291.

CHAN, K., VAN ZWIETEN, L., MESZAROS, I., DOWNIE, A. & JOSEPH, S. 2008a. Using poultry litter biochars as soil amendments. *Soil Research,* 46**,** 437-444.

CHAN, K. Y., VAN ZWIETEN, L., MESZAROS, I., DOWNIE, A. & JOSEPH, S. 2008b. Agronomic values of greenwaste biochar as a soil amendment. *Soil Research,* 45**,** 629-634.

CHEN, T., ZHANG, Y., WANG, H., LU, W., ZHOU, Z., ZHANG, Y. & REN, L. 2014. Influence of pyrolysis temperature on characteristics and heavy metal adsorptive performance of biochar derived from municipal sewage sludge. *Bioresource technology,* 164**,** 47-54.

CHEN, X., CHEN, G., CHEN, L., CHEN, Y., LEHMANN, J., MCBRIDE, M. B. & HAY, A. G. 2011. Adsorption of copper and zinc by biochars produced from pyrolysis of hardwood and corn straw in aqueous solution. *Bioresource technology,* 102**,** 8877-8884.

CHEN, Y., YANG, H., WANG, X., ZHANG, S. & CHEN, H. 2012. Biomass-based pyrolytic polygeneration system on cotton stalk pyrolysis: influence of temperature. *Bioresource technology,* 107**,** 411-418.

CHENG, C.-H., LEHMANN, J. & ENGELHARD, M. H. 2008. Natural oxidation of black carbon in soils: changes in molecular form and surface charge along a climosequence. *Geochimica et Cosmochimica Acta,* 72**,** 1598-1610.

CHUN, Y., SHENG, G., CHIOU, C. T. & XING, B. 2004. Compositions and sorptive properties of crop residue-derived chars. *Environmental science & technology,* 38**,** 4649-4655.

CLAOSTON, N., SAMSURI, A., AHMAD HUSNI, M. & MOHD AMRAN, M. 2014. Effects of pyrolysis temperature on the physicochemical properties of empty fruit bunch and rice husk biochars. *Waste Management & Research,* 32**,** 331-339.

CORNELISSEN, G., MARTINSEN, V., SHITUMBANUMA, V., ALLING, V., BREEDVELD, G. D., RUTHERFORD, D. W., SPARREVIK, M., HALE, S. E., OBIA, A. & MULDER, J. 2013. Biochar effect on maize yield and soil characteristics in five conservation farming sites in Zambia. *Agronomy,* 3**,** 256-274.

DAI, Z., MENG, J., MUHAMMAD, N., LIU, X., WANG, H., HE, Y., BROOKES, P. C. & XU, J. 2013. The potential feasibility for soil improvement, based on the properties of biochars pyrolyzed from different feedstocks. *Journal of soils and sediments,* 13**,** 989-1000.

DEMIRBAS, A. 2004. Effects of temperature and particle size on bio-char yield from pyrolysis of agricultural residues. *Journal of analytical and applied pyrolysis,* 72**,** 243-248.

DING, W., DONG, X., IME, I. M., GAO, B. & MA, L. Q. 2014. Pyrolytic temperatures impact lead sorption mechanisms by bagasse biochars. *Chemosphere,* 105**,** 68-74.

DING, Y., LIU, Y.-X., WU, W.-X., SHI, D.-Z., YANG, M. & ZHONG, Z.-K. 2010. Evaluation of biochar effects on nitrogen retention and leaching in multi-layered soil columns. *Water, Air, & Soil Pollution,* 213**,** 47-55.

DING, Z., HU, X., WAN, Y., WANG, S. & GAO, B. 2016. Removal of lead, copper, cadmium, zinc, and nickel from aqueous solutions by alkali-modified biochar: Batch and column tests. *Journal of Industrial and Engineering Chemistry,* 33**,** 239-245.

DOWNIE, A. E., VAN ZWIETEN, L., SMERNIK, R. J., MORRIS, S. & MUNROE, P. R. 2011. Terra Preta Australis: Reassessing the carbon storage capacity of temperate soils. *Agriculture, ecosystems & environment,* 140**,** 137-147.

DUKU, M. H., GU, S. & HAGAN, E. B. 2011. Biochar production potential in Ghana—a review. *Renewable and Sustainable Energy Reviews,* 15**,** 3539-3551.

FRIŠTÁK, V., PIPÍŠKA, M., LESNÝ, J., SOJA, G., FRIESL-HANL, W. & PACKOVÁ, A. 2015. Utilization of biochar sorbents for Cd2+, Zn2+, and Cu2+ ions separation from aqueous solutions: comparative study. *Environmental monitoring and assessment,* 187**,** 4093.

FU, P., YI, W., BAI, X., LI, Z., HU, S. & XIANG, J. 2011. Effect of temperature on gas composition and char structural features of pyrolyzed agricultural residues. *Bioresource Technology,* 102**,** 8211-8219.

GAI, X., WANG, H., LIU, J., ZHAI, L., LIU, S., REN, T. & LIU, H. 2014. Effects of feedstock and pyrolysis temperature on biochar adsorption of ammonium and nitrate. *PloS one,* 9**,** e113888.

GAO, F., XUE, Y., DENG, P., CHENG, X. & YANG, K. 2015. Removal of aqueous ammonium by biochars derived from agricultural residuals at different pyrolysis temperatures. *Chemical Speciation & Bioavailability,* 27**,** 92-97.

GASKIN, J., STEINER, C., HARRIS, K., DAS, K. & BIBENS, B. 2008. Effect of low-temperature pyrolysis conditions on biochar for agricultural use. *Transactions of the ASABE,* 51**,** 2061-2069.

GERLACH, R., BAUMEWERD-SCHMIDT, H., VAN DEN BORG, K., ECKMEIER, E. & SCHMIDT, M. W. 2006. Prehistoric alteration of soil in the Lower Rhine Basin, Northwest Germany— archaeological, 14 C and geochemical evidence. *Geoderma,* 136**,** 38-50.

GLASER, B., BALASHOV, E., HAUMAIER, L., GUGGENBERGER, G. & ZECH, W. 2000. Black carbon in density fractions of anthropogenic soils of the Brazilian Amazon region. *Organic Geochemistry,* 31**,** 669-678.

GLASER, B., HAUMAIER, L., GUGGENBERGER, G. & ZECH, W. 2001. The'Terra Preta'phenomenon: a model for sustainable agriculture in the humid tropics. *Naturwissenschaften,* 88**,** 37-41.

HAN, Y., BOATENG, A. A., QI, P. X., LIMA, I. M. & CHANG, J. 2013. Heavy metal and phenol adsorptive properties of biochars from pyrolyzed switchgrass and woody biomass in correlation with surface properties. *Journal of environmental management,* 118**,** 196-204.

HERNANDEZ-MENA, L. E., PÉCORAA, A. A. & BERALDOB, A. L. 2014. Slow pyrolysis of bamboo biomass: Analysis of biochar properties. *CHEMICAL ENGINEERING,* 37.

HOSSAIN, M. K., STREZOV, V., CHAN, K. Y., ZIOLKOWSKI, A. & NELSON, P. F. 2011. Influence of pyrolysis temperature on production and nutrient properties of wastewater sludge biochar. *Journal of Environmental Management,* 92**,** 223-228.

HOUBEN, D., EVRARD, L. & SONNET, P. 2013. Mobility, bioavailability and pH-dependent leaching of cadmium, zinc and lead in a contaminated soil amended with biochar. *Chemosphere,* 92**,** 1450-1457.

HU, L., LI, X., LIU, B., GU, M. & DAI, J. 2009. Organic structure and possible origin of ancient charred paddies at Chuodun Site in southern China. *Science in China Series D: Earth Sciences,* 52**,** 93-100.

HUANG, M., YANG, L., QIN, H., JIANG, L. & ZOU, Y. 2014. Fertilizer nitrogen uptake by rice increased by biochar application. *Biology and fertility of soils,* 50**,** 997-1000.

JIEN, S.-H. & WANG, C.-S. 2013. Effects of biochar on soil properties and erosion potential in a highly weathered soil. *Catena,* 110**,** 225-233.

JONES, D., ROUSK, J., EDWARDS-JONES, G., DELUCA, T. & MURPHY, D. 2012. Biochar-mediated changes in soil quality and plant growth in a three year field trial. *Soil Biology and Biochemistry,* 45**,** 113-124.

JOSEPH, S., CAMPS-ARBESTAIN, M., LIN, Y., MUNROE, P., CHIA, C., HOOK, J., VAN ZWIETEN, L., KIMBER, S., COWIE, A. & SINGH, B. 2010. An investigation into the reactions of biochar in soil. *Soil Research,* 48**,** 501-515.

KIM, K. H., KIM, J.-Y., CHO, T.-S. & CHOI, J. W. 2012. Influence of pyrolysis temperature on physicochemical properties of biochar obtained from the fast pyrolysis of pitch pine (Pinus rigida). *Bioresource technology,* 118**,** 158-162.

KIZITO, S., WU, S., KIRUI, W. K., LEI, M., LU, Q., BAH, H. & DONG, R. 2015. Evaluation of slow pyrolyzed wood and rice husks biochar for adsorption of ammonium nitrogen from

piggery manure anaerobic digestate slurry. *Science of The Total Environment,* 505**,** 102-112.

KOŁODYŃSKA, D., WNĘTRZAK, R., LEAHY, J., HAYES, M., KWAPIŃSKI, W. & HUBICKI, Z. 2012. Kinetic and adsorptive characterization of biochar in metal ions removal. *Chemical Engineering Journal,* 197**,** 295-305.

KUMAR, S. & GUPTA, R. B. 2009. Biocrude production from switchgrass using subcritical water. *Energy & Fuels,* 23**,** 5151-5159.

LAIRD, D., FLEMING, P., WANG, B., HORTON, R. & KARLEN, D. 2010. Biochar impact on nutrient leaching from a Midwestern agricultural soil. *Geoderma,* 158**,** 436-442.

LEE, J. W., KIDDER, M., EVANS, B. R., PAIK, S., BUCHANAN III, A., GARTEN, C. T. & BROWN, R. C. 2010. Characterization of biochars produced from cornstovers for soil amendment. *Environmental Science & Technology,* 44**,** 7970-7974.

LEHMANN, J. & JOSEPH, S. 2015. *Biochar for environmental management: science, technology and implementation*, Routledge.

LIU, L., SHEN, G., SUN, M., CAO, X., SHANG, G. & CHEN, P. 2014. Effect of biochar on nitrous oxide emission and its potential mechanisms. *Journal of the Air & Waste Management Association,* 64**,** 894-902.

LIU, N., SUN, Z. T., WU, Z. C., ZHAN, X. M., ZHANG, K., ZHAO, E. F. & HAN, X. R. Adsorption characteristics of ammonium nitrogen by biochar from diverse origins in water. Advanced Materials Research, 2013. Trans Tech Publ, 305-312.

LU, H., ZHANG, W., WANG, S., ZHUANG, L., YANG, Y. & QIU, R. 2013. Characterization of sewage sludge-derived biochars from different feedstocks and pyrolysis temperatures. *Journal of Analytical and Applied Pyrolysis,* 102**,** 137-143.

MÉNDEZ, A., TARQUIS, A., SAA-REQUEJO, A., GUERRERO, F. & GASCÓ, G. 2013a. Influence of pyrolysis temperature on composted sewage sludge biochar priming effect in a loamy soil. *Chemosphere,* 93**,** 668-676.

MÉNDEZ, A., TERRADILLOS & GASCÓ, G. 2013b. Physicochemical and agronomic properties of biochar from sewage sludge pyrolysed at different temperatures. *Journal of Analytical and Applied Pyrolysis,* 102**,** 124-130.

MUKHERJEE, A. & ZIMMERMAN, A. R. 2013. Organic carbon and nutrient release from a range of laboratory-produced biochars and biochar–soil mixtures. *Geoderma,* 193**,** 122-130.

NAMGAY, T., SINGH, B. & SINGH, B. P. 2010. Influence of biochar application to soil on the availability of As, Cd, Cu, Pb, and Zn to maize (Zea mays L.). *Soil Research,* 48**,** 638-647.

NDOR, E., AMANA, S. & ASADU, C. 2015. Effect of biochar on soil properties and organic carbon sink in degraded soil of Southern Guinea Savanna Zone, Nigeria. *Int. J. Plant Soil Sci,* 4**,** 252-258.

NIGUSSIE, A., KISSI, E., MISGANAW, M. & AMBAW, G. 2012. Effect of biochar application on soil properties and nutrient uptake of lettuces (Lactuca sativa) grown in chromium polluted soils. *American-Eurasian Journal of Agriculture and Environmental Science,* 12**,** 369-376.

NOVAK, J. M., LIMA, I., XING, B., GASKIN, J. W., STEINER, C., DAS, K., AHMEDNA, M., REHRAH, D., WATTS, D. W. & BUSSCHER, W. J. 2009. Characterization of designer biochar produced at different temperatures and their effects on a loamy sand. *Annals of Environmental Science,* 3**,** 195-206.

O'NEILL, B., GROSSMAN, J., TSAI, M., GOMES, J., LEHMANN, J., PETERSON, J., NEVES, E. & THIES, J. 2009. Bacterial community composition in Brazilian anthrosols and adjacent soils characterized using culturing and molecular identification. *Microbial Ecology,* 58**,** 23-35.

OGAWA, M. & OKIMORI, Y. 2010. Pioneering works in biochar research, Japan. *Soil Research,* 48**,** 489-500.

ONAY, O. 2007. Influence of pyrolysis temperature and heating rate on the production of bio-oil and char from safflower seed by pyrolysis, using a well-swept fixed-bed reactor. *Fuel Processing Technology,* 88**,** 523-531.

PAETHANOM, A. & YOSHIKAWA, K. 2012. Influence of pyrolysis temperature on rice husk char characteristics and its tar adsorption capability. *Energies,* 5**,** 4941-4951.

PARK, J.-H., OK, Y. S., KIM, S.-H., CHO, J.-S., HEO, J.-S., DELAUNE, R. D. & SEO, D.-C. 2016. Competitive adsorption of heavy metals onto sesame straw biochar in aqueous solutions. *Chemosphere,* 142**,** 77-83.

PARK, J. H., CHOPPALA, G. K., BOLAN, N. S., CHUNG, J. W. & CHUASAVATHI, T. 2011. Biochar reduces the bioavailability and phytotoxicity of heavy metals. *Plant and soil,* 348**,** 439.

PELLERA, F.-M., GIANNIS, A., KALDERIS, D., ANASTASIADOU, K., STEGMANN, R., WANG, J.-Y. & GIDARAKOS, E. 2012. Adsorption of Cu (II) ions from aqueous solutions on biochars prepared from agricultural by-products. *Journal of Environmental Management,* 96**,** 35-42.

PUGA, A. P., MELO, L. C. A., DE ABREU, C. A., COSCIONE, A. R. & PAZ-FERREIRO, J. 2016. Leaching and fractionation of heavy metals in mining soils amended with biochar. *Soil and Tillage Research,* 164**,** 25-33.

REGMI, P., MOSCOSO, J. L. G., KUMAR, S., CAO, X., MAO, J. & SCHAFRAN, G. 2012. Removal of copper and cadmium from aqueous solution using switchgrass biochar produced via hydrothermal carbonization process. *Journal of environmental management,* 109**,** 61-69.

SARKHOT, D., GHEZZEHEI, T. & BERHE, A. 2013. Effectiveness of biochar for sorption of ammonium and phosphate from dairy effluent. *Journal of environmental quality,* 42**,** 1545-1554.

SMITH, N. J. 1980. ANTHROSOLS AND HUMAN CARRYING CAPACITY IN AMAZONIA∗. *Annals of the Association of American Geographers,* 70**,** 553-566.

SONG, W. & GUO, M. 2012. Quality variations of poultry litter biochar generated at different pyrolysis temperatures. *Journal of analytical and applied pyrolysis,* 94**,** 138-145.

SONG, Y., WANG, F., BIAN, Y., KENGARA, F. O., JIA, M., XIE, Z. & JIANG, X. 2012. Bioavailability assessment of hexachlorobenzene in soil as affected by wheat straw biochar. *Journal of hazardous materials,* 217**,** 391-397.

SPOKAS, K. A. 2010. Review of the stability of biochar in soils: predictability of O: C molar ratios. *Carbon Management,* 1**,** 289-303.

SPOKAS, K. A., CANTRELL, K. B., NOVAK, J. M., ARCHER, D. W., IPPOLITO, J. A., COLLINS, H. P., BOATENG, A. A., LIMA, I. M., LAMB, M. C. & MCALOON, A. J. 2012a. Biochar: a synthesis of its agronomic impact beyond carbon sequestration. *Journal of environmental quality,* 41**,** 973-989.

SPOKAS, K. A., NOVAK, J. M. & VENTEREA, R. T. 2012b. Biochar's role as an alternative N-fertilizer: ammonia capture. *Plant and soil,* 350**,** 35-42.

SUN, Y., GAO, B., YAO, Y., FANG, J., ZHANG, M., ZHOU, Y., CHEN, H. & YANG, L. 2014. Effects of feedstock type, production method, and pyrolysis temperature on biochar and hydrochar properties. *Chemical Engineering Journal,* 240**,** 574-578.

TAGHIZADEH-TOOSI, A., CLOUGH, T. J., SHERLOCK, R. R. & CONDRON, L. M. 2012. A wood based low-temperature biochar captures NH3-N generated from ruminant urine-N, retaining its bioavailability. *Plant and Soil,* 353**,** 73-84.

TAKAYA, C., FLETCHER, L., SINGH, S., ANYIKUDE, K. & ROSS, A. 2016. Phosphate and ammonium sorption capacity of biochar and hydrochar from different wastes. *Chemosphere,* 145**,** 518-527.

TATARKOVÁ, V., HILLER, E. & VACULÍK, M. 2013. Impact of wheat straw biochar addition to soil on the sorption, leaching, dissipation of the herbicide (4-chloro-2-methylphenoxy) acetic acid and the growth of sunflower (Helianthus annuus L.). *Ecotoxicology and environmental safety,* 92**,** 215-221.

TRENKEL, M. E. 2010. *Slow-and controlled-release and stabilized fertilizers: An option for enhancing nutrient use efficiency in agriculture*, IFA, International fertilizer industry association.

UZOMA, K., INOUE, M., ANDRY, H., FUJIMAKI, H., ZAHOOR, A. & NISHIHARA, E. 2011. Effect of cow manure biochar on maize productivity under sandy soil condition. *Soil use and management,* 27**,** 205-212.

VAN ZWIETEN, L., KIMBER, S., MORRIS, S., CHAN, K., DOWNIE, A., RUST, J., JOSEPH, S. & COWIE, A. 2010. Effects of biochar from slow pyrolysis of papermill waste on agronomic performance and soil fertility. *Plant and soil,* 327**,** 235-246.

VU, T. M., DOAN, D. P., VAN, H. T., NGUYEN, T. V., VIGNESWARAN, S. & NGO, H. H. 2017. Removing ammonium from water using modified corncob-biochar. *Science of the Total Environment,* 579**,** 612-619.

WANG, D., ZHANG, W. & ZHOU, D. 2013a. Antagonistic effects of humic acid and iron oxyhydroxide grain-coating on biochar nanoparticle transport in saturated sand. *Environmental science & technology,* 47**,** 5154-5161.

WANG, Y., HU, Y., ZHAO, X., WANG, S. & XING, G. 2013b. Comparisons of biochar properties from wood material and crop residues at different temperatures and residence times. *Energy & fuels,* 27**,** 5890-5899.

WAQAS, M., KHAN, S., QING, H., REID, B. J. & CHAO, C. 2014. The effects of sewage sludge and sewage sludge biochar on PAHs and potentially toxic element bioaccumulation in Cucumis sativa L. *Chemosphere,* 105**,** 53-61.

WIEDNER, K. & GLASER, B. 2015. Traditional use of biochar. *Biochar for Environmental Management: Science, Technology and Implementation,* 15.

XU, X., CAO, X. & ZHAO, L. 2013. Comparison of rice husk-and dairy manure-derived biochars for simultaneously removing heavy metals from aqueous solutions: role of mineral components in biochars. *Chemosphere,* 92**,** 955-961.

YAKKALA, K., YU, M.-R., ROH, H., YANG, J.-K. & CHANG, Y.-Y. 2013. Buffalo weed (Ambrosia trifida L. var. trifida) biochar for cadmium (II) and lead (II) adsorption in single and mixed system. *Desalination and Water Treatment,* 51**,** 7732-7745.

YAMATO, M., OKIMORI, Y., WIBOWO, I. F., ANSHORI, S. & OGAWA, M. 2006. Effects of the application of charred bark of Acacia mangium on the yield of maize, cowpea and peanut, and soil chemical properties in South Sumatra, Indonesia. *Soil science & plant nutrition,* 52**,** 489-495.

YANG, L., LIAO, F., HUANG, M., YANG, L. & LI, Y. 2015. Biochar improves sugarcane seedling root and soil properties under a pot experiment. *Sugar Tech,* 17**,** 36-40.

YANG, X., LIU, J., MCGROUTHER, K., HUANG, H., LU, K., GUO, X., HE, L., LIN, X., CHE, L. & YE, Z. 2016. Effect of biochar on the extractability of heavy metals (Cd, Cu, Pb, and Zn) and enzyme activity in soil. *Environmental Science and Pollution Research,* 23**,** 974-984.

YANG, Y., LIN, X., WEI, B., ZHAO, Y. & WANG, J. 2014. Evaluation of adsorption potential of bamboo biochar for metal-complex dye: equilibrium, kinetics and artificial neural network modeling. *International Journal of Environmental Science and Technology,* 11**,** 1093-1100.

YAO, Y., GAO, B., INYANG, M., ZIMMERMAN, A. R., CAO, X., PULLAMMANAPPALLIL, P. & YANG, L. 2011. Biochar derived from anaerobically digested sugar beet tailings: characterization and phosphate removal potential. *Bioresource technology,* 102**,** 6273-6278.

YAO, Y., GAO, B., ZHANG, M., INYANG, M. & ZIMMERMAN, A. R. 2012. Effect of biochar amendment on sorption and leaching of nitrate, ammonium, and phosphate in a sandy soil. *Chemosphere,* 89**,** 1467-1471.

YU, Q., XIA, D., LI, H., KE, L., WANG, Y., WANG, H., ZHENG, Y. & LI, Q. 2016. Effectiveness and mechanisms of ammonium adsorption on Biochars derived from biogas residues. *RSC Advances,* 6**,** 88373-88381.

YUAN, H., LU, T., ZHAO, D., HUANG, H., NORIYUKI, K. & CHEN, Y. 2013. Influence of temperature on product distribution and biochar properties by municipal sludge pyrolysis. *Journal of Material Cycles and Waste Management,* 15**,** 357-361.

YUAN, J.-H., XU, R.-K. & ZHANG, H. 2011. The forms of alkalis in the biochar produced from crop residues at different temperatures. *Bioresource technology,* 102**,** 3488-3497.

YUAN, J. H. & XU, R. K. 2011. The amelioration effects of low temperature biochar generated from nine crop residues on an acidic Ultisol. *Soil Use and Management,* 27**,** 110-115.

ZHANG, M. & GAO, B. 2013. Removal of arsenic, methylene blue, and phosphate by biochar/AlOOH nanocomposite. *Chemical engineering journal,* 226**,** 286-292.

ZHANG, M., GAO, B., VARNOOSFADERANI, S., HEBARD, A., YAO, Y. & INYANG, M. 2013. Preparation and characterization of a novel magnetic biochar for arsenic removal. *Bioresource technology,* 130**,** 457-462.

ZHANG, Y., LI, Z. & MAHMOOD, I. B. 2014. Recovery of NH 4+ by corn cob produced biochars and its potential application as soil conditioner. *Frontiers of Environmental Science & Engineering,* 8**,** 825-834.

ZHENG, H., WANG, Z., DENG, X., ZHAO, J., LUO, Y., NOVAK, J., HERBERT, S. & XING, B. 2013. Characteristics and nutrient values of biochars produced from giant reed at different temperatures. *Bioresource Technology,* 130**,** 463-471.

ZHENG, R.-L., CAI, C., LIANG, J.-H., HUANG, Q., CHEN, Z., HUANG, Y.-Z., ARP, H. P. H. & SUN, G.-X. 2012. The effects of biochars from rice residue on the formation of iron plaque and the accumulation of Cd, Zn, Pb, As in rice (Oryza sativa L.) seedlings. *Chemosphere,* 89**,** 856-862.

ZHOU, Z., YUAN, J. & HU, M. 2015. Adsorption of ammonium from aqueous solutions on environmentally friendly barbecue bamboo charcoal: characteristics and kinetic and thermodynamic studies. *Environmental Progress & Sustainable Energy,* 34**,** 655-662.

ZIELIŃSKA, A. & OLESZCZUK, P. 2015. Evaluation of sewage sludge and slow pyrolyzed sewage sludge-derived biochar for adsorption of phenanthrene and pyrene. *Bioresource technology,* 192**,** 618-626.

ZIMMERMAN, A. R. 2010. Abiotic and microbial oxidation of laboratory-produced black carbon (biochar). *Environmental science & technology,* 44**,** 1295-1301.

ZORNOZA, R., MORENO-BARRIGA, F., ACOSTA, J., MUÑOZ, M. & FAZ, A. 2016. Stability, nutrient availability and hydrophobicity of biochars derived from manure, crop residues, and municipal solid waste for their use as soil amendments. *Chemosphere,* 144**,** 122-130.

Chapter 2. Biochar production and general methodology

2.1 Biochar production

2.1.1 Biomass feedstock collection

The feedstocks used for this study were collected from small processing factories in a suburb of Hanoi city, Vietnam. The wood and bamboo residues were chopped into suitable pieces to fit into the Top-Lid Updraft Drum (TLUD) equipment (see section 2.1.2 below) which was used to produce the biochars. In each case, the biomass was air-dried and then packed into plastic containers and stored in the biomass sample storage unit of the Soils and Fertilizers Research Institute, Hanoi, Vietnam prior to undergoing the pyrolysis process.

2.1.2 Biochar production equipment

The TLUD equipment was designed by Prof. Joseph Stephen (University of New South Wales, Australia) with the outline drawing illustrated in Figure 2.1. The TLUD in this study was made from a metal barrel (208.190 L, height 0.87 m, diameter 0.58 m) with a 20 cm diameter chimney (see Figure 2.2). The construction of the TLUD was conducted by Prof. Joseph Stephen (New South Wales, Australia) and Dang Duc Khoi (Population, Environment and Development Centre, Vietnam). The TLUD technology design and construction were supported by the project "Piloting Pyrolytic Cookstoves and Sustainable Biochar Soil Enrichment in Northern Vietnam Uplands", reference code 03-V-387. The TLUD was designed to allow control of heat and pyrolysis time for reproducible biochar production to facilitate study of the resulting biochar, yet be simple enough to be applied in the field by small farmers in northern Vietnam
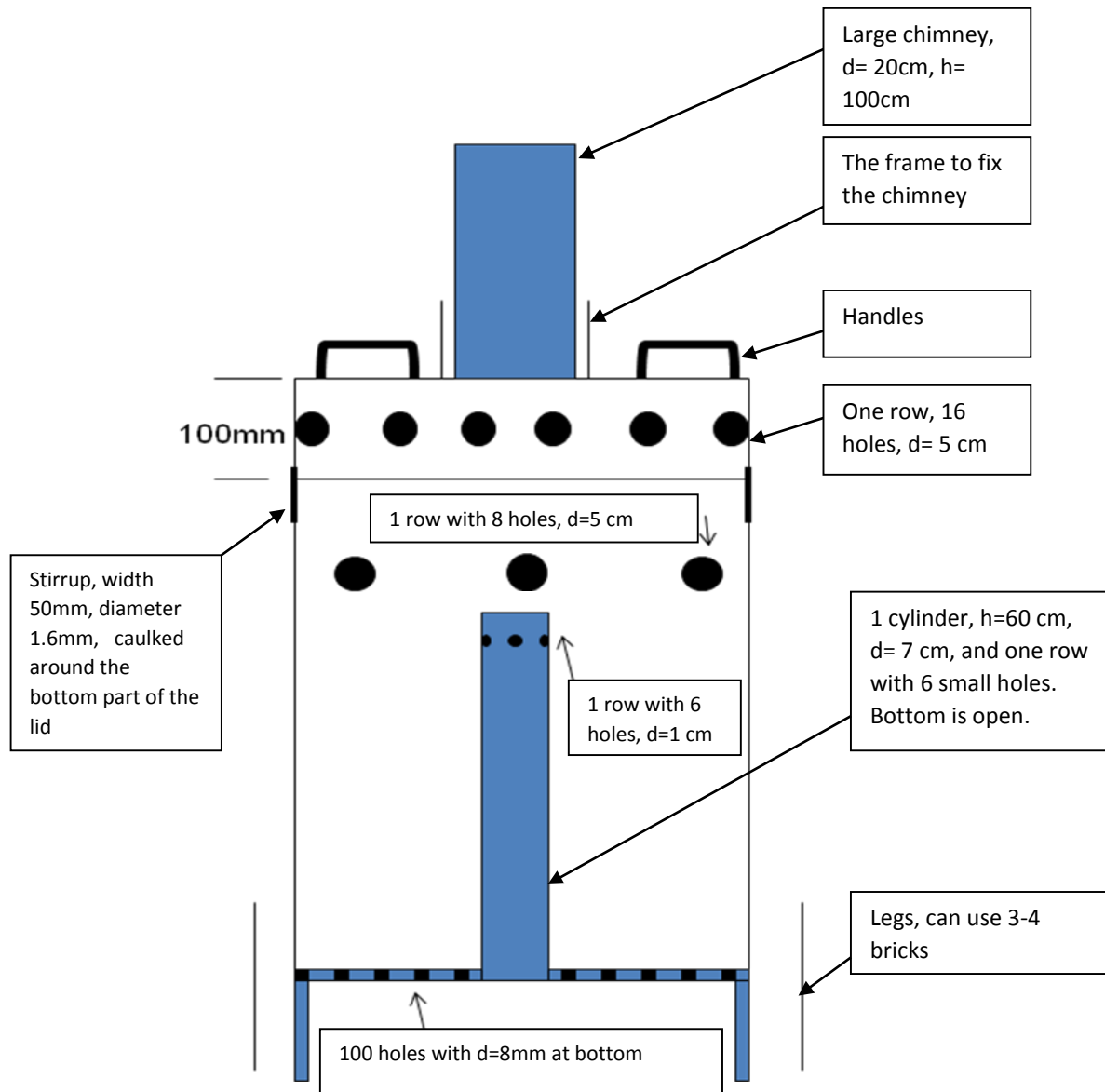
Figure 2.1. Illustrative geometry of the TLUD used for biochar production in this thesis.

This TLUD was initially used to access the applicability of this new technology as a means to develop widespread local biochar production in northern Vietnam, as an alternative to the current practice of burning the rice straw on the fields after harvesting. The equipment was successfully run by the famers to turn rice straw and other residues (rice husk and plant branches) into biochar at household scale, and the biochar was subsequently applied to soil to support rice and vegetable growth as well as being mixed with farm yard manure for composting.

Top of drum with secondary air holes and 20 cm diameter chimney

Bottom of drum with 100 air holes (d=8mm)
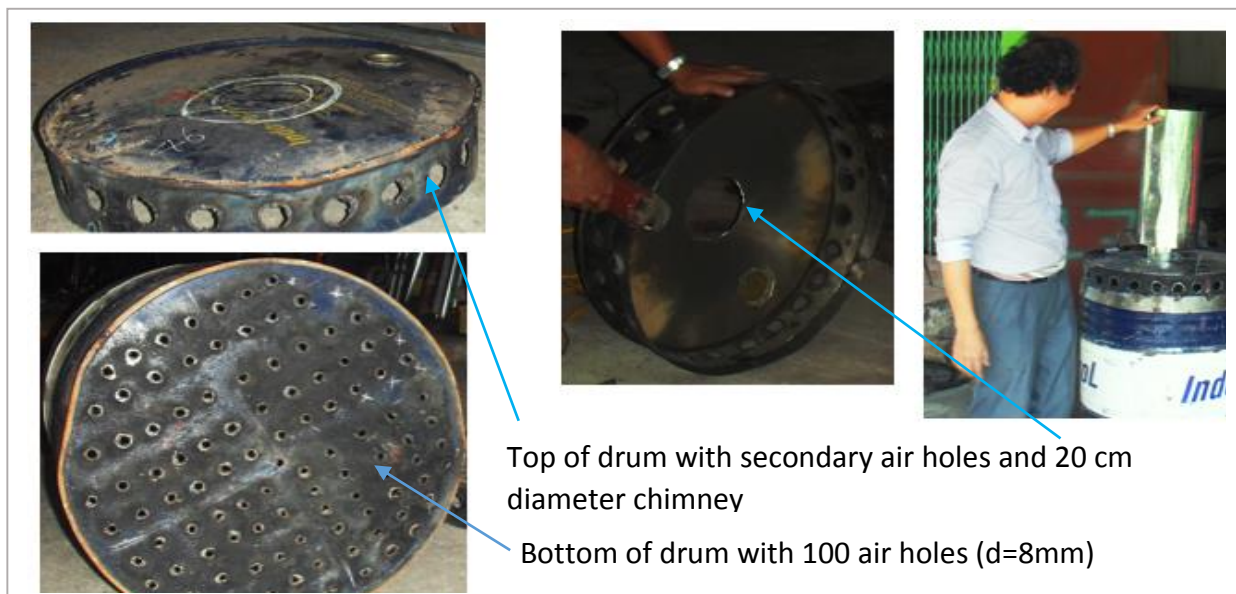
Figure 2.2. The TLUD designed from a metal barrel.

2.1.3 Biochar production

The three different biochars (wood chip, rice husk and bamboo) were produced simultaneously in a TLUD that has been modified to allow the use of various feedstocks in parallel, resulting in biochars produced under identical conditions. The feedstock materials were put into the drum in parallel layers of about 20 cm thickness to ensure uniformity in temperature for each feedstock. The final layer was wood, as wood keeps the flame and heat for a long time, and thus is used to reduce the smoke formed during the pyrolysis process.

A fire was started at the top of the biomass material and then the lid and chimney were placed on top, once a flame was established. The flame burned off, when it moved to the middle of the TLUD. A sandy material was used to cut off the air (see Figure 2.3), which led to burn off of the flame. The total pyrolysis process took approximately 3 hours, then the lid was removed and water was sprayed inside the drum to cool off the biochar. Upon cooling, the layers of biochar can be removed and separated. After that, 1kg of each biochar from wood (WBC), rice husk (RBC), and bamboo (BBC) biomass was stored in air tight plastic bags and shipped to the

University of Birmingham (UoB), UK. Then, the samples were stored in plastic bottles sealed with caps and kept in the UoB lab at room temperature. All studies in this thesis were performed using the same batch of the three biochars.

Figure 2.3. The pyrolysis process for biochar production using the TLUD equipment.

2.2 Experimental methodology

2.2.1 Biochar characterisation

BET surface area:

Surface area was determined by the Brunauer, Emmett, and Teller (BET) method (Brunauer et al., 1938a). The method is based on Langmuir's theory for monolayer molecular adsorption up to multilayer adsorption with the hypotheses that physical adsorption of gas molecules onto a solid occurs in layers, with no interaction between each adsorption layer. A Surface Area Analyzer (model SA 3100) was used for this analysis. Approximately 1g of biochar

(adsorbent), sieved through a 2mm mesh, was loaded into the vessel. Prior to the determination of the adsorption isotherm, outgassing was conducted to remove the physically adsorbed substances from the adsorbent at 250 °C for three hours. After degassing was complete, the sample vessel was weighed to determine exactly the weight of the adsorbent, which was used for BET surface analysis. Then, nitrogen gas (adsorbate) was admitted into the sample vessel at cryogenic temperature by the gas adsorption technique. The pressure in the sample vessels was measured for each volume of the gas added until the adsorbate and adsorbent are in equilibrium. The surface area of the samples was measured by plotting the data as a straight line with y= 1/v[(Po/P)-1] and x=P/Po following equations (equations 1 and 2):

$$\frac{1}{V\left[\left(\frac{P_o}{P}\right)-1\right]} = \frac{C-1}{C}\left(\frac{P}{P_o}\right) + \frac{1}{V_m C} \qquad \text{(equation 1)}$$

where P_0 and P are the equilibrium and the saturation pressure of the adsorbate, V is the volume of adsorbed gas, and V_m is the volume of the monolayer-adsorbed gas, C is the BET constant, and:

$$C = \exp\left(\frac{E_1 - E_l}{RT}\right) \qquad \text{(equation 2)}$$

where E_1 and E_l are the heats of adsorption for the first and higher layers, respectively.

A total surface area $S_{BET,total}$ and a specific surface area S_{BET} were estimated using the following equation (equation 3):

$$S_{BET,\ total} = \frac{V_m N_s}{V} \qquad \text{and} \qquad S_{BET} = \frac{S_{total}}{\alpha} \qquad \text{(equation 3)}$$

 where N is Avogadro's number, s is the adsorption cross section of the adsorbing species, and α is the mass of adsorbent (g).

Proximate analysis:

Moisture, ash, and volatile matter were analysed by the method of the American Society for Testing and Materials Standard –D1762-84 (Standard, 2009). Moisture was measured by the loss of weight when fixed masses of the biochars were heated in the oven at 105°C for 2 hours. Volatile mater was determined by the weight loss as the biochars were heated at 950°C for 6 minutes. Ash was obtained after continuously heating the samples up to 750°C for 6 hours. Fixed carbon was calculated as the remainder after ash, moisture, and volatile matter were measured and subtracted from the total sample dry weight.

Elemental analysis (C, N, H, O):

The biochar samples, sieved through a 2mm mesh, were loaded into a tin capsule and placed into an autosampler drum to remove any atmospheric nitrogen. The sample was then put into a vertical quartz tube and heated at 1,000 °C with constant helium flow and pure oxygen in order to combust (oxidize) the sample completely. The gas mixture containing the three components (C, N, H) from the oxidation step was separated via a chromatographic column and detected by a thermoconductivity detector. The elemental analyzer used was a Carlo Erba EA1110 Model, Italy. The total O was calculated following the ASTM method as follows:

$$O\ (\%w/w) = 100 - ash\ (\%w/w) - C\ (\%w/w) - N\ (\%w/w) - H\ (\%w/w)$$

pH:

The pH of the biochars was determined using the method of Rajkovich et al. (2012). The biochar samples (1g), sieved through a 2mm mesh, were mixed with distilled (DI) water (25 mL) in a 50mL centrifuge tube with a lid. The mixtures were put on an orbital table shaker and shaken for 1.5h to ensure good contact between the water and the biochar's internal surface. Then, the solvent was stirred again using a steel spatula and the pH of the solvent was continuously measured using a calibrated Thermo Orion 3 star pH meter.

Cation Exchange Capacity (CEC):

CEC determination was based on the method of Rajkovich et al. (2012). The exchangeable cations on the surface of the biochar samples were measured by saturating 1.0 g of the biochar, sieved through a 2mm mesh, mixed with 50 mL of 1N CH_3COONH_4 (pH=7) in Falcon centrifuge tube (50mL) with a lid, and the mixture solutions were shaken on a shaker table overnight which ensured that the biochar surfaces were sufficiently wetted. After shaking, the solution was filtered by corning bottle – top vacuum filter system (pore size = 0.22 μm, Sigma – Aldrich) and then an additional 40 mL of the 1M CH_3COONH_4 was added to each, and then immediately extracted by filtration. Next, 60 mL of ethanol (80%) was used to wash all unbound NH_4^+ from around the samples. After that, 50 mL of 1N KCl solution was added to the mixtures to which were kept for 16 h in order to reach equilibrium during which time the NH_4^+ absorbed to the biochar was completely replaced by K^+, then immediately another 40 mL of 1N KCl was added for subsequent replacement. The sample solutions containing NH_4^+ (which had been displaced by K^+ during the extraction steps) were quantified by Ion Chromatography (Dionex DX500). For this, the samples were diluted 25 times, which brought the NH_4^+ concentration into the range of the standards (0, 0.5, 5, 10, 20, 50 mg NH_4^+/L and not more than 100 mg NH_4^+/L as per the requirements of the machine. After that, the sample/standard solution was poured into the 5mL AS40 polyvials to reach two thirds full, and the filter cap was pressed into each vial. The vials were added into the Autosampler (AS40) of the machine for analysis. The analysis process ran 9 samples (3 replicated of wood BC, 3 replicates of rice husk BC, and 3 replicates of bamboo BC) and it took 22 mins per sample.

Scanning electron microscopy (SEM):

Small pieces of the initially produced biochar were selected and further dried at 60 ºC in an oven overnight. Then, 4-5 small pieces (4-5 mm) of each biochar sample were coated with 10

nm Au/Pt film by a Cressington SC7640 sputter coater and kept in a desiccator overnight. A scanning electron microscope (Philips ESEM XL30 FEG model) operating at accelerating voltages of 10-20 kV was used to image the biochars. 5 images of each biochar were taken with dimensions and magnifications as shown in Table 2.1.

Table 2.1. Dimensions and magnifications for the SEM images of the biochars.

Dimension	20 μm	50 μm	100 μm	200 μm	500 μm
Magnification	x 1000	x 500	x 200	x 100	x 50

Functional group analysis:

The FTIR analysis is relied on the vibrations of atoms of molecules. When infrared radiation was passed through the sample (biochar), the infrared spectrum of the sample was recorded. And the fraction of the incident radiator adsorbed at a specific energy was also determined. The peak in the adsorption spectrum at the energy was corresponded to the vibration frequency of the sample molecule. In order to conduct this analysis, approximately 0.5 g of each biochar, sieved through a 2mm mesh and then dried at $60^{o}C$ for 24h, was used for Fourier Transform Infrared (FTIR) analysis. The FTIR spectra of the biochar samples were measured using a Varian 660 spectrometer. The spectra were an average of 32 scans at 4 cm^{-1} resolution from 4000–400 cm^{-1} region.

2.2.2 Assessment for the effectiveness of biochar for fertilizer capture

Methodology:

The adsorption ability of the biochars for fertilizer (represented as NH_4^+-N) was evaluated by adsorption experiments. The experiments included different dosages of biochars (0, 0.25, 0.50, 1.0, and 2.0 g), various initial concentrations of NH_4^+-N (0, 20, 40, 80, 160, 320 mg/L), and different contact times (30, 60, 90, 120, 240, and 480 mins) in order to probe the optimal

conditions. The data of the different initial concentrations experiment were assessed using the Langmuir, Freundlich and Temkin isotherm models to identify whether the NH_4^+-N adsorbed onto the biochars as a monolayer or/and multilayer and whether the adsorption was onto a homogeneous and/or heterogeneous surface. The results of the contact time experiment were evaluated using Pseudo-first order and Pseudo-second order models in order to determine whether the adsorption was controlled by physical adsorption and/or chemical adsorption. In addition, the intraparticle diffusion model was used to investigate the diffusion mechanisms of NH_4^+-N onto the porous biochar particles. All of the models utilised are fully described in Chapter 4.

Set up of adsorption experiments:

- *The biochar dosage experiments:*

The different dosages of biochar (0, 0.25, 0.5, 1.0, 2.0 g) were mixed with NH_4^+-N solution (40 mL, NH_4^+-N = 40 mg/L, pH =7), see Table 2.2 for full details, and then the mixtures were shaken for 24 hours (400 rpm), after which extraction of the biochar absorbed NH_4^+-N was carried out as described below:

Table 2.2. Experimental treatments for assessment of the impact of biochar dose on the effectiveness of adsorption of N-containing fertilizer.

Biochar	Treatments for one replicate			
0g	DI water	DI water	DI water	0
0.25g	0.25gWBC+NH_4^+-N	0.25gRBC+NH_4^+-N	0.25gBBC+NH_4^+-N	Control
0.5g	0.5gWBC+NH_4^+-N	0.5gRBC+NH_4^+-N	0.5gBBC+NH_4^+-N	Control
1.0g	1.0gWBC+NH_4^+-N	1.0gRBC+NH_4^+-N	1.0gBBC+NH_4^+-N	Control
2.0g	2.0gWBC+NH_4^+-N	2.0gRBC+NH_4^+-N	2.0gBBC+NH_4^+-N	Control

Control: WBC + DI water, RBC + DI water, BBC + DI water. Note the volume was 40 mL in all cases. WBC = Wood biochar; RBC = rice husk biochar; BBC = bamboo biochar.

The aim of this experiment was to indentify the suitable dose of biochar for adsorption with the NH_4^+-N concentration in range of 0 -40 mg/L.

- *The NH_4^+-N concentration experiments:*

0.5 g of each biochar was mixed with 40 mL of NH_4^+-N solution with various concentrations (NH_4^+-N = 0, 20, 40, 80, 160, 320 mg/L, pH=7) as per Table 2.3. The mixtures were then shaken for 24 hours (400 rpm), following which extraction of the biochar absorbed NH_4^+-N was carried out as described below.

Table 2.3. Experimental treatments for assessment of the impact of NH_4^+-N concentration on the effectiveness of biochars for adsorption of N-containing fertilizer.

NH_4^+-N	Treatments for one replicate		
0 (control)	WBC+DI water	RBC+DI water	BBC+DI water
20 mg/L	$0.5gWBC+NH_4^+$-N	$0.5gRBC+NH_4^+$-N	$0.5gBBC+NH_4^+$-N
40 mg/L	$0.5gWBC+NH_4^+$-N	$0.5gRBC+NH_4^+$-N	$0.5gBBC+NH_4^+$-N
80 mg/L	$0.5gWBC+NH_4^+$-N	$0.5gRBC+NH_4^+$-N	$0.5gBBC+NH_4^+$-N
160 mg/L	$0.5gWBC+NH_4^+$-N	$0.5gRBC+NH_4^+$-N	$0.5gBBC+NH_4^+$-N
320 mg/L	$0.5gWBC+NH_4^+$-N	$0.5gRBC+NH_4^+$-N	$0.5gBBC+NH_4^+$-N

The aim of this experiment was to create the data for the isotherm models (Langmir, Freundlich, and Temkin models, see chapter 4) which determined the adsorption of NH4+-N onto biochar by mono and/or multi layers on homogenous and/or hecterogenous surface.

- *The contact time experiments:*

0.5g of the biochars was added into 40 mL of NH_4^+-N solution (40 mg/L, pH=7), and then the suspension was shaken at 400 rpm for the desired times (30, 60, 120, 240, and 360 mins) as per Table 2.4, after which extraction of the biochar-absorbed NH_4^+-N was carried out as described below.

Table 2.4. Experimental treatments for assessment of the impact of contact time on the effectiveness of biochars for adsorption of N-containing fertilizer.

Time	Treatments for one replicate			
30 mins	0.5gWBC+NH$_4^+$-N	0.5gRBC+NH$_4^+$-N	0.5gBBC+NH$_4^+$-N	Control
60 mins	0.5gWBC+NH$_4^+$-N	0.5gRBC+NH$_4^+$-N	0.5gBBC+NH$_4^+$-N	Control
120 mins	0.5gWBC+NH$_4^+$-N	0.5gRBC+NH$_4^+$-N	0.5gBBC+NH$_4^+$-N	Control
240 mins	0.5gWBC+NH$_4^+$-N	0.5gRBC+NH$_4^+$-N	0.5gBBC+NH$_4^+$-N	Control
360 mins	0.5gWBC+NH$_4^+$-N	0.5gRBC+NH$_4^+$-N	0.5gBBC+NH$_4^+$-N	Control

Control: WBC + DI water, RBC + DI water, BBC + DI water.

The data of these experiments were fited by Pseudo-first order and Pseudo-second order models (see chapter 4) to identify the adsorption mechanism for NH$_4^+$-N, and intrapartical diffusion model (see chapter 4) to determine the diffusion steps of NH$_4^+$-N onto biochar.

Steps in the adsorption experiments:

The biochars were crushed using a pestle and mortar and sieved (0.5 mm mesh) to obtain a uniform particle size between 500-800 µm as per the method of Hollister et al. (2013). All experiments were conducted in triplicate at room temperature (22 ± 0.5 °C), and the mixtures were shaken using an orbital shaker at 400 rpm for the desired times (e.g 24h or 30 min). Then, the supernatants were filtered through an acrodisc syringe filter (0.20 µm) as shown in Figure 2.4, and analysed for remaining NH$_4^+$-N content.
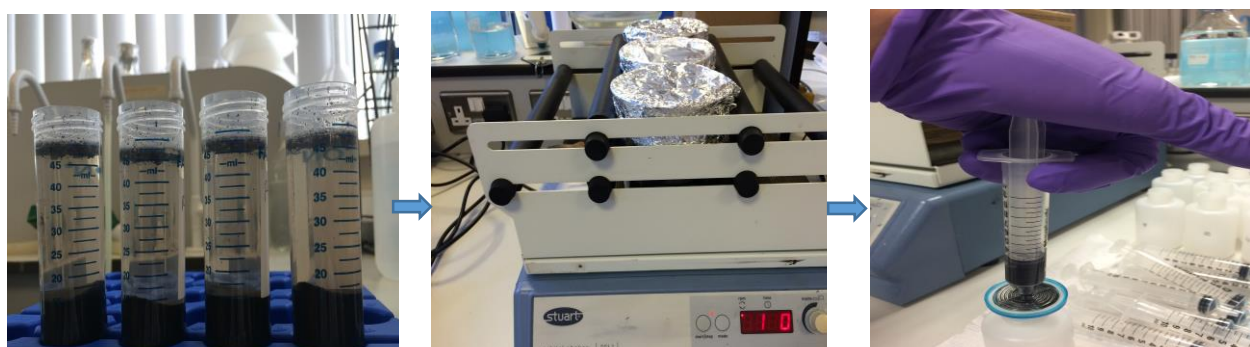
1. NH$_4^+$-N solution added to biochar   2. The mixture being shaken   3. The mixture being filtered

Figure 2.4. Steps in the biochar adsorption experiments.

After filtering, the supernatant was used to determine the concentration of adsorbent (NH_4^+-N) by Ion Chromatography (Dionex DX500). Three blank samples (DI water) were run at the beginning and end of every run. The adsorption capacity (mg/g) and % removal were calculated using equations (2.1) and (2.2), respectively.

$$q = \frac{(C_o - C_x)V}{m} \quad (2.1) \qquad \text{and} \qquad \%removal = \frac{C_o - C_x}{C_o} \times 100 \quad (2.2)$$

where C_o is the initial concentration of adsorbate (40 mg/L of NH_4^+-N or as added), C_x is the concentration of adsorbate at the contact time; V (L) is the volume of the adsorbate; and m is the mass of adsorbent (g).

Method limitation:

The neutral pH (pH = 7) of the NH_4^+-N solution may impact on the the transformation of NH_4^+-N to NH_3 which was emited during the experiment. And the amount of NO_3^- transformed from NH_4^+-N was also measured in this experiment.

2.2.3 Evaluating the adsorption capacity of biochar for heavy metal pollutants

Methodology:

The biochar-adsorbed-heavy metal (Zn^{2+}) concentration was evaluated by various adsorption experiments. The experiments had a similar set-up to those for the NH_4^+-N adsorption including different dosages of biochars, various initial concentrations of Zn^{2+}, and different contact times. The isotherm models (Langmuir and Freundlich), the kinetic models (Pseudo-first order and Pseudo-second order models), and the intraparticle diffusion model were also used to identify the adsorption mechanism of the heavy metal onto the biochars.

Set-up of the adsorption experiments:

-*The biochar dosage experiment:* The different dosages of biochar (0, 0.25, 0.5, 0.75, and 1.0 g) were mixed with Zn^{2+} solution (40 mL, Zn^{2+} = 60 mg/L, pH =5.5) as indicated in Table 2.5, and then the mixture was shaken for 24 hours.

Table 2.5. Treatments used to investigate the effect of biochar dosage on Zn^{2+} adsorption.

Biochar	Treatments for one replicate			
0 g	DI water	DI water	DI water	0
0.25 g	0.25g WBC + Zn^{2+}	0.25g RBC + Zn^{2+}	0.25g BBC + Zn^{2+}	Control
0.5 g	0.5g WBC + Zn^{2+}	0.5g WBC + Zn^{2+}	0.5g WBC + Zn^{2+}	Control
0.75 g	0.75g WBC + Zn^{2+}	0.75g WBC + Zn^{2+}	0.75g WBC + Zn^{2+}	Control
1.0 g	1.0g WBC + Zn^{2+}	1.0g WBC + Zn^{2+}	1.0g WBC + Zn^{2+}	Control

Control: WBC+DI water, RBC+DI water, BBC+DI water.

These experiments aimed to indentify the suitable dose of biochar for adsorption with the Zn^{2+} concentration in range of below 60 mg/L.

-*The Zn^{2+} concentration experiment:* 0.5 g of biochar was mixed with 40 mL of Zn^{2+} solution with various concentrations (Zn^{2+} = 0, 20, 40, 60, 80, 160, 320 mg/L, pH=5.5) as shown in Table 2.6. The mixture was then shaken for 24 hours.

Table 2.6. Experimental treatments to investigate the effect of different NH_4^+-N concentrations.

Zn^{2+} conc.	Treatments for one replicate		
0 mg/L (control)	WBC + DI water	RBC + DI water	BBC + DI water
20 mg/L	0.5g WBC + Zn^{2+}	0.5g WBC + Zn^{2+}	0.5g WBC + Zn^{2+}
40 mg/L	0.5g WBC + Zn^{2+}	0.5g WBC + Zn^{2+}	0.5g WBC + Zn^{2+}
80 mg/L	0.5g WBC + Zn^{2+}	0.5g WBC + Zn^{2+}	0.5g WBC + Zn^{2+}
160 mg/L	0.5g WBC + Zn^{2+}	0.5g WBC + Zn^{2+}	0.5g WBC + Zn^{2+}
320 mg/L	0.5g WBC + Zn^{2+}	0.5g WBC + Zn^{2+}	0.5g WBC + Zn^{2+}

The aim of this experiment was similar to the NH4+-N adsorption as creating the data for the isotherm models (Langmir, Freundlich, and Temkin models, see chapter 5) which determined the adsorption of Zn2+ onto biochar by mono and/or multilayer on homogenous and/or hecterogenous surface.

-*The contact time experiment:* 0.5g of the biochars was added into 40 mL of Zn^{2+} solution (60 mg/L, pH=5.5), and then the mixture was shaken for the desired times (30, 60, 90, 120, 150, 240 mins) as per Table 2.7.

Table 2.7. Treatments for the contact time experiment.

Time	Treatments for one replicate			
30 mins	0.5g WBC + Zn^{2+}	0.5g WBC + Zn^{2+}	0.5g WBC + Zn^{2+}	Control
60 mins	0.5g WBC + Zn^{2+}	0.5g WBC + Zn^{2+}	0.5g WBC + Zn^{2+}	Control
90 mins	0.5g WBC + Zn^{2+}	0.5g WBC + Zn^{2+}	0.5g WBC + Zn^{2+}	Control
120 mins	0.5g WBC + Zn^{2+}	0.5g WBC + Zn^{2+}	0.5g WBC + Zn^{2+}	Control
150 mins	0.5g WBC + Zn^{2+}	0.5g WBC + Zn^{2+}	0.5g WBC + Zn^{2+}	Control
240 mins	0.5g WBC + Zn^{2+}	0.5g WBC + Zn^{2+}	0.5g WBC + Zn^{2+}	Control

Control: WBC + DI water, RBC + DI water, BBC + DI water.

Alike the NH_4^+-N experiments, the data of these experiments were used to fit the kinetic models (Pseudo-first order and Pseudo-second order models, see chapter 5) to identify the adsorption mechanism of biochar for Zn^{2+}. The data were also used for the intrapartical diffusion model (see chapter 5) to determine the diffusion steps of Zn^{2+} onto biochar.

Carrying out the adsorption experiments:

All steps were conducted as described for the NH_4^+-N experiments. After the filtration step, the Zn^{2+} concentration of the filtered solution was measured by Flame Atomic Adsorption Spectrometry (Perkin Elmer AAnalyst 300 model) with various Zn^{2+} standards (0, 0.25, 0.5,1.0 and 2 ppm). All experiments were conducted in three replications. The adsorption capacity

and % removal of Zn^{2+} by the biochars were calculated as per the equations presented for the NH_4^+-N experiments (see section 2.2.2).

2.2.4 Pollutant removal from landfill leachate by biochar

Methodology:

In this study, the adsorption capacity of the three biochars was assessed through experiments with real landfill leachate containing complex pollutants rather than the artificial solutions described above with single adsorbates like or Zn^{2+}. The main objectives were to evaluate how the NH_4^+-N adsorption onto the biochars was affected by the competition from other adsorbates (Ca^{2+}, Mg^+, K^+ and Na^+) in the leachate, and to elucidate which cations on the surface of the biochar participated in the cation exchange to facilitate the NH_4^+-N adsorption. The adsorption capacity and % removal were evaluated via equilibrium and column experiments.

Set up of the equilibrium adsorption experiment:

The equilibrium adsorption experiments of the single biochar and mixed biochars using the leachate were similar to the equilibrium experiments with NH_4^+-N and Zn^{2+} model solutions**.** 0.5g biochar was mixed with 40 mL of the leachate, and the mixture was shaken on the shaker for 24h at room temperature (22 ± 0.5 ^oC) as shown in Table 2.8. After that, the solvent was filtered through an acrodisc syringe filter (0.20μm). The filtrate was diluted 50 – 75 times with DI water, to produce solutions whose analyte concentrations were in the range of the standard curve (0.5, 1, 5, 10, 20, 50 mg/L of NH_4^+-N, Ca^{2+}, Mg^{2+}, K^+, and Na^+) before being analyzed by Ion Chromatography machine (Dionex DX500 model).

Table 2.8. Treatments for the leachate adsorption by biochar.

Treatments for single biochar	Treatments for mixed biochars
1. Landfill leachate	4. Wood BC + rice husk BC + leachate
2. Wood BC + leachate	5. Rice husk BC + bamboo BC + leachate
3. Rice husk BC + leachate	6. Bamboo BC + wood BC + leachate
4. Bamboo BC + leachate	7. Wood + rice husk + bamboo BCs + leachate

Set up of the biochar column experiment*:*

In this study, mixed biochar (wood BC + rice husk BC + bamboo BC in a 1:1:1 ratio) was packed into glass chromatography columns (30.48 cm length, 2.54 cm inside diameter). After that, the mixture was washed with DI water to remove any impurities before the leachate was flowed through.

| Equipment preparation | The dirty being removed | The leachate being filtered |

Figure 2.5. Conducting the biochar filter for the landfill leachate.

Then, 750 mL of the leachate was passed through the column with a flow rate of 1mL/min. The process was periodically stopped at the end of the day, and the solution after passing the column each day was kept in the fridge for use in the process the next day. The process was undergone for four days, which means the initial leachate was passed through the column four times. The samples of each day were collected and diluted to 50 – 75 times with DI water to ensure the analyte concentrations in the filtrates fell within the range of the standards

(calibration curve). Then, the diluted samples were analyzed for the cations (NH_4^+-N, Ca^{2+}, Mg^{2+}, K^+, and Na^+) by Ion Chromatography machine(Dionex DX500 model).

2.2.5 Statistic analysis

Excell 2013 and IPM SPSS statistic 22 sorfwares were used for statistic analysis for the data of the experiments of this thesis.

References

BRUNAUER, S., EMMETT, P. H. & TELLER, E. 1938. Adsorption of gases in multimolecular layers. *Journal of the American chemical society,* 60**,** 309-319.

HOLLISTER, C. C., BISOGNI, J. J. & LEHMANN, J. 2013. Ammonium, nitrate, and phosphate sorption to and solute leaching from biochars prepared from corn stover (Zea mays L.) and oak wood (Quercus spp.). *Journal of environmental quality,* 42**,** 137-144.

RAJKOVICH, S., ENDERS, A., HANLEY, K., HYLAND, C., ZIMMERMAN, A. R. & LEHMANN, J. 2012. Corn growth and nitrogen nutrition after additions of biochars with varying properties to a temperate soil. *Biology and Fertility of Soils,* 48**,** 271-284.

STANDARD, A. 2009. Standard test method for chemical analysis of wood charcoal. *American Society for Testing and Materials, Conshohocken, PA*.

Chapter 3. Physicochemical Characterization of Biomass Residue–Derived Biochars in Vietnam

Nguyen Van Hien[a,b], Eugenia Valsami-Jones[a], Nguyen Cong Vinh[b] , Tong Thi Phu[b], Nguyen Thi Thanh Tam[b], Iseult Lynch[a*]

[a] School of Geography, Earth and Environmental Sciences, University of Birmingham, Edgbaston, B15 2TT, UK

[b] Department of Land Use, Soils and Fertilizers Research Institute, Hanoi, Vietnam

[*] Corresponding author: i.lynch@bham.ac.uk

Abstract

This study compares the physico-chemical characteristics of three different types of biochar produced from biomass residues in Vietnam as a basis for optimising their application in water purification and soil fertilisation. Wood biochar (WBC), rice husk biochar (RBC), and bamboo biochar (BBC) were produced under limited oxygen conditions using equipment available locally in Vietnam, known as a Top-Lid Updraft Drum (TLUD). The resulting biochars were characterised using a suite of state-of-the-art methods to understand their morphology, surface chemistry and cation exchange capacity. Surface areas (measured by BET) for WBC and BBC were 479.34 m^2/g and 434.53 m^2/g, respectively, significantly higher than that of RBC which was only 3.29 m^2/g. The morphology as shown in SEM images corresponds with the BET surface area, showing a smooth surface for RBC, a hollow surface for BBC, and a rough surface for WBC. All three biochars produced alkaline, with pH values around 10, and all have high carbon contents (47.95 - 82.1 %). Cation exchange capacity (CEC) was significantly different ($p < 0.05$) among the biochars, being 26.70 cmol/kg for RBC, 20.7 cmol/kg for BBC, and 13.53 cmol/kg for WBC, which relates to the cations (Ca, Mg, K) and functional groups with negative charge (carboxyl, hydroxyl) present on the biochar surfaces. The highest contents of Ca, Mg and K in rice husk BC may explain its highest CEC values. Thus, although

the biochars were produced by the same method, the various feedstocks lead to quite different physico-chemical properties.   Ongoing work is linking these physico-chemical properties to the biochar efficiencies in terms of ammonia capture capacities for use as fertilisers, and for adsorption of heavy metals (Zn, Cu) or water filtration, in order to design optimal biochar properties for specific applications.

Key words: physico-chemical characteristics, biochar, BET surface area, SEM, total carbon, CEC, FTIR, feedstock

1. Introduction

Biochar is the carbonized product gained by pyrolysis of biomass under restricted or absent oxygen conditions (Mukherjee and Zimmerman, 2013, Paethanom and Yoshikawa, 2012), but without an activation step and thus differs from so-called activated carbon (Qiu et al., 2009). The justification for carbonization through pyrolysis is to avoid the negative influences on human health and the environment that result from direct (in field) burning of biomass residues which releases carbon dioxide, one of the most important greenhouse gases (Al-Wabel et al., 2013).   Biomass-derived biochar is formed via a complex process (Kim et al., 2012), but the reaction mechanism of biomass pyrolysis can be described as occurring mainly via three steps (Demirbas, 2004) as follows:

Stage 1: Biomass $\xrightarrow{\text{Heat}}$ Moisture + Dry residues

Stage 2: Dry residues $\xrightarrow{\text{Heat}}$ (Volatile and Gases) + Pre-biochar

Stage 3: Pre-biochar $\xrightarrow{\text{Heat}}$ (Volatile and Gases) + Biochar

The first step is loss of moisture from the biomass, which becomes dry feedstock by heating. Then pre-biochar and volatile compounds are formed. In the last step, chemical compounds in the biosolid rearrange and form a carbon-rich solid product known as biochar. The volatiles, are either condensable such as bio-oil, or noncondensable gases (Duku et al., 2011) known as syngas, including hydrogen (50%), carbon dioxides (30%), nitrogen (5%), methane (5%), and others (Sohi et al., 2009). As a result of its aromatic structure (Schmidt and Noack, 2000) biochar can be recalcitrant to microbial decomposition and mineralization (Zheng et al., 2010) which leads to its persistence in soil for hundreds of years (Zheng et al., 2010). In fact, biochar found in dark soil known as 'Terra Preta soil' in Amazônia was reported as being about 500-2,500 years old (Neves et al., 2003) while biochar found in ocean sediment was estimated to date from 2,400 to 13,000 years ago (Masiello and Druffel, 1998).

The benefits of biochar were demonstrated by several previous research efforts. For instance, wood biochar applied into a Colombian savanna Oxisol increased available Ca and Mg concentrations and pH, and reduced toxicity of Al (Major et al., 2010). In addition, biochar improved soil structure (Jones et al., 2011) created a carbon sink in soil (Sohi et al., 2010) and reduced CH_4 emissions (Liu, 2011). Hale (2013) reported that biochar can absorb NH_4^+-N via cation exchange, thereby reducing the leaching of nitrogen fertilizer from soil (Huang et al., 2014). Interestingly, biochar can be recalcitrant to microbial attack (Lehmann and Rondon, 2006) while compost or plant biomass are rapidly decomposed to greenhouse gases (CH_4, CO_2), especially in tropical regions (Jenkinson and Ayanaba, 1977). Thus, the application of biochar has a positive effect on soil fertility, particularly in tropical regions (Joseph and Lehmann, 2009). However, several studies have found no or negative influences of biochar application. For example, in calcareous soils, biochar did not improve pH or available P and cations (Lentz and Ippolito, 2012). Additionally, greenhouse gas emission (CO_2) was increased

for an Inceptisol type soil to which wood biochar produced at 350°C was applied (Ameloot et al., 2013). These disadvantages may relate to biomass type and conditions of biochar production, and soil type.

Pyrolysis conditions impact on the physicochemical characteristics of the biochar (Angın, 2013, Abo-Farha et al., 2009, Novak et al., 2009). For example, Méndez et al. (2013) observed that the ash content, pH, and BET surface area increased, while CEC, volatile matter and microspore area declined in biochar produced from sewage sludge at 600 °C compared to biochar prepared at 400 °C. On the other hand, a dramatic increase from 0.007 m^2/g to 274 m^2/g in micropore (defined as being < 2 nm) area was observed for biochars derived from Cottonseed hull when the pyrolysis temperature increased from 650 °C to 800 °C (Uchimiya et al., 2011). Decreases in total N, organic carbon (OC), and CEC were also found in poultry litter biochar when the pyrolysis temperature rose from 300 °C to 600 °C, while the opposite trend was seen for pH and BET surface area (Song and Guo, 2012). Similar trends also were observed by (Mukherjee et al., 2011) and Chen et al. (2008) who explained that at low temperature (<300 °C) compounds containing -OH, aliphatic C-O and ester C=O groups were removed from the outer surface, while volatile matter shielding or connecting to aromatic cores were destroyed or partly emitted at higher temperatures (>300 °C). Thus, micropores dominating the biochar surface are filled by volatile compounds, which are emitted during pyrolysis as the temperature increases (Mukherjee et al., 2011) and dramatically enlarge the surface area of the resulting biochar (Cheng et al., 2008).

The biomass materials used for biochar production also have a major influence on the resulting biochar properties (Mukome et al., 2013). For instance, wood and grass biomass-derived biochar normally contain low nutrient elements, in part due to emissions of nitrogen

during the pyrolysis process, so the resulting biochar has much lower N content than fertilizers (Cantrell et al., 2012). Song and Guo (2012) reported that biochars formed from waste wheat straw and tree leaves contained higher organic carbon (OC) content (64% - 73.9%) than that of poultry litter-derived biochar (36.10%) produced at the same temperature (400 $^{\circ}$C). In addition, the different original biomass affects the morphology of the resulting biochar; for instance, the exoskeleton of tracheids (elongated cells in the xylem of vascular plants that serve in the transport of water and mineral salts) was an important contributor to structure for wood biochar, while a heterogeneous structure resulted from chicken manure biochar (Joseph et al., 2010). The CEC and pH of poultry litter-produced biochar were observed to be higher than those of pine chip biochar and peanut hull biochar (Gaskin et al., 2008).

The properties of biochar are not static once formed: the environmental conditions following biochar application were also found to affect biochar properties (Nguyen and Lehmann, 2009). Surface oxidation of biochar particles was observed to occur when the biochar was applied into soil (Liang et al., 2006) resulting in an increase of between 10% and 16% in surface negative charge (carboxyl groups) of biochars (350-600 $^{\circ}$C) derived from corn stover residues and oak wood when applied under alternative water regimes (i.e. wet and dry conditions) (Nguyen and Lehmann, 2009). However, aliphatic groups (CH_2, CH_3) were decreased by 18-42% in the wet conditions, and by 4-30% in the dry conditions (Nguyen and Lehmann, 2009). Cheng et al. (2006) reported that abiotic oxidation governed the increase of negative surface charge and CEC of wood biochar (black locust) in soil, rather than biotic oxidation (microbial activities). Surface oxidation increased over time, progressing from phenolic groups to carboxylic groups, which were the main (cation) adsorption sites of the biochar (Cheng et al., 2006). Yang et al. (2016) reported that the content of C=O and COOH groups of walnut shell biochar incubated with $FeCl_3$ or kaolinite was enhanced 2.0 and 2.5 times, respectively,

compared with the fresh biochar. The surface groups of the fresh biochars were negatively charged and so adsorbed only cations (NH_4^+) via CEC (Mukherjee et al., 2011). However, the O-containing groups of biochar could react with soil cations such as Al^{3+}, Fe^{3+}/Fe^{2+}, Ca^{2+}, Mg^{2+} to form organometallic complexes (Yang et al., 2016) and therefore could adsorb nutrient anions such as NO_3^-, PO_4^{3-} (Mukherjee et al., 2011).

Biochar application has thus been shown to have positive effects on the physico-chemical properties of soil. However, as different biomass and pyrolysis conditions give various biochar characteristics, which have different effects on soil properties and plants, it is not always clear what the optimal biomass composition should be for specific local applications. Vietnam, for example, has tropical weather leading to highly decomposed soil organic matter, and has high rain annual fall causing severe erosion and leaching. Currently, the agricultural and forestry residues in several regions in Vietnam are burnt or left to decompose in the fields, which results in carbon dioxide release from the biomass into the atmosphere. Therefore, turning the biomass into biochar will bring more benefits for soil enrichment and reduce the environmental impact of agriculture. Hence, the objectives of this study were to identify the physicochemical properties of three different biochars formed from acacia wood chip, rice husk, and bamboo by the Top-Lid Updraft Drum (TLUD) technology, a biomass production method commonly used in this region.

2. Materials and methods

2.1 Biochar production

• Materials for biochar production:

The biomass residues used for biochar production in this study were collected from small processing factories in a suburb of Hanoi city. The feedstocks include acacia wood chip, rice husk and bamboo. The wood and bamboo were chopped into suitable pieces to fit into the Top-Lid Updraft Drum equipment and air-dried before the pyrolysis process. According to Nasser and Aref (2014) the chemical composition of acacia wood is 48% of cellulose, 22% hemicelluloses, and 30% lignin, while rice husk contains 28-38% cellulose, 9-20% lignin, and 18.8-22.3% SiO_2.(Guo et al., 2002) In comparison, bamboo is 47.5% cellulose, 15.35% hemicelluloses, 26.25% lignin, and 0.7% silica.(Hernandez-Mena et al., 2014)

• Technology of biochar production:

The TLUD technology was inherited from the project 'Piloting Pyrolytic Cookstoves and Sustainable Biochar Soil Enrichment in Northern Vietnam Uplands' (Grant Agreement No 3-V-048). It consisted of a barrel (208.190 L, height 0.87 m, diameter 0.58 m) with a chimney, which is described in detail in Figure 1. The three different biochars were produced simultaneously in a TLUD that has been modified to allow the use of various feedstocks in parallel, resulting in biochars produced under identical conditions. The materials are put into the drum in parallel layers of about 20 cm thickness to ensure uniformity in temperature for each feedstock. The final layer is wood, as wood keeps the flame for a long time, and thus is used to reduce the smoke formed during the pyrolysis process. A fire is started at the top of the material and then the lid and chimney are placed on top, once a flame is established. After the biochar starts to form, small amounts of water are injected inside the drum via the 16 hole (d = 5 cm) and 8 hole (d = 5 cm) rows in order to maintain a temperature between 400 – 550

°C. The total process takes about 3 hours, then the lid is removed and water is sprayed inside

the drum to extinguish the fire and cool the biochar. Upon cooling, the layers of biochar can

be removed and separated. After that, 1kg of each biochar from wood (WBC), rice husk (RBC),

and bamboo (BBC) biomass was stored in air tight plastic bags and shipped to the University

of Birmingham, UK. Finally, the samples were kept at room temperature in the lab for analysis.

The samples were characterized through BET surface area, Scanning Electron Microscopy

(SEM), Fourier transform infrared spectroscopy (FTIR), elemental and proximate analysis, and

CEC, with reference to the COST Action guidelines for standardisation of biochar analysis

(Bachmann et al., 2016) where appropriate.
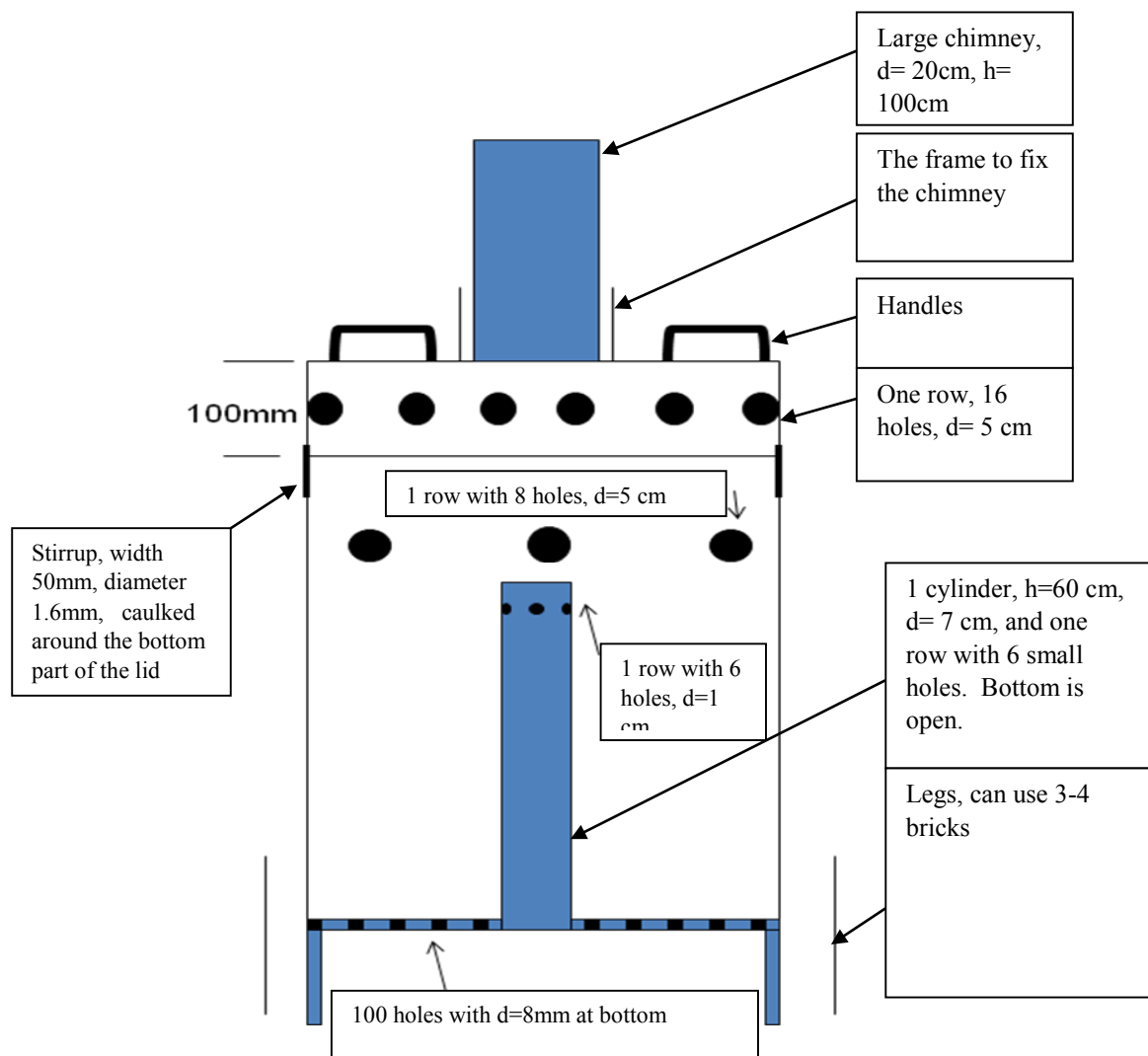
Figure 1: Modified TLUD for biochar production.

2.2 Analysis methods

pH$_{H2O}$ analysis:

Biochars, sieved through a 2mm mesh, were analyzed for pH using the method of (Rajkovich et al., 2012). Briefly, distilled water, with ratio of biochar to DI water of 1:25 (w/v), was added to the biochar and the mixture was shaken for 1.5h to ensure good contact between the water and the biochar's internal surface. Then, the solvent was stirred again by steel spatula and pH of the solvent was continuously measured using a Thermo Orion 3 star pH meter.

Cation exchange capacity (CEC):

CEC was determined using the method described in (Rajkovich et al., 2012). In brief, 1.0 g of the biochar sieved through a 2mm mesh was saturated with 50 mL of 1N CH_3COONH_4 (pH=7) and the mixture solution was shaken on a shaker table overnight which ensured that the biochar surfaces were sufficiently wetted. After shaking, the solution was filtered by vacuum filter (0.22 μm) and then an additional 40 mL of the 1N CH_3COONH_4 was added and then immediately extracted by the filtration. Next, 60 ml of ethanol (80%) was used to wash all unbound NH_4^+ from around the samples. The biochar samples were placed into a glass beaker and 50 mL of 1N KCl was added. The solution was kept for 16 h in order to reach equilibrium during which time the NH_4^+ absorbed to the biochar was completely replaced by K^+, then immediately another 40 mL of 1N KCl was added for a subsequent extraction. The solutions containing NH_4^+ which replaced by K^+ were quantified by Ion Chromatography (Dionex DX500) using 6 standards (0, 0.5, 1.0, 5.0, 10.0, 20, 50 mg/L of NH_4^+).

Scanning electron microscopy (SEM):

Small pieces of initial biochar were selected and further dried at 60 $^{\circ}$C in an oven overnight. Then, 4-5 small pieces of each biochar sample were coated with 10 nm Au/Pt film by a Cressington SC7640 sputter coater and kept in a desiccator overnight. A scanning electron

microscope (Philips ESEM XL30 FEG model) operating at accelerating voltages of 10-20 kV was used to image the biochars.

BET surface area:

Surface area was determined by the Brunauer, Emmett, and Teller (BET) method (1983). The method is based on Langmuir's theory for monolayer molecular adsorption to multilayer adsorption with the hypotheses that physical adsorption of gas molecules onto a solid occurs in layers, with no interaction between each adsorption layer. A Surface Area Analyzer (model SA 3100) was used for this analysis. Approximately 1g of biochar (adsorbent), sieved through a 2mm mesh, was loaded into the vessel. Prior to the determination of the adsorption isotherm, outgassing was conducted to remove the physically adsorbed substances from the adsorbent at 250 °C for three hours. After degassing was complete, the sample vessel was weighed to determine exactly the weight of the adsorbent, which was used for BET surface analysis. Then, a known volume of nitrogen gas (adsorbate) was admitted into the sample vessel at cryogenic temperature by the gas adsorption technique. The pressure in the sample vessels was measured for each volume of the gas added until the adsorbate and adsorbent are in equilibrium. The surface area of the samples was measured by plotting the data as straight line with y= 1/v[(Po/P)-1] and x=P/Po following equations (equations 1 and 2):(Brunauer et al., 1938)

$$\frac{1}{V[(\frac{P_o}{P})-1]} = \frac{C-1}{C}\left(\frac{P}{P_o}\right) + \frac{1}{V_m C} \qquad \text{(equation 1)}$$

where P_0 and P are the equilibrium and the saturation pressure of the adsorbate, V is the volume of adsorbed gas, and V_m is the volume of the monolayer-adsorbed gas, C is BET constant, and:

$$C = \exp\left(\frac{E_1 - E_l}{RT}\right) \qquad \text{(equation 2)}$$

where E_1 and E_l are the heats of adsorption for the first and higher layers, respectively.

A total surface area $S_{BET,total}$ and a specific surface area S_{BET} were estimated using the following equation (equation 3):

$$S_{BET,total} = \frac{V_m N_s}{V} \quad \text{and} \quad S_{BET} = \frac{S_{total}}{\alpha} \quad \text{(equation 3)}$$

where N is Avogadro's number, s is the adsorption cross section of the adsorbing species, α is the mass of adsorbent (g).

Proximate analysis:

Moisture, ash, and volatile matter were analysed by the method of the American Society for Testing and Materials Standard (ASTM standard –D1762-84). Approximately 1g of biochar, sieved through a 2mm mesh, was added into a porcelain crucible and the moisture content was calculated from the loss in weight at 105 °C in the oven for 2h. After that, the crucibles used for moisture measurement were heated to 950 °C in a muffle furnace for a period of 6 minutes to measure volatile mater. Ash content was then calculated from the loss in weight of the samples contained in the crucibles (used for volatile matter) following heating at 750 °C for 6h.

Elemental analysis (C, N, H):

5mg of biochar, sieved through a 2mm mesh, was loaded into a tin capsule and placed into an autosampler drum to remove any atmospheric nitrogen. The sample was then put into a vertical quartz tube and heated at 1,000 °C with constant helium flow and pure oxygen in order to combust (oxidize) the sample completely. The gas mixture containing the three components (C, N, H) from the oxidation step was separated via a chromatographic column and detected by a thermoconductivity detector. The elemental analyzer used was a Carlo Erba EA1110 Model, Italy. The total O was calculated following the ASTM method as follows:

O (%w/w) = 100 – ash (%w/w) – C (%w/w) – N (%w/w) – H (%w/w)   (equation 4).

Total P, Ca, Mg, and K:

Total P, Ca, Mg, K were measured after biochar (0.5g) was put into a porcelain crucible heated to 500°C over 2 h, and held at 500 °C for 8 h for dry combustion. The sample was then moved into the combustion vessel. Next, 5 mL HNO_3 was added to each vessel and the samples were digested by a heating block at 120°C until dryness (5h). The tubes were allowed to cool before adding 1.0 mL HNO_3 and 4.0 mL H_2O_2. After that, samples were preheated to 120°C to dryness, and then dissolved with 1.43 mL HNO_3, made up with 18.57 mL deionized water to achieve 5% acid concentration, sonicated for 10 min, and filtered. The total P was measured by spectroscopy using a UV-Vis 2000 model with quartz cuvette at λ=725 nm with 6 standards (0, 0.02, 0.04, 0.06, 0.08, 0.1 mg P_2O_5/100mL) to establish the standard curve. Ca and Mg were titrated by EDTA (0.01 M) with murexide (the ammonium salt of purpuric acid) indicator for Ca and Eriochrome Black T for Mg, and K was analyzed by Flame Atomic Adsorption Spectroscopy (FAAS 2900 model) with 4 standards (0.25, 0.5, 1.0, and 2.0 mg K/L).

Surface functional group analysis (Fourier-transform infrared -FTIR) spectroscopy):

Approximately 0.5 g of biochar, sieved through a 2mm mesh and dried at 60°C, was used for FTIR analysis. The FTIR spectra of the biochar were measured using a Varian 660 spectrometer. The spectra were an average of 32 scans at 4 cm^{-1} resolution from 4000–400 cm^{-1} region.

Statistical analysis:

Microsoft office excel 2007 was used for determination of standard deviation (SD) and IBM SPSS statistic 22 software was used for ANOVA analysis.

3. Results and discussion

3.1 Elemental components

The biochar samples were analyzed in duplicate for C, H, N, P, K, Ca, and Mg, whereas O was calculated using equation 4 shown in section 2.2 above. The data are presented as mean ± SD

(standard deviation) in Table 1. Results indicate that all three biochars had high carbon content, and that there was a difference (p<0.05) among the biochars. Wood BC had the highest value (82.10 ± 0.21 %C), while rice husk BC was lowest with only 47.82 ± 0.18 %C. A high carbon concentration is an important property of biochar for soil enrichment. Nitrogen (N) accounted for a very low proportion in the ultimate analysis, with similar values (p>0.05) for all three biochar samples with N in the range 0.62 ± 0.06 - 0.72 ± 0.02% N in the order rice husk BC < wood BC < bamboo BC. Hydrogen content was also low and similar across the three biochars, ranging from 2.07 ± 0.04) % to 2.33 (± 0.01%) H, with wood BC < rice husk BC = bamboo BC. Unlike the carbon content, the oxygen content of rice husk and bamboo were similar (p>0.05), fluctuating between 8.25 ± 0.28% and 8.86 ± 0.02%, whereas wood biochar oxygen was 12.93 ± 0.16%. There was no statistical difference of phosphorous (P_2O_5) content (p>0.05) among the biochars nor for potassium (K) or magnesium (Mg), although the absolute values varied. However, the Ca content of rice husk BC (2.37 ± 0.18 %) was significantly different (p<0.05) in comparison with those of wood BC (0.65 ± 0.06%) and bamboo BC (0.57 ± 0.01%)

Table 1. Elemental composition of the three different biochar samples.

Parameters	Wood BC	Rice husk BC	Bamboo BC
C, %	82.10 ±0.21 c	47.82 ±0.18 a	80.27 ±0.08 b
H, %	2.33 ±0.01 a	2.07 ±0.04 a	2.07 ±0.04 a
N, %	0.71 ±0.05 a	0.62 ±0.06 a	0.72 ±0.02 a
O, %	12.93 ±0.16 a	8.25 ±0.28 b	8.86 ±0.02 b
P,%	0.22 ±0.21 a	0.22 ±0.20 a	0.88 ±0.13 a
K,%	1.58 ±0.62 a	1.89 ±0.63 a	0.47 ±0.13 a
Ca,%	0.65 ±0.06 a	2.37 ±0.18 b	0.57 ±0.01 a
Mg,%	0.21 ±0.05 a	0.26 ±0.10 a	0.14 ±0.03 a

The biochars produced from plant residues normally contain a low portion of nutrient elements (Cantrell et al., 2012). The loss of H and N via volatile matter is related to the degree of carbonization during pyrolysis, explaining in part the low H and N values (Bagreev et al., 2001). Cantrell et al. (2012) reported that H and N contents in initial biomass were volatised 50-85% and 21.4%-77.5%, respectively, when pyrolysis temperatures increased from 350 °C to 700 °C. However, N content can be preserved in biochar due to the transformation of the amine functionality in the original feedstocks into pyridine-like compounds during pyrolysis (Bagreev et al., 2001). The very low N contents determined here (Table 1) suggests that most were volatilised, and that low pyridine functionality can be expected from the FTIR analysis.

3.2 Proximate analysis, pH and CEC of the biochar samples

Samples were run in duplicate for moisture, volatile mater, and ash proportions, and in triplicate for pH and CEC. The results are shown in Table 2 and are presented as mean ± SD. The data indicate that the biochars were all alkaline with pH values ranging from 9.51 (± 0.02) to 10.11 (± 0.04) in the order Rice BC < Bamboo BC < Wood BC. Several previous studies proved that the alkalinity of biochar is attributed to the presence of alkaline metals such as Ca, Mg, and K (Song and Guo, 2012, Gundale and DeLuca, 2006) carbonate ($CaCO_3$ and $MgCO_3$), and organic functional groups (Yuan et al., 2011). This is consistent with the data from Table 1, where the Rice husk BC had the highest values of Ca, Mg and K, and the Bamboo BC having the lowest concentrations of each. The pH is known as a pivotal parameter of soils, which impacts on available nutrients and plant growth (Lee et al., 2013). Thus, the high pH of these biochars suggests their suitability for use as soil amendments to ameliorate acidic soils (Lee et al., 2013) which may also contain aluminium, iron and manganese which can be toxic to crops and cause nutrient (P, Mo, Mg, Ca) deficiencies in several soils (Yuan et al., 2011). For example, Fe^{2+} is toxic to rice when soil pH<5.0 due to excessive Fe^{2+} uptake. A high Fe^{2+} content

in soil can also lead to poor root oxidation due to accumulation in the rhizosphere of H_2S and FeS which inhibit respiration (Yuan et al., 2011).

The ash content of the biochars, as determined by the ASTM method, shows significant differences among the various biochars ($p < 0.05$). The largest proportion of ash was found in the rice husk BC, with 41.24 (± 0.49) % ash, while the lowest was observed for wood BC (1.93 ± 0.03 %). Rice husk BC has been reported previously to have a relatively high ash content, e.g., 54.0% (Shen et al., 2014) which is due to the biomass having lower abundance of lignin, e.g., 9-20% (Guo et al., 2002) as compared to woody residues, e.g., 20-40% (Sharma et al., 2004). In addition, biochar with higher ash contents was found to correspond to lower values of fixed carbon, as reported in several previous studies.e.g.(Yargicoglu et al., 2015). Interestingly, although there were significant differences ($p < 0.05$) in both the ash and fixed carbon (rice husk BC < bamboo BC < wood BC) proportions among the biochars, their volatile matter values were similar ($p > 0.05$), ranging between 45.61 (± 0.54) % and 48.72 (± 3.22) % (rice husk BC < wood BC < bamboo BC). The low fixed carbon content of rice husk BC (7.82 ± 0.10 %) means that this material is less resistant to biotic decomposition and thus has a shorter existence in soil (Yargicoglu et al., 2015). However, rice husk BC's high pH and CEC are useful properties for soil enrichment (Budai et al., 2014).

Table 2. CEC, pH, and composition of the three biochars.

Parameters	Wood BC	Rice husk BC	Bamboo BC
pH	10.11 ±0.04 a	9.51 ±0.02 a	9.94 ±0.02 a
CEC, Cmol/kg	13.53 ±0.65 a	26.70 ±1.57 c	20.77 ±1.21 b
Moisture,%	5.45 ±0.03 a	5.37 ±0.05 a	6.11 ±0.11 a
Volatile,%	46.68 ±1.68 a	45.61 ±0.54 a	48.72 ±3.22 a
Ash,%	1.93 ±0.03 a	41.24 ±0.49 c	8.08 ±0.20 b
Fixed carbon,%	45.94 ±1.68 c	7.82 ±0.10 a	37.09 ±3.32 b

There were significant differences of CEC values among the three biochars (p<0.05). In fact, rice husk BC had the highest CEC with 26.70 Cmol/kg, while bamboo and wood BC were 20.77 Cmol/kg and 13.53 Cmol/kg, respectively. A high CEC indicates the ability of biochar to adsorb cationic nutrients (e.g. Ca^{2+}, Mg^{2+}, NH_4^+, K^+) and thus high CEC biochars reduce the leaching of these nutrients along a soil profile (Song and Guo, 2012). CEC depends on the presence of negatively charged surface functional groups (Essington, 2015) and other sources like metal hydroxides and silica phytoliths in biochar ash (Harvey et al., 2011). In addition, ageing and oxidization of biochar surface following application in the environment (soil) contributes to increased CEC values (Cheng et al., 2006), thus enhancing the adsorption and retention capacities of soil for nutrient cations (Yuan et al., 2011).

3.3 FTIR spectroscopy

FTIR spectra of wood, rice husk, and bamboo BCs are shown in Figure 2. The characteristic vibration was interpreted based on Stuart (2004) and (Özçimen and Ersoy-Meriçboyu, 2010). The band at 2922 cm^{-1} of both bamboo and wood BC refers to the aliphatic C-H stretching of alkenes. The O-H stretching of carboxylic acids in the three BCs is observed in the region of 2588-2532 cm^{-1}, while O–H and P–H stretching of ester compounds are assigned in the range of 2362-2348 cm^{-1}. The bands that appear at around 2160 cm^{-1} in rice husk and wood BC are attributed to aliphatic isonitrile –N≡C stretching, C≡C stretching of alkynes, as well as Si-H stretching of silicon compounds.
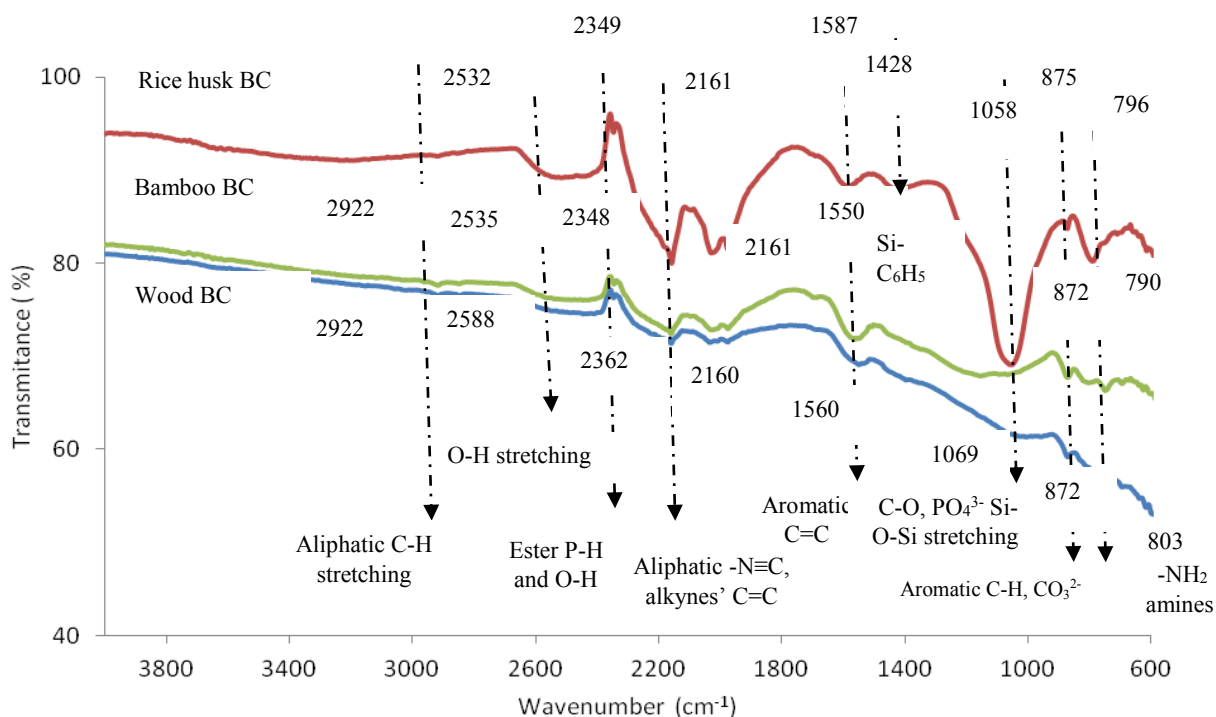
Figure 2. FTIR spectra of the three different biochars in the range 4000 – 400 cm^{-1}.

The C=C stretching bands of aromatic compounds of the biochars appeared in the range 1587-1550 cm^{-1}, whereas aromatic C=C stretching and C-H bending bands are assigned between 875 cm^{-1} and 872 cm^{-1}. Interestingly, there was one band near 1430 cm^{-1} for rice husk BC only, suggesting silicon attachment to the ring of benzene. Bands in the range of Si-O-Si asymmetric stretching (1000-1130 cm^{-1}) were observed for both wood BC (1069 cm^{-1}) and rice husk BC (1058 cm^{-1}). This finding was in contrast with the report of Nasser and Aref (2014) who found no Si content in wood BC from six Acacia species in Saudi Arabia. In addition, CO_3^{2-} groups were also represented in the bands at 872 cm^{-1} for wood BC and bamboo BC or at 875 cm^{-1} for rice husk BC, while the bands appearing in the range of 950-1100 m^{-1} for wood BC (1069 m^{-1}) and rice husk BC (1058 m^{-1}) are assigned to PO_4^{3-} ions. In the range 1069-1058 cm^{-1}, C-O stretching bands of alcohols and phenols and aliphatic C-O stretching of esters were found in wood and rice husk BC, but were not present in bamboo BC. The bands observed between

70

803-796 cm^{-1} for all three biochars were associated with NH$_2$ wagging and twisting of amines, and aliphatic symmetric P–O–C stretching.   Similarly, =C-H bending of alkynes and C-S stretching bands were assigned in the range of 700-600 cm^{-1} and were present in all three biochars. Thus, the three biochars were dominated by the aromatic structure (Fang et al., 2014) which results from the transformation of cellulose, hemicelluloses, and lignin and protein present in the parental feedstocks (Cantrell et al., 2012, Keiluweit et al., 2010) to form condensed structures via aromatization (Harvey et al., 2011) during the pyrolysis process. This is consistent with the alkaline pHs found for all three biochars. Additionally, carboxylic acid, alcohol, phenol, and amine functional groups were found to have formed on the biochar surfaces, which play an important role in cation and anion adsorption capacity of biochar, and indeed is consistent with the original biomass components.

3.4 BET and SEM

The BET surface area of the three biochars is presented in Figure 3, with values varying significantly with different parental biomass (p<0.05). The biochar produced from rice husk has the lowest BET surface area of 3.29 ± 0.02 m^2/g while bamboo and wood biochar both resulted in higher values of 434.53 ± 2.79 and 479.34 ± 0.88 m^2/g, respectively. The low value of surface area of rice husk BC corresponds with its less complicated morphology as indicated in the SEM images (Figure 4 c & d), compared to wood and bamboo BCs (Figure 4). In genaral, the surface area of biomass biochar is increased by the development of a porous system during the pyrolysis process (Paethanom and Yoshikawa, 2012). However, the high ash content of rice husk (41.24%, see Table 2) can result in blocking of the pores (Yargicoglu et al., 2015) which contributes to the reduction in surface area. In addition, softening, melting, fusing, and carbonizing during pyrolysis process, which can result in significant blocking of the pores, also causes a decease of the surface area values (Fu et al., 2011). According to

Rouquerol et al. (1994) biochar porosity was characterized by the International Union of Pure and Applied Chemistry (IUPAC) as micropores (<2 nm), mesopores (2-50 nm), and macropores (>50 nm). In fact macropores do not contribute to the measured surface area, while meso- and micropores do (Lee et al., 2013).

Scanning electron microscopy (SEM) was used to characterize the morphology of the three biochar samples. The pore shape, size and morphology are visualised by SEM, providing information on the structure of the three biochars after pyrolysis of the different biomasses. Figure 4 shows representative images of each biochar, at two different magnifications (20μm x 1000 μm and 200 μm x 100 μm). These pictures demonstrate the difference in porous structure among the biochars. In fact, the surface of the wood biochar has a complicated and rough surface with hollow structure (Figure 4a) and various pores (Figure 4b), representative of volatile compound release (Cetin et al., 2004). In contrast, the morphology of rice husk shows elongated hollow regions (resembling the shape of a boat) (Figure 4d) with one side having rough surface formed by mostly closed vesicles in rows, which were presumably formed by the melting of lignin while transporting the volatiles towards the surface (Sharma et al., 2002) and cracking and polymerization of hydrocarbons (Septien et al., 2013). In addition, there are crystals of inorganic salts present as individual particles and soot particles (Septien et al., 2013) covering the surface (figure 4c). In contrast, the other side of the wood biochar (Figure 4d) was observed as a smooth surface. Liu et al. (2010) reported that the melting and fusion process of lignin and other small organic molecules could be the cause of smooth surface formation.
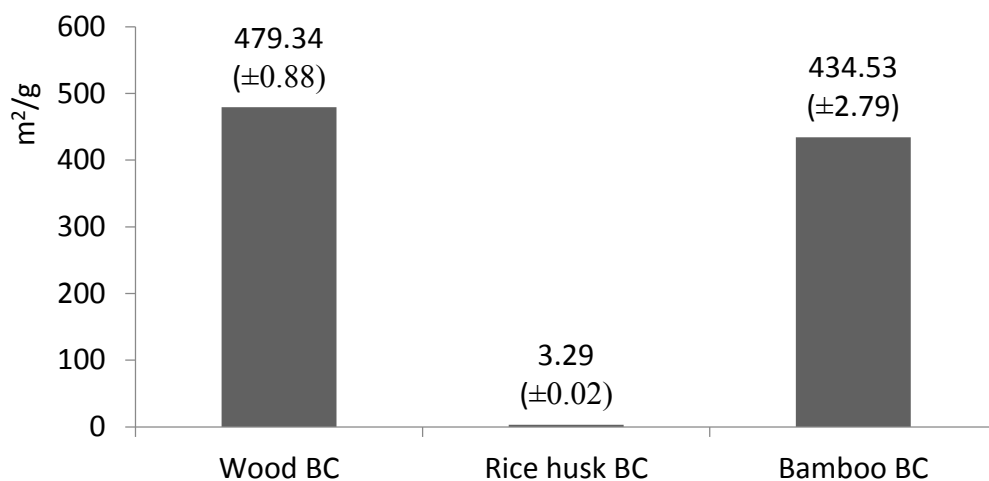
Figure 3. BET surface area of three different biochars.

Several mineral crystals (Figure 4a) were observed on the surface of rice husk BC. Septien et al. (2012) proposed that the mineral grains moved to the surface and then coalesced after fusion or re-condensed volatiles. Interestingly, the porous structure did not show on the SEM images of rice husk BC, while this parameter plays a key role in surface area of biochar, particularly, mesopores and micropores (Lee et al., 2013). In addition, a porous system serves as habitat for soil microorganisms such as bacteria, fungi, and protozoa which interact with the rhizosphere to improve the ability of plant for nutrient uptake (Thies and Rillig, 2009). Thus, these limitations suggest that risk husk BC may be less suitable as a soil nutrient, due to the lower BET surface area of this biochar. In comparison, bamboo BC (Figure 4e & f) had a special morphology, appearing as a hollow honeycomb-like structure with various pore sizes. The volatile compounds released quickly during the pyrolysis process created an internal overpressure and led to the coalescence of small pores, which lead to inner cavities and a more open structure (Guerrero et al., 2005, Onay, 2007). Such open pores with dominant micropores are the main source of this biochar's high surface area (Sharma et al., 2002). Thus, the complicated surface structure of both wood BC and bamboo BC allows them to have higher BET surfaces than rice husk BC.
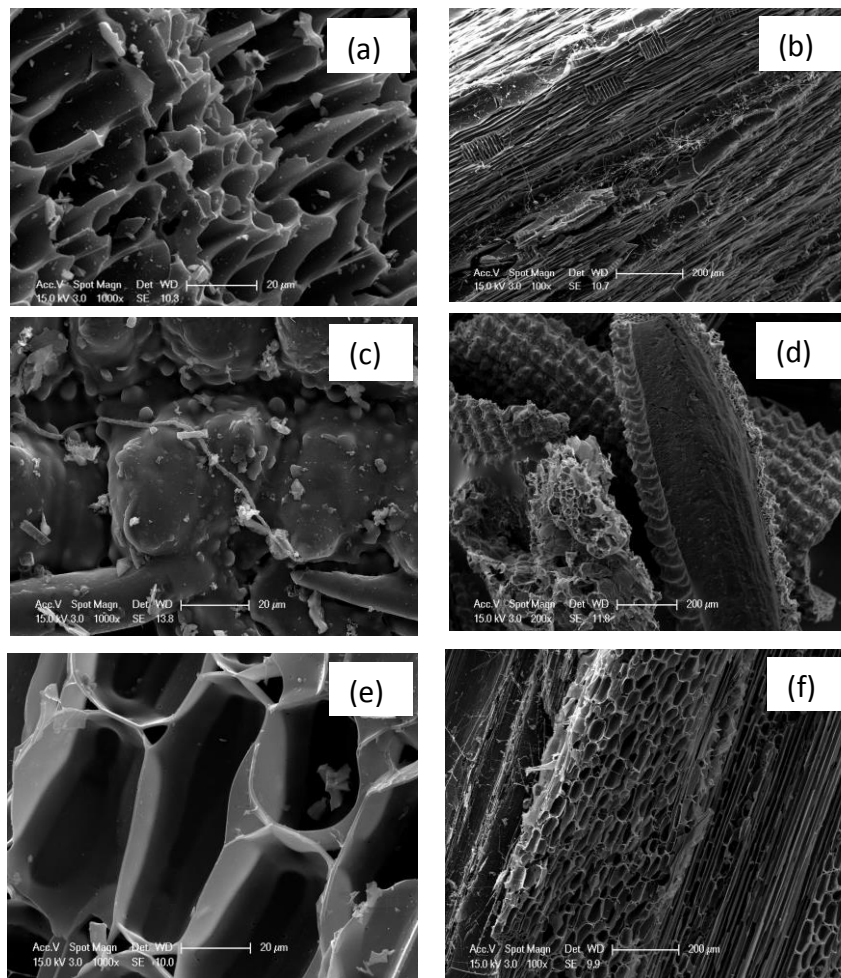
Figure 4. SEM photographs of biochar samples, (a, b) wood BC, (c, d) rice husk BC, and (e, f) bamboo BC. Magnifications are included in the images, all of which were taken from the same sample orientations.

3.5 Optimising the biochar selection for specific applications

The detailed characterisation of the biochars presented here is the first step in an ongoing project to support local agriculture in Vietnam by optimising the functional capacity of biochars through selection of the most suitable biomass or combination of biomass sources to produce biochars with the desired functional characteristics depending on the intended application. Thus, where the goal is improvement of soil quality, for example via providing a carbon sink or encouraging colonisation by microorganisms the set of desired BC properties needed would be different than those required for applications such as binding of heavy

metals or other toxicants or indeed for soil conditioning via enhanced retention of vital nutrients. Table 3 below presents an initial analysis of the BC properties required for the three main applications of interest in this work, and a first mapping of the physical-chemical properties of the three biochars analysed here (wood, risk husk and bamboo) to these requirements. Subsequent work will confirm experimentally that the properties identified in theory as correlating with key functional behaviours, which translate in practice to assessing the ammonium-nitrogen binding and heavy metal binding capacity of the different biochars and correlating these with key physico-chemical properties driving the reactive potential of the biochars.

Table 3: Summary of the BC properties required for different applications and an initial assessment of the suitability of the different BCs match to these properties.

Environmental application	Wood BC	Rice BC	Bamboo BC
Improving soil quality (C sink)			
- High C content	✔	X	✔
- Low Ash content	✔	X	✔
- Alkaline pH	✔	✔	✔
- High surface area	✔	X	✔
- Highly porous structure (habitat for microrganisms and water holding capacity)	✔	X	✔
Binding of heavy metals (remediation)			
- Alkaline pH	✔	✔	✔
- High CEC	X	✔	✔
- High surface area	✔	X	✔
- Alcohol groups / phenols / esters	✔	✔	✔
- Acidic groups (COO$^-$, CO$_3^{2-}$)	✔	✔	✔
- Other groups (PO$_4^{3-}$)	✔	✔	X
Retention of nutrients (fertilisation)			
- High CEC	X	✔	✔
- High Surface area	✔	X	✔
- Porous structure	✔	X	✔
- Acidic groups (COO$^-$, CO$_3^{2-}$)	✔	✔	✔
- Other groups (PO$_4^{3-}$, Si-O-Si)	✔	✔	X

4. Conclusions

The comparison of three biochars, from different biomass sources widely available in Vietnam (i.e. Acacia wood, rice husk and bamboo), produced using a pyrolysis approach indicated important differences of the physicochemical properties among the biochars produced under identical conditions. The high carbon content and alkaline pH of the three BCs makes them suitable for creating a carbon sink and improving the pH of acidic soils, as well as theoretically providing the capability to reduce mobility of toxic metals by precipitation. The immobility of heavy metals governed by changes pH in soil amended with biochar was reported by precious studies (Park et al., 2011). The formation of metal hydr(oxide), carbonate, and phospate precipitates are one of possible mechanisms for the immobility of the metals (Park et al., 2011). Testing of the metal mobility reduction of the biochars is underway and will be reported separately.

CEC and BET surface area are important parameters determining the adsorption capacity of a BC for ion nutrients or heavy metals, so the high CEC values (rice husk BC) and BET surface area values (bamboo BC and wood BC) are useful for soil enrichment and environmental mitigation. The values of CEC relate to cation binding capacity (Ca^{2+}, Mg^2, K^+, Na^+) and functional groups on surface, while BET surface area corresponds to surface morphology, as observed by SEM. The complex morphology with variously sized pores present in bamboo and wood BC not only serves as habitat for microorganisms (Zackrisson et al., 1996, Rillig and Thies, 2012), but also potentially improves the water holding capacity of soil (Basso et al., 2013, Yu et al., 2013).

Thus, the detailed characterisation of the biochars is the first step towards optimisation of the selection of biochars for specific applications, as part of an ongoing project to support local

agriculture. Indeed, it might be that mixtures of different biomass sources could be developed to fully optimise the functionality of the BCs for a range of agricultural applications.

Acknowledgements

References

ABO-FARHA, S., ABDEL-AAL, A., ASHOUR, I. & GARAMON, S. 2009. Removal of some heavy metal cations by synthetic resin purolite C100. Journal of hazardous materials, 169, 190-194.

AL-WABEL, M. I., AL-OMRAN, A., EL-NAGGAR, A. H., NADEEM, M. & USMAN, A. R. A. 2013. Pyrolysis temperature induced changes in characteristics and chemical composition of biochar produced from conocarpus wastes. Bioresource Technology, 131, 374-379.

AMELOOT, N., DE NEVE, S., JEGAJEEVAGAN, K., YILDIZ, G., BUCHAN, D., FUNKUIN, Y. N., PRINS, W., BOUCKAERT, L. & SLEUTEL, S. 2013. Short-term CO_2 and N_2O emissions and microbial properties of biochar amended sandy loam soils. Soil Biology and Biochemistry, 57, 401-410.

ANGIN, D. 2013. Effect of pyrolysis temperature and heating rate on biochar obtained from pyrolysis of safflower seed press cake. Bioresource technology, 128, 593-597.

BACHMANN, H. J., BUCHELI, T. D., DIEGUEZ-ALONSO, A., FABBRI, D., KNICKER, H., SCHMIDT, H.-P., ULBRICHT, A., BECKER, R., BUSCAROLI, A., BUERGE, D., CROSS, A., DICKINSON, D., ENDERS, A., ESTEVES, V. I., EVANGELOU, M. W. H., FELLET, G., FRIEDRICH, K., GASCO GUERRERO, G., GLASER, B., HANKE, U. M., HANLEY, K., HILBER, I., KALDERIS, D., LEIFELD, J., MASEK, O., MUMME, J., CARMONA, M. P., CALVELO PEREIRA, R., REES, F., ROMBOLÀ, A. G., DE LA ROSA, J. M., SAKRABANI, R., SOHI, S., SOJA, G., VALAGUSSA, M., VERHEIJEN, F. & ZEHETNER, F. 2016. Toward the Standardization of Biochar Analysis: The COST Action TD1107 Interlaboratory Comparison. Journal of Agricultural and Food Chemistry, 64, 513-527.

BAGREEV, A., BANDOSZ, T. J. & LOCKE, D. C. 2001. Pore structure and surface chemistry of adsorbents obtained by pyrolysis of sewage sludge-derived fertilizer. Carbon, 39, 1971-1979.

BASSO, A. S., MIGUEZ, F. E., LAIRD, D. A., HORTON, R. & WESTGATE, M. 2013. Assessing potential of biochar for increasing water-holding capacity of sandy soils. Gcb Bioenergy, 5, 132-143.

BRUNAUER, S., EMMETT, P. H. & TELLER, E. 1938. Adsorption of gases in multimolecular layers. J. Am. Chem. Soc, 60, 309-319.

BUDAI, A., WANG, L., GRONLI, M., STRAND, L. T., ANTAL JR, M. J., ABIVEN, S., DIEGUEZ-ALONSO, A., ANCA-COUCE, A. & RASSE, D. P. 2014. Surface properties and chemical

composition of corncob and Miscanthus biochars: effects of production temperature and method. Journal of agricultural and food chemistry, 62, 3791-3799.

CANTRELL, K. B., HUNT, P. G., UCHIMIYA, M., NOVAK, J. M. & RO, K. S. 2012. Impact of pyrolysis temperature and manure source on physicochemical characteristics of biochar. Bioresource technology, 107, 419-428.

CETIN, E., MOGHTADERI, B., GUPTA, R. & WALL, T. 2004. Influence of pyrolysis conditions on the structure and gasification reactivity of biomass chars. Fuel, 83, 2139-2150.

CHEN, B., ZHOU, D. & ZHU, L. 2008. Transitional adsorption and partition of nonpolar and polar aromatic contaminants by biochars of pine needles with different pyrolytic temperatures. Environmental Science & Technology, 42, 5137-5143.

CHENG, C.-H., LEHMANN, J. & ENGELHARD, M. H. 2008. Natural oxidation of black carbon in soils: Changes in molecular form and surface charge along a climosequence. Geochimica et Cosmochimica Acta, 72, 1598-1610.

CHENG, C.-H., LEHMANN, J., THIES, J. E., BURTON, S. D. & ENGELHARD, M. H. 2006. Oxidation of black carbon by biotic and abiotic processes. Organic Geochemistry, 37, 1477-1488.

DEMIRBAS, A. 2004. Effects of temperature and particle size on bio-char yield from pyrolysis of agricultural residues. Journal of analytical and applied pyrolysis, 72, 243-248.

DUKU, M. H., GU, S. & HAGAN, E. B. 2011. Biochar production potential in Ghana—a review. Renewable and Sustainable Energy Reviews, 15, 3539-3551.

ENDERS, A., HANLEY, K., WHITMAN, T., JOSEPH, S. & LEHMANN, J. 2012. Characterization of biochars to evaluate recalcitrance and agronomic performance. Bioresource Technology, 114, 644-653.

ESSINGTON, M. E. 2015. Soil and water chemistry: An integrative approach, CRC press.

FANG, Q., CHEN, B., LIN, Y. & GUAN, Y. 2014. Aromatic and Hydrophobic Surfaces of Wood-derived Biochar Enhance Perchlorate Adsorption via Hydrogen Bonding to Oxygen-containing Organic Groups. Environmental Science & Technology, 48, 279-288.

FU, P., YI, W., BAI, X., LI, Z., HU, S. & XIANG, J. 2011. Effect of temperature on gas composition and char structural features of pyrolyzed agricultural residues. Bioresource Technology, 102, 8211-8219.

GASKIN, J., STEINER, C., HARRIS, K., DAS, K. & BIBENS, B. 2008. Effect of low-temperature pyrolysis conditions on biochar for agricultural use. Trans. Asabe, 51, 2061-2069.

GUERRERO, M., RUIZ, M., ALZUETA, M., BILBAO, R. & MILLERA, A. 2005. Pyrolysis of eucalyptus at different heating rates: studies of char characterization and oxidative reactivity. Journal of Analytical and Applied Pyrolysis, 74, 307-314.

GUNDALE, M. J. & DELUCA, T. H. 2006. Temperature and source material influence ecological attributes of ponderosa pine and Douglas-fir charcoal. Forest Ecology and Management, 231, 86-93.

GUO, Y., YANG, S., YU, K., ZHAO, J., WANG, Z. & XU, H. 2002. The preparation and mechanism studies of rice husk based porous carbon. Materials chemistry and physics, 74, 320-323.

HALE, S. E. A., V.; MARTINSEN, V.; MULDER, J.; BREEDVELD, G. D.; CORNELISSEN, G. 2013. The sorption and desorption of phosphate-P, ammonium-N and nitrate-N in cacao shell and corn cob biochars. Chemosphere 91, 1612-1619.

HARVEY, O. R., HERBERT, B. E., RHUE, R. D. & KUO, L.-J. 2011. Metal interactions at the biochar-water interface: energetics and structure-sorption relationships elucidated by flow adsorption microcalorimetry. Environmental science & technology, 45, 5550-5556.

HERNANDEZ-MENA, L. E., PÉCORAA, A. A. & BERALDOB, A. L. 2014. Slow pyrolysis of bamboo biomass: Analysis of biochar properties. CHEMICAL ENGINEERING, 37.

HUANG, M., YANG, L., QIN, H., JIANG, L. & ZOU, Y. 2014. Fertilizer nitrogen uptake by rice increased by biochar application. Biology and Fertility of Soils, 50, 997-1000.

JENKINSON, D. & AYANABA, A. 1977. Decomposition of carbon-14 labeled plant material under tropical conditions. Soil Science Society of America Journal, 41, 912-915.

JONES, D. L., EDWARDS-JONES, G. & MURPHY, D. V. 2011. Biochar mediated alterations in herbicide breakdown and leaching in soil. Soil Biology and Biochemistry, 43, 804-813.

JOSEPH, S., CAMPS-ARBESTAIN, M., LIN, Y., MUNROE, P., CHIA, C., HOOK, J., VAN ZWIETEN, L., KIMBER, S., COWIE, A. & SINGH, B. 2010. An investigation into the reactions of biochar in soil. Soil Research, 48, 501-515.

JOSEPH, S. & LEHMANN, J. 2009. Biochar for environmental management: science and technology, London, GB: Earthscan.

KEILUWEIT, M., NICO, P. S., JOHNSON, M. G. & KLEBER, M. 2010. Dynamic molecular structure of plant biomass-derived black carbon (biochar). Environmental science & technology, 44, 1247-1253.

KIM, K. H., KIM, J.-Y., CHO, T.-S. & CHOI, J. W. 2012. Influence of pyrolysis temperature on physicochemical properties of biochar obtained from the fast pyrolysis of pitch pine (Pinus rigida). Bioresource Technology, 118, 158-162.

LEE, Y., PARK, J., RYU, C., GANG, K. S., YANG, W., PARK, Y.-K., JUNG, J. & HYUN, S. 2013. Comparison of biochar properties from biomass residues produced by slow pyrolysis at 500 C. Bioresource technology, 148, 196-201.

LEHMANN, J. & RONDON, M. 2006. Bio-char soil management on highly weathered soils in the humid tropics. Biological approaches to sustainable soil systems. CRC Press, Boca Raton, FL, 517-530.

LENTZ, R. & IPPOLITO, J. 2012. Biochar and manure affect calcareous soil and corn silage nutrient concentrations and uptake. Journal of environmental quality, 41, 1033-1043.

LIANG, B., LEHMANN, J., SOLOMON, D., KINYANGI, J., GROSSMAN, J., O'NEILL, B., SKJEMSTAD, J. O., THIES, J., LUIZÃO, F. J., PETERSEN, J. & NEVES, E. G. 2006. Black Carbon Increases Cation Exchange Capacity in Soils. Soil Science Society of America Journal, 70.

LIU, Y. Y., M.; WU, Y.; WANG, H.; CHEN, Y.; WU, W. 2011. Reducing CH4 and CO2 emissions from waterlogged paddy soil with biochar. J Soils Sediments, 11, 930-939.

LIU, Z., ZHANG, F.-S. & WU, J. 2010. Characterization and application of chars produced from pinewood pyrolysis and hydrothermal treatment. Fuel, 89, 510-514.

MAJOR, J., RONDON, M., MOLINA, D., RIHA, S. J. & LEHMANN, J. 2010. Maize yield and nutrition during 4 years after biochar application to a Colombian savanna oxisol. Plant and soil, 333, 117-128.

MASIELLO, C. A. & DRUFFEL, E. R. M. 1998. Black Carbon in Deep-Sea Sediments. Science, 280, 1911-1913.

MÉNDEZ, A., TARQUIS, A. M., SAA-REQUEJO, A., GUERRERO, F. & GASCÓ, G. 2013. Influence of pyrolysis temperature on composted sewage sludge biochar priming effect in a loamy soil. Chemosphere, 93, 668-676.

MUKOME, F. N., ZHANG, X., SILVA, L. C., SIX, J. & PARIKH, S. J. 2013. Use of chemical and physical characteristics to investigate trends in biochar feedstocks. Journal of agricultural and food chemistry, 61, 2196-2204.

MUKHERJEE, A., ZIMMERMAN, A. & HARRIS, W. 2011. Surface chemistry variations among a series of laboratory-produced biochars. Geoderma, 163, 247-255.

MUKHERJEE, A. & ZIMMERMAN, A. R. 2013. Organic carbon and nutrient release from a range of laboratory-produced biochars and biochar–soil mixtures. Geoderma, 193, 122-130.

NASSER, R. A.-S. & AREF, I. M. 2014. Fuelwood Characteristics of Six Acacia Species Growing Wild in the Southwest of Saudi Arabia as Affected by Geographical Location.

NEVES, E. G., PETERSEN, J. B., BARTONE, R. N. & DA SILVA, C. A. 2003. Historical and socio-cultural origins of Amazonian dark earth. Amazonian dark earths. Springer.

NOVAK, J. M., LIMA, I., XING, B., GASKIN, J. W., STEINER, C., DAS, K., AHMEDNA, M., REHRAH, D., WATTS, D. W. & BUSSCHER, W. J. 2009. Characterization of designer biochar produced at different temperatures and their effects on a loamy sand. Annals of Environmental Science.

NGUYEN, B. T. & LEHMANN, J. 2009. Black carbon decomposition under varying water regimes. Organic Geochemistry, 40, 846-853.

ONAY, O. 2007. Influence of pyrolysis temperature and heating rate on the production of bio-oil and char from safflower seed by pyrolysis, using a well-swept fixed-bed reactor. Fuel Processing Technology, 88, 523-531.

ÖZÇIMEN, D. & ERSOY-MERIÇBOYU, A. 2010. Characterization of biochar and bio-oil samples obtained from carbonization of various biomass materials. Renewable Energy, 35, 1319-1324.

PAETHANOM, A. & YOSHIKAWA, K. 2012. Influence of pyrolysis temperature on rice husk char characteristics and its tar adsorption capability. Energies, 5, 4941-4951.

PARK, J. H., CHOPPALA, G. K., BOLAN, N. S., CHUNG, J. W. & CHUASAVATHI, T. 2011. Biochar reduces the bioavailability and phytotoxicity of heavy metals. Plant and soil, 348, 439.

QIU, Y., ZHENG, Z., ZHOU, Z. & SHENG, G. D. 2009. Effectiveness and mechanisms of dye adsorption on a straw-based biochar. Bioresour Technol, 100, 5348-51.

RAJKOVICH, S., ENDERS, A., HANLEY, K., HYLAND, C., ZIMMERMAN, A. R. & LEHMANN, J. 2012. Corn growth and nitrogen nutrition after additions of biochars with varying properties to a temperate soil. Biology and Fertility of Soils, 48, 271-284.

RILLIG, M. C. & THIES, J. E. 2012. Characteristics of biochar: biological properties. Biochar for environmental management. Routledge.

ROUQUEROL, J., AVNIR, D., FAIRBRIDGE, C., EVERETT, D., HAYNES, J., PERNICONE, N., RAMSAY, J., SING, K. & UNGER, K. 1994. Recommendations for the characterization of porous solids (Technical Report). Pure and Applied Chemistry, 66, 1739-1758.

SCHMIDT, M. W. & NOACK, A. G. 2000. Black carbon in soils and sediments: analysis, distribution, implications, and current challenges. Global biogeochemical cycles, 14, 777-793.

SEPTIEN, S., VALIN, S., DUPONT, C., PEYROT, M. & SALVADOR, S. 2012. Effect of particle size and temperature on woody biomass fast pyrolysis at high temperature (1000–1400 C). Fuel, 97, 202-210.

SEPTIEN, S., VALIN, S., PEYROT, M., SPINDLER, B. & SALVADOR, S. 2013. Influence of steam on gasification of millimetric wood particles in a drop tube reactor: Experiments and modelling. Fuel, 103, 1080-1089.

SHARMA, R. K., WOOTEN, J. B., BALIGA, V. L., LIN, X., GEOFFREY CHAN, W. & HAJALIGOL, M. R. 2004. Characterization of chars from pyrolysis of lignin. Fuel, 83, 1469-1482.

SHARMA, R. K., WOOTEN, J. B., BALIGA, V. L., MARTOGLIO-SMITH, P. A. & HAJALIGOL, M. R. 2002. Characterization of char from the pyrolysis of tobacco. Journal of agricultural and food chemistry, 50, 771-783.

SHEN, Y., ZHAO, P. & SHAO, Q. 2014. Porous silica and carbon derived materials from rice husk pyrolysis char. Microporous and Mesoporous Materials, 188, 46-76.

SOHI, S., LOPEZ-CAPEL, E., KRULL, E. & BOL, R. 2009. Biochar, climate change and soil: A review to guide future research. CSIRO Land and Water Science Report, 5, 17-31.

SOHI, S. P., KRULL, E., LOPEZ-CAPEL, E. & BOL, R. 2010. Chapter 2 - A Review of Biochar and Its Use and Function in Soil. Advances in Agronomy. Academic Press.

SONG, W. & GUO, M. 2012. Quality variations of poultry litter biochar generated at different pyrolysis temperatures. Journal of analytical and applied pyrolysis, 94, 138-145.

STUART, B. H. 2004. Spectral analysis. Infrared spectroscopy: fundamentals and applications, 45-70.

THIES, J. E. & RILLIG, M. C. 2009. Characteristics of biochar: biological properties. Biochar for environmental management: Science and technology, 85-105.

UCHIMIYA, M., WARTELLE, L. H., KLASSON, K. T., FORTIER, C. A. & LIMA, I. M. 2011. Influence of pyrolysis temperature on biochar property and function as a heavy metal sorbent in soil. Journal of Agricultural and Food Chemistry, 59, 2501-2510.

YANG, F., ZHAO, L., GAO, B., XU, X. & CAO, X. 2016. The Interfacial Behavior between Biochar and Soil Minerals and Its Effect on Biochar Stability. Environmental science & technology, 50, 2264-2271.

YARGICOGLU, E. N., SADASIVAM, B. Y., REDDY, K. R. & SPOKAS, K. 2015. Physical and chemical characterization of waste wood derived biochars. Waste Management, 36, 256-268.

YU, O.-Y., RAICHLE, B. & SINK, S. 2013. Impact of biochar on the water holding capacity of loamy sand soil. International Journal of Energy and Environmental Engineering, 4, 44.

YUAN, J.-H., XU, R.-K. & ZHANG, H. 2011. The forms of alkalis in the biochar produced from crop residues at different temperatures. Bioresource Technology, 102, 3488-3497.

ZACKRISSON, O., NILSSON, M.-C. & WARDLE, D. A. 1996. Key ecological function of charcoal from wildfire in the Boreal forest. Oikos, 10-19.

ZHENG, W., GUO, M., CHOW, T., BENNETT, D. N. & RAJAGOPALAN, N. 2010. Sorption properties of greenwaste biochar for two triazine pesticides. Journal of Hazardous Materials, 181, 121-126.

Chapter 4. Adsorption of ammonium nitrogen (NH$_4^+$-N) ions onto various Vietnamese Biomass Residue–derived Biochars (wood, rice husk and bamboo)

Nguyen Van Hien[a,b], Eugenia Valsami-Jones[a] , Nguyen Cong Vinh[b], Tong Thi Phu[b], Nguyen Thi Thanh Tam[b] , Iseult Lynch[a]

[a] School of Geography, Earth and Environmental Sciences, University of Birmingham, Edgbaston, B15 2TT, UK

[b] Department of Land Use, Soils and Fertilizers Research Institute, Hanoi, Vietnam

Corresponding author: i.lynch@bham.ac.uk

Abstract

This study evaluates adsorption of ammonium nitrogen (NH$_4^+$-N) ions onto various biochars produced from biomass residues in Vietnam as a function of their physicochemical characteristics. Three biochars, including wood biochar (WBC), rice husk biochar (RBC), and bamboo biochar (BBC), were produced under limited oxygen conditions using Top-Lid Updraft Drum technology at temperatures of 450-550ºC. Physicochemical characterization (BET surface area, Cation exchange capacity (CEC), Scanning Electron Microscopy, Fourier Transform Infrared Spectroscopy) of the biochars was performed in order to link their porosity and surface functional groups with their NH$_4^+$-N capture capacities. The adsorption capacity was evaluated using various parameters such as adsorbent dosage, contact time, and initial adsorbate concentration. The equilibrium adsorption data were analyzed by Langmuir, Freundlich and Temkin adsorption isotherm models. The Freundlich model best describes the adsorption of NH$_4^+$-N onto the three biochars. The capacities of the biochars for NH$_4^+$-N adsorption were in the order RBC > BBC > WBC, which correlates with their overall CECs. The Lagergren-first order and pseudo-second order models were also used to evaluate the kinetics of adsorption, and the adsorption data of NH$_4^+$-N showed a good fit with the later model. Thus, the experimental data indicates that all three Vietnamese agricultural residue-derived biochars are suitable for maximising NH$_4^+$-N adsorption from aqueous solutions (e.g. from

fertiliser application), with rice husk BC being especially effective. The increased adsorption capacity of RBC correlated with its having the highest CEC despite having the lowest surface area, suggesting that surface chemistry plays the greatest role in the NH_4^+-N adsorption of all the physico-chemical parameters investigated.

Key words: Adsorption, biochar, ammonium, physico-chemical characterization, equilibrium adsorption, and adsorption kinetics

1. Introduction

Ammonia compounds in water have attracted increasing intention around the world for their influence on drinking and waste water, and aquaculture. Ammonia is present in water in two forms, either unionised ammonia, NH_3, or as the ammonium cation, NH_4^+ (Chien, 1992). The nitrogen sources resulting in water pollution mainly result from industrial and agricultural activities like food, rubber and fish processing, steel and leather production, animal husbandry, and fertilizer application (Le Leuch and Bandosz, 2007, Zhu et al., 2012), and from aquaculture. In agriculture, nitrogen fertilizer applied as urea – $CO(NH_2)_2$ is widely used due to its high N content (46% N), low manufacturing costs, and easy shipping (Hagin and Tucker, 1982). However, the main problem of this product is the low use efficiency, with 40-70% of the applied nitrogen lost to the environment (Wu and Lui, 2007) via leaching, volatilization, run off, and erosion (Bouwman and Boumans, 2002).

High ammonia concentrations in drinking water can have harmful impacts on human health, while in industrial wastewater ammonia is linked to oxidation of the pipe systems draining the wastewater (Halim et al., 2013), and excessive amounts in lakes and rivers with slow flow is a major cause of eutrophication (Zhu et al., 2012) and is toxic for fish (Chien, 1992). Hence,

several studies have focussed on approaches for removal of ammonia from aqueous solution. The methods employed for ammonia removal from wastewater include ion exchange by natural zeolite (Alshameri et al., 2014, Malovanyy et al., 2013, Thornton et al., 2007), bioadsorption by biofilm (Sabbah et al., 2013, Qiao et al., 2010), ozone treatment (Schroeder et al., 2011, Tanaka and Matsumura, 2003), and adsorption by carbon nanotubes (Moradi and Zare, 2013), synthetic zeolite (Otal et al., 2013, Arslan and Veli, 2012) or low cost materials such as wheat straw or volcanic tuff (Ma et al., 2011, Maranon et al., 2006). Among the potential methods, adsorption is considered to be a promising technology for removal of ammonia contaminants from wastewater (Zhu et al., 2012). From the various porous solids described, low-cost adsorbents known as biochar (BC), the carbonized product gained by pyrolysis of biomass under restricted or absent oxygen conditions (Mukherjee and Zimmerman, 2013a, Paethanom and Yoshikawa, 2012) present a prospective option for industrial or household-scale removal of pollutants. Advantages of biochar include their porous structures, high surface area, and negative surface charge, and the fact that it can be produced in kilns on-site by small farmer groups in developing countries utilising materials that would otherwise simply be burned.

Removal of ammonia from aqueous solution by biochar was assessed by several researches using biochars produced from different feedstocks. The results showed that different kinds of biochar gave various adsorption capacities. For example, Zeng et al. (2013) reported that biochar produced from four phytoremediation plants at high temperature (700°C) had higher adsorption capacity for ammonia than those produced at lower temperatures (500-600°C), while the opposite trend was observed by Wang et al. (2015c) for oak sawdust BCs (300-600°C). The effect of various concentrations of HNO_3 used to modify the surface of corncob BC on NH_4^+-N adsorption was reported by Vu et al. (2017) with the best ratio of BC/HNO_3 found to be 1:5 (w/v). Thus, although BC has been shown to be effective for ammonia

adsorption, the mechanism for the adsorption is still not fully understood. Surface-chemistry driven adsorption was assumed as the mechanism for most studies, but whether NH_4^+-N is adsorbed on biochar as a monolayer or multilayer on homogenous and/or heterogeneous surfaces is still under debate.

Vietnam is known as an agricultural country: agriculture accounted for 17% of GDP in 2014 and employs nearly half of the workforce (World Bank, 2006). Biomass residues like wood chips, sawdust, rice husk, and bamboo are abundant by-products of processing plants in Vietnam. According to statistics from the Ministry of Agriculture and Rural Development (Vietnam), average rice production in Vietnam from 2011-2015 was around 43 million tons, which corresponds to around 8 million tons of rice husk discharged in this 4 year period. These discharged by-products are normally used for cooking, as bedding for animals or are left for decomposition in fields, rather than being turned into novel products like biochar for industrial and agricultural applications. In recent years, several research efforts in Vietnam have investigated the potential application of these products, particularly evaluating their effectiveness for water purification, as waste water treatment has become a hot issue in some region, but the results are still limited. Hence, in this work, three selected typical Vietnamese biomass sources were turned into biochar and evaluated for (ammonium) adsorption as a function of their physicochemical characteristics. The goal of this research was to provide evidence-based recommendations to local farmers on the selection of the appropriate biomass to convert to biochar in order to achieve specific treatment goals.

2. Materials and Methodology

2.1 Biochar preparation and characterization

Three biochars from *Acacia* wood chip, rice husk, and bamboo were produced by TLUD technology under limited oxygen condition, as described in **section 2.1 of Chapter 2**. The

biochars were extensively characterized in terms of their pH, CEC (cation exchange capacity), BET surface area, FTIR (Fourier-Transform Infrared Spectroscopy) for surface chemistry, proximate and element analysis. All three biochars were alkaline with pH = 9.51-10.11. CEC decreased in the order rice husk BC (26.70 Cmol/kg) > bamboo BC (20.77 Cmol/kg) > wood BC (13.53 Cmol/kg), while the opposite trend was observed for BET surface area. Measurement methodologies were described in detail in section **2.2.1 of Chapter 2**.

2.2 Adsorption experiments

The stock solution with 500 mg/L of NH_4^+-N was prepared by dissolving NH_4Cl in distilled water. Solutions for adsorption experiments with the three biochars were diluted from the stock solution, with exposure concentrations (20 – 320 mg/L) selected to ensure concentrations much higher than the normal concentration of ammonia (0.2 mg/L) in surface water (Organization, 2004a). The pH of the experimental solutions was adjusted to a constant value (pH=7) by adding small volumes of 0.1M NaOH or 0.1M HCl, and measured by a pH meter (Thermo Orion 3 star model). The adsorption experiments were conducted including different dosages of adsorbents (biochars), various initial concentrations of adsorbate (NH_4^+-N), and different contact times. The initial concentration of NH_4^+-N (40mg/L) in solution for the experiments of biochar mass and contact time was chosen based on the experiments of Zhu et al. (2012). In the first experiment assessing the effect of biochar concentration, 0, 0.25, 0.50, 1.0, and 2.0g of biochar were added into falcon tubes and mixed with 40mL of NH_4^+-N (40 mg/L, pH=7). Then, the tubes were put on an orbital shaker and shaken at 300 rpm for 24h hours at ambient temperature (22 ± 0.5^{o}C). After the desired time, the solution was centrifuging at 5,000 rpm for 10 mins, and the supernatant was filtered using an acrodisc syringe filter (0.20 μm) after which the NH_4^+-N concentration in the filtered solution was

measured by Ion Chromatography (Dionex DX500 model) and calculated using a standard curve determined using standard solutions of 0.5, 1, 5, 10, 20, 50 mg/L of NH_4^+-N.

For the second set of experiments, assessing the effect of NH_4^+-N concentration on the absorption efficiency, 0.5g biochocar was added into falcon tubes and mixed with 40 mL of NH_4^+-N (pH=7) with various concentrations (0, 20, 40, 80, 160, 320 mg/L of NH_4^+-N), and shaken for 24h at 300 rpm at room temperature (22 ± 0.5 °C). Other steps were the same as in the first study, to measuring the NH_4^+-N concentration remaining on solution.

In the final set of adsorption experiments, assessing the effect of adsorption time, 0.5g biochar mixed with 40mL NH_4^+-N (40 mg/L, pH=7) was shaken for the desired times (30, 60, 90, 120, 240, and 480 mins), and then each sample was centrifuged and filtered as described above to evaluate the adsorption capacity of biochar as a function of the contact time. Other steps were similar to the above two experiments.

All the experiments were conducted in triplicate, and data were presented as mean ± SD (standard deviation). The NH_4^+-N adsorption at equilibrium q_e, at a specific incubation time q_t and the proportion of removal (%) were calculated using the follow equations.

Equations 1 and 2 describe the equilibrium experiments:

$$q_e = \frac{(C_o - C_e)V}{m} \quad (1) \qquad \text{and} \qquad \%\text{removal} = \frac{C_o - C_e}{C_o} \times 100 \quad (2)$$

where C_o are the initial concentration of adsorbate (40 mg/L of NH_4^+-N), C_e is the concentration of adsorbate at equilibrium (i.e. at 24h where no further change in the concentration in solution occur); V (L) is the volume of the adsorbate; and m is the dosage of adsorbent (g).

Equations 3 and 4 describe the contact time experiments:

$$q_t = \frac{(C_o - C_t)V}{m} \qquad (3) \qquad \text{and} \qquad \%\text{removal} = \frac{C_o - C_t}{C_o} \times 100 \qquad (4)$$

where C_o and C_t are the initial and time t concentrations of NH_4^+-N (i.e. C_t is the concentration of NH_4^+-N at time t); V (L) is the volume of the adsorbate; and m is the dosage of adsorbent (g).

Data Analysis

Langmuir isotherm, Freundlich isotherm, and Temkin isotherm models were used to evaluate the data of adsorption of NH_4^+-N in order to provide insights into the adsorption process and arrangement of the adsorbed NH_4^+-N on the biochar surfaces.

The Langmuir model (Langmuir, 1917) was successfully used to simulate the adsorption isotherms of adsorbate onto solid. Langmuir theory assumes that sorption occurs at a surface with homogenous adsorption sites, without interactions between the adsorbed molecules and with constant heat of adsorption for all active sites of the adsorbent (Chowdhury et al., 2011, Gupta et al., 2010). Additionally, the maximum adsorption is associated with a monolayer impregnated with molecules of adsorbate on a homogeneous adsorbent surface (Long et al., 2008). The model equation (5) was described as follows:

$$\frac{1}{q_e} = \frac{1}{q_{max}} + \frac{1}{q_{max}K_L}\frac{1}{C_e} \qquad (5)$$

where q_e (mg/g) is the adsorption capacity at equilibrium, C_e (mg/L) is the concentration of adsorbate (remaining in solution in our measurements) at equilibrium, C_o (mg/L) is initial concentration of adsorbate, K_L (L/mg) is the Langmuir adsorption constant relative to the adsorption energy, and q_{max} (mg/g) is the maximum monolayer adsorption capacity of the adsorbent. Values of K_L and q_{max} are calculated by plotting $1/q_e$ versus $1/C_e$.

The Freundlich isotherm (1906) was used to predict multilayer adsorption on a heterogeneous surface between liquid and solid phases. The theory of the Freundlich isotherm assumes that the adsorbate molecules are adsorbed onto a heterogeneous surface via a multilayer of adsorbent (Long et al., 2008) and that the heat of adsorption is not equally distributed to all the adsorption sites (Chowdhury et al., 2011). The equation is presented in Equation 6, as follows:

$$\ln q_e = \frac{1}{n} \ln C_e + \ln K_F \qquad (6)$$

where q_e (mg/g) is the adsorption capacity at equilibrium, C_e (mg/L) is the concentration of adsorbate at equilibrium, C_o is the initial concentration of adsorbate, KF (mg/g) is the multilayer adsorption capacity, $1/n$ is the intensity of adsorption. Values of K_F and $1/n$ are calculated by plotting $\ln q_e$ versus $\ln C_e$.

The Temkin isotherm is based on the assumption that the adsorption heat impacts all molecules in a solid layer and increases linearly due to the interaction between adsorbent and adsorbate. The equation for this model was described by Chowdhury et al. (2011) as indicated in Equation 7 below:

$$q_e = \frac{RT}{b} \ln A + \frac{RT}{b} \ln C_e \qquad (7)$$

where q_e (mg/g) is the adsorption capacity in equilibrium, C_e (mg/L) is the equilibrium concentration of adsorbate, $B = RT/b$ (J/mol) is the Temkin constant related to adsorption heat, A (L/g) is the equilibrium constant of binding related to the maximum energy of binding. Values of A and B are calculated by plotting q_e versus $\ln C_e$.

Kinetics of adsorption:

Pseudo-first order and Pseudo-second order models were used to evaluate the mechanism of solid adsorption. The equations (8 and 9, respectively) are below as follows:

$$\ln(q_e - q_t) = \ln q_{e*} - k_1 t \qquad (8) \qquad \text{and} \qquad \frac{t}{q_t} = \frac{1}{k_2 q_{e**}^2} + \frac{t}{q_e} \qquad (9)$$

where q_t (mg/g) is the amount of adsorbate (NH_4^+-N in this case) adsorbed onto the biochar

at time t (min), q_e (mg/g) is the adsorption capacity at equilibrium, k_1 (min^{-1}) and k_2 (g/mg min)

are the Pseudo-first order and Pseudo-second order rate constants, respectively. q_{e*} is

calculated from a plot of $\ln(q_e - q_t)$ versus t, while q_{e**} is obtained from a plot of t/q_t versus t.

Thus, q_{e*} and q_{e**} are called $q_{e\text{-cal}1}$ and $q_{e\text{-cal}2}$ as they are the calculated values as opposed to

the experimentally determined ones.

Intraparticle diffusion model:

An Intraparticle diffusion model, based on the theory of Weber and Morris (1963), was used

to evaluate the diffusion mechanisms and rate controlling steps in the adsorption of NH_4^+-N

onto the different biochars.   The equation is given as:

$$q_t = k_{id} t^{1/2} + C \qquad (10)$$

where k_{id} is the rate constant of the intraparticle diffusion (mg/g $min^{1/2}$), and C is the

thickness of the boundary layer. C and k_{id} are calculated from the plot of q_t versus $t^{1/2}$.

3. Results and discussion

3.1 Effect of biochar mass on ammonium adsorption

The data showing the effect of biochar concentration (adsorbent mass) on NH_4^+-N adsorption

are presented in Figure 1. In this study, various concentrations of each of the three biochars

were added into NH_4^+-N solutions with initial concentration of 40mg/L and pH=7 to investigate

the adsorption capacity of the different biochars for NH_4^+-N.   The results show that the

adsorption capacity of the three biochars decreased with increasing biochar dosages (see

Figure 1). In fact, when adsorbent dosages increased from 6.25 g/L to 50 g/L, the adsorption

of NH_4^+-N onto wood BC, rice husk BC and bamboo BC decreased from 2.49 ± 0.02 mg/g to

0.57 ± 0.07 mg/g , 2.75 ± 0.14 mg/g to 0.51 ± 0.004 mg/g, and 2.52 ± 0.67 mg/g to 0.50 ± 0.02 mg/g, respectively. This finding corresponded with the results of Zhu et al. (2012). This phenomenon could be explained by the fact that as the biochar mass increased the total adsorption sites on the biochar surface increased with increased biochar mass, while the NH_4^+-N concentration in the initial solution was constant, and thus not all binding sites were occupied over the timescale of the experiment.
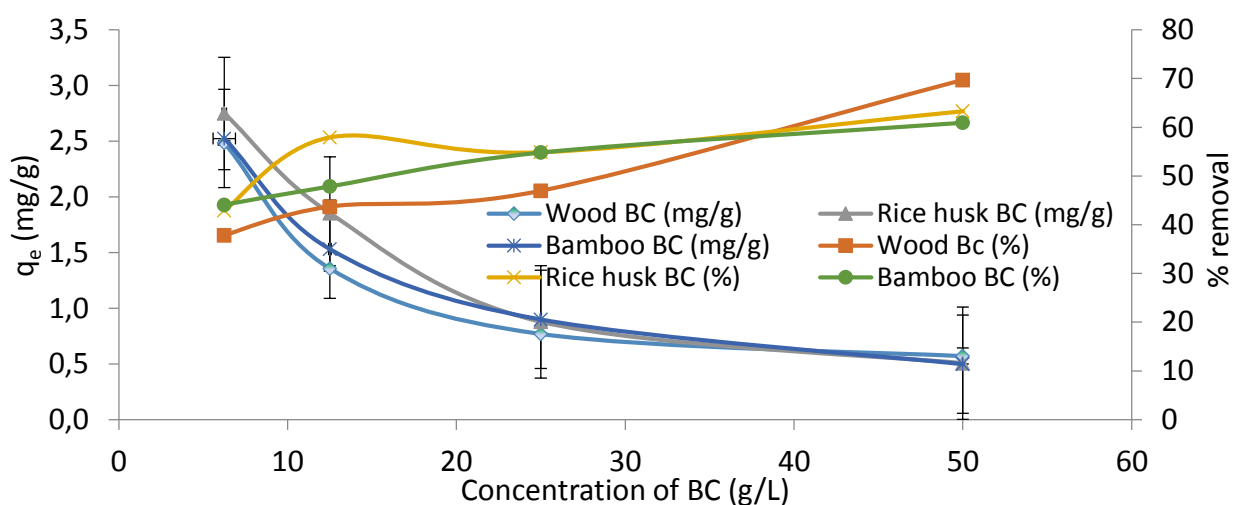
Figure 1: Effect of adsorbent (biochar) concentration on NH_4^+-N adsorption, where the concentration of NH_4^+-N was constant at 40 mg/L, plotted as adsorption at equilibrium, q_e, (left hand axis) and as the proportion of initial NH_4^+-N removed (%) on the right hand axis. N=3 in all cases.

The relative adsorption abilities of the three biochars varied with increasing dosage. For example, when the mass of biochar was between 6.25g/L and 25g/L, the adsorption capacity of three biochars were in order rice husk BC > bamboo BC > wood BC. However, when concentration of biochar was higher 25g/L, the adsorption of the biochars was similar (see Figure 1). The effect of biochar concentration on % removal was in contrast with the adsorption ability, with % removal increasing linearly with increasing dosage of biochar. This trend also was reported in the study of Zhu et al. (2012). It could be seen in Figure 1 that when

the biochar concentrations rose from 6.25g/L to 50g/L, the percentage of NH_4^+-N removal increased from 37.85 ± 0.76% to 69.71 ± 9.22% for wood BC, from 42.96 ± 2.17% to 63.29 ± 0.54% for rice husk biochar, and from 44.09 ± 0.72% to 60.95 ± 4.39% for bamboo BC.

3.2 Effect of Ammonium Concentration on Adsorption Capacity of Biochars

The effect of initial NH_4^+-N concentration with a constant adsorbent value (12.5g/L) on adsorption ability and % NH_4^+-N removal of the biochars is illustrated in Figure 2. The results are in contrast with the effect of adsorbent dosages. In fact, the adsorption capacity of biochar for NH_4^+-N increased dramatically with increasing initial NH_4^+-N concentration, while % removal of NH_4^+-N was increased initially and then decreased. When the initial concentration of NH_4^+-N was increased from 20mg/L to 40mg/L, % removal of NH_4^+-N by the three biochars showed a sharp increase, with the order being rice husk BC (45.79 ± 9.21 - 56.00 ± 3.47%) > Bamboo (38.15 ± 4.30 − 47.86 ± 2.42%) > wood BC (30.83 ± 4.44 − 41.19 ± 2.19%). Interestingly, the % NH_4^+-N removal by both rice husk BC and wood BC reached a peak at 40mg/L of NH_4^+-N, and gradually declined with higher concentrations. In contrast, % removal of bamboo continuously rose and reached the highest value (51.23 ± 4.70%) at around 70mg/L of NH_4^+-N. Hence, the concentration of NH_4^+-N at 40mg/L provided maximal removal for both wood BC and rice husk BC at dosage of 12.25g/L, while 60- 80 mg/L of NH_4^+-N were optimal for bamboo BC at the dosage. Note that the concentrations testes here are much higher than typical water concentrations in Vietnam, including the Lower Mekong Basin where total ammonia ranged from 0.013 mg/L to 1.3 mg/L, with maximum values (i.e. greater than 1 mg/L) for all the sites in the swamps of Laos (Chea et al., 2016), suggesting that biochar would be able to continuing removing ammonia over extended periods before being saturated.
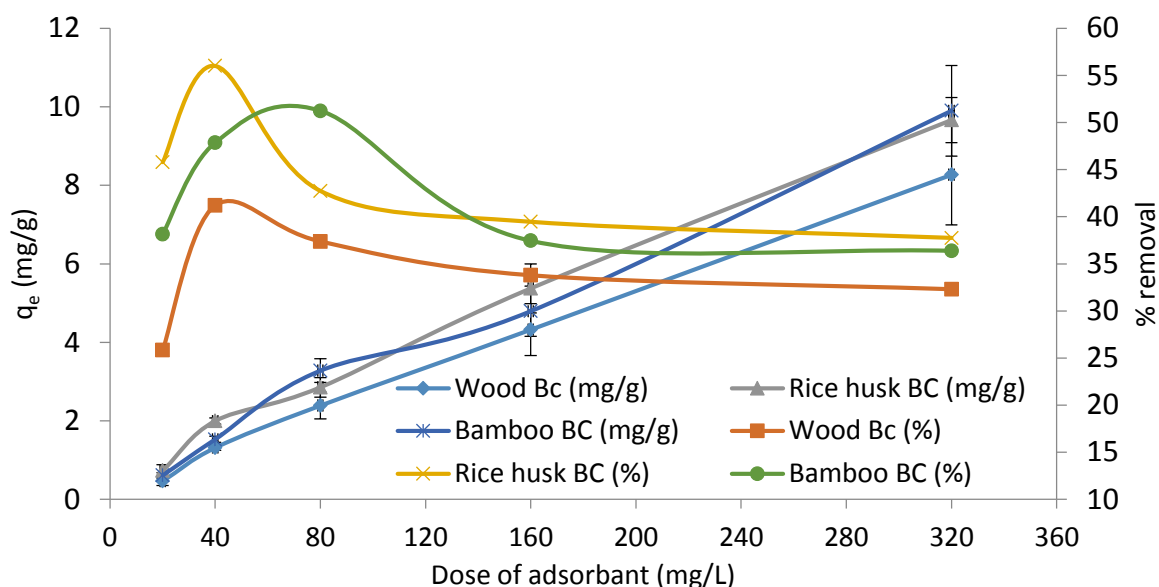
Figure 2. Effect of adsorbate concentration on adsorption capacity of the three biochars at a biochar concentration of 12.5g/L, plotted as adsorption at equilibrium, q_e, (left hand axis) and as the proportion of initial NH_4^+-N removed (%) (right side axis). N=3 in all cases.

The order of % removal among three biochars also changed with increasing initial concentration of NH_4^+-N. For instance, % removal was in order bamboo BC > rice husk BC > wood BC for NH_4^+-N concentrations from 60 mg/L to 130 mg/L, whereas this order was reversed (rice husk BC > bamboo BC > wood BC) at NH_4^+-N concentrations higher than 130 mg/L, although wood BC was always the lowest. Thus, the increase in adsorption capacity of the three biochars with increasing initial absorbant concentration plays an important role in nutrient retention and waste water treatment, particularly when N fertilizers have just been applied into soil or wastewater at high NH_4^+-N concentrations. Extremely high concentration of NH_4^+-N in wastewater was reported by previous studies, such as 1635 - 1810 mg/L in landfill leachate of Kyungjoo City in South Korea (Im et al., 2001) or 2070 - 2540 mg/L in the municipal solid waste of Seville in Spain (Luna et al., 2007).

3.3 Effect of contact time on Ammonium Adsorption by Biochars

Adsorption capacity and % removal of NH_4^+-N by the three biochars was affected by contact time, as presented in Figure 3. It has been observed that the trends of adsorption and NH_4^+-N removal by the three biochars were quite different with increasing contact time. As contact time was increased from 30 to 480 mins, the adsorption ability of wood BC was nearly in equilibrium (1.27 ± 0.01 mg/g) after 30 mins, and after that mainly kept stable. In contrast, there was an increase in adsorption for rice husk BC from 1.38 ± 0.02 mg/g to 1.75 ± 0.02 mg/g in the period of 30-60 mins, and absorption was then nearly unchanged during 120 - 480 mins. The sharp increase of adsorption for the initial time (60 mins) for rice husk BC could be the result of the high NH_4^+-N in solution and the large number of available adsorption sites on the adsorbent surface. The high initial concentration of NH_4^+-N (40 mg/L) increased the driving force and collisions between the biochar and adsorbate-NH_4^+-N (Hou et al., 2016), and the available adsorption sites (CEC and functional groups) were attractive to NH_4^+-N ions. Thus, the adsorption process of rice husk BC for NH_4^+-N took place in more than one stage - a rapid adsorption step initially when there were lots of binding sites, an intermediate binding rate as sites became harder to find, and equilibrium when the on and off rates were equal.
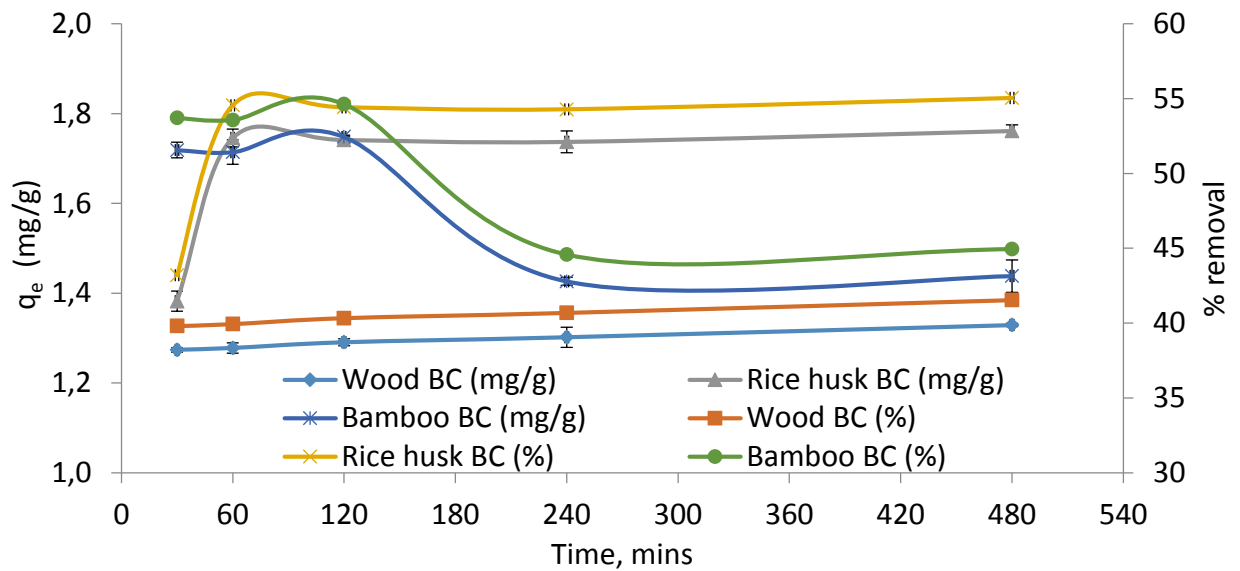
Figure 3. Effect of contact time on adsorption capacity of biochar, plotted as adsorption at t time, q_t, (left axis) and as the proportion of initial NH_4^+-N removed (%) (right axis). Biochar concentrations were 0.5g and the initial NH_4^+-N concentration was 40 mg/L. N=3 in all cases.

However, the opposite results were observed for bamboo BC when contact time increased. For example, the highest adsorption was obtained during the initial period of 30-120 mins with values between 1.71 ± 0.03 mg/g and 1.75 ± 0.004 mg/g. There was a significant decline in adsorption from 1.75 ± 0.004 mg/g to 1.43 ± 0.01 mg/g when the contact time increased from 120 to 240 mins. After that, a slight increase occurred during 240 – 480 mins before reaching equilibrium. The main reasons for these phenomena could be described as follows. Bamboo BC was found to have a comb-like structure with a highly porous distribution (see supplemental data showing Scanning Electron Microscopy images of the bamboo biochar compared to the rice husk and wood). So, during the initial stage of adsorption (<120 mins), NH_4^+-N ions could move quickly into macro and meso-pores by diffusion of the concentration gradient, where they may have been trapped by physical adsorption and adsorbed by negative charges on the bamboo biochar surface. According to Wang et al. (2015b), mesopores occupied 90% of the total porous system of bamboo BC, where the physical adsorption mainly

occurred. However, our data suggest that surface chemistry effects, resulting arising from functional groups with negative charge mainly governed ammonium adsorption, rather than physical adsorption by surface area or porous structure as reported previously. More detailed mechanisms of adsorption of ammonium to the three biochars are explained in the sections on adsorption isotherms and adsorption kinetics.

3.4 Adsorption Isotherms

Isotherm models of Langmuir, Freundlich, and Temkin were used to describe the association between the initial concentration of dissolved adsorbate (NH_4^+-N) and the content of adsorbate adsorbed onto the surface of biochar from aqueous solutions at equilibrium at a certain temperature (22 °C) and pH (7.0). The analysis of data for NH_4^+-N adsorption to biochar is necessary for identification of which equations are suitable to fit and describe the results. Particularly, these parameters could explain for the physicochemical properties of the adsorbent surface responsible for adsorbate adsorption at a fixed temperature and pH. All the parameters fitted by the three models are given in Table 1, and an illustration (Figure 4) was modified from Medveď and Černý (2011) for the assumed adsorption of Langmuir isotherm (Figure 4a) and Freudlich isotherm (Figure 4b).

Table 1. Langmuir, Freundlich, and Temkin constants for NH_4^+-N adsorption to the three biochars studied (wood BC = WBC, rice husk BC = RBC, and bamboo BC = BBC).

Biochar	Langmuir model (Eq5)			Freundlich model (Eq6)			Temkin model (Eq7)		
	q_{max}	K_L	R^{2*}	K_F	1/n	R^{2**}	B	A	R^{2***}
WBC	-8.09	-0.28	0.9295	0.04	0.985	0.9658	2.64	-2.66	0.9114
RBC	88.50	6.73	0.9111	0.14	0.801	0.9489	2.80	-2.31	0.8994
BBC	-12.55	-0.64	0.9425	0.08	0.911	0.9460	3.06	-2.51	0.9109

Note: q_{max} and K_L , K_F and 1/n, A and B were described in equation (5), (6) and (7) above, respectively. R^{2*}, R^{2**}, and R^{2***} were obtained by the plotting described in equation (5), (6) and (7) with data from Figure 2.

The results indicated that the Langmuir and Temkin models are not suitable for exploring NH_4^+-N adsorption onto the biochars due to the low linear regression (R^2 values) and several parameters such as q_{max}, K_L, and A having negative values. Although having a low R^2 value (R^2 = 0.9111), the maximum adsorption of rice husk BC for NH_4^+-N was estimated by the Langmuir model being 88.50 mg/g. In contrast, the experimental data is better explained by the Freundlich isotherm for the adsorption of ammonium for all biochars. According to Baocheng et al. (2008) and Öztürk and Bektaş (2004), K_f could be used to compare the adsorption capacity among the three biochars as when C_e=1, the K_f value concurs with q_e.

a) Monolayer adsorption on homogenous   b) Multilayer adsorption on heterogeneous surface
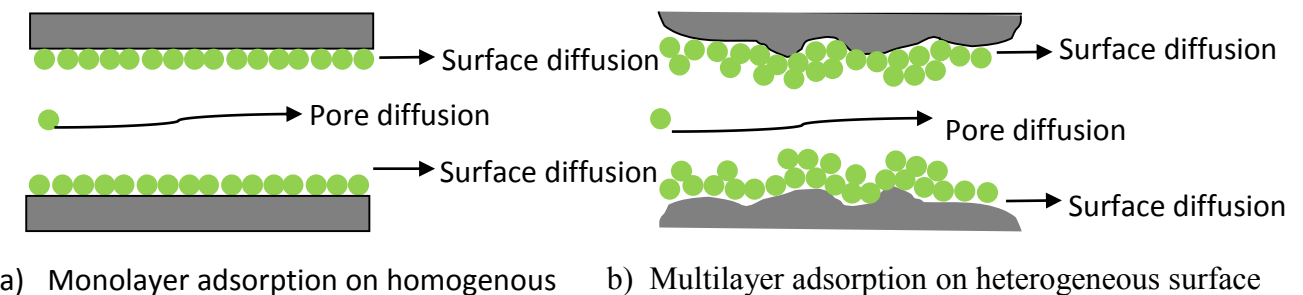
Figure 4. An illustration of NH_4^+-N ions adsorbed onto biochar surfaces as a monolayer (a) or a multilayer (b). Multilayer adsorption is more likely on heterogeneous surfaces such as biochar.

As shown in Table 1, the K_f values of the three biochars were in the order rice husk BC > bamboo BC > wood BC, meaning that rice husk biochar had the highest adsorption ability for NH_4^+-N. In addition, the values of n and 1/n were used to classify the adsorption isotherm (Asiagwu and Owamah, 2013, Bhandari and Xu, 2001). The favourability of the adsorption process is evaluated by the magnitude of n, while 1/n, is a heterogeneous factor that indicates the adsorption intensity of the adsorbent (Huang et al., 2014b). The n values (calculated from 1/n values from Table1) of the three biochars were in the order rice husk BC (1.25) > bamboo BC (1.09) > wood BC (1.05) and all were higher than 1 which means favourable adsorption (Huang et al., 2014b). The values of 1/n were between 0 and 1, which showed high adsorption intensity (Hou et al., 2016). Thus, it could be concluded that the adsorption of NH_4^+-N onto each of the three biochars involved multilayer coating, and available adsorption sites on the surface of the biochars were distributed randomly rather than uniformly. These findings were also supported by Zeng et al. (2013) for twelve biochars produced at different temperatures (500°C, 600°C, and 700°C) from four phytoremediation plants, and by Hale et al. (2013) for corncob BC (300-350°C). However, our results were in contrast with Wang et al. (2015c) for oak sawdust BC (300-600°C), Vu et al. (2017) for modified corncob BC (400°C), and Kizito et al. (2015) for mixed wood BC and rice husk BC (600°C), suggesting that the biomass structure and surface chemistry and the resulting biochar surface chemistry and structure play an important role. The oak sawdust and mixed wood and rice husk BC results were well fitted with the Langmuir isotherm which means that adsorption of NH_4^+-N by the adsorbents was related to monolayer formation with constant heat of adsorption for all sites on a homogeneous surface. Interestingly, Saleh et al. (2012) reported that the NH_4^+-N adsorption by peanut biochar (produced at 450°C) was attributed to both monolayer and multilayer adsorption on heterogeneous surface, while Gao et al. (2015) found that multiple mechanisms

could govern NH_4^+-N adsorption due to neither the Langmuir model nor the Freundlich model being suitable for data of peanut shell BC, corncob BC and corn stalk BC (300°C, 450°C, 600°C). Thus, the different initial biomass and various pyrolysis temperatures may result in differences of NH_4^+-N adsorption onto biochar. More detail of the adsorption mechanisms are described in sections 3.5 and 3.6.

3.5 Adsorption Kinetics

Adsorption kinetics studies are widely used to understand the mechanisms involved in adsorbent and adsorbate interactions. Adsorption processes depend on the physicochemical characteristics of the adsorbent as well as the migration of the adsorbate (mass transfer). In order to predict the adsorption mechanism of NH_4^+-N to the different biochars, Pseudo-first order and Pseudo-second order models were used to investigate the adsorption kinetics. The best fitting model was evaluated based on both the linear regression coefficient (R^2) and the q_{e-cal} value, i.e., the calculated value of adsorption at equilibrium. The parameters calculated from the two models are presented in Table 2. It can be seen that the Pseudo-first order model did not fit the experimental data. The values of q_{e-cal} of wood BC (0.09 mg/g) and rice husk BC (0.02 mg/g) were extremely low compared to the experimental values, while q_{e-cal1}, K_1, and R^{2*} values of bamboo BC are absent in Table 1 due to its experimental data being not suitable for plotting $\ln(q_e-q_t)$ versus t. Thus, the graph plotting the Pseudo-first order fit to the data was not presented.

Table 2. Rate parameters for the adsorption of NH_4^+-N onto the various biochars (wood BC= WBC, rice husk BC = RBC, and bamboo BC = BBC).

Biochar	q_{e-exp}	Pseudo - first order			Pseudo - second order			Intraparticle diffusion		
		q_{e-cal1}	K_1	R^{2*}	q_{e-cal2}	K_2	R^{2**}	K_{id}	C	R^{2***}
WBC	1.36	0.09	0.002	0.9912	1.33	0.24	0.9999	0.013	1.57	0.9189
RBC	1.85	0.02	0.002	0.3158	178	0.13	0.9998	0.086	1.71	0.7339
BBC	1.53	-	-	-	1.40	-0.06	0.9982	-0.084	1.99	0.6863

Note: q_{e-cal1}, K_1 and R^{2*} were obtained by plotting equation (8); q_{e-cal2}, K_2 and R^{2**} were calculated from the plot of equation (9); K_{id}, C and R^{2***} were determined from the plot of equation (10). The data used for all these plots was from Figure 3.

In contrast, the Pseudo – second order model fit the data of NH_4^+-N adsorption onto three biochars with high correlation coefficients ($R^2 > 0.998$ see Figure 6). In addition, the q_{e-cal} values obtained from the model also agreed with the experimental Q_{e-exp} values, particularly for wood BC and rice husk BC. This supports the assumption that the rate-limiting step of NH_4^+-N adsorption onto the three biochars may be governed by chemical adsorption, which involves covalent forces arising from sharing or exchanging electrons between adsorbent and adsorbate (Ho and McKay, 1999, Kumar et al., 2010) and CEC. These findings correspond well to the physicochemical properties of these biochars (see supplementary data) in which rice husk BC had the lowest BET surface area but the highest CEC. In addition, alongside hydroxyl and carboxyl groups, the Si-O-Si groups on rice husk BC (see supplementary Table S1) also played an important role as ammonium adsorption sites, which was proven by (Yu et al., 2016). Hence, rice husk BCs adsorption capacity was higher than those of bamboo BC and wood BC (see Table 2) which had higher BET surface areas but lower CEC values than rice husk. The adsorption of NH_4^+-N by biochar related to CEC was reported by Zeng et al. (2013) for

biochars from phytoremediation plants and Vu et al. (2017) for corncob BC. Thus, it can be concluded that the adsorption of NH_4^+-N ions onto the three biochars assessed here was affected by functional groups with negative charge on surface and CEC rather than surface area. This is also in agreement with other previous studies (Saleh et al., 2012, Wang et al., 2015a, Takaya et al., 2016).
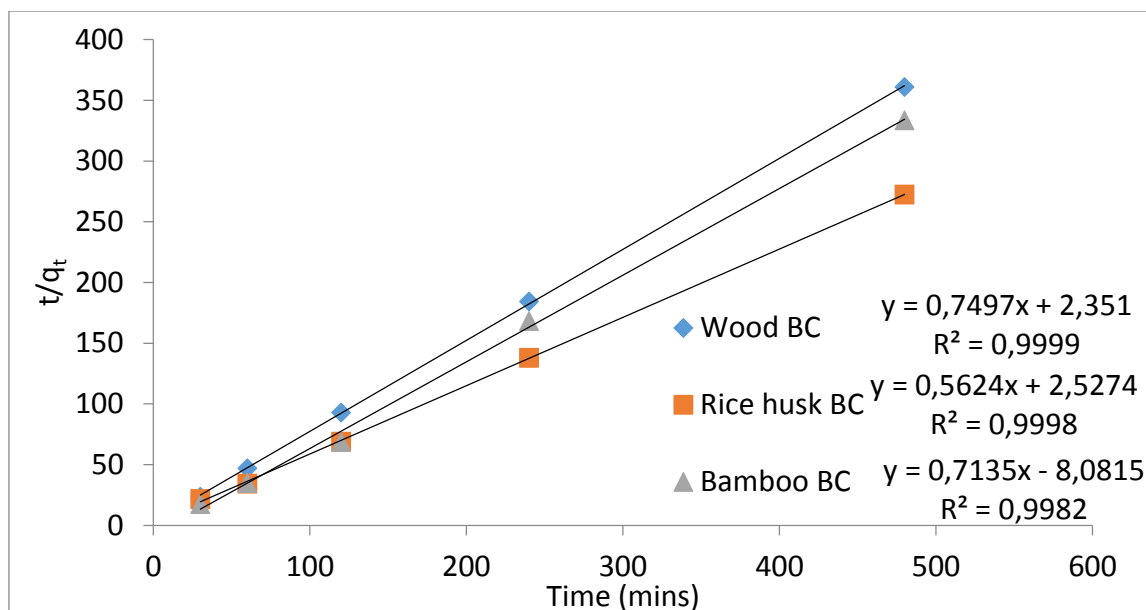
Figure 5. Plotting t/q_t versus t of Pseudo – second order data from the dataset plotted in Figure 3 assessing the effect of exposure time on the absorption amount to reveal the kinetics of adsorption.

3.6 Intraparticle diffusion model

Since the diffusion mechanism could not be identified by either the Pseudo – first order or Pseudo – second order models (Chen et al., 2010, Hameed et al., 2008, Radnia et al., 2011), the intraparticle diffusion model was also used to investigate the diffusion of NH_4^+-N into the three biochars. In order to understand the actual process involved in the adsorption of NH_4^+-N ions onto the porous system of biochar, a model (Equation 10), described by Weber and Morris (1962), was used as empirically it has been found that most adsorption process depend

105

on $t^{1/2}$ rather than being linearly related to time t. If a plot of q_t versus $t^{1/2}$ is linear and passes through the origin, intraparticle diffusion is the sole rate limiting step in the adsorption process (Foo and Hameed, 2012). In fact, the plot (see Figure 7) did not pass via the origin, which means the adsorption process occurred via more than one step.
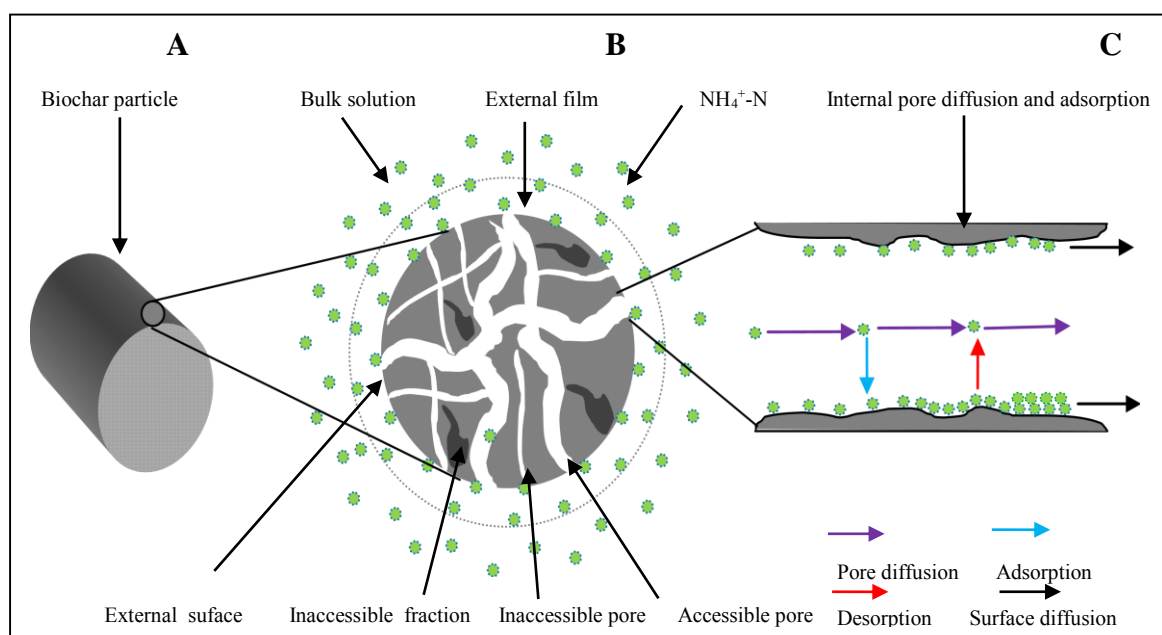
Figure 6. Assumed biochar geometry and the interparticle diffusion model for analyte adsoprtion. Part A illustrates an entire biochar particle. Part B illustrates the porous distribution with accessible pores (e.g., 30 nm) and small inaccessible pores, and assumed inaccessible fractions are shown in darker colour. Part C shows the internal pore diffusion, adsorption, and assumed desorption.

The diffusion process was illustrated in Figure 6 which was developed by integrating ideas of Zhang et al. (2016), Luterbacher et al. (2013), and Medveď and Černý (2011), and suggests that adsorption of NH_4^+-N ions underwent four main continuous steps (Worch, 2012) as follows:

Step 1: NH_4^+-N ions are transported from the bulk solution to the boundary layer (external film) located around the biochar particles.

Step 2: After the transport to the external surface of biochar, transport through the film occurs as external diffusion or film diffusion.

Step 3: Then transport into the interior of biochar particles, called intraparticle diffusion or internal diffusion by pore diffusion and/or surface diffusion (see Figure 4) occurs.

Step 4: The energetic interaction (overcoming of the activation energy) between NH_4^+-N ions and adsorption sites occurs, driven by the chemisorption processes.

The rate of an adsorption process is normally governed by the film and/or intraparticle diffusion due to the fact that the first and fourth steps occur quickly (Worch, 2012). The plots of q_t versus square root t ($t^{1/2}$) for the three biochars are illustrated for the intraparticle diffusion of the three biochar (Figure 7), and the fitting parameters are given in Table 2.

.
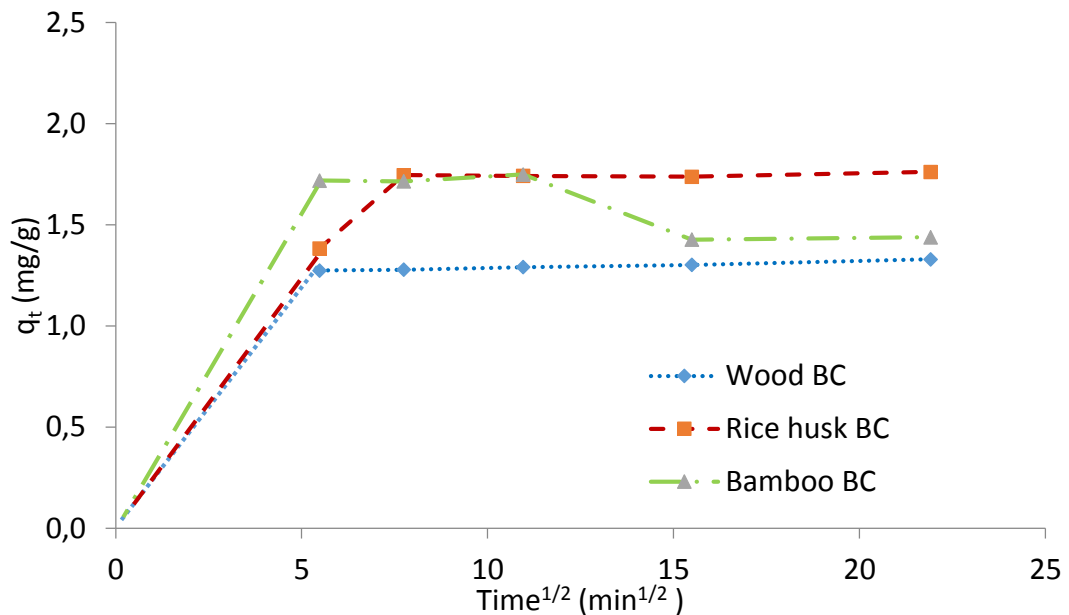
Figure 7. Intraparticle diffusion plots for NH_4^+-N ions adsorbed onto the porous adsorbents, i.e. the three biochars studied here. Data is replotted form Figure 3.

It could be seen that the plots (Figure 7) did not pass through the origin, so intraparticle diffusion was not the sole rate–limiting step. The first sharp portion (see Figure 7) is attributed to the diffusion of NH_4^+-N ions through the boundary layer (film) to the external surface of the biochar, and It was took place during the initial ~30 mins (around 5 min$^{1/2}$). The second part (5- 11 min$^{1/2}$ or 30 -120 mins) describes the process of intraparticle diffusion (pore diffusion and/or surface diffusion) of NH_4^+-N ions in porous system or on surface of the biochars. According to Worch (2012), the mass transfer into the interior of the adsorbent particles mainly occurs in the macropores (>50 nm) and mesopores (2-50 nm), while the adsorption take place in the microspore volume (<2 nm). The porous classification was followed the International Union of Pure and Applied Chemistry (Rouquerol et al., 1994). Thus, the porous structures of wood BC and bamboo BC (see SEM in supplementary data) may facilitate intraparticle diffusion. The final step was observed from 120 mins (11 min$^{1/2}$) onwards, which was the final equilibrium stage when intraparticle diffusion began slowly due to thee low concentration of adsorbate in solution (Cheung et al., 2007) and their being no more available adsorption sites. For bamboo BC, the complex structure (see supplementary data) and porous distribution and surface impacted on the diffusion process. The fast attainment of equilibrium in the period of 5- 11 min$^{1/2}$ or 30 -120 mins 30-120 was relative to the initial rapid adsorption uptake occurring in macropores and mesopores where there was a high rate of diffusion (Medveď and Černý, 2011). After that (11 min$^{1/2}$ or 120 mins), the diffusion (surface diffusion and pore diffusion) decreased due to the macropores and mesopores being filled by the adsorbate (presented in the Figure 7) which restricted the diffusion in microspores (branched pores).

4. Conclusions

The three biochars produced from biomass residues in Vietnam showed good adsorption capacity for NH_4^+-N in aqueous solution, especially rice husk BC. The adsorption of NH_4^+-N onto the biochars was governed by chemical adsorption (CEC, surface functional groups) rather than physical adsorption (surface area), and took place in a manner consistent with the heterogeneous surface with multilayer adsorption model. The biochar adsorption increased with increase of adsorbent concentration, which is important for ensuring its suitability for practical use in water purification and nutrient capture. In addition, biochars with high stability of aromatic carbon and adsorption of NH_4^+-N by the adsorbents via chemical adsorption (e.g., CEC and hydroxyl, carboxyl and O-Si-O surface functional groups) may be suitable for use as novel amendments for soil enrichment or fertilizer coating, known as slow release fertilizer to reduce the nutrient loss via leaching and/or emission (NO_x) . Particularly, the high silicon (18.8 – 22.3 % SiO_2) content in rice husk biomass (Guo et al., 2002) which was converted to Si-O-Si groups or converted into aromatic rings of carbon (Si-C_6H_5) of the biochar, plays a key role not only in nutrient capture but also recovery and return of organic Si sources to soil.

References

ALSHAMERI, A., IBRAHIM, A., ASSABRI, A. M., LEI, X., WANG, H. & YAN, C. 2014. The investigation into the ammonium removal performance of Yemeni natural zeolite: Modification, ion exchange mechanism, and thermodynamics. *Powder Technology,* 258**,** 20-31.

ARSLAN, A. & VELI, S. 2012. Zeolite 13X for adsorption of ammonium ions from aqueous solutions and hen slaughterhouse wastewaters. *Journal of the Taiwan institute of chemical engineers,* 43**,** 393-398.

ASIAGWU, A. K. & OWAMAH, H. I. 2013. Kinetic Model for the Sorption of Ni (II), Cu (II) and Zn (II) onto Coconut (Cocos nucifera) Fibers Waste Biomass from Aqueous Solution. *Journal Of International Environmental Application And Science,* 8**,** 343.

BAOCHENG, Q., JITI, Z., XIANG, X., ZHENG, C., HONGXIA, Z. & XIAOBAI, Z. 2008. Adsorption behavior of Azo Dye CI Acid Red 14 in aqueous solution on surface soils. *Journal of Environmental Sciences,* 20**,** 704-709.

BHANDARI, A. & XU, F. 2001. Impact of peroxidase addition on the sorption– desorption behavior of phenolic contaminants in surface soils. *Environmental science & technology,* 35**,** 3163-3168.

CHEA, R., GRENOUILLET, G. & LEK, S. 2016. Evidence of water quality degradation in lower Mekong basin revealed by self-organizing map. *PloS one,* 11**,** e0145527.

CHEN, S., ZHANG, J., ZHANG, C., YUE, Q., LI, Y. & LI, C. 2010. Equilibrium and kinetic studies of methyl orange and methyl violet adsorption on activated carbon derived from Phragmites australis. *Desalination,* 252**,** 149-156.

CHEUNG, W., SZETO, Y. & MCKAY, G. 2007. Intraparticle diffusion processes during acid dye adsorption onto chitosan. *Bioresource technology,* 98**,** 2897-2904.

CHIEN, Y.-H. Water quality requirements and management for marine shrimp culture. Proceedings of the Special Session on Shrimp Farming, 1992. World Aquaculture Society Baton Rouge, LA, USA, 144-156.

CHOWDHURY, Z. Z., ZAIN, S. M., RASHID, A. & KHALID, K. 2011. Linear regression analysis for kinetics and isotherm studies of sorption of manganese (II) ions onto activated palm ash from waste water. *Orient. J. Chem,* 27**,** 405-415.

FOO, K. & HAMEED, B. 2012. Textural porosity, surface chemistry and adsorptive properties of durian shell derived activated carbon prepared by microwave assisted NaOH activation. *Chemical engineering journal,* 187**,** 53-62.

GAO, F., XUE, Y., DENG, P., CHENG, X. & YANG, K. 2015. Removal of aqueous ammonium by biochars derived from agricultural residuals at different pyrolysis temperatures. *Chemical Speciation & Bioavailability,* 27**,** 92-97.

GUO, Y., YANG, S., YU, K., ZHAO, J., WANG, Z. & XU, H. 2002. The preparation and mechanism studies of rice husk based porous carbon. *Materials chemistry and physics,* 74**,** 320-323.

GUPTA, V. K., RASTOGI, A. & NAYAK, A. 2010. Biosorption of nickel onto treated alga (Oedogonium hatei): application of isotherm and kinetic models. *Journal of Colloid and Interface Science,* 342**,** 533-539.

HAGIN, J. & TUCKER, B. 1982. *Fertilization of dryland and irrigated soils*, Springer.

HALE, S., ALLING, V., MARTINSEN, V., MULDER, J., BREEDVELD, G. & CORNELISSEN, G. 2013. The sorption and desorption of phosphate-P, ammonium-N and nitrate-N in cacao shell and corn cob biochars. *Chemosphere,* 91**,** 1612-1619.

HALIM, A. A., LATIF, M. T. & ITHNIN, A. 2013. Ammonia removal from aqueous solution using organic acid modified activated carbon. *World Applied Sciences Journal,* 24**,** 01-06.

HAMEED, B., TAN, I. & AHMAD, A. 2008. Adsorption isotherm, kinetic modeling and mechanism of 2, 4, 6-trichlorophenol on coconut husk-based activated carbon. *Chemical Engineering Journal,* 144**,** 235-244.

HO, Y.-S. & MCKAY, G. 1999. Pseudo-second order model for sorption processes. *Process biochemistry,* 34**,** 451-465.

HOU, J., HUANG, L., YANG, Z., ZHAO, Y., DENG, C., CHEN, Y. & LI, X. 2016. Adsorption of ammonium on biochar prepared from giant reed. *Environmental Science and Pollution Research,* 23**,** 19107-19115.

HUANG, Y., LI, S., LIN, H. & CHEN, J. 2014. Fabrication and characterization of mesoporous activated carbon from Lemna minor using one-step H 3 PO 4 activation for Pb (II) removal. *Applied Surface Science,* 317**,** 422-431.

IM, J.-H., WOO, H.-J., CHOI, M.-W., HAN, K.-B. & KIM, C.-W. 2001. Simultaneous organic and nitrogen removal from municipal landfill leachate using an anaerobic-aerobic system. *Water research,* 35**,** 2403-2410.

KIZITO, S., WU, S., KIRUI, W. K., LEI, M., LU, Q., BAH, H. & DONG, R. 2015. Evaluation of slow pyrolyzed wood and rice husks biochar for adsorption of ammonium nitrogen from piggery manure anaerobic digestate slurry. *Science of the Total Environment,* 505**,** 102-112.

KUMAR, P. S., RAMAKRISHNAN, K., KIRUPHA, S. D. & SIVANESAN, S. 2010. Thermodynamic and kinetic studies of cadmium adsorption from aqueous solution onto rice husk. *Brazilian Journal of Chemical Engineering,* 27**,** 347-355.

LANGMUIR, I. 1917. The constitution and fundamental properties of solids and liquids. *Journal of the Franklin Institute,* 183**,** 102-105.

LE LEUCH, L. & BANDOSZ, T. 2007. The role of water and surface acidity on the reactive adsorption of ammonia on modified activated carbons. *Carbon,* 45**,** 568-578.

LONG, X. L., CHENG, H., XIN, Z. L., XIAO, W. D., LI, W. & YUAN, W. K. 2008. Adsorption of ammonia on activated carbon from aqueous solutions. *Environmental Progress,* 27**,** 225-233.

LUNA, Y., OTAL, E., VILCHES, L., VALE, J., QUEROL, X. & PEREIRA, C. F. 2007. Use of zeolitised coal fly ash for landfill leachate treatment: A pilot plant study. *Waste Management,* 27**,** 1877-1883.

LUTERBACHER, J. S., PARLANGE, J. Y. & WALKER, L. P. 2013. A pore-hindered diffusion and reaction model can help explain the importance of pore size distribution in enzymatic hydrolysis of biomass. *Biotechnology and bioengineering,* 110**,** 127-136.

MA, Z., LI, Q., YUE, Q., GAO, B., LI, W., XU, X. & ZHONG, Q. 2011. Adsorption removal of ammonium and phosphate from water by fertilizer controlled release agent prepared from wheat straw. *Chemical Engineering Journal,* 171**,** 1209-1217.

MALOVANYY, A., SAKALOVA, H., YATCHYSHYN, Y., PLAZA, E. & MALOVANYY, M. 2013. Concentration of ammonium from municipal wastewater using ion exchange process. *Desalination,* 329**,** 93-102.

MARANON, E., ULMANU, M., FERNANDEZ, Y., ANGER, I. & CASTRILLÓN, L. 2006. Removal of ammonium from aqueous solutions with volcanic tuff. *Journal of Hazardous materials,* 137**,** 1402-1409.

MEDVEĎ, I. & ČERNÝ, R. 2011. Surface diffusion in porous media: A critical review. *Microporous and Mesoporous Materials,* 142**,** 405-422.

MORADI, O. & ZARE, K. 2013. Adsorption of ammonium ion by multi-walled carbon nanotube: kinetics and thermodynamic studies. *Fullerenes, Nanotubes and Carbon Nanostructures,* 21**,** 449-459.

MUKHERJEE, A. & ZIMMERMAN, A. R. 2013. Organic carbon and nutrient release from a range of laboratory-produced biochars and biochar–soil mixtures. *Geoderma,* 193–194**,** 122-130.

ORGANIZATION, W. H. 2004. Back ground document for evelopment of WHO Guidelines for drinking water quality. PP.

OTAL, E., VILCHES, L. F., LUNA, Y., POBLETE, R., GARCÍA-MAYA, J. M. & FERNÁNDEZ-PEREIRA, C. 2013. Ammonium ion adsorption and settleability improvement achieved in a synthetic zeolite-amended activated sludge. *Chinese Journal of Chemical Engineering,* 21**,** 1062-1068.

ÖZTÜRK, N. & BEKTAŞ, T. E. 2004. Nitrate removal from aqueous solution by adsorption onto various materials. *Journal of hazardous materials,* 112**,** 155-162.

PAETHANOM, A. & YOSHIKAWA, K. 2012. Influence of pyrolysis temperature on rice husk char characteristics and its tar adsorption capability. *Energies,* 5**,** 4941-4951.

QIAO, S., MATSUMOTO, N., SHINOHARA, T., NISHIYAMA, T., FUJII, T., BHATTI, Z. & FURUKAWA, K. 2010. High-rate partial nitrification performance of high ammonium containing wastewater under low temperatures. *Bioresource technology,* 101**,** 111-117.

RADNIA, H., GHOREYSHI, A. A. & YOUNESI, H. 2011. Isotherm and kinetics of Fe (II) adsorption onto chitosan in a batch process. *Iranica Journal of Energy and Environment,* 2**,** 250-257.

ROUQUEROL, J., AVNIR, D., FAIRBRIDGE, C., EVERETT, D., HAYNES, J., PERNICONE, N., RAMSAY, J., SING, K. & UNGER, K. 1994. Recommendations for the characterization of porous solids (Technical Report). *Pure and Applied Chemistry,* 66**,** 1739-1758.

SABBAH, I., BARANSI, K., MASSALHA, N., DAWAS, A., SAADI, I. & NEJIDAT, A. 2013. Efficient ammonia removal from wastewater by a microbial biofilm in tuff-based intermittent biofilters. *Ecological engineering,* 53**,** 354-360.

SALEH, M. E., MAHMOUD, A. H. & RASHAD, M. 2012. Peanut biochar as a stable adsorbent for removing N [H. sub. 4]-N from wastewater: a preliminary study. *Advances in environmental biology***,** 2170-2177.

SCHROEDER, J., CROOT, P., VON DEWITZ, B., WALLER, U. & HANEL, R. 2011. Potential and limitations of ozone for the removal of ammonia, nitrite, and yellow substances in marine recirculating aquaculture systems. *Aquacultural engineering,* 45**,** 35-41.

TAKAYA, C., FLETCHER, L., SINGH, S., ANYIKUDE, K. & ROSS, A. 2016. Phosphate and ammonium sorption capacity of biochar and hydrochar from different wastes. *Chemosphere,* 145**,** 518-527.

TANAKA, J. & MATSUMURA, M. 2003. Application of ozone treatment for ammonia removal in spent brine. *Advances in Environmental Research,* 7**,** 835-845.

THORNTON, A., PEARCE, P. & PARSONS, S. 2007. Ammonium removal from digested sludge liquors using ion exchange. *Water research,* 41**,** 433-439.

VU, T. M., DOAN, D. P., VAN, H. T., NGUYEN, T. V., VIGNESWARAN, S. & NGO, H. H. 2017. Removing ammonium from water using modified corncob-biochar. *Science of the Total Environment,* 579**,** 612-619.

WANG, B., LEHMANN, J., HANLEY, K., HESTRIN, R. & ENDERS, A. 2015a. Adsorption and desorption of ammonium by maple wood biochar as a function of oxidation and pH. *Chemosphere,* 138**,** 120-126.

WANG, Y., LU, J., WU, J., LIU, Q., ZHANG, H. & JIN, S. 2015b. Adsorptive Removal of
Fluoroquinolone Antibiotics Using Bamboo Biochar. *Sustainability,* 7**,** 12947-12957.

WANG, Z., GUO, H., SHEN, F., YANG, G., ZHANG, Y., ZENG, Y., WANG, L., XIAO, H. & DENG, S.
2015c. Biochar produced from oak sawdust by Lanthanum (La)-involved pyrolysis for
adsorption of ammonium (NH 4+), nitrate (NO 3−), and phosphate (PO 4 3−).
Chemosphere, 119**,** 646-653.

WEBER, W. J. & MORRIS, J. C. 1963. Kinetics of adsorption on carbon from solution. *Journal
of the Sanitary Engineering Division,* 89**,** 31-60.

WORCH, E. 2012. *Adsorption technology in water treatment: fundamentals, processes, and
modeling*, Walter de Gruyter.

YU, Q., XIA, D., LI, H., KE, L., WANG, Y., WANG, H., ZHENG, Y. & LI, Q. 2016. Effectiveness and
mechanisms of ammonium adsorption on Biochars derived from biogas residues. *RSC
Advances,* 6**,** 88373-88381.

ZENG, Z., LI, T.-Q., ZHAO, F.-L., HE, Z.-L., ZHAO, H.-P., YANG, X.-E., WANG, H.-L., ZHAO, J. &
RAFIQ, M. T. 2013. Sorption of ammonium and phosphate from aqueous solution by
biochar derived from phytoremediation plants. *Journal of Zhejiang University Science
B,* 14**,** 1152-1161.

ZHANG, H., CHEN, L., LU, M., LI, J. & HAN, L. 2016. A novel film–pore–surface diffusion model
to explain the enhanced enzyme adsorption of corn stover pretreated by ultrafine
grinding. *Biotechnology for biofuels,* 9**,** 181.

ZHU, K., FU, H., ZHANG, J., LV, X., TANG, J. & XU, X. 2012. Studies on removal of NH 4+-N
from aqueous solution by using the activated carbons derived from rice husk.
Biomass and bioenergy, 43**,** 18-25.

Chapter 5. Removal of Zinc (Zn^{2+}) from Aqueous Solution by various Vietnamese Biomass Residue–derived Biochars (wood, rice husk and bamboo)

Nguyen Van Hien[a,b], Eugenia Valsami-Jones[a] , Nguyen Cong Vinh[b], Tong Thi Phu[b], Nguyen Thi Thanh Tam[b] , Iseult Lynch[a]

[a] School of Geography, Earth and Environmental Sciences, University of Birmingham, Edgbaston, B15 2TT, UK

[b] Department of Land Use, Soils and Fertilizers Research Institute, Hanoi, Vietnam

Corresponding author: i.lynch@bham.ac.uk

Abstract

Removal of Zinc (Zn^{2+}) from aqueous solution by various biochars (BC) produced from biomass residues in Vietnam, including acacia wood chip, rice husk, and bamboo, was assessed. These residues were pyrolized by Top-Lid Updraft Drum (TLUD) technology under limited oxygen conditions. The impact of various parameters, such as adsorbent (biochar) dosages, contact time, and initial adsorbate (Zn^{2+}) concentration, were investigated in order to assess the adsorption capacity of the three biochars for Zn^{2+} representing one of the important heavy metals of high toxicity to aqueous organisms and thus whose levels in drinking water need to be strictly controlled. The experimental data was analyzed by the Langmuir and Freundlich models which indicated that the adsorption isotherm of Zn^{2+} to all three biochars was well fit by the Freundlich model. The adsorption capacity was in the order bamboo BC > rice husk BC ~ wood BC, and a pseudo-second order model was suitable to describe the adsorption kinetics of Zn^{2+} onto the three biochars. The results indicated that all three biochars are good for removal of Zn^{2+} from aqueous solution, with bamboo BC being especially efficient (removal of 96 - 98% Zn^{2+} for Zn^{2+} concentrations in the range 40-80 mg/L). The adsorption was governed by organic groups (-COOH, $-OH^-$) on the biochars which formed complexes and chelates, and via precipitation with inorganic groups (CO_3^{2-}, PO_4^{2-}) present on the biochars, rather than by ion exchange.

Key words: Adsorption, biochar, Zinc, functional groups, inorganic groups, adsorption isotherms, adsorption kinetic

1. Introduction

Contamination of aqueous environments by Inorganic pollutants is a considerable concern for many countries (Shaheen et al., 2013). These problems have been occurring especially in developing countries where wastewater and solid waste treatments or recycling are limited due to the lack of affordable treatment technologies and suitable management processes. The presence of heavy metals in the environment leads to toxicity to aqueous flora and fauna (Nadeem et al., 2006, Mohan et al., 2007), and may cause impacts to human health via the food chain (Abo-Farha et al., 2009). According to Srivastava and Majumder (2008), metal elements having atomic weights in the range 63.5 – 200.6 g/mol (or Daltons) and having a speciific gravity higher than 5.0 are called heavy metals. One of those metals that has attracted significant research is Zinc (Zn), because both plants and humans require some Zn for growth, but too much is extremely toxic. In fact, the most important role of Zn in both plants and humans is related to the activities of several enzymes (Kabata-Pendias, 2010, Dali-Youcef et al., 2006). However, excess Zn in humans leads to toxicity and effects such as vomiting, dehydration, electrolyte imbalance, abdominal pain, nausea, lethargy, dizziness and lack of muscular coordination (Dali-Youcef et al., 2006), while in plants the consequences of excess Zn include decreased growth and chlorosis (loss of their green colour from leaves) (Kabata-Pendias, 2010). Hence, the level of Zn in drinking water is limited to 3 mg/L (Organization, 2004b) to ensure that sufficient is available to meet the bodily needs, but that there is no risk of accummulation and toxicity.

The sources of Zn released into wastewater or soil environments are mainly from industrial activities such as steel production or mining activities (Mohan and Singh, 2002, Kabata-Pendias, 2010). Several technologies have been developed to control or remove heavy metal and other pollutants before they are discharged into environment, including chemical

precipitation (Gonzalez-Munoz et al., 2006, Alvarez et al., 2007, Chen et al., 2009), ion exchange (Doula, 2009, Abo-Farha et al., 2009, Hui et al., 2005), membrane filtration (Samper et al., 2009, Landaburu-Aguirre et al., 2010, Barakat and Schmidt, 2010), coagulation and flocculation (Hankins et al., 2006, Heredia and Martín, 2009, Duan et al., 2010), and adsorption (Karnib et al., 2014, Mubarak et al., 2013, Kołodyńska et al., 2012). Among these methods, the latter is now known as a potential approach for the removal of heavy metals using various adsorbents such as activated carbon (Moreno-Barbosa et al., 2013, Depci et al., 2012, Kobya et al., 2005), carbon nanotubes (Lu and Chiu, 2006, Moosa et al., 2016, Cho et al., 2009), and biochar (Beesley and Marmiroli, 2011, Han et al., 2013, Chen et al., 2011). However, activated carbon and carbon nanotubes are costly for application, so low–cost products such as biochar bring advantages especially for developing countries.

Biochar (BC) is mainly produced from biomass residues at both industrial and local levels, and can be recycled and re-used numerous times. The key feature of biochar that makes it useful for heavy metal adsorption is that it carries a lot of negative charges (Yuan et al., 2011, Yao et al., 2011) which arise mainly from acidic functional groups (-COOH, -OH$^-$) on the biochar surface. In addition, biochar also contains several inorganic groups (CO_3^{2-}, PO_4^{3-}) which combine with heavy metals to form precipitates. Therefore, the heavy metal removal by biochar combines ion exchange arising from the high Cation Exchange Capacity (CEC) of biochars with precipitation by inorganic groups to form metal salts, and chelation or complexation of metals by surface organic groups. Therefore, the adsorbent is attractive to study for water purification and soil enrichment.

Heavy metal (Zn^{2+}) removed by biochar from aquatic environments has been assessed by several studies. For example, Kołodyńska et al. (2012) used pig and cow manure-derived biochars to assess the adsorption of Cu^{2+}, Cd^{2+}, Pb^{2+}, and Zn^{2+}, and found that complexation

and precipitation mainly governed the heavy metals adsorption, with the adsorption capacity (q_e) being 50.42 - 80.88 mg/g for Zn^{2+}; 74.95 - 94.71 mg/g for Cu^{2+}; 79.55 - 122.11 mg/g for Cd^{2+}, and 153.76 - 229.98 mg/g for Pb^{2+}. Lower adsorption capacity was observed for Zn^{2+} and Cu^{2+} with 6.79 and 4.54 mg/g respectively for hard wood BC and 12.52 and 11.0 mg/g respectively for corn straw BCs by Chen et al. (2011), while the biochars produced from beech wood chips and garden green waste residues adsorbed only 0.97 - 2.23 mg/g Zn^{2+}, 1.99 – 7.80 mg/g Cd^{2+}, and 2.5 – 3.65 mg/g Cu^{2+} in studies by Frišták et al. (2015). Although the different biochars had different adsorption capacities, their experimental data were well fit by the Langmuir model which means that the adsorption resulted in formation of a monolayer on a homogenous surface. In contrast, optimal fitting with the Freundlich model was observed by Mubarak et al. (2013) for magnetic biochar, Komkiene and Baltrenaite (2016) for Scots pine and Silver birch BCs (produced at both 450 °C and 700 °C), and for five biochars produced from sugarcane bagasse, eucalyptus forest residues, castor meal, green pericarp of coconut, and water hyacinth (Doumer et al. (2016)). Hence, although biochar was found to be effective for removal of heavy metals and most studies proved surface-chemistry driven adsorption, whether the adsorption occurred on homogenous and/or heterogeneous surfaces by a monolayer and/or multilayer is still under debate, and indeed may be dependent on specific features of the biochar and its originating biomass.

Vietnam is a developing country with significant pollution issues and emerging industrialisation. Industrial production has been replacing agricultural production in several regions. Many benefits arise from the industry, but the country is faced with a polluted environment whose protection and remediation is limited by lack of management expertise and available cost-effective treatment technology. For example, an environmental accident in 2016, the so-called Formosa incident whereby waste water was discharged from Ha Tinh Formosa Steel of Taiwan's Formosa Plastics Corp in Ha Tinh province of Vietnam, resulted in

pollution of more than 125 miles of the Vietnamese coast and the death of 255 tons of fish and 64 tons of clams. However, pollution of waste water can be reduced by several of the methods mentioned above, particularly low-cost adsorbents such as biochar which can be produced from biomass residues. These by-products are abundant in the country, with readily available biomass including wood chip, rice husk, and bamboo formed after processing of the respective plants. For instance, around 8 million tons of rice husk were discharged annually (2011- 2015) from average rice production of 43 million tons (statistics from the Ministry of Agriculture and Rural Development, Vietnam). In fact, the feedstocks are normally used for cooking, as bedding for animals or are left for decomposition, while turning them into novel products like biochar for water purification or agricultural applications is still limited. Hence, in this work, three selected biomass were turned into biochar adsorbents with the aim of evaluating their effectiveness for pollutant removal using the heavy metal Zinc as an exemplar, and correlating adsorption efficiency with their physicochemical characteristics to understand the mode(s) of binding to the different biochars.

2. Materials and Methodology

2.1 Biochar preparation and characterization

The technology known as TLUD was used to produce the three biochars from acacia wood chip, rice husk, and bamboo under limited oxygen conditions at a temperature between $450^{O}C$ and $550^{o}C$. The physicochemical characterization of the biochars was described in detail in **Chapter 3**. In summary, BET surface area values were observed to follow the order rice husk BC (3.29 ±0.02 m^2/g) < bamboo BC (434.53 ±2.79 m^2/g) < wood BC (479.34 ±0.88 m^2/g). This trend was consistent with their morphology (as determined by Scanning Electron Microscopy) such as the rough outer surface and smooth inner surface for rice husk BC, the comb-like structure evident in the bamboo BC, and the hollow structure of the wood BC. In contrast, the

opposite trend was seen for CEC with rice husk BC (26.70 Cmol/kg) > bamboo BC (20.77 Cmol/kg) > wood BC (13.53 Cmol/kg). Carboxyl and hydroxyl functional groups were observed for all the biochars, while Si-O-Si asymmetric stretching was evident in the Fourier Transformed Infrared (FTIR) spectra of both wood and rice husk BC. Interestingly, silicon attachment to the ring of benzene ($Si-C_6H_5$) was only apparent in rice husk BC. As per several previous studies, the three biochars had alkaline pHs ranging from 9.51 ± 0.02 to 10.11 ± 0.04.

2.2 Biochar adsorption experiments

The stock solution (500 mg Zn^{2+}/L) was formed by dissolving $Zn(NO_3)_2.6H_2O$ in distilled water, and this was used to prepare the Zn^{2+} solutions for adsorption experiments with various Zn^{2+} and biochar concentrations. The experimental solutions were adjusted to pH 5.5 ± 0.2 by 0.1M NaOH and/or 0.1M HCl. The adsorption of Zn^{2+} onto the biochars was evaluated through methods modified from Kołodyńska et al. (2012) and Xu et al. (2013b) with systematic variation of the initial concentrations of adsorbate (5g biochar mixed with 40mL of 0, 20, 40, 60, 80, 160, and 320 mg Zn^{2+}/L and shaken for 24h), different dosages of adsorbent (0, 0.25, 0.75, and 1.0 g of the BC mixed with 40mL of 60mg Zn^{+2}/L and shaken for 24h), and different contact times (0.5g biochar mixed with 40mL of 60mg Zn^{+2}/L and shaken for 30, 60, 90, 120, 150, 180, and 240 mins). The suspensions were shaken on orbital shaker at 300 rpm to reach the desired times at ambient temperature (20 ± 0.5 °C). At the appointed time, the suspensions were centrifuged at 5,000 rpm for 5 mins and the supernatants filtered by acrodisc syringe filter (0.20 μm). The Zn^{2+} concentration in the filtered supernatant was measured by Flame Atomic Adsorption Spectrometry (Perkin Elmer AAnalyst 300 model) with various standards (0, 0.25, 0.5, 1.0 and 2.0 ppm Zn^{2+}). All the experiments were conducted in thriplicate. The Zn^{2+} adsorption onto biochar at equilibrium (q_e), at t time (q_t), and the proportion of removal (%) were calculated using the equations presented below.

For equilibrium experiments:

$$q_e = \frac{(C_o - C_e)V}{m} \quad (1) \qquad \text{and} \qquad \%\text{removal} = \frac{C_o - C_e}{C_o} \times 100 \ (2)$$

where C_o and C_e are the initial and equilibrium concentrations of Zn^{2+}; V (L) is the volume of

the adsorbate (Zn^{2+} in this case); and m is the mass of adsorbent (biochar in this case) (g).

For the contact time experiments:

$$q_t = \frac{(C_o - C_t)V}{m} \quad (3) \quad \text{and} \quad \%\text{removal} = \frac{C_o - C_t}{C_o} \times 100 \ (4)$$

where C_o (mg/L) and C_t (mg/L) are the initial and time t concentrations of Zn^{2+}; V (L) is the

volume of the adsorbate solution; and m is the dosage of adsorbent (g).

Data analysis

The Langmuir isotherm and Freundlich isotherm models were used to evaluate the adsorption

of Zn^{2+} onto the three biochars. The theory of Langmuir (1917) assumes that adsorption of an

adsorbate onto an adsorbent take place as a homogenous surface monolayer (Long et al.,

2008) with constant adsorption heat for all active sites and no interactions between the

adsorbed molecules (Chowdhury et al., 2011, Gupta et al., 2010). The model equation is as

follows:

$$\frac{1}{q_e} = \frac{1}{q_{max}} + \frac{1}{q_{max}K_L}\frac{1}{C_e} \quad (5)$$

where q_e (mg/g) and q_{max} (mg/g) are the adsorption capacity of the adsorbent and the

maximum monolayer adsorption capacity of the adsorbent in equilibrium, respectively; K_L

(L/mg) is the Langmuir adsorption constant relating to the adsorption energy; C_e (mg/L) is the

concentration of the adsorbate at equilibrium.

The theory of Freundlich (1906) assumes that the adsorbate molecules adsorb onto the adsorbent as a heterogeneous multilayer (Long et al., 2008) with unequal adsorption heats for the adsorption sites (Chowdhury et al., 2011). The equation is described as follows:

$$\ln q_e = \frac{1}{n}\ln C_e + \ln K_F \ (6)$$

where q_e (mg/g) and C_e (mg/L) are the adsorption capacity of adsorbent and concentration of adsorbate in equilibrium, respectively; $1/n$ is the intensity of adsorption; and K_F (mg/g) is the Freundlich affinity coefficient.

Adsorption Kinetics:

The adsorption mechanism of porous adsorbents can be assessed by Pseudo-first order and Pseudo-second order models to understand the adsorption kinetics. The equations with linear form are shown, respectively as follows:

$$\ln\left(q_{e\text{-}exp} - q_t\right) = \ln q_{e\text{-}cal1} - k_1 t \ (8) \quad \text{and} \quad \frac{t}{q_t} = \frac{1}{k_2 q_{e\text{-}cal2}^2} + \frac{t}{q_{e\text{-}cal2}} \ (9)$$

where $q_{e\text{-}exp}$ (mg/g) is the experimentally obtained adsorption capacity of adsorbent at equilibrium; q_t (mg/g) is the amount of adsorbate adsorbed onto the biochar at time t (min); k_1 (min^{-1}) and k_2 (g/mg min) are the Pseudo-first order and Pseudo-second order rate constants, respectively; $q_{e\text{-}cal1}$ is calculated from plots of $\ln(q_{e\text{-}cal1} - q_t)$ versus t, while $q_{e\text{-}cal2}$ is obtained from plots of t/q_t versus t.

Intraparticle diffusion model:

The intraparticle diffusion model, based on the theory of Weber and Morris (1963), was used to evaluate the diffusion mechanisms of the porous adsorbents. The equation is given as:

$$q_t = k_{id} t^{1/2} + C \quad (10)$$

where k_{id} is the rate constant of the intraparticle diffusion (mg/g min$^{1/2}$), and C is the thickness of the boundary layer. C and k_{id} are calculated from the plot of q_t versus $t^{1/2}$.

3. Results and discussion

3.1 Effect of Zinc concentration on the adsorption capacity of biochars

The impact of different initial Zn^{2+} concentrations on adsorption ability and % Zn^{2+} removal of the biochars at a constant adsorbent value (12.5g/L) is shown in Figure 1. The results indicated that the Zn^{2+} adsorption onto the three biochars increased as the initial Zn^{2+} concentration increased. In fact, there was a sharp increase in the adsorption for bamboo BC when the adsorbate concentrations rose from 20 mg/L to 80 mg/L, while this trend occurred for rice husk and wood BCs at Zn^{2+} concentration lower than 40 mg/L. The adsorption to the three biochars slowed down gradually at the higher concentrations (e.g., > 80 mg Zn^{2+}/L for bamboo BC or > 40 mg Zn^{2+}/L for both wood BC and rice husk BC). Interestingly, all three biochars had similar adsorption abilities when the Zn^{2+} concentrations were lower than 40mg/L, while at the the higher Zn^{2+} concentrations the adsorption capacity followed the order bamboo BC > wood BC ~ rice husk BC for.
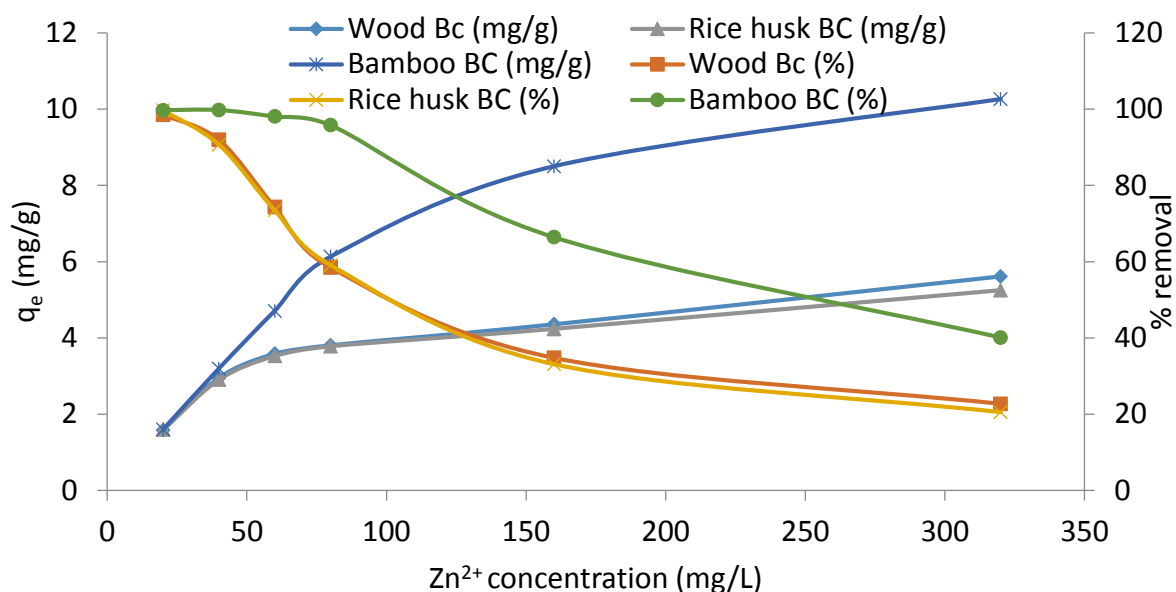
Figure 1: Effect of initial adsorbate (Zn^{2+}) concentration on Zn^{2+} adsorption by biochar, where the biochar concentration was constant at 12.5 g/L, plotted as adsorption at equilibrium, q_e, and as the proportion of initial Zn^{2+} removed (%).

The Zn^{2+} removal (%) by the biochars, however, had an opposite trend compared to the adsorption (see Figure 1). In fact, although the % removals showed a dramatic decrease, the Zn^{2+} total (mg) removed by the biochars (12.5g/L) increased with enhancing the initial concentrations (see Table 1). For instance, when increasing the adsorbate concentration from 20 mg/L to 320 mg/L, the total amount of Zn^{2+} removed by both wood BC and rice husk BC was similar and increased from 19.76 ± 0.50 mg/L to 70.18 ± 3.40 mg/L. The increase in the total amount of Zn^{2+} removed also was observed for bamboo BC but with higher amounts, rising from 19.95 ± 0.02 mg/L to 128.30 ± 3.11 mg/L based on 12.5g biochar.

Table 1. The mass of Zn^{2+} removed by biochar at the various initial Zn^{2+} concentrations.

Zn^{2+} initial Conc (mg/L)	Wood BC		Rice husk BC		Bamboo BC	
	C_e, mg/L	Removal[1], mg	C_e, mg/L	Removal[2], mg	Ce, mg/L	Removal[3], mg
20	0.24±0.05	19.76±0.05	0.07±0.01	19.93±0.01	0.05±0.02	19.95±0.02
40	3.13±0.07	36.87±0.07	3.71±0.25	36.29±0.25	0.08±0.00	39.92±0.00
60	15.23±0.69	44.77±0.69	15.91±0.76	44.09±0.76	1.16±0.08	58.84±0.08
80	32.43±0.71	47.57±0.71	32.75±0.1.26	47.25±1.26	3.37±0.42	76.63±0.42
160	105.55±1.02	54.45±1.02	107.04±4.74	52.96±4.74	53.74±0.53	106.26±0.53
320	249.82±3.40	70.18±3.40	254.38±1.15	65.62±1.15	191.70±3.11	128.30±3.11

Note: The biochar concentration was constant (12.5g/L); C_e (mg/L) was the Zn^{2+} concentration in the filtered supernatant. The Zn^{2+} removal[1,2&3] (mg) was calculated for 12.5g biochar (total).

Interestingly, the biochar concentration of 12.5 g/L for both wood BC and rice husk BC could remove 99% of the Zn^{2+} in the solution containing 20 mg Zn^{2+}/L, while 90-92% removals were observed for the solution of 40 mg Zn^{2+}/L, which nearly meets the requirement for drinking water quality, which require values <3.0 mg Zn^{2+}/L (Organization, 2004b), where the residual Zn^{2+} concentrations were 3.13 ± 0.07 mg/L for wood BC and 3.71 ± 0.25 mg/L for rice husk BC following incubation for 24 hours. In contrast, bamboo BC (12.5 g/L) could remove more than 98% of Zn^{2+} (the residual Zn^{2+} concentrations = 0.05 ± 0.02-1.16 ± 0.08 mg/L) from the 20 and 40 mg/L solutions, resulting in water that was fully compliant with the drinking water requirements, whereas 96% removal (residual Zn^{2+} concentration 3.37 ± 0.42 mg/L) was seen for the solution with initial concentration of 80 mg Zn^{2+}/L (see Figure 1 & Table 1). Hence, bamboo BC is better able to remove heavy metal (Zn^{2+}) at higher contamination levels than wood or rice husk BCs.

3.2 Effect of biochar dosage on Zinc adsorption

The results of Zn^{2+} ion adsorbption onto the three biochars at various biochar masses are shown in Figure 2. The results indicate that increasing the concentrations of biochar actually decreases the adsorption effectiveness of all three biochars for Zn^{2+} at the Zn^{2+} concentrations evaluated. These trends were similar to several previous reports, such as Chen et al. (2011) for hard wood and corn straw BCs, Kołodyńska et al. (2012) for pig and cow manure BCs or Pellera et al. (2012) for rice husk, olive pomance, orange waste, and compost BCs (for Cu^{2+} adsorption). For example, when the adsorbent dosage increased four-fold from 6.25g/L to 25g/L, the Zn^{2+} adsorption onto wood BC and rice husk BC decreased by half from 4.06 ± 0.27 mg Zn^{2+}/g biochar to 2.06 ± 0.01 mg Zn^{2+}/g biochar, while the adsorption reduction of bamboo BC was even greater going from 6.97 ± 0.12 mg Zn^{2+}/g biochar to 2.35 ± 2.16 mg Zn^{2+}/g biochar.
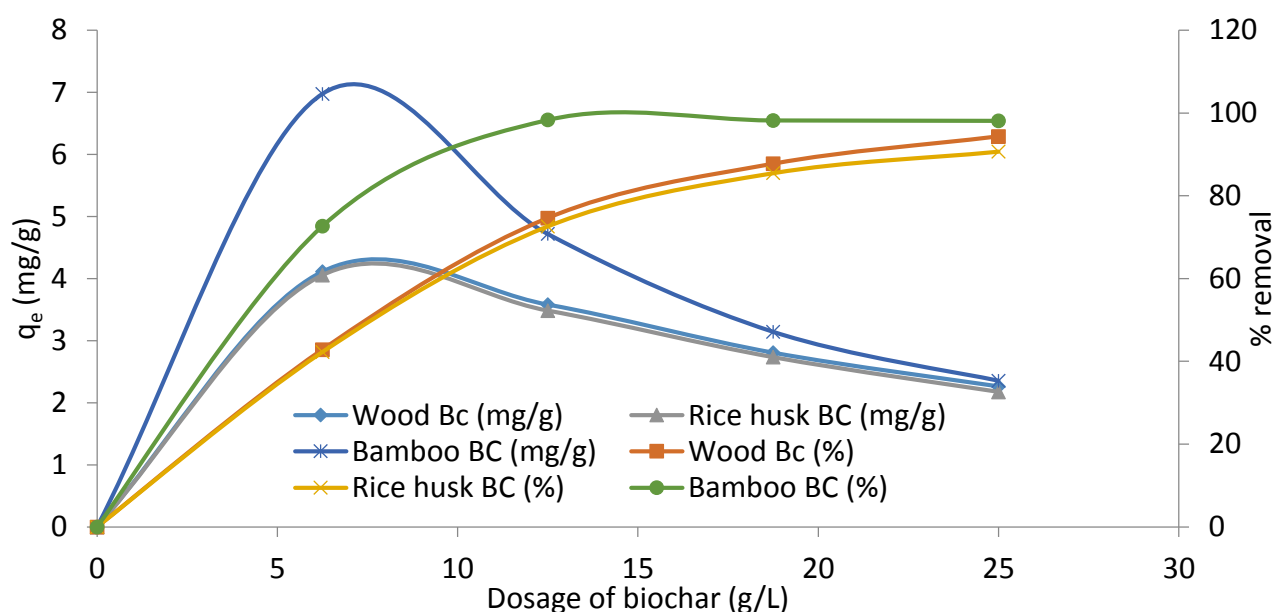
Figure 2: Effect of adsorbent (biochar) concentration on Zn^{2+} adsorption at constant Zn^{2+} concentration (60 mg/L), plotted as adsorption at equilibrium, q_e, and as the proportion of initial Zn^{2+} removed (%).

The trend of Zn^{2+} removal (%) increased with increacing adsorbent concentration. For instance, there was a sharp increase in the Zn^{2+} removal for the three biochars when the adsorbent mass was increased from 6.25 g/L to 12.5 g/L. Beyond 12.5 g/L biochar, the %

removal remained stable at around 98% for bamboo BC at biochar contents ≥ 12.5 g/L, while % removal by both wood BC and rice husk BC decreased gradually. These results indicated that the adsorbent dosage of 12.5g/L was a turning point of adsorption for the biochars for 60mg/L of adsorbate, and for this reason 12.5 g/L was chosen as the biochar dosage for the subsequent experiments in this study. Note however, that this would need to be reconfirmed if higher absorbate concentration solutions were to be remediated, e.g. wastewater sludge.

The adsorption mechanism of Zn^{2+} onto the biochar remains unclear. In fact, rice husk BC has the highest CEC (26.70 ± 1.57 Cmol/kg and the lowest BET surface area (3.29 m^2/g), but had similar adsorption capacity as wood BC whose CEC is much lower at 13.53 ± 0.65 Cmol/kg and whose BET surface area is much higher at 479.34 m^2/g. Additionally, the removal and adsorption capacity of all three biochars were similar when the biochar concentration reached 25g/L. Further analysis of the data was thus performed to shed light on the adsorption mechanisms.

3.3 Effect of contact time on Zinc adsorption by biochars

The effect of contact time on adsorption capacity and % removal of Zn^{2+} by the three biochars is presented in Figure 3. The data showed that the adsorption capacity and removal of Zn^{2+} by the three biochars were quite different, and followed the order bamboo BC > rice husk BC > wood BC with increasing contact time. There was a fast adsorption for Bamboo BC in the first period (30 mins) with 90.64 ± 1.75 % of Zn^{2+} removed, and the removal increased slowly (an additional 4.15 ± 1.49 %) after 240 mins before reaching equilibrium.
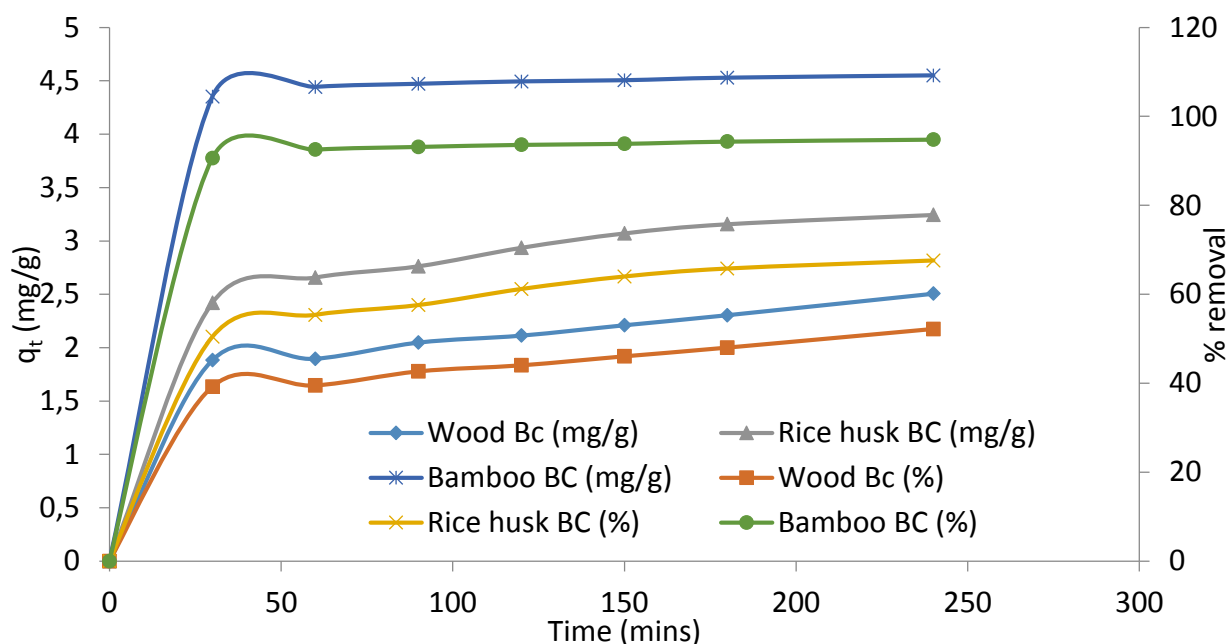
Figure 3. Effect of contact time on biochar adsorption capacity, plotted as adsorption at time t, q_t, and as the proportion of initial Zn^{2+} removed (%). Adsorbent and adsorbate concentrations were 0.5g and 60 mg/L, respectively.

In contrast, wood BC and rice husk BC both showed a gradual increase, although higher adsorption was seen for the later. The removal of Zn^{2+} by rice husk BC in the first 30 mins and after 240 mins was 50.43 ± 7.01 % and 67.59 ± 1.28 %, respectively, while only 52.19 ± 1.28 % of the adsorbate was removed over 240 mins by wood BC. Interestingly, although the same biochars were used for NH_4^+ adsorption experiments, the adsorption trend for Zn^{2+} was different than that of NH_4^+ during the contact time experiments. Thus, it could be concluded that the adsorption capacity depends not only on the adsorbents but also the adsorbate type, as different adsorption mechanisms are available.

3.4 Adsorption Isotherms

The Langmuir and Freundlich Isotherm models are normally used to describe the relationship of the initial concentration of adsorbate (Zn^{2+}) in solution and the adsorbate content adsorbed by the adsorbent (biochar) at equilibrium at a certain temperature and pH. The Zn^{2+} adsorbed onto the biochars was analyzed to identify which model best describes (fits) the adsorption of

130

adsorbate onto the biochar surface: i.e., whether the adsorption results in monolayer or multilayer formation according to the theory of the two models. The Zn^{2+} adsorption isotherm was constructed using the data of the effect of initial concentration of Zn^{2+} which ranged from 20 mg/L to 320 mg/L on adsorption, as presented previously (Figure 1). The fitting parameters obtained from the two models are shown in Table 1.

Table 2. Langmuir and Freundlich constants derived from the data for Zn^{2+} adsorption onto the three biochars studied (wood, rice husk and bamboo).

Adsorbent	Langmuir model			Freundlich model		
	q_{max}	K_L	R^{2*}	K_F	$1/n$	R^{2**}
Wood BC	4.02	2.62	0.9257	2.17	0.16	0.9668
Rice husk BC	3.82	1.03	0.9030	2.35	0.14	0.9924
Bamboo BC	7.62	5.63	0.8981	4.73	0.15	0.9915

Note: q_{max}, K_L, and R^{2*} were obtained by plotting $1/q_e$ versus $1/C_e$ (equation 5), while K_F, $1/n$ and R^{2**} were calculated from a plot of $\ln q_e$ versus $\ln C_e$ (equation 6), respectively, using the data from Figure 1.

The parameters indicated that the Freundlich model (R^2=0.9668-0.9924) is a better fit to the data than the Langmuir model (R^2=0.8981-0.9257), as indicated by the linear regression values. The q_{max} values of the Langmuir model, calculated from the plot of $1/q_e$ versus $1/C_e$ were also lower than the q_e values from experiments (see Figure 1). In addition, the heterogeneity coefficient ($1/n$) of the three biochars was in the range between 0 and 1, which indicated favourable adsorption (Radnia et al., 2011). This trend was also supported by Mubarak et al. (2013) for magnetic biochar, Komkiene and Baltrenaite (2016) for biochars produced from Scots pine (*P. Sylvestris L.*) and Silver birch (*B. bendula*) plants (at 450 ºC and 700 ºC), Doumer et al. (2016) for five biochars produced from sugarcane bagasse, eucalyptus forest residues, castor meal, green pericarp of coconut, and water hyacinth. However, these

findings were opposite to several previous studies which supported a Langmuir model to explain the adsorption of the heavy metal (Zn^{2+}) to biochars, such as Chen et al. (2011) for hardwood BC (450 ^oC) and corn straw BC (600 ^oC), Kołodyńska et al. (2012) for pig and cow manure BCs (400 ^oC and 600 ^oC), Han et al. (2013) for swithgrass and wood BC (500 ^oC), Frišták et al. (2015) for beech wood chip BC and garden waste green residue BC (500 ^oC). Thus, biochars produced from different biomasses and at various temperatures were found to have different adsorption capacities and adsorption mechanisms for Zinc. In this study Zn^{2+} adsorption onto the three biochars was best fit using the Freundlich model, which means that the adsorption occurred as a heterogeneous surface multilayer. The mechanism for the Zn^{2+} adsorption by biochar will be explained in more detail in Sections 3.5 & 3.6.

3.5 Adsorption Kinetics

The adsorption mechanism of the adsorbate (Zn^{2+}) by the biochars was evaluated through adsorption kinetics studies. Two kinetics models were investigated, a Pseudo-first order and a Pseudo-second order model, were used to identify the adsorption mechanism. Both linear regression coefficients (R^2) and q_{e-cal} values are normally used to assess the goodness of fit of kinetics models. The parameters obtained from the two models are shown in Table 2.

Table 3. Rate parameters for the adsorption of Zn^{2+} onto the three biochars (wood BC = WBC, rice husk BC = RBC, and bamboo BC = BBC)

Biochar	Pseudo first order				Pseudo second order			Intraparticle diffusion		
	q_{e-exp}	q_{e-cal}	K_1	R^2	q_{e-cal}	K_2	R^2	K_{id}	C	R^2
WBC	3.58	1.88	0.002	0.9792	2.64	0.017	0.9897	0.064	1.46	0.9487
RBC	3.53	1.33	0.413	0.9885	3.45	0.016	0.9979	0.086	1.98	0.9834
BBC	4.71	0.32	0.003	0.9232	4.58	0.110	1.0000	0.019	4.28	0.9260

It can be seen that the pseudo first order model did not fit well to the experimental data (data from Figure 3). This finding was proven by the q_{e-cal} values (0.32-1.88 mg/g) which were observed to be much lower than the experimental values (q_{e-exp} = 3.58-4.71 mg/g), and the linear regression coefficient values (R^2 = 0.9232-0.9885) were lower than those obtained from the pseudo second order model (R^2 = 0.9897-1). In contrast, the values of q_{e-cal} (2.64-4.58 mg/g) calculated from the pseudo second order model were similar to the experimental values, and the R^2 values were higher than those of Pseudo first order model, particularly for bamboo BC (R^2= 1). The high correlation coefficients ($\geq$ 0.9897) suggest that the Pseudo second order model could be applied for the entire adsorption process in all three biochars.

Furthermore, it could be concluded that the rate-limiting step of the adsorption of Zn^{2+} onto the biochars was controlled by chemical adsorption occurring on the heterogeneous biochar surface as a result of multilayer adsorption. These findings were also supported by Kołodyńska et al. (2012) for pig and cow manure BCs, by Chen et al. (2011) for hard wood BC and corn straw BC, and by Mubarak et al. (2013) for magnetic biochars. According to Kołodyńska et al. (2012), inner-sphere complexation, i.e., ions binding directly to the surface with no intervening water molecules, and precipitation were responsible for the Zn^{2+} adsorption to the biochars, while electrostatic-driven ion exchange played essentially no role in the adsorption process.
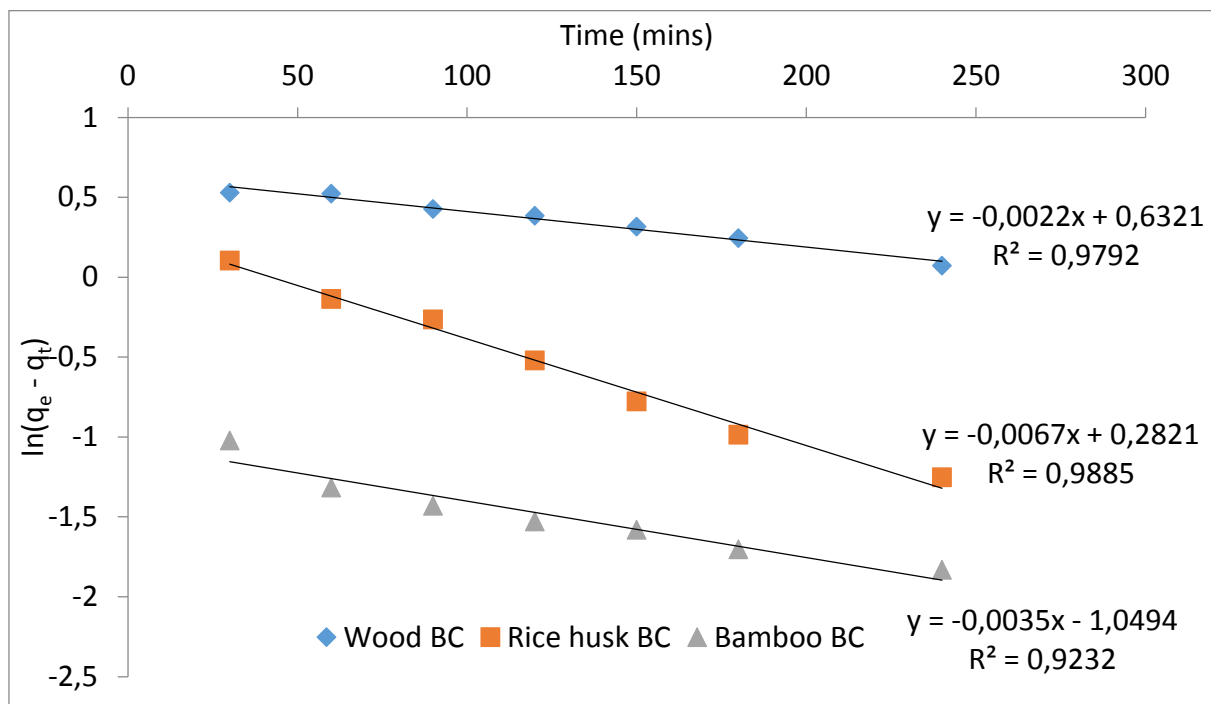
Figure 4. Plot of ln (q_e-q_t) versus t by using data of q_t (mg/g) and t (mins) from Figure 3, and $q_{e\text{-exp}}$ (mg/g) from Table 2) and fitting with the Pseudo – first order model

According to Xu et al. (2013a), heavy metal ions formed the complexation with negatively charged surface functional groups (e.g. hydroxyl groups) was reported by and/or precipitate with PO_4^{3-} and CO_3^{2-} groups. All of these organic and inorganic groups were reported to be present in the three Vietnamese biochars studied here (see section 3.3 in chapter 3). The negligible adsorption of Zn^{2+} via electrostatic cation exchange was evidenced by rice husk BC which had the highest CEC (26.70 ±1.57 Cmol/kg) in comparison with wood BC (13.53 ±0.65 Cmol/kg) and bamboo BC (20.77 ±1.21 Cmol/kg), but which had a similar adsorption capacity as wood BC (see Figures 1 & 2). These findings were opposite to the adsorption behaviour of the same three biochars for NH_4^+-N, which was adsorbed in the order rice husk BC > bamboo BC > wood BC, indicating that depending on the nature of the pollutant to be remediated different biochars will be more or less suitable, depending on the mechanism of adsorption and the surface functionalization of the specific biochar. Clearly, adsorption via cation

exchange was not the driving factor governing the adsorption of Zn^{2+} onto the three Vietnamese biochars.
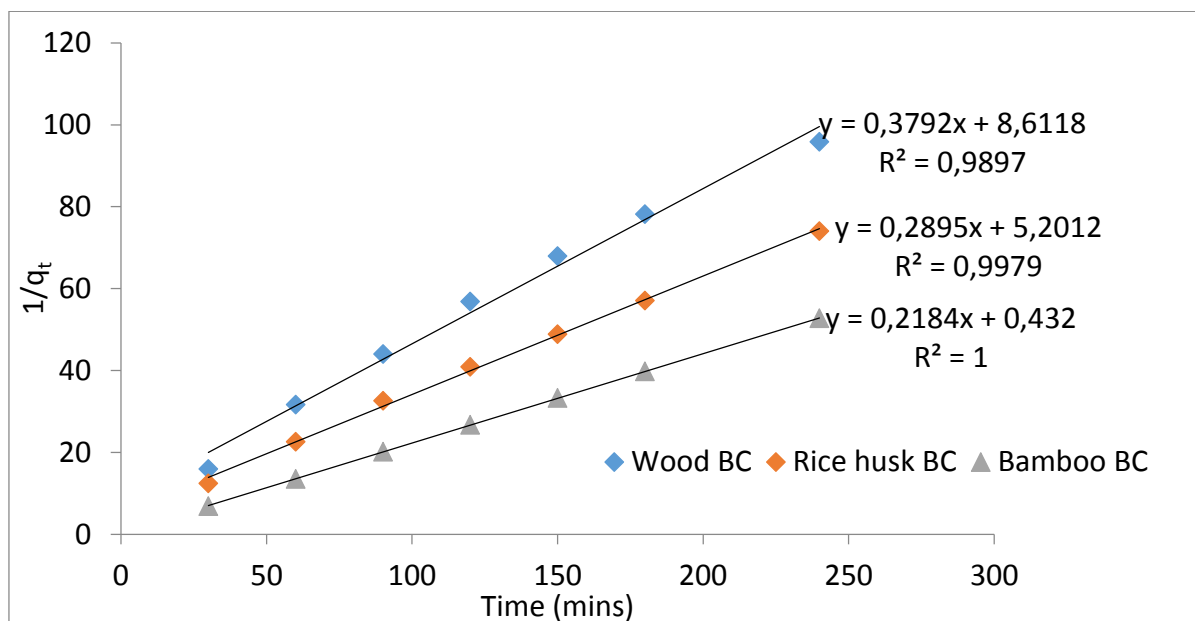
Figure 5. Plot of $1/q_t$ versus t (data from Figure 3) fit using the pseudo – second order model.

3.6 Intraparticle diffusion

Intraparticle diffusion is normally investigated in order to understand the diffusion mechanism of an adsorbate onto a porous adsorbent like biochar. Thus, the Weber and Morris model (Equation 10) was used to stimulate the adsorption process of Zn^{2+} ions onto the biochars, by plotting q_t versus $t^{1/2}$. If the plot is linear and passes through the origin, intraparticle diffusion is the sole rate limiting step in the adsorption process (Foo and Hameed, 2012). However, the plot did not pass via the origin (see Figure 6), so the adsorption process of Zn^{2+} onto the biochars by intraparticle diffusion occurred in more than one step. The intraparticle diffusion of Zn^{2+} adsorbed onto the three biochars was presented in Figure 6 and the model fitting parameters are shown in Table 2.
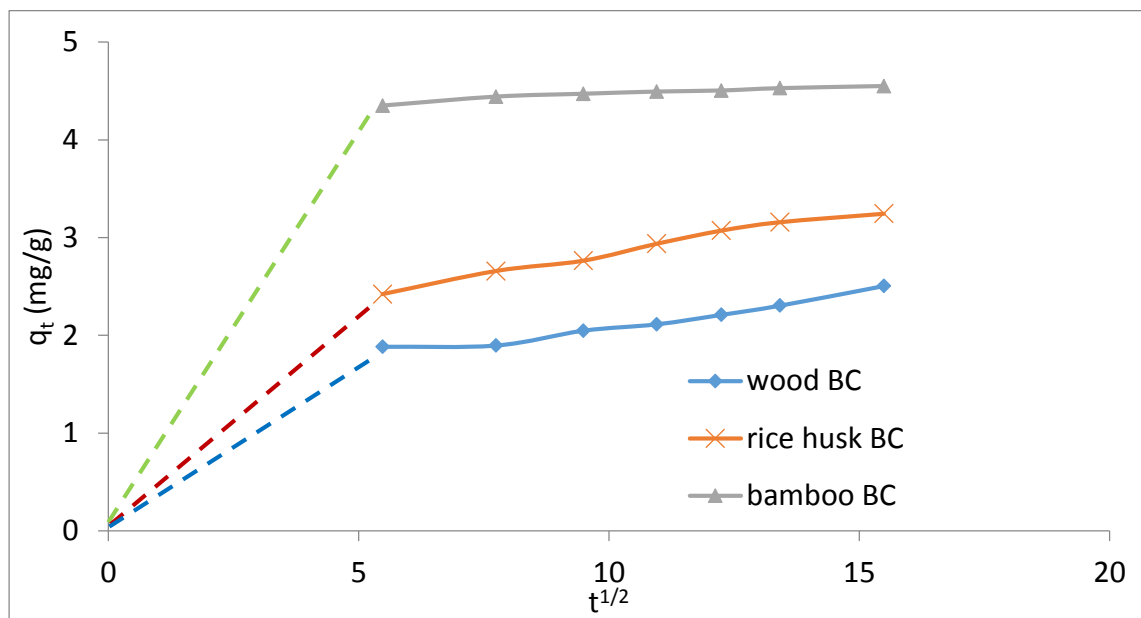
Figure 6. Intraparticle diffusion plots for Zn^{2+} ions adsorbed onto the biochars. The value of q_t and the square root of t ($t^{1/2}$) were calculated using values from Figure 3.

It could be seen that the first steep increase (see Figure 6) during the initial 30 mins (around 5.5 $min^{1/2}$) was the diffusion of Zn^{2+} ions through the boundary layer (film) which surrounds the biochar particles to the external surface of the biochar. After that, the pore diffusion and/or surface diffusion (intraparticle diffusion) of Zn^{2+} ions in the porous system of the biochars took place over 30-60 mins (around 5.5 -7.7 $min^{1/2}$) for bamboo BC, and over 30-150 mins (around 5.5 -13.4 $min^{1/2}$) for both rice husk and wood BCs. Worch (2012) reported that intraparticle diffusion mainly occurs in the macrospores (>50 nm) and mesopores (2-50 nm) of biochars, whereas the microspore volume (<2 nm) as per the classification of the International Union of Pure and Applied Chemistry (Rouquerol et al., 1994) is attributed to adsorption. The final steps in the Zn^{2+} absorption were observed to be the slowdown of the diffusion which occurred after 60 mins (7.7 $min^{1/2}$) for bamboo BC, while after 150 mins (7.7 $min^{1/2}$) for both rice husk and wood BCs. The decrease of the diffusion was caused by the low concentration of adsorbate in solution (Cheung et al., 2007) and the porous system (macrospores and mesopores) becoming filled by adsorbate. In comparison, the diffusion of

Zn^{2+} onto the biochars was different compared to that of NH_4^+ (see Hien et al, 2018b) from which it may be concluded that diffusion depends not only on the structure of the adsorbent but also on the nature and chemistry of the adsorbent. In this case, bamboo BC had the biggest boundary layer (C_i=4.28) and the lowest rate constant for intraparticle diffusion with k_i=0.019 (see Table 2), but it had the highest adsorption capacity for Zn^{2+}. Thus, the increase of thickness of boundary layer enhanced the driving force of adsorption process.

4. Conclusion

The biomass residue–derived biochars from Vietnam showed good results for adsorption of Zn^{2+} from aqueous solution, especially bamboo BC. The data for Zn^{2+} adsorption onto the biochars fit the Freundlich model and thus occurred as a heterogeneous multilayer adsorption to the surface. The process was governed by chemical adsorption, mainly based on complexation (organic groups) and precipitation (inorganic groups) rather than via the classical cation exchange. The adsorption capacity of the three biochars for Zn^{2+} was in the order bamboo BC > wood BC ~ rice husk BC. The biochar adsorption increased with increasing adsorbent (biochar) concentrations for the three biochars, while only the adsorption to bamboo BC increased as the concentration of adsorbate (Zn^{2+}) increased. The results in this study indicated that the biochars produced from wood, rice husk, and bamboo biomass area promising adsorbents for heavy metal removal from wastewater, particularly bamboo BC. In fact, bamboo BC (12.5g/L) could remove 96% of Zn^{2+} from the aqueous solution containing Zn^{2+} concentration up to 80 mg/L (see section 3.1). In addition, bamboo biochar also proved to have a significant removal capacity for textile dyes (Yang et al., 2014, Mui et al., 2010). Thus, bamboo biochar is a promising product as a low cost and eco-friendly adsorbent for removing multiple contaminants from aqueous solution.

Acknowledgements

References

ABO-FARHA, S., ABDEL-AAL, A., ASHOUR, I. & GARAMON, S. 2009. Removal of some heavy metal cations by synthetic resin purolite C100. *Journal of hazardous materials,* 169**,** 190-194.

ALVAREZ, M. T., CRESPO, C. & MATTIASSON, B. 2007. Precipitation of Zn (II), Cu (II) and Pb (II) at bench-scale using biogenic hydrogen sulfide from the utilization of volatile fatty acids. *Chemosphere,* 66**,** 1677-1683.

BARAKAT, M. & SCHMIDT, E. 2010. Polymer-enhanced ultrafiltration process for heavy metals removal from industrial wastewater. *Desalination,* 256**,** 90-93.

BEESLEY, L. & MARMIROLI, M. 2011. The immobilisation and retention of soluble arsenic, cadmium and zinc by biochar. *Environmental Pollution,* 159**,** 474-480.

CHEN, Q., LUO, Z., HILLS, C., XUE, G. & TYRER, M. 2009. Precipitation of heavy metals from wastewater using simulated flue gas: sequent additions of fly ash, lime and carbon dioxide. *Water research,* 43**,** 2605-2614.

CHEN, X., CHEN, G., CHEN, L., CHEN, Y., LEHMANN, J., MCBRIDE, M. B. & HAY, A. G. 2011. Adsorption of copper and zinc by biochars produced from pyrolysis of hardwood and corn straw in aqueous solution. *Bioresource technology,* 102**,** 8877-8884.

CHEUNG, W., SZETO, Y. & MCKAY, G. 2007. Intraparticle diffusion processes during acid dye adsorption onto chitosan. *Bioresource technology,* 98**,** 2897-2904.

CHO, H.-H., WEPASNICK, K., SMITH, B. A., BANGASH, F. K., FAIRBROTHER, D. H. & BALL, W. P. 2009. Sorption of aqueous Zn [II] and Cd [II] by multiwall carbon nanotubes: the relative roles of oxygen-containing functional groups and graphenic carbon. *Langmuir,* 26**,** 967-981.

CHOWDHURY, Z. Z., ZAIN, S. M., RASHID, A. & KHALID, K. 2011. Linear regression analysis for kinetics and isotherm studies of sorption of manganese (II) ions onto activated palm ash from waste water. *Orient. J. Chem,* 27**,** 405-415.

DALI-YOUCEF, N., OUDDANE, B. & DERRICHE, Z. 2006. Adsorption of zinc on natural sediment of Tafna River (Algeria). *Journal of hazardous materials,* 137**,** 1263-1270.

DEPCI, T., KUL, A. R. & ÖNAL, Y. 2012. Competitive adsorption of lead and zinc from aqueous solution on activated carbon prepared from Van apple pulp: study in single-and multi-solute systems. *Chemical Engineering Journal,* 200**,** 224-236.

DOULA, M. K. 2009. Simultaneous removal of Cu, Mn and Zn from drinking water with the use of clinoptilolite and its Fe-modified form. *Water Research,* 43**,** 3659-3672.

DOUMER, M., RIGOL, A., VIDAL, M. & MANGRICH, A. 2016. Removal of Cd, Cu, Pb, and Zn from aqueous solutions by biochars. *Environmental Science and Pollution Research,* 23**,** 2684-2692.

DUAN, J., LU, Q., CHEN, R., DUAN, Y., WANG, L., GAO, L. & PAN, S. 2010. Synthesis of a novel flocculant on the basis of crosslinked Konjac glucomannan-graft-polyacrylamide-co-sodium xanthate and its application in removal of Cu 2+ ion. *Carbohydrate Polymers,* 80**,** 436-441.

FOO, K. & HAMEED, B. 2012. Textural porosity, surface chemistry and adsorptive properties of durian shell derived activated carbon prepared by microwave assisted NaOH activation. *Chemical engineering journal,* 187**,** 53-62.

FREUNDLICH, H. 1906. Over the adsorption in solution. *J. Phys. Chem,* 57**,** e470.

FRIŠTÁK, V., PIPÍŠKA, M., LESNÝ, J., SOJA, G., FRIESL-HANL, W. & PACKOVÁ, A. 2015. Utilization of biochar sorbents for Cd2+, Zn2+, and Cu2+ ions separation from aqueous solutions: comparative study. *Environmental monitoring and assessment,* 187**,** 4093.

GONZALEZ-MUNOZ, M. J., RODRIGUEZ, M. A., LUQUE, S. & ALVAREZ, J. R. 2006. Recovery of heavy metals from metal industry waste waters by chemical precipitation and nanofiltration. *Desalination,* 200**,** 742-744.

GUPTA, V. K., RASTOGI, A. & NAYAK, A. 2010. Biosorption of nickel onto treated alga (Oedogonium hatei): application of isotherm and kinetic models. *Journal of Colloid and Interface Science,* 342**,** 533-539.

HAN, Y., BOATENG, A. A., QI, P. X., LIMA, I. M. & CHANG, J. 2013. Heavy metal and phenol adsorptive properties of biochars from pyrolyzed switchgrass and woody biomass in

correlation with surface properties. *Journal of environmental management,* 118**,** 196-204.

HANKINS, N. P., LU, N. & HILAL, N. 2006. Enhanced removal of heavy metal ions bound to humic acid by polyelectrolyte flocculation. *Separation and Purification Technology,* 51**,** 48-56.

HEREDIA, J. B. & MARTÍN, J. S. 2009. Removing heavy metals from polluted surface water with a tannin-based flocculant agent. *Journal of hazardous materials,* 165**,** 1215-1218.

HUI, K., CHAO, C. Y. H. & KOT, S. 2005. Removal of mixed heavy metal ions in wastewater by zeolite 4A and residual products from recycled coal fly ash. *Journal of Hazardous Materials,* 127**,** 89-101.

KABATA-PENDIAS, A. 2010. *Trace elements in soils and plants*, CRC press.

KARNIB, M., KABBANI, A., HOLAIL, H. & OLAMA, Z. 2014. Heavy metals removal using activated carbon, silica and silica activated carbon composite. *Energy Procedia,* 50**,** 113-120.

KOBYA, M., DEMIRBAS, E., SENTURK, E. & INCE, M. 2005. Adsorption of heavy metal ions from aqueous solutions by activated carbon prepared from apricot stone. *Bioresource technology,* 96**,** 1518-1521.

KOŁODYŃSKA, D., WNĘTRZAK, R., LEAHY, J., HAYES, M., KWAPIŃSKI, W. & HUBICKI, Z. 2012. Kinetic and adsorptive characterization of biochar in metal ions removal. *Chemical Engineering Journal,* 197**,** 295-305.

KOMKIENE, J. & BALTRENAITE, E. 2016. Biochar as adsorbent for removal of heavy metal ions [Cadmium (II), Copper (II), Lead (II), Zinc (II)] from aqueous phase. *International Journal of Environmental Science and Technology,* 13**,** 471-482.

LANDABURU-AGUIRRE, J., PONGRÁCZ, E., PERÄMÄKI, P. & KEISKI, R. L. 2010. Micellar-enhanced ultrafiltration for the removal of cadmium and zinc: use of response surface methodology to improve understanding of process performance and optimisation. *Journal of hazardous materials,* 180**,** 524-534.

LANGMUIR, I. 1917. The constitution and fundamental properties of solids and liquids. *Journal of the Franklin Institute,* 183**,** 102-105.

LONG, X. L., CHENG, H., XIN, Z. L., XIAO, W. D., LI, W. & YUAN, W. K. 2008. Adsorption of ammonia on activated carbon from aqueous solutions. *Environmental Progress,* 27**,** 225-233.

LU, C. & CHIU, H. 2006. Adsorption of zinc (II) from water with purified carbon nanotubes. *Chemical Engineering Science,* 61**,** 1138-1145.

MOHAN, D., PITTMAN JR, C. U., BRICKA, M., SMITH, F., YANCEY, B., MOHAMMAD, J., STEELE, P. H., ALEXANDRE-FRANCO, M. F., GÓMEZ-SERRANO, V. & GONG, H. 2007. Sorption of arsenic, cadmium, and lead by chars produced from fast pyrolysis of wood and bark during bio-oil production. *Journal of colloid and interface science,* 310**,** 57-73.

MOHAN, D. & SINGH, K. P. 2002. Single-and multi-component adsorption of cadmium and zinc using activated carbon derived from bagasse—an agricultural waste. *Water research,* 36**,** 2304-2318.

MOOSA, A. A., RIDHA, A. M. & HUSSIEN, N. A. 2016. Removal of Zinc Ions from Aqueous Solution by Bioadsorbents and CNTs. *American Journal of Materials Science,* 6**,** 105-114.

MORENO-BARBOSA, J. J., LÓPEZ-VELANDIA, C., DEL PILAR MALDONADO, A., GIRALDO, L. & MORENO-PIRAJÁN, J. C. 2013. Removal of lead (II) and zinc (II) ions from aqueous

solutions by adsorption onto activated carbon synthesized from watermelon shell and walnut shell. *Adsorption,* 19**,** 675-685.

MUBARAK, N., ALICIA, R., ABDULLAH, E., SAHU, J., HASLIJA, A. A. & TAN, J. 2013. Statistical optimization and kinetic studies on removal of Zn 2+ using functionalized carbon nanotubes and magnetic biochar. *Journal of Environmental Chemical Engineering,* 1**,** 486-495.

MUI, E. L., CHEUNG, W., VALIX, M. & MCKAY, G. 2010. Dye adsorption onto char from bamboo. *Journal of hazardous materials,* 177**,** 1001-1005.

NADEEM, M., MAHMOOD, A., SHAHID, S., SHAH, S., KHALID, A. & MCKAY, G. 2006. Sorption of lead from aqueous solution by chemically modified carbon adsorbents. *Journal of Hazardous Materials,* 138**,** 604-613.

ORGANIZATION, W. H. 2004. *Guidelines for drinking-water quality*, World Health Organization.

PELLERA, F.-M., GIANNIS, A., KALDERIS, D., ANASTASIADOU, K., STEGMANN, R., WANG, J.-Y. & GIDARAKOS, E. 2012. Adsorption of Cu (II) ions from aqueous solutions on biochars prepared from agricultural by-products. *Journal of Environmental Management,* 96**,** 35-42.

RADNIA, H., GHOREYSHI, A. A. & YOUNESI, H. 2011. Isotherm and kinetics of Fe (II) adsorption onto chitosan in a batch process. *Iranica Journal of Energy and Environment,* 2**,** 250-257.

ROUQUEROL, J., AVNIR, D., FAIRBRIDGE, C., EVERETT, D., HAYNES, J., PERNICONE, N., RAMSAY, J., SING, K. & UNGER, K. 1994. Recommendations for the characterization of porous solids (Technical Report). *Pure and Applied Chemistry,* 66**,** 1739-1758.

SAMPER, E., RODRÍGUEZ, M., DE LA RUBIA, M. & PRATS, D. 2009. Removal of metal ions at low concentration by micellar-enhanced ultrafiltration (MEUF) using sodium dodecyl sulfate (SDS) and linear alkylbenzene sulfonate (LAS). *Separation and purification technology,* 65**,** 337-342.

SHAHEEN, S. M., EISSA, F. I., GHANEM, K. M., EL-DIN, H. M. G. & AL ANANY, F. S. 2013. Heavy metals removal from aqueous solutions and wastewaters by using various byproducts. *Journal of environmental management,* 128**,** 514-521.

SRIVASTAVA, N. & MAJUMDER, C. 2008. Novel biofiltration methods for the treatment of heavy metals from industrial wastewater. *Journal of hazardous materials,* 151**,** 1-8.

WEBER, W. J. & MORRIS, J. C. 1963. Kinetics of adsorption on carbon from solution. *Journal of the Sanitary Engineering Division,* 89**,** 31-60.

WORCH, E. 2012. *Adsorption technology in water treatment: fundamentals, processes, and modeling*, Walter de Gruyter.

XU, X., CAO, X. & ZHAO, L. 2013a. Comparison of rice husk-and dairy manure-derived biochars for simultaneously removing heavy metals from aqueous solutions: role of mineral components in biochars. *Chemosphere,* 92**,** 955-961.

XU, X., CAO, X., ZHAO, L., WANG, H., YU, H. & GAO, B. 2013b. Removal of Cu, Zn, and Cd from aqueous solutions by the dairy manure-derived biochar. *Environmental Science and Pollution Research,* 20**,** 358-368.

YANG, Y., LIN, X., WEI, B., ZHAO, Y. & WANG, J. 2014. Evaluation of adsorption potential of bamboo biochar for metal-complex dye: equilibrium, kinetics and artificial neural network modeling. *International Journal of Environmental Science and Technology,* 11**,** 1093-1100.

YAO, Y., GAO, B., INYANG, M., ZIMMERMAN, A. R., CAO, X., PULLAMMANAPPALLIL, P. & YANG, L. 2011. Biochar derived from anaerobically digested sugar beet tailings: characterization and phosphate removal potential. *Bioresource technology,* 102**,** 6273-6278.

YUAN, J.-H., XU, R.-K. & ZHANG, H. 2011. The forms of alkalis in the biochar produced from crop residues at different temperatures. *Bioresource technology,* 102**,** 3488-3497.

Chapter 6. Remediation of Landfill Leachate by various Vietnamese Biomass Residue–derived Biochars (wood, rice husk and bamboo): Equilibrium and Column Studies

Nguyen Van Hien[a,b], Eugenia Valsami-Jones[a] , Nguyen Cong Vinh[b], Tong Thi Phu, Nguyen Thi Thanh Tam[b] , Iseult Lynch[a]

[a] School of Geography, Earth and Environmental Sciences, University of Birmingham, Edgbaston, B15 2TT, UK

[b] Department of Land Use, Soils and Fertilizers Research Institute, Hanoi, Vietnam

Corresponding author: i.lynch@bham.ac.uk

Abstract

Biochars produced by Top-Lid Updraft Drum (TLUD) technology from Vietnamese biomass residues including acacia wood chip, rice husk, and bamboo were investigated for their performance as low cost adsorbents for landfill leachate remediation. Equilibrium (batch) and column experiments were conducted to assess the adsorption capacity and efficiency of removal of NH_4^+-N and other cations from the leachate by the three biochars individually, their binary mixtures (wood + rice husk BCs, wood + bamboo BCs, rice husk + bamboo BCs), and a 1:1:1 mixture of the three biochars. The data indicated that all three biochars were individually good for ammonium (NH_4^+-N) adsorption. The highest adsorption ($P<0.05$) belonged to rice husk BC (44.06 ± 1.55 NH_4^+-N mg/g) in comparison with both bamboo BC (40.41 ± 0.95 NH_4^+-N mg/g) and wood BC (38.90 ± 1.78 NH_4^+-N mg/g) which were similar in the adsorption ($p > 0.05$). Meanwhile, the adsorption of NH_4^+-N onto the binary mixtures was not significantly different ($p>0.05$), which fluctuated between 39.89 ± 1.76 and 43.10 ± 2.22 mg/g. Finally, NH_4^+-N removal by the bichar column (wood + rice husk + bamboo BCs) was 43.69 ± 2.15 % at a flow rate of 1 mL/min after four days (12 hours per day) with the solution passed again for 4 times (four days). Particularly, the NH_4^+-N adsorption capacity of the individual biochars under the competitive conditions (landfill leachate) was higher than their CEC (Cation Exchange Capacity) values, which means that cation exchange was not the main mechanism

to govern the adsorption. In addition, K^+ ion on the surface of the biochars was found the main cation to exchange with the cations (NH_4^+-N, Ca^{2+}, Mg^{2+}, and Na^+) in the landfill leachate.

Key words: Biochar, landfill leachate, NH_4^+-N, adsorption, CEC, remediation

1. Introduction

Landfill is one of the common methods to be used for managing the disposal of municipal solid waste (Kurniawan et al., 2006). The advantages of this method include its low cost, simplicity, and potential for landscape restoration following mineral workings (Aziz et al., 2011). However, the decomposition of the organic waste after landfilling by hydrological and chemical reactions (Azmi et al., 2016) and percolation of rainwater results in the production of the highly polluted solution known as "leachate" (Kurniawan et al., 2006). Landfill leachate has a complex mixture of pollutants such as organic matter, sodium, and heavy metals, as well as having high alkalinity (bicarbonate and carbonate) as reported by previous studies (Shehzad et al., 2016, Aziz et al., 2010, El-Salam and Abu-Zuid, 2015). For example, Amr et al. (2013) reported that the landfill leachate in Malaysia had chemical oxygen demand (COD) of 2,025 mg/L , biochemical oxygen demand (BOD_5) of 93 mg/L and 810 mg/L of NH_3-N. Even higher values were observed in landfill leachate from South Korea with COD of 24,400 mg/L, BOD_5 of 10,800 mg/L, NH_4^+-N at 1,682 mg/L and 3,160 mg/L of Cl^- (Im et al., 2001). According to Foo and Hameed (2009), landfill leachate is normally classified into three ages: < 5 years (young), 5 – 10 years (medium), and > 10 years (old), and the ratio of BOD/COD is commonly used to indicate the age (Ahmed and Lan, 2012). A BOD/COD ratio in range of 0.5 - 1.0 indicates a young leachate, 0.1 – 0.5 indicates a medium leachate, and less than 0.1 is typical for old leachates.

The combination of the various compounds at high concentration makes the remediation of landfill leachate challenging, especially given the need to remove all of the pollutants at the same time. Several methods have been used for leachate treatment, which were reviewed by Renou et al. (2008). For example, aerobic (Li and Zhao, 2001, Orupold et al., 2000, Matthews et al., 2009), or anaerobic (Uygur and Kargı, 2004, Kennedy and Lentz, 2000, Lin and Chang, 2000) biological treatments were used due to their low cost, simplicity, and reliability (Renou et al., 2008). In general, biological methods are evaluated in terms of their COD removal efficiency due to the fact that biodegradable compounds are removed (El-Gohary and Kamel, 2016), but the removal efficiency of ammonia by these approaches was very low (less than 20%) because of the high salinity and the presence of inhibitory compounds such ammonia (Di Iaconi et al., 2006). The high ammonia concentration normally observed in medium and old landfill leachates significantly inhibits the microbial activity, which leads to reduced COD removal efficiency (El-Gohary and Kamel, 2016). Thus, a combination of physicochemical remediation processes are needed to decrease the presence of ammonia before biological treatment is applied (Li and Zhao, 2001, El-Gohary and Kamel, 2016).

The combination of physical and/or chemical treatments has widely been used to reduce the pollutant concentrations of the leachate, which includes flotation (Zouboulis et al., 2003), coagulation – flocculation (Monje-Ramirez and De Velasquez, 2004, Tatsi et al., 2003), chemical oxidation (QURESI-II et al., 2002, Steensen, 1997), air stripping (Marttinen et al., 2002, CHEUNG et al., 1997), and adsorption (Kargı and Pamukoglu, 2004). Among these methods, adsorption is considered to have several advantages (Azmi et al., 2016) such as the low initial cost, easy recovery, reusable adsorbent, and design simplicity (Bhatnagar et al., 2013). Adsorption via a superior adsorbent (activated carbon) has been proven as one of the most effective treatments (Azmi et al., 2016, Kargi and Pamukoglu, 2004). However, the high

cost for production (Azmi et al., 2016) and non-renewable sources (coal) are the main limitations for using this product for the treatment and remediation of leachate.

Nowadays, the utilization of the low cost adsorbent known as biochar, produced from biomass residues (wood, rice husk, bamboo, corncob, etc.), has been receiving considerable attention. In fact, Shehzad et al. (2016) reported that the biochar produced from sea mango removed up to 95.1% of the colour, reduced COD by 84.94% and NH_3-N by 95.77%. A very high effectiveness of E.coli removal (96%) by soft wood biochar has also been observed by Mohanty and Boehm (2014). Li et al. (2016) indicated that a biotrickling filter packed with palm wood biochar removed 80% of ammonium and 68% of phosphorus from the wastewater having high nitrogen (NH_4^+-N = 10,000 mg/L and phosphorus (PO_4^{3-} = 2,500 mg/L) contents. In addition, the biochar filter was reported to have a significantly higher COD removal compared to activated carbon for wastewater having COD concentrations higher than 500 mg/L (Huggins et al., 2016). However, although the adsorption of NH_4^+-N onto biochar was proven to be controlled by multiple mechanisms (Gao et al., 2015), which of them is the main driver or governs the adsorption is still a topic of controversy. For example, Gai et al. (2014) and Zheng et al. (2013) supported that CEC predominantly governed, but Takaya et al. (2016) showed that oxygen – containing functional groups on the biochar surface were more involved rather than CEC. This suggests that the mechanism may be biochar biomass specific. Moreover, most of the studies to date have assessed the effect of a single biochar on the adsorption rather than mixed biochars, which may have different (or combination) mechanisms of adsorption.

This study assessed the utility of single biochars versus mixed biochars for pollutant removal (NH_4^+-N and other cations) from the landfill leachate by both batch (equilibrium) and column experiments. In addition, the adsorption results were used to evaluate the role of CEC of biochar for the process as well as which of cations on particle biochar surface participates on

that. The biochars were produced from acacia wood, rice husk, and bamboo residues which are known as redundant agricultural waste in Vietnam.

2. Materials and Methodology

2.1 Biochar preparation and characterization

The three biochars were produced from acacia wood chip, rice husk, and bamboo by The TLUD (Top-Lid Updraft Drum) technology at a temperature between $450^{\circ}C$ and $550^{\circ}C$. The main physicochemical characteristics of these biochars were summarised on Table 1. In fact, the three biochars were alkaline with pH ranging from 9.51 - 10.11, and had high carbon content, particularly wood BC (82.10 %) and bamboo BC (80.27 %). The CEC values was in order as rice husk BC (26.70 Cmol/kg) > bamboo BC (20.77 Cmol/kg) > wood BC (13.53 Cmol/kg). In addition, the highest ash content was also observed for rice husk BC (41.24 %), while wood BC and Bamboo BC contained only 1.93 % and 8.08 %, respectively. In contrast, BET surface was observed to this opposite trend with the order as wood BC (497.34 m^2/g) > bamboo BC (434.53 m^2/g) > rice husk(3.29 m^2/g). Their morphology (SEM – Scanning electron microscopy) and surface function groups (FTIR - Fourier-transform infrared (FTIR) spectroscopy) were described in detail in Chapter 3.

Table 1. Characteristics of the three biochars used for the bath and column leaching experiments (mean of 3 replications, ± STDEV).

Characteristics	Wood BC	Rice husk BC	Bamboo BC
pH	10.11 ±0.04	9.51 ±0.02	9.94 ±0.02
C, %	82.10 ±0.21	47.82 ±0.18	80.27 ±0.08
H, %	2.33 ±0.01	2.07 ±0.04	2.07 ±0.04
N, %	0.71 ±0.05	0.62 ±0.06	0.72 ±0.02
O, %	12.93 ±0.16	8.25 ±0.28	8.86 ±0.02
P_2O_5, %	0.51 ±0.21	0.50 ±0.20	0.19 ±0.13
K, %	1.58 ±0.62	1.89 ±0.63	0.47 ±0.13
Ca, %	0.65 ±0.06	2.37 ±0.18	0.57 ±0.01
Mg, %	0.21 ±0.05	0.26 ±0.10	0.14 ±0.03
CEC, mmol/kg	13.53 ±0.65	26.70 ±1.57	20.77 ±1.21
BET surface are, m^2/g	497.34 ±0.88	3.29 ±0.02	434.53 ±2.79
Moisture, %	5.45 ±0.03	5.37 ±0.05	6.11 ±0.11
Ash, %	1.93 ±0.03	41.24 ±0.49	8.08 ±0.20
Volatile mater, %	46.68 ±1.68	45.61 ±0.54	48.72 ±3.22
Fixed carbon, %	45.94 ±1.68	7.82 ±0.10	37.09 ±3.32

2.2 Landfill leachate

Landfill leachate was collected from Pound Bottom landfill (Salisbury, Wiltshire SP5 2PU) on Tuesday 6th June 2017 and stored in a 1 m^3 plastic tank outdoors at University of Birmingham. The pH of the leachate was recorded as alkaline (8.68 ± 0.5), and the concentration of ammonium (NH_4^+-N) was determined to be 1790.18 ± 2.53 mg/L. The exchangeable cations (Ca^{2+}, Mg^{2+}, K^+, and Na^+) in the leachate were also measured, with their values being 366.02 ± 0.12 mg/L for Ca^{2+}, 156.85 ± 0.02 mg/L for Mg^{2+}, 256.44 ± 0.01 mg/L for K^+, and 1614.14 ± 0.11 mg/L for Na^+. The initial concentrations of the exchangeable cations in the leachate will be compared to those in the solution after adsorption by the biochars, to determine the

effectiveness of the biochars at remediating the landfill leachate and to identify the mechanism of adsorption of ammonium by the biochars.

2.3 Experimental set-up

2.3.1. Equilibrium adsorption experiment

The adsorbent (0.5g) was added into plastic falcon tubes (50 mL) and mixed with the landfill leachate (40 mL). Next, the mixtures were placed on an orbital shaker and shaken at 300 rpm for24h at ambient temperature (20 ± 0.5 °C) to equilibrate. After that, the mixtures were centrifuged at 5,000 rpm for 5 mins and the supernatant filtered through Acrodisc syringe filters (0.20µm). Then, the filtered solutions were diluted 100 times with DI water to ensure that the analyte concentrations were within the range of the standard curve (0.5, 1, 5, 10, 20, 50 mg/L of NH_4^+-N, Ca^{2+}, Mg^{2+}, K^+, and Na^+). The concentration of NH_4^+-N, Ca^{2+}, Mg^{2+}, K^+, and Na^+ in the filtered solution were measured by Ion Chromatography (Dionex DX500 model), and calculated using equations (1) & (2):

$$q_e \; = \; \frac{(C_o - C_e)V}{m} \;\; (1) \qquad \text{and} \qquad \%\text{removal} = \frac{C_o - C_e}{C_o} \; x \; 100 \;\; (2)$$

where C_o and C_e are the initial and equilibrium concentrations of the cations in the leachate; V is the volume of the leachate (L) ; and m is the mass of adsorbent (g).

2.3.2 Adsorption filter experiment
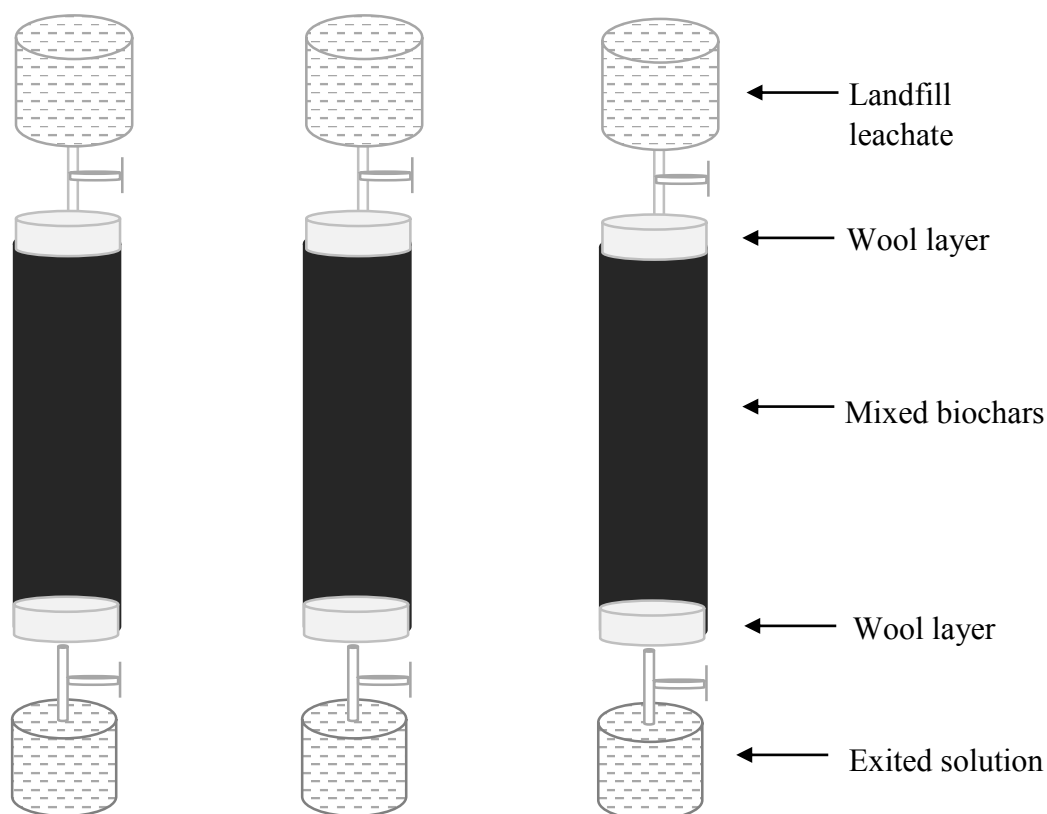
Figure 1. Biochar columns (filters) for pollutant removal from landfill leachate.

The column test is a kind of leaching experiment, which is normally used to investigate the filtering process of adsorption materials (substrates) for the leaching solution. In this study, a continuous flow of landfill leachate was leached through mixed biochars (wood + rice husk + bamboo BCs) packed in glass chromatography columns (30.48 cm length, 2.54 cm inside diameter). The three biochars were mixed well with ration 1:1:1 (w:w:w) before the packing. Dry packing was chosen rather than wet packing to prevent floating and nonuniform distribution of the biochar layers (Mohanty et al,). The mixed biochar packing was shown in Figure 1. Then, DI water was used to wash impurities from the biochars before the leachate solution was passed through. Each column was a separate composition, which presented for one replication. Thus, the solution passed through only one column with 4 times (four days with 12 hours per day). The experiment was carried out in three replications. The flow rate

was controlled to 1 mL/min (Mohanty and Boehm, 2014), and the experiment was periodically stopped at the end of the day by turning off the pump and storing the solutions in the fridge (Sprynskyy et al., 2005). Analysis sample was also periodically collected from the exit solution when the process was stopped (at the end of each day). The solution was kept in the fridge and injected into the tank again (Figure 1) the next experimental day. The concentrations of NH_4^+-N, Ca^{2+}, Mg^{2+}, K^+ and Na^+ in the samples were analysed by Ion Chromatography (Dionex DX500 model), and then calculated using equations (3) & (4).

For the column experiments:

$$q_t = \frac{(C_o - C_t)V}{m} \ (3) \quad \text{and} \quad \%\text{removal} = \frac{C_o - C_t}{C_o} \ x \ 100 \ (4)$$

where C_o (mg/L) and C_t (mg/L) are the initial and time t concentrations of the cations; V is the volume of the adsorbate solution (L); and m is the mass of adsorbent (g) packed in the column.

2.3.3. Data analysis

The data experiments were analyzed by Excell 2013 and IBI SPSS statistic 22 sorfwares.

3. Results and discussion

3.1 The adsorption capacity of biochar in the equilibrium study

The adsorption capacity of each biochar assessed singly for NH_4^+-N in the landfill leachate is presented in Figure 2. The data indicated that the three biochars had good adsorption capacity for ammonium (NH_4^+-N) for the leachate solution containing a high NH_4^+-N concentration. In fact, the values were in the order rice husk BC (44.06 ± 1.55 mg/g) > bamboo BC (40.41 ± 0.95 mg/g) ~ wood BC (38.90 ± 1.78 mg/g), and the % removals corresponded to 30.76 ± 1.08, 28.28 ± 0.66, and 27.16 ± 1.30 %, respectively. The statistic analysis indicated that the NH_4^+-N adsorption of rice husk BC was significant difference (p < 0.05) with both the wood BC and

bamboo BC. Meanwhile, bamboo BC and wood BC were observed to have the similar adsorption capacity ($p > 0.05$) for NH_4^+-N in the landfill leachate. However, the adsorption capacity of these three biochars for the cation (NH_4^+-N) was monitored only in range of 0.47 - 9.90 mg/g when the experiments conducted with the artificial solution containing single NH_4^+ cation with concentrations from 20 to 320 mg/L (Hien et al, 2018). Thus, the adsorption capacity of the three biochars strongly depends on the initial NH_4^+-N concentration. The wood BC and rice husk BC were also observed to have good adsorption capacity for NH_4^+-N from wastewater of pig manure biogas which had an ammonium concentration of 1,400 mg/L (Kizito et al., 2015), with the adsorption capacity of wood BC (42.02 mg/g) being higher than that of rice husk BC (37.63 mg/g). The effect of initial NH_4^+-N concentration on biochar adsorption capacity was also evident from the results of Yu et al. (2016) which indicated that pig manure BC and straw BC had NH_4^+-N adsorption values of only 27.04 and 20.24 mg/g, respectively, for wastewater from pig manure biogas having NH_4^+-N concentration of 855 ± 12.64 mg/L.
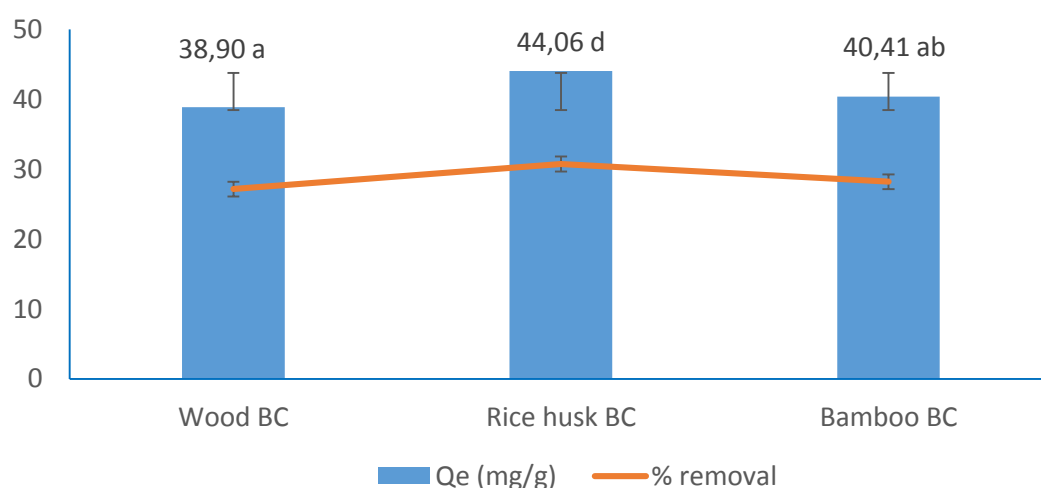
Figure 2. Effect of various biochars on NH_4^+-N adsorption and removal (rice husk BC > bamboo BC ~ wood BC, $p < 0.05$). Data are mean values ± standard deviation. The same letters indicate no significant difference (p<0.05).

The NH$_4^+$-N adsorption was also assessed through mixed biochars (Figure 3) to assess whether the combination of characteristics would enhance the adsorption capacity. The data indicated that the adsorption of three binary mixtures of biochars including wood + rice husk BC; bamboo + rice husk BC; and a ternary mixture of wood + rice husk + bamboo BC for NH$_4^+$-N in the leachate had similar values (p > 0.05) which fluctuated between 42.37 ± 1.35 and 43.10 ± 2.22 mg/g. The % removals were observed around 30 %. Although, the mixture of wood + bamboo BC had NH$_4^+$-N absorption efficiency of 39.89 ± 1.76 mg/g, and % removal of 27.86 ± 1.23 %, there was not different with the adsorption values of the other mixture (p > 0.05). The effectiveness of the mixed biochars for adsorption NH$_4^+$-N from diary effluent with NH$_4^+$-N concentration up to 1,000 mg/L was also assessed by Sarkhot et al. (2013), but the adsorption capacity was only 5.3 mg/g for the mixed wood biochars (300 °C) produced from maple, aspen, choke cherry, and alder. Thus, rice husk BC was a good adsorbent to mix with other biochars for pollutant removal.
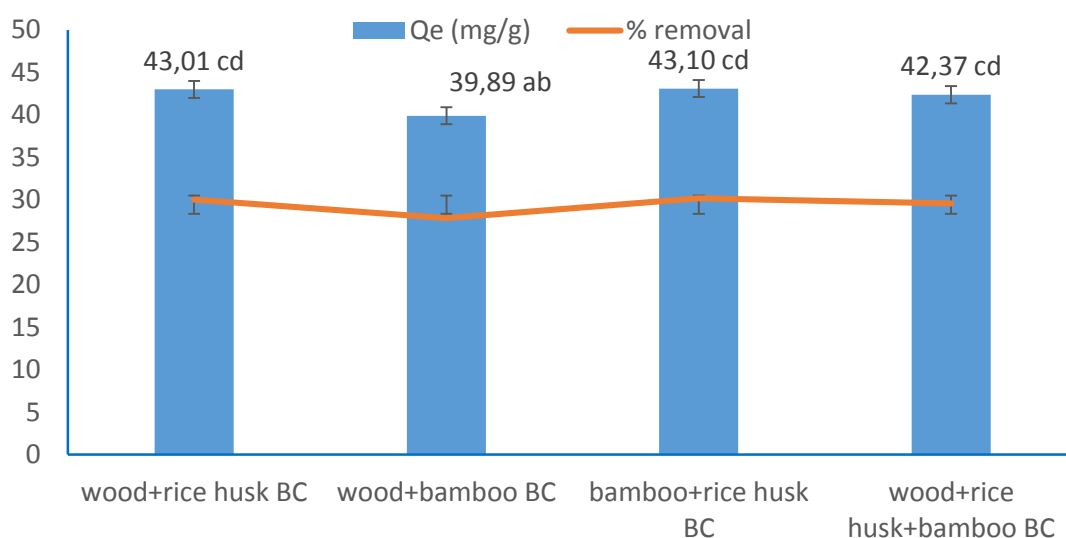
Figure 3. Effect of mixed biochars on NH$_4^+$-N adsorption and removal. Data are mean values ± standard deviation. The same letters indicate no significant difference (p<0.05).

The above results showed that the three biochars and their mixtures produced from acacia wood, rice husk, and bamboo residues had good adsorption capacity for NH_4^+-N from landfill leachate. However, the adsorption capacity was still lower than the maximum adsorption capacity (q_{max} = 88.50 mg/g for rice husk BC), which was calculated from the Langmuir model (Hien et al, 2018). Similarly, Kizito et al. (2015) also reported that wood BC and rice husk BC had maximum adsorption capacities of 44.64 and 39.80 mg/g, respectively, which are higher than the values at equilibrium adsorption as described above (42.02 and 37.63 mg/g, respectively).

Table 2. Absorption of the other exchangeable cations competing with NH_4^+-N for adsorption to the BC samples. Data are mean values ± standard deviation.

Biochar	NH_4^+-N	Ca^{2+}	Mg^{2+}	K^+	Na^+
	q_e (mg/g)				
WBC	38.90 ± 1.78	15.94 ± 0.99	2.01 ± 0.24	-2.06 ± 0.30	-2.75 ± 0.82
RBC	44.06 ± 1.55	21.39 ± 0.12	1.60 ± 0.05	-20.27 ± 3.12	7.74 ± 0.52
BBC	40.41 ± 0.95	23.75 ± 0.64	-0.78 ± 0.04	-30.49 ± 0.47	11.23 ± 1.32
WBC+RBC	43.01 ± 0.46	21.11 ± 0.50	1.98 ± 0.45	-2.47 ± 0.47	15.58 ± 0.21
WBC+BBC	39.89 ± 1.76	21.86 ± 1.25	1.46 ± 0.38	-19.20 ± 2.43	10.88 ± 0.66
BBC+RBC	43.10 ± 2.22	8.70 ± 0.24	1.73 ± 0.14	-21.77 ± 0.19	4.20 ± 0.19
WBC+RBC+BBC	42.37±1.35	21.46±1.05	-0.72±0.24	-26.35±1.18	8.59 ± 0.59

WBC = wood BC; RBC = rice husk BC; BBC = bamboo BC

In addition, Yu et al. (2016) showed that the maximum NH_4^+-N adsorption was recorded at 44.64 ± 0.60 mg/g for wood BC and 39.80 ± 0.54 mg/g for rice husk BC as compared to the adsorption of 27.04 and 20.24 mg/g at equilibrium, respectively for wastewater of pig manure biogas (NH_4^+-N concentration = 855 ± 12.64 mg/L). Hence, the reduction of ammonium adsorption onto biochar may come from the competition of other cations in the wastewater. In fact, the effect of other cations was complicated, as shown in Table 2. For example, Ca^{2+}

and Mg^{2+} in the leachate were also adsorbed onto wood BC (15.94 ± 0.99 and 2.01 ± 0.24 mg/g respectively), while K^+ and Na^+ on the surface of the biochar was exchanged into the exiting solution. The exchangeable values of the two cations (K^+ and Na^+) were 2.06 ± 0.3 and $2.75.0.82$ mg/g, respectively. By contrast, in the wood + rice husk BCs, wood + bamboo BCs, and bamboo + rice husk BCs only K^+ was found to be displaced by the NH_4^+-N adsorption, while bamboo BC and the mixed ternary biochar both Mg^{2+} and K^+ were found to be exchanged and released into the leachate solution. Interestingly, none of the biochars adsorbed potassium cation (K^+), even though there was a high concentration ($K^+ = 256.44 \pm 0.01$ mg/L) in the leachate. The highest exchanged K^+ concentration was recorded for bamboo BC (30.49 ± 0.47 mg/g), while the lowest was wood BC (2.06 ± 30 mg/g). Thus, ammonium adsorption to the biochars involved cation exchange with displacement particularly of potassium cations. According to Yu et al. (2016), K^+ nearly vanished from both pig manure BC and straw BC, while Ca^{2+} and Mg^{2+} strongly declined after the adsorption. In addition, the important role of Ca^{2+} and Mg^{2+} for NH_4^+-N adsorption was also reported in the results of Zheng et al. (2013). Thus, the findings of Yu et al. (2016) and Zheng et al. (2013) about Ca^{2+} participation in exchange for the adsorption of NH_4^+-N was opposite with the results presented here. In addition, the NH_4^+-N adsorption capacity of the three biochars via cation exchange converted from their CEC values (wood BC = 13.53 Cmol/kg, rice husk BC = 26.70 Cmol/kg, and 20.77 Cmol/kg) was 2.44 mg/g, 4.81 mg/g, and 3.74 mg/g, respectively. These values indicated that the NH_4^+-N adsorption through the CEC of the biochars occupied only 6.27 % for wood BC, 10.92 % for rice husk BC, and 8.49 % for bamboo BC in comparison with the total (wood BC = 38.90 mg/g, rice husk BC = 44.06 mg/g, and bamboo BC = 40.41 mg/g), which means that the CEC of the biochars did not play a major role in the NH_4^+-N adsorption. Hence, the major portion of the adsorption may have mainly occurred via the adsorption to the organic functional groups (carboxyl and hydroxyl groups) and inorganic groups (CO_3^{2-}, PO_4^{3-}, SiO_2) of the biochars. The

158

NH$_4^+$-N adsorption being driven by the functional groups present on the biochars was also supported by Takaya et al. (2016) and Yu et al. (2016). Particularly, Yu et al. (2016) reported that not only SiO$_2$ groups but also CO$_3^{2-}$ groups are involved in the adsorption of NH$_4^+$-N. In addition, Takaya et al. (2016) suggested that soluble organic matter on surface biochar also possibly participates in the adsorption of ammonium. The adsorption of Ca^{2+} and Mg^{2+}, and Na$^+$ onto the adsorbents may involve the formation of complexes or mineral salts with surface functional groups of the biochar (see Figure 4).

3.2 Effect of biochar column on NH$_4^+$-N adsorption

The effectiveness of biochar for landfill leachate treatment performance was assessed in column filters (Figure 1). Based on the results of the equilibrium adsorption experiments, the mixture of the three biochars was used to assess whether the pollutant removal efficiency could be enhanced by combining (layering) the biochars. The concentration of NH$_4^+$-N and other cations, such as Ca^{2+}, Mg^{2+}, K$^+$, and Na$^+$, was measured every day during the experiment, which aims to calculate the % NH$_4^+$-N adsorption and removal (Figure 3), and identify which of the cations are participating in the adsorption (Table 3).
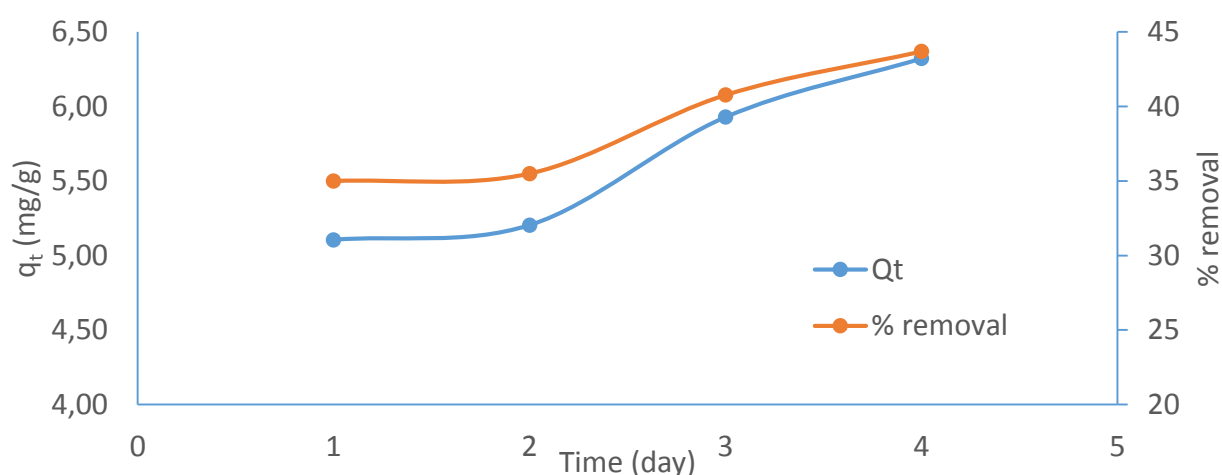
Figure 4. Dynamics of NH$_4^+$-N adsorbed by the biochar in the column experiment over four days.

The data indicated that the NH_4^+-N adsorption capacity of the column increased with increased time. In fact, the NH_4^+-N adsorption gradually increased from 5.11 ± 1.31 to 6.32 ± 1.33 mg/g when the leachate had flowed through the filter for 4 times (4 days with 12 hours per day). In addition, the % removal showed a similar trend, and increased over time from 34.99 ± 2.03 % (the first day) to 43.69 ± 2.15 % (the fourth day), which corresponded to the concentration of ammonium (NH_4^+-N) in the effluent solution decreasing from 1,128.34 ± 0.24 mg/L (the first day) to 980.80 ± 0.26 mg/L (the fourth day). Thus, the amount of NH_4^+-N removed from the landfill leachate by the biochar filter at a flow rate of 1 mL/minute after 4 days was 809.38 mg/L compared with the initial concentration of the leachate (1790.18 mg/L). The adsorption capacity of the column was lower than that of equilibrium experiment (see Table 2), which was due to effect of flow process and the amount of adsorbent packed into the column. The flow rate affected the diffusion of NH_4^+- N from the bulk solution into the porous system of biochar particles, while the amount of biochar related to competition among the adsorption sites available on the biochar surface. Hence, a suitable flow rate and an appropriate times for re-circulation of the influent are needed to increase the contact time of the adsorbates with the adsorbents.

The competition of the other cations on the surface of the biochar and in the leachate with NH_4^+-N adsorption is shown in Table 3.

Table 3. Absorption of the other exchangeable cations competing with NH_4^+-N adsorption. Data are mean values ± standard deviation.

Time	NH_4^+-N	Ca^{2+}	Mg^{2+}	K^+	Na^+
			q_t (mg/g)		
Day1	5.11 ± 1.31	0.33 ± 0.12	-0.13 ± 0.05	-2.88 ± 0.65	3.81 ± 0.94
Day2	5.20 ± 1.48	0.48 ± 0.14	-0.06 ± 0.01	-2.63 ± 0.63	3.71 ± 1.00
Day3	5.93 ± 1.43	0.61 ± 0.10	-0.26 ± 0.05	-3.40 ± 0.19	3.55 ± 1.05
Day4	6.32 ± 1.33	0.91 ± 0.36	0.03 ± 0.01	-2.40 ± 0.68	3.73 ± 0.66

The data in Table 3 indicated that the cations competed with NH_4^+-N adsorped onto the mixed biochar column showed a similar trend to the mixture of three biochars in the equilibrium experiment (see Table 2). In fact, both Ca^{2+} and Na^+ ions in the landfill leachate (Ca^{2+}= 366.02 mg/L; Na^+ = 1614.14 mg/L) were adsorbed onto the biochar in the column with 0.33 - 0.91 mg/g and 3.55 – 3.81 mg/g, respectively. In contrast, the biochar did not adsorb K^+ and Mg^{2+} (except the day 4) from the leachate. For example, K^+ and Mg^{2+} ions on the biochar surface (in the column) were exchanged into the effluent solution with 2.63 – 3.40 mg/g, and 0.06 – 0.23 mg/g. Thus, NH_4^+-N, Ca^{2+}, and Na^+ from the leachate were adsorbed onto the filter during the experiment, meanwhile the K^+ and Mg^{2+} of the biochars were mainly exchanged into the exiting solution.

3.3 Adsorption mechanisms of biochar with cations in the leachate

The adsorption mechanisms of the various biochars with the cations present in the landfill leachate is presented schematically in Figure 4. The illustration was compiled from mechanisms proposed by Ding et al. (2014), Spokas et al. (2012b), and Zhou and Chen (2001). The results indicated that the adsorption of NH_4^+-N and the other cations from the leachate onto the biochar particles may involve several processes. The first adsorption mechanism was controlled by the intraparticle diffusion (1), which was proven in **Chapter 4** for NH_4^+-N),

particularly with wood BC and bamboo BC both of which were shown to have sophisticatedly porous structures (see **section 3.4 of Chapter 3**). In this mechanism the NH_4^+, Ca^{2+}, and Na^+ cations diffused from the bulk solution to the external film surrounding the biochar particles before moving to the external surface by film diffusion, and then being transported into the particles by porous diffusion and/or surface diffusion. The second proposed mechanism utilises the NH_3 in the leachate as a Brownsted and/ or Lewis acid (2) which reacts with functional groups (carboxyl and hydroxyl groups) on surface of the biochars to form ammonium salt or amide (Spokas et al., 2012b).
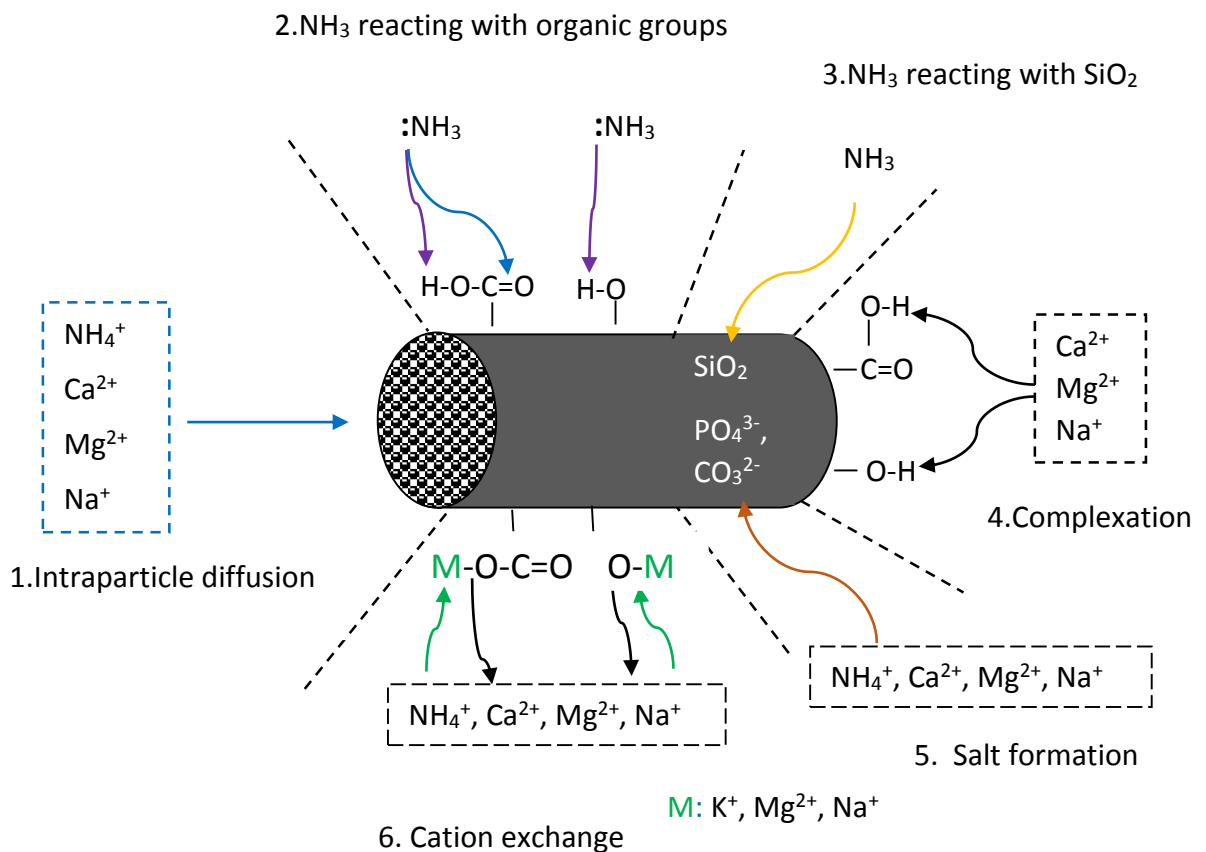
Figure 5. Schematic of the geometry of the cations present in the landfill leachate adsorbed onto a biochar particle.

A third potential adsorption mechanism involves NH_3 reacting with SiO_2 (3) which was confirmed to be present on the surface of the rice husk and wood BCs (see **section 3.3 of**

Chapter 3), to create $SiO_2 - NH_3$ complex or $H_2NSiOOH$ molecules (Zhou and Chen, 2001). For rice husk biomass, the SiO_2 content was in range $18.8 - 22.3\%$ (Guo et al., 2002), which explained the good ammonia adsorption of rice husk BC. In addition, NH_4^+ ions combined with the other inorganic groups such as PO_4^{3-} and CO_3^{2-} to form ammonium salts (5). The cation exchange was the final adsorption mechanism for NH_4^+-N, which exchanged with cations (K^+, Mg^{2+}, and Na^+) on the biochar surface (6). Meanwhile, the adsorption of Ca^{2+}, Mg^{2+} and Na^+ onto the three biochars was related to cation exchange (6), complexation (4), precipitation of mineral salts with the inorganic groups (5), and intraparticle diffusion (1). The formation of the salts, particularly via Ca^{2+} and Mg^{2+} reacting with PO_4^{3-} was also supported by (Mukherjee et al. (2011)).

4. Conclusion

The three biochars and their 1:1:1 mixture had the good adsorption capacity for NH_4^+-N and Ca^{2+} as well as Na^+ from the leachate. The adsorption occurred through various processes which related to the surface functional groups (organic and inorganic groups), cation exchange, and intraparticle diffusion. Particularly, the results indicated that the contribution of CEC of the biochars for the NH_4^+-N adsorption was only $6.27 - 10.92 \%$ of the adsorbed NH_4^+-N total. That means the high concentration of adsorbate (NH_4^+-N = 1790.18 mg/L in the leachate exceeds the adsorption ability of the biochars via CEC (cation exchange). But, the findings for the important role of K^+ ions of the biochars for NH_4^+-N adsorption may give good research ideas for enriching and controlling this cation (K^+) on the biochar surface for participation of the cation exchange with NH_4^+-N. In addition, although competing strongly with NH_4^+-N, the adsorption of Ca^{2+}, Mg^{2+} and Na^+ from the leachate onto the biochars is the valuable findings for using the biochas for remediation of these metals in the waste water.

Acknowledgements

References

AHMAD, M., LEE, S. S., DOU, X., MOHAN, D., SUNG, J.-K., YANG, J. E. & OK, Y. S. 2012. Effects of pyrolysis temperature on soybean stover-and peanut shell-derived biochar properties and TCE adsorption in water. Bioresource technology, 118, 536-544.

AHMAD, M., LEE, S. S., RAJAPAKSHA, A. U., VITHANAGE, M., ZHANG, M., CHO, J. S., LEE, S.-E. & OK, Y. S. 2013. Trichloroethylene adsorption by pine needle biochars produced at various pyrolysis temperatures. Bioresource technology, 143, 615-622.

AHMED, F. N. & LAN, C. Q. 2012. Treatment of landfill leachate using membrane bioreactors: A review. Desalination, 287, 41-54.

AL-WABEL, M. I., AL-OMRAN, A., EL-NAGGAR, A. H., NADEEM, M. & USMAN, A. R. A. 2013. Pyrolysis temperature induced changes in characteristics and chemical composition of biochar produced from conocarpus wastes. Bioresource Technology, 131, 374-379.

AL-WABEL, M. I., USMAN, A. R., EL-NAGGAR, A. H., ALY, A. A., IBRAHIM, H. M., ELMAGHRABY, S. & AL-OMRAN, A. 2015. Conocarpus biochar as a soil amendment for reducing heavy metal availability and uptake by maize plants. Saudi journal of biological sciences, 22, 503-511.

ALAMIN, A. H. & KAEWSICHAN, L. 2015. Adsorption of Zn (II) and Cd (II) ions from aqueous solutions by Bamboo biochar cooperation with Hydroxyapatite and Calcium Sulphate. International Journal of ChemTech Research, 7, 2159-2170.

ALLER, M. F. 2016. Biochar properties: Transport, fate, and impact. Critical Reviews in Environmental Science and Technology, 46, 1183-1296.

ALSHAMERI, A., IBRAHIM, A., ASSABRI, A. M., LEI, X., WANG, H. & YAN, C. 2014. The investigation into the ammonium removal performance of Yemeni natural zeolite: Modification, ion exchange mechanism, and thermodynamics. Powder Technology, 258, 20-31.

ALVAREZ, M. T., CRESPO, C. & MATTIASSON, B. 2007. Precipitation of Zn (II), Cu (II) and Pb (II) at bench-scale using biogenic hydrogen sulfide from the utilization of volatile fatty acids. Chemosphere, 66, 1677-1683.

AMELOOT, N., DE NEVE, S., JEGAJEEVAGAN, K., YILDIZ, G., BUCHAN, D., FUNKUIN, Y. N., PRINS, W., BOUCKAERT, L. & SLEUTEL, S. 2013. Short-term CO 2 and N 2 O emissions and microbial properties of biochar amended sandy loam soils. Soil Biology and Biochemistry, 57, 401-410.

AMR, S. S. A., AZIZ, H. A., ADLAN, M. N. & BASHIR, M. J. 2013. Pretreatment of stabilized leachate using ozone/persulfate oxidation process. Chemical Engineering Journal, 221, 492-499.

ANGıN, D. 2013. Effect of pyrolysis temperature and heating rate on biochar obtained from pyrolysis of safflower seed press cake. Bioresource technology, 128, 593-597.

ARSLAN, A. & VELI, S. 2012. Zeolite 13X for adsorption of ammonium ions from aqueous solutions and hen slaughterhouse wastewaters. Journal of the Taiwan institute of chemical engineers, 43, 393-398.

ASIAGWU, A. K. & OWAMAH, H. I. 2013. Kinetic Model for the Sorption of Ni (II), Cu (II) and Zn (II) onto Coconut (Cocos nucifera) Fibers Waste Biomass from Aqueous Solution. Journal Of International Environmental Application And Science, 8, 343.

AZIZ, S. Q., AZIZ, H. A., YUSOFF, M. S. & BASHIR, M. J. 2011. Landfill leachate treatment using powdered activated carbon augmented sequencing batch reactor (SBR) process: Optimization by response surface methodology. Journal of Hazardous Materials, 189, 404-413.

AZIZ, S. Q., AZIZ, H. A., YUSOFF, M. S., BASHIR, M. J. & UMAR, M. 2010. Leachate characterization in semi-aerobic and anaerobic sanitary landfills: a comparative study. Journal of environmental management, 91, 2608-2614.

AZMI, N. B., BASHIR, M. J., SETHUPATHI, S. & NG, C. A. 2016. Anaerobic stabilized landfill leachate treatment using chemically activated sugarcane bagasse activated carbon: kinetic and equilibrium study. Desalination and Water Treatment, 57, 3916-3927.

BACHMANN, H. J., BUCHELI, T. D., DIEGUEZ-ALONSO, A., FABBRI, D., KNICKER, H., SCHMIDT, H.-P., ULBRICHT, A., BECKER, R., BUSCAROLI, A., BUERGE, D., CROSS, A., DICKINSON, D., ENDERS, A., ESTEVES, V. I., EVANGELOU, M. W. H., FELLET, G., FRIEDRICH, K., GASCO GUERRERO, G., GLASER, B., HANKE, U. M., HANLEY, K., HILBER, I., KALDERIS, D.,

LEIFELD, J., MASEK, O., MUMME, J., CARMONA, M. P., CALVELO PEREIRA, R., REES, F., ROMBOLÀ, A. G., DE LA ROSA, J. M., SAKRABANI, R., SOHI, S., SOJA, G., VALAGUSSA, M., VERHEIJEN, F. & ZEHETNER, F. 2016. Toward the Standardization of Biochar Analysis: The COST Action TD1107 Interlaboratory Comparison. Journal of Agricultural and Food Chemistry, 64, 513-527.

BAGREEV, A., BANDOSZ, T. J. & LOCKE, D. C. 2001. Pore structure and surface chemistry of adsorbents obtained by pyrolysis of sewage sludge-derived fertilizer. Carbon, 39, 1971-1979.

BAOCHENG, Q., JITI, Z., XIANG, X., ZHENG, C., HONGXIA, Z. & XIAOBAI, Z. 2008. Adsorption behavior of Azo Dye CI Acid Red 14 in aqueous solution on surface soils. Journal of Environmental Sciences, 20, 704-709.

BARAKAT, M. & SCHMIDT, E. 2010. Polymer-enhanced ultrafiltration process for heavy metals removal from industrial wastewater. Desalination, 256, 90-93.

BASSO, A. S., MIGUEZ, F. E., LAIRD, D. A., HORTON, R. & WESTGATE, M. 2013. Assessing potential of biochar for increasing water-holding capacity of sandy soils. Gcb Bioenergy, 5, 132-143.

BEESLEY, L. & MARMIROLI, M. 2011. The immobilisation and retention of soluble arsenic, cadmium and zinc by biochar. Environmental Pollution, 159, 474-480.

BEESLEY, L., MORENO-JIMÉNEZ, E. & GOMEZ-EYLES, J. L. 2010. Effects of biochar and greenwaste compost amendments on mobility, bioavailability and toxicity of inorganic and organic contaminants in a multi-element polluted soil. Environmental pollution, 158, 2282-2287.

BHANDARI, A. & XU, F. 2001. Impact of peroxidase addition on the sorption– desorption behavior of phenolic contaminants in surface soils. Environmental science & technology, 35, 3163-3168.

BHATNAGAR, A., HOGLAND, W., MARQUES, M. & SILLANPÄÄ, M. 2013. An overview of the modification methods of activated carbon for its water treatment applications. Chemical Engineering Journal, 219, 499-511.

BOATENG, A. A., GARCIA-PEREZ, M., MASEK, O., BROWN, R. & DEL CAMPO, B. 2015. Biochar production technology. Biochar for Environmental Management: Science, Technology and Implementation, 2.

BOGUSZ, A., OLESZCZUK, P. & DOBROWOLSKI, R. 2015. Application of laboratory prepared and commercially available biochars to adsorption of cadmium, copper and zinc ions from water. Bioresource technology, 196, 540-549.

BREWER, C. E., SCHMIDT-ROHR, K., SATRIO, J. A. & BROWN, R. C. 2009. Characterization of biochar from fast pyrolysis and gasification systems. Environmental Progress & Sustainable Energy, 28, 386-396.

BRIDGWATER, A. 1994. Catalysis in thermal biomass conversion. Applied Catalysis A: General, 116, 5-47.

BROWN, R., CAMPO, B. D., BOATENG, A. A., GARCIA-PEREZ, M. & MASEK, O. 2015. Fundamentals of biochar production. Biochar for Environmental Management. Routledge, London, 39-62.

BRUNAUER, S., EMMETT, P. H. & TELLER, E. 1938a. Adsorption of gases in multimolecular layers. Journal of the American chemical society, 60, 309-319.

BRUNAUER, S., EMMETT, P. H. & TELLER, E. 1938b. Adsorption of gases in multimolecular layers. J. Am. Chem. Soc, 60, 309-319.

BUDAI, A., WANG, L., GRONLI, M., STRAND, L. T., ANTAL JR, M. J., ABIVEN, S., DIEGUEZ-ALONSO, A., ANCA-COUCE, A. & RASSE, D. P. 2014. Surface properties and chemical composition of corncob and Miscanthus biochars: effects of production temperature and method. Journal of agricultural and food chemistry, 62, 3791-3799.

168

CANTRELL, K. B., HUNT, P. G., UCHIMIYA, M., NOVAK, J. M. & RO, K. S. 2012. Impact of pyrolysis temperature and manure source on physicochemical characteristics of biochar. Bioresource Technology, 107, 419-428.

CAO, X., MA, L., GAO, B. & HARRIS, W. 2009. Dairy-manure derived biochar effectively sorbs lead and atrazine. Environmental science & technology, 43, 3285-3291.

CETIN, E., MOGHTADERI, B., GUPTA, R. & WALL, T. 2004. Influence of pyrolysis conditions on the structure and gasification reactivity of biomass chars. Fuel, 83, 2139-2150.

CLAOSTON, N., SAMSURI, A., AHMAD HUSNI, M. & MOHD AMRAN, M. 2014. Effects of pyrolysis temperature on the physicochemical properties of empty fruit bunch and rice husk biochars. Waste Management & Research, 32, 331-339.

CORNELISSEN, G., MARTINSEN, V., SHITUMBANUMA, V., ALLING, V., BREEDVELD, G. D., RUTHERFORD, D. W., SPARREVIK, M., HALE, S. E., OBIA, A. & MULDER, J. 2013. Biochar effect on maize yield and soil characteristics in five conservation farming sites in Zambia. Agronomy, 3, 256-274.

CHAN, K., VAN ZWIETEN, L., MESZAROS, I., DOWNIE, A. & JOSEPH, S. 2008a. Using poultry litter biochars as soil amendments. Soil Research, 46, 437-444.

CHAN, K. Y., VAN ZWIETEN, L., MESZAROS, I., DOWNIE, A. & JOSEPH, S. 2008b. Agronomic values of greenwaste biochar as a soil amendment. Soil Research, 45, 629-634.

CHEA, R., GRENOUILLET, G. & LEK, S. 2016. Evidence of water quality degradation in lower Mekong basin revealed by self-organizing map. PloS one, 11, e0145527.

CHEN, B., ZHOU, D. & ZHU, L. 2008. Transitional adsorption and partition of nonpolar and polar aromatic contaminants by biochars of pine needles with different pyrolytic temperatures. Environmental Science & Technology, 42, 5137-5143.

CHEN, Q., LUO, Z., HILLS, C., XUE, G. & TYRER, M. 2009. Precipitation of heavy metals from wastewater using simulated flue gas: sequent additions of fly ash, lime and carbon dioxide. Water research, 43, 2605-2614.

CHEN, S., ZHANG, J., ZHANG, C., YUE, Q., LI, Y. & LI, C. 2010. Equilibrium and kinetic studies of methyl orange and methyl violet adsorption on activated carbon derived from Phragmites australis. Desalination, 252, 149-156.

CHEN, T., ZHANG, Y., WANG, H., LU, W., ZHOU, Z., ZHANG, Y. & REN, L. 2014. Influence of pyrolysis temperature on characteristics and heavy metal adsorptive performance of biochar derived from municipal sewage sludge. Bioresource technology, 164, 47-54.

CHEN, X., CHEN, G., CHEN, L., CHEN, Y., LEHMANN, J., MCBRIDE, M. B. & HAY, A. G. 2011. Adsorption of copper and zinc by biochars produced from pyrolysis of hardwood and corn straw in aqueous solution. Bioresource technology, 102, 8877-8884.

CHEN, Y., YANG, H., WANG, X., ZHANG, S. & CHEN, H. 2012. Biomass-based pyrolytic polygeneration system on cotton stalk pyrolysis: influence of temperature. Bioresource technology, 107, 411-418.

CHENG, C.-H., LEHMANN, J. & ENGELHARD, M. H. 2008. Natural oxidation of black carbon in soils: Changes in molecular form and surface charge along a climosequence. Geochimica et Cosmochimica Acta, 72, 1598-1610.

CHENG, C.-H., LEHMANN, J., THIES, J. E., BURTON, S. D. & ENGELHARD, M. H. 2006. Oxidation of black carbon by biotic and abiotic processes. Organic Geochemistry, 37, 1477-1488.

CHEUNG, K. C., CHU, L. M. & WONG, M. H. 1997. Ammonia stripping as a pretreatment for landfill leachate. Water, air, and soil pollution, 94, 209-220.

CHEUNG, W., SZETO, Y. & MCKAY, G. 2007. Intraparticle diffusion processes during acid dye adsorption onto chitosan. Bioresource technology, 98, 2897-2904.

CHIEN, Y.-H. Water quality requirements and management for marine shrimp culture. Proceedings of the Special Session on Shrimp Farming, 1992. World Aquaculture Society Baton Rouge, LA, USA, 144-156.

CHO, H.-H., WEPASNICK, K., SMITH, B. A., BANGASH, F. K., FAIRBROTHER, D. H. & BALL, W. P. 2009. Sorption of aqueous Zn [II] and Cd [II] by multiwall carbon nanotubes: the relative roles of oxygen-containing functional groups and graphenic carbon. Langmuir, 26, 967-981.

CHOWDHURY, Z. Z., ZAIN, S. M., RASHID, A. & KHALID, K. 2011. Linear regression analysis for kinetics and isotherm studies of sorption of manganese (II) ions onto activated palm ash from waste water. Orient. J. Chem, 27, 405-415.

CHUN, Y., SHENG, G., CHIOU, C. T. & XING, B. 2004. Compositions and sorptive properties of crop residue-derived chars. Environmental science & technology, 38, 4649-4655.

DAI, Z., MENG, J., MUHAMMAD, N., LIU, X., WANG, H., HE, Y., BROOKES, P. C. & XU, J. 2013. The potential feasibility for soil improvement, based on the properties of biochars pyrolyzed from different feedstocks. Journal of soils and sediments, 13, 989-1000.

DALI-YOUCEF, N., OUDDANE, B. & DERRICHE, Z. 2006. Adsorption of zinc on natural sediment of Tafna River (Algeria). Journal of hazardous materials, 137, 1263-1270.

DEMIRBAS, A. 2004. Effects of temperature and particle size on bio-char yield from pyrolysis of agricultural residues. Journal of analytical and applied pyrolysis, 72, 243-248.

DEPCI, T., KUL, A. R. & ÖNAL, Y. 2012. Competitive adsorption of lead and zinc from aqueous solution on activated carbon prepared from Van apple pulp: study in single-and multi-solute systems. Chemical Engineering Journal, 200, 224-236.

DI IACONI, C., RAMADORI, R. & LOPEZ, A. 2006. Combined biological and chemical degradation for treating a mature municipal landfill leachate. Biochemical Engineering Journal, 31, 118-124.

DING, W., DONG, X., IME, I. M., GAO, B. & MA, L. Q. 2014. Pyrolytic temperatures impact lead sorption mechanisms by bagasse biochars. Chemosphere, 105, 68-74.

DING, Y., LIU, Y.-X., WU, W.-X., SHI, D.-Z., YANG, M. & ZHONG, Z.-K. 2010. Evaluation of biochar effects on nitrogen retention and leaching in multi-layered soil columns. Water, Air, & Soil Pollution, 213, 47-55.

DING, Z., HU, X., WAN, Y., WANG, S. & GAO, B. 2016. Removal of lead, copper, cadmium, zinc, and nickel from aqueous solutions by alkali-modified biochar: Batch and column tests. Journal of Industrial and Engineering Chemistry, 33, 239-245.

DOULA, M. K. 2009. Simultaneous removal of Cu, Mn and Zn from drinking water with the use of clinoptilolite and its Fe-modified form. Water Research, 43, 3659-3672.

DOUMER, M., RIGOL, A., VIDAL, M. & MANGRICH, A. 2016. Removal of Cd, Cu, Pb, and Zn from aqueous solutions by biochars. Environmental Science and Pollution Research, 23, 2684-2692.

DOWNIE, A. E., VAN ZWIETEN, L., SMERNIK, R. J., MORRIS, S. & MUNROE, P. R. 2011. Terra Preta Australis: Reassessing the carbon storage capacity of temperate soils. Agriculture, ecosystems & environment, 140, 137-147.

DUAN, J., LU, Q., CHEN, R., DUAN, Y., WANG, L., GAO, L. & PAN, S. 2010. Synthesis of a novel flocculant on the basis of crosslinked Konjac glucomannan-graft-polyacrylamide-co-sodium xanthate and its application in removal of Cu 2+ ion. Carbohydrate Polymers, 80, 436-441.

DUKU, M. H., GU, S. & HAGAN, E. B. 2011. Biochar production potential in Ghana—a review. Renewable and Sustainable Energy Reviews, 15, 3539-3551.

EL-GOHARY, F. A. & KAMEL, G. 2016. Characterization and biological treatment of pre-treated landfill leachate. Ecological Engineering, 94, 268-274.

EL-SALAM, M. M. A. & ABU-ZUID, G. I. 2015. Impact of landfill leachate on the groundwater quality: A case study in Egypt. Journal of advanced research, 6, 579-586.

ENDERS, A., HANLEY, K., WHITMAN, T., JOSEPH, S. & LEHMANN, J. 2012. Characterization of biochars to evaluate recalcitrance and agronomic performance. Bioresource Technology, 114, 644-653.

ESSINGTON, M. E. 2015. Soil and water chemistry: An integrative approach, CRC press.

FANG, Q., CHEN, B., LIN, Y. & GUAN, Y. 2014. Aromatic and Hydrophobic Surfaces of Wood-derived Biochar Enhance Perchlorate Adsorption via Hydrogen Bonding to Oxygen-containing Organic Groups. Environmental Science & Technology, 48, 279-288.

FOO, K. & HAMEED, B. 2009. An overview of landfill leachate treatment via activated carbon adsorption process. Journal of hazardous materials, 171, 54-60.

FOO, K. & HAMEED, B. 2012. Textural porosity, surface chemistry and adsorptive properties of durian shell derived activated carbon prepared by microwave assisted NaOH activation. Chemical engineering journal, 187, 53-62.

FREUNDLICH, H. 1906. Over the adsorption in solution. J. Phys. Chem, 57, e470.

FRIŠTÁK, V., PIPÍŠKA, M., LESNÝ, J., SOJA, G., FRIESL-HANL, W. & PACKOVÁ, A. 2015. Utilization of biochar sorbents for Cd2+, Zn2+, and Cu2+ ions separation from aqueous solutions: comparative study. Environmental monitoring and assessment, 187, 4093.

FU, P., YI, W., BAI, X., LI, Z., HU, S. & XIANG, J. 2011. Effect of temperature on gas composition and char structural features of pyrolyzed agricultural residues. Bioresource Technology, 102, 8211-8219.

GAI, X., WANG, H., LIU, J., ZHAI, L., LIU, S., REN, T. & LIU, H. 2014. Effects of feedstock and pyrolysis temperature on biochar adsorption of ammonium and nitrate. PloS one, 9, e113888.

GAO, F., XUE, Y., DENG, P., CHENG, X. & YANG, K. 2015. Removal of aqueous ammonium by biochars derived from agricultural residuals at different pyrolysis temperatures. Chemical Speciation & Bioavailability, 27, 92-97.

GASKIN, J., STEINER, C., HARRIS, K., DAS, K. & BIBENS, B. 2008a. Effect of low-temperature pyrolysis conditions on biochar for agricultural use. Transactions of the ASABE, 51, 2061-2069.

GASKIN, J., STEINER, C., HARRIS, K., DAS, K. & BIBENS, B. 2008b. Effect of low-temperature pyrolysis conditions on biochar for agricultural use. Trans. Asabe, 51, 2061-2069.

GERLACH, R., BAUMEWERD-SCHMIDT, H., VAN DEN BORG, K., ECKMEIER, E. & SCHMIDT, M. W. 2006. Prehistoric alteration of soil in the Lower Rhine Basin, Northwest Germany— archaeological, 14 C and geochemical evidence. Geoderma, 136, 38-50.

GLASER, B., BALASHOV, E., HAUMAIER, L., GUGGENBERGER, G. & ZECH, W. 2000. Black carbon in density fractions of anthropogenic soils of the Brazilian Amazon region. Organic Geochemistry, 31, 669-678.

GLASER, B., HAUMAIER, L., GUGGENBERGER, G. & ZECH, W. 2001. The'Terra Preta'phenomenon: a model for sustainable agriculture in the humid tropics. Naturwissenschaften, 88, 37-41.

GONZALEZ-MUNOZ, M. J., RODRIGUEZ, M. A., LUQUE, S. & ALVAREZ, J. R. 2006. Recovery of heavy metals from metal industry waste waters by chemical precipitation and nanofiltration. Desalination, 200, 742-744.

GUERRERO, M., RUIZ, M., ALZUETA, M., BILBAO, R. & MILLERA, A. 2005. Pyrolysis of eucalyptus at different heating rates: studies of char characterization and oxidative reactivity. Journal of Analytical and Applied Pyrolysis, 74, 307-314.

GUNDALE, M. J. & DELUCA, T. H. 2006. Temperature and source material influence ecological attributes of ponderosa pine and Douglas-fir charcoal. Forest Ecology and Management, 231, 86-93.

GUO, Y., YANG, S., YU, K., ZHAO, J., WANG, Z. & XU, H. 2002. The preparation and mechanism studies of rice husk based porous carbon. Materials chemistry and physics, 74, 320-323.

GUPTA, V. K., RASTOGI, A. & NAYAK, A. 2010. Biosorption of nickel onto treated alga (Oedogonium hatei): application of isotherm and kinetic models. Journal of Colloid and Interface Science, 342, 533-539.

HAGIN, J. & TUCKER, B. 1982. Fertilization of dryland and irrigated soils, Springer.

HALE, S., ALLING, V., MARTINSEN, V., MULDER, J., BREEDVELD, G. & CORNELISSEN, G. 2013. The sorption and desorption of phosphate-P, ammonium-N and nitrate-N in cacao shell and corn cob biochars. Chemosphere, 91, 1612-1619.

HALE, S. E. A., V.; MARTINSEN, V.; MULDER, J.; BREEDVELD, G. D.; CORNELISSEN, G. 2013. The sorption and desorption of phosphate-P, ammonium-N and nitrate-N in cacao shell and corn cob biochars. Chemosphere 91, 1612-1619.

HALIM, A. A., LATIF, M. T. & ITHNIN, A. 2013. Ammonia removal from aqueous solution using organic acid modified activated carbon. World Applied Sciences Journal, 24, 01-06.

HAMEED, B., TAN, I. & AHMAD, A. 2008. Adsorption isotherm, kinetic modeling and mechanism of 2, 4, 6-trichlorophenol on coconut husk-based activated carbon. Chemical Engineering Journal, 144, 235-244.

HAN, Y., BOATENG, A. A., QI, P. X., LIMA, I. M. & CHANG, J. 2013. Heavy metal and phenol adsorptive properties of biochars from pyrolyzed switchgrass and woody biomass in correlation with surface properties. Journal of environmental management, 118, 196-204.

HANKINS, N. P., LU, N. & HILAL, N. 2006. Enhanced removal of heavy metal ions bound to humic acid by polyelectrolyte flocculation. Separation and Purification Technology, 51, 48-56.

HARVEY, O. R., HERBERT, B. E., RHUE, R. D. & KUO, L.-J. 2011. Metal interactions at the biochar-water interface: energetics and structure-sorption relationships elucidated by flow adsorption microcalorimetry. Environmental science & technology, 45, 5550-5556.

HEREDIA, J. B. & MARTÍN, J. S. 2009. Removing heavy metals from polluted surface water with a tannin-based flocculant agent. Journal of hazardous materials, 165, 1215-1218.

HERNANDEZ-MENA, L. E., PÉCORAA, A. A. & BERALDOB, A. L. 2014. Slow pyrolysis of bamboo biomass: Analysis of biochar properties. CHEMICAL ENGINEERING, 37.

HO, Y.-S. & MCKAY, G. 1999. Pseudo-second order model for sorption processes. Process biochemistry, 34, 451-465.

HOLLISTER, C. C., BISOGNI, J. J. & LEHMANN, J. 2013. Ammonium, nitrate, and phosphate sorption to and solute leaching from biochars prepared from corn stover (Zea mays L.) and oak wood (Quercus spp.). Journal of environmental quality, 42, 137-144.

HOSSAIN, M. K., STREZOV, V., CHAN, K. Y., ZIOLKOWSKI, A. & NELSON, P. F. 2011. Influence of pyrolysis temperature on production and nutrient properties of wastewater sludge biochar. Journal of Environmental Management, 92, 223-228.

HOU, J., HUANG, L., YANG, Z., ZHAO, Y., DENG, C., CHEN, Y. & LI, X. 2016. Adsorption of ammonium on biochar prepared from giant reed. Environmental Science and Pollution Research, 23, 19107-19115.

HOUBEN, D., EVRARD, L. & SONNET, P. 2013. Mobility, bioavailability and pH-dependent leaching of cadmium, zinc and lead in a contaminated soil amended with biochar. Chemosphere, 92, 1450-1457.

HU, L., LI, X., LIU, B., GU, M. & DAI, J. 2009. Organic structure and possible origin of ancient charred paddies at Chuodun Site in southern China. Science in China Series D: Earth Sciences, 52, 93-100.

HUANG, M., YANG, L., QIN, H., JIANG, L. & ZOU, Y. 2014a. Fertilizer nitrogen uptake by rice increased by biochar application. Biology and Fertility of Soils, 50, 997-1000.

HUANG, Y., LI, S., LIN, H. & CHEN, J. 2014b. Fabrication and characterization of mesoporous activated carbon from Lemna minor using one-step H_3PO_4 activation for Pb (II) removal. Applied Surface Science, 317, 422-431.

HUGGINS, T. M., HAEGER, A., BIFFINGER, J. C. & REN, Z. J. 2016. Granular biochar compared with activated carbon for wastewater treatment and resource recovery. Water research, 94, 225-232.

HUI, K., CHAO, C. Y. H. & KOT, S. 2005. Removal of mixed heavy metal ions in wastewater by zeolite 4A and residual products from recycled coal fly ash. Journal of Hazardous Materials, 127, 89-101.

IM, J.-H., WOO, H.-J., CHOI, M.-W., HAN, K.-B. & KIM, C.-W. 2001. Simultaneous organic and nitrogen removal from municipal landfill leachate using an anaerobic-aerobic system. Water research, 35, 2403-2410.

JENKINSON, D. & AYANABA, A. 1977. Decomposition of carbon-14 labeled plant material under tropical conditions. Soil Science Society of America Journal, 41, 912-915.

JIEN, S.-H. & WANG, C.-S. 2013. Effects of biochar on soil properties and erosion potential in a highly weathered soil. Catena, 110, 225-233.

JONES, D., ROUSK, J., EDWARDS-JONES, G., DELUCA, T. & MURPHY, D. 2012. Biochar-mediated changes in soil quality and plant growth in a three year field trial. Soil Biology and Biochemistry, 45, 113-124.

JONES, D. L., EDWARDS-JONES, G. & MURPHY, D. V. 2011. Biochar mediated alterations in herbicide breakdown and leaching in soil. Soil Biology and Biochemistry, 43, 804-813.

JOSEPH, S., CAMPS-ARBESTAIN, M., LIN, Y., MUNROE, P., CHIA, C., HOOK, J., VAN ZWIETEN, L., KIMBER, S., COWIE, A. & SINGH, B. 2010. An investigation into the reactions of biochar in soil. Soil Research, 48, 501-515.

JOSEPH, S. & LEHMANN, J. 2009. Biochar for environmental management: science and technology, London, GB: Earthscan.

KABATA-PENDIAS, A. 2010. Trace elements in soils and plants, CRC press.

KARGı, F. & PAMUKOGLU, M. Y. 2004. Adsorbent supplemented biological treatment of pre-treated landfill leachate by fed-batch operation. Bioresource Technology, 94, 285-291.

KARGI, F. & PAMUKOGLU, M. Y. 2004. Repeated fed-batch biological treatment of pre-treated landfill leachate by powdered activated carbon addition. Enzyme and Microbial Technology, 34, 422-428.

KARNIB, M., KABBANI, A., HOLAIL, H. & OLAMA, Z. 2014. Heavy metals removal using activated carbon, silica and silica activated carbon composite. Energy Procedia, 50, 113-120.

KEILUWEIT, M., NICO, P. S., JOHNSON, M. G. & KLEBER, M. 2010. Dynamic molecular structure of plant biomass-derived black carbon (biochar). Environmental science & technology, 44, 1247-1253.

KENNEDY, K. & LENTZ, E. 2000. Treatment of landfill leachate using sequencing batch and continuous flow upflow anaerobic sludge blanket (UASB) reactors. Water Research, 34, 3640-3656.

KIM, K. H., KIM, J.-Y., CHO, T.-S. & CHOI, J. W. 2012. Influence of pyrolysis temperature on physicochemical properties of biochar obtained from the fast pyrolysis of pitch pine (Pinus rigida). Bioresource technology, 118, 158-162.

KIZITO, S., WU, S., KIRUI, W. K., LEI, M., LU, Q., BAH, H. & DONG, R. 2015. Evaluation of slow pyrolyzed wood and rice husks biochar for adsorption of ammonium nitrogen from piggery manure anaerobic digestate slurry. Science of the Total Environment, 505, 102-112.

KOBYA, M., DEMIRBAS, E., SENTURK, E. & INCE, M. 2005. Adsorption of heavy metal ions from aqueous solutions by activated carbon prepared from apricot stone. Bioresource technology, 96, 1518-1521.

KOŁODYŃSKA, D., WNĘTRZAK, R., LEAHY, J., HAYES, M., KWAPIŃSKI, W. & HUBICKI, Z. 2012. Kinetic and adsorptive characterization of biochar in metal ions removal. Chemical Engineering Journal, 197, 295-305.

KOMKIENE, J. & BALTRENAITE, E. 2016. Biochar as adsorbent for removal of heavy metal ions [Cadmium (II), Copper (II), Lead (II), Zinc (II)] from aqueous phase. International Journal of Environmental Science and Technology, 13, 471-482.

KUMAR, P. S., RAMAKRISHNAN, K., KIRUPHA, S. D. & SIVANESAN, S. 2010. Thermodynamic and kinetic studies of cadmium adsorption from aqueous solution onto rice husk. Brazilian Journal of Chemical Engineering, 27, 347-355.

KUMAR, S. & GUPTA, R. B. 2009. Biocrude production from switchgrass using subcritical water. Energy & Fuels, 23, 5151-5159.

KURNIAWAN, T. A., LO, W.-H. & CHAN, G. Y. 2006. Physico-chemical treatments for removal of recalcitrant contaminants from landfill leachate. Journal of hazardous materials, 129, 80-100.

LAIRD, D., FLEMING, P., WANG, B., HORTON, R. & KARLEN, D. 2010. Biochar impact on nutrient leaching from a Midwestern agricultural soil. Geoderma, 158, 436-442.

LANDABURU-AGUIRRE, J., PONGRÁCZ, E., PERÄMÄKI, P. & KEISKI, R. L. 2010. Micellar-enhanced ultrafiltration for the removal of cadmium and zinc: use of response surface

methodology to improve understanding of process performance and optimisation. Journal of hazardous materials, 180, 524-534.

LANGMUIR, I. 1917. The constitution and fundamental properties of solids and liquids. Journal of the Franklin Institute, 183, 102-105.

LE LEUCH, L. & BANDOSZ, T. 2007. The role of water and surface acidity on the reactive adsorption of ammonia on modified activated carbons. Carbon, 45, 568-578.

LEE, J. W., KIDDER, M., EVANS, B. R., PAIK, S., BUCHANAN III, A., GARTEN, C. T. & BROWN, R. C. 2010. Characterization of biochars produced from cornstovers for soil amendment. Environmental Science & Technology, 44, 7970-7974.

LEE, Y., PARK, J., RYU, C., GANG, K. S., YANG, W., PARK, Y.-K., JUNG, J. & HYUN, S. 2013. Comparison of biochar properties from biomass residues produced by slow pyrolysis at 500 C. Bioresource technology, 148, 196-201.

LEHMANN, J. & JOSEPH, S. 2015. Biochar for environmental management: science, technology and implementation, Routledge.

LEHMANN, J. & RONDON, M. 2006. Bio-char soil management on highly weathered soils in the humid tropics. Biological approaches to sustainable soil systems. CRC Press, Boca Raton, FL, 517-530.

LENTZ, R. & IPPOLITO, J. 2012. Biochar and manure affect calcareous soil and corn silage nutrient concentrations and uptake. Journal of environmental quality, 41, 1033-1043.

LI, W., LOYOLA-LICEA, C., CROWLEY, D. E. & AHMAD, Z. 2016. Performance of a two-phase biotrickling filter packed with biochar chips for treatment of wastewater containing high nitrogen and phosphorus concentrations. Process Safety and Environmental Protection, 102, 150-158.

LI, X. & ZHAO, Q. 2001. Efficiency of biological treatment affected by high strength of ammonium-nitrogen in leachate and chemical precipitation of ammonium-nitrogen as pretreatment. Chemosphere, 44, 37-43.

LIANG, B., LEHMANN, J., SOLOMON, D., KINYANGI, J., GROSSMAN, J., O'NEILL, B., SKJEMSTAD, J. O., THIES, J., LUIZÃO, F. J., PETERSEN, J. & NEVES, E. G. 2006. Black Carbon Increases Cation Exchange Capacity in Soils. Soil Science Society of America Journal, 70.

LIN, S. H. & CHANG, C. C. 2000. Treatment of landfill leachate by combined electro-Fenton oxidation and sequencing batch reactor method. Water Research, 34, 4243-4249.

LIU, L., SHEN, G., SUN, M., CAO, X., SHANG, G. & CHEN, P. 2014. Effect of biochar on nitrous oxide emission and its potential mechanisms. Journal of the Air & Waste Management Association, 64, 894-902.

LIU, N., SUN, Z. T., WU, Z. C., ZHAN, X. M., ZHANG, K., ZHAO, E. F. & HAN, X. R. Adsorption characteristics of ammonium nitrogen by biochar from diverse origins in water. Advanced Materials Research, 2013. Trans Tech Publ, 305-312.

LIU, Y. Y., M.; WU, Y.; WANG, H.; CHEN, Y.; WU, W. 2011. Reducing CH4 and CO2 emissions from waterlogged paddy soil with biochar. J Soils Sediments, 11, 930-939.

LIU, Z., ZHANG, F.-S. & WU, J. 2010. Characterization and application of chars produced from pinewood pyrolysis and hydrothermal treatment. Fuel, 89, 510-514.

LONG, X. L., CHENG, H., XIN, Z. L., XIAO, W. D., LI, W. & YUAN, W. K. 2008. Adsorption of ammonia on activated carbon from aqueous solutions. Environmental Progress, 27, 225-233.

LU, C. & CHIU, H. 2006. Adsorption of zinc (II) from water with purified carbon nanotubes. Chemical Engineering Science, 61, 1138-1145.

LU, H., ZHANG, W., WANG, S., ZHUANG, L., YANG, Y. & QIU, R. 2013. Characterization of sewage sludge-derived biochars from different feedstocks and pyrolysis temperatures. Journal of Analytical and Applied Pyrolysis, 102, 137-143.

LUNA, Y., OTAL, E., VILCHES, L., VALE, J., QUEROL, X. & PEREIRA, C. F. 2007. Use of zeolitised coal fly ash for landfill leachate treatment: A pilot plant study. Waste Management, 27, 1877-1883.

LUTERBACHER, J. S., PARLANGE, J. Y. & WALKER, L. P. 2013. A pore-hindered diffusion and reaction model can help explain the importance of pore size distribution in enzymatic hydrolysis of biomass. Biotechnology and bioengineering, 110, 127-136.

MA, Z., LI, Q., YUE, Q., GAO, B., LI, W., XU, X. & ZHONG, Q. 2011. Adsorption removal of ammonium and phosphate from water by fertilizer controlled release agent prepared from wheat straw. Chemical Engineering Journal, 171, 1209-1217.

MAJOR, J., RONDON, M., MOLINA, D., RIHA, S. J. & LEHMANN, J. 2010. Maize yield and nutrition during 4 years after biochar application to a Colombian savanna oxisol. Plant and soil, 333, 117-128.

MALOVANYY, A., SAKALOVA, H., YATCHYSHYN, Y., PLAZA, E. & MALOVANYY, M. 2013. Concentration of ammonium from municipal wastewater using ion exchange process. Desalination, 329, 93-102.

MARANON, E., ULMANU, M., FERNANDEZ, Y., ANGER, I. & CASTRILLÓN, L. 2006. Removal of ammonium from aqueous solutions with volcanic tuff. Journal of Hazardous materials, 137, 1402-1409.

MARTTINEN, S., KETTUNEN, R., SORMUNEN, K., SOIMASUO, R. & RINTALA, J. 2002. Screening of physical–chemical methods for removal of organic material, nitrogen and toxicity from low strength landfill leachates. Chemosphere, 46, 851-858.

MASIELLO, C. A. & DRUFFEL, E. R. M. 1998. Black Carbon in Deep-Sea Sediments. Science, 280, 1911-1913.

MATTHEWS, R., WINSON, M. & SCULLION, J. 2009. Treating landfill leachate using passive aeration trickling filters; effects of leachate characteristics and temperature on rates and process dynamics. Science of the total environment, 407, 2557-2564.

MEDVEĎ, I. & ČERNÝ, R. 2011. Surface diffusion in porous media: A critical review. Microporous and Mesoporous Materials, 142, 405-422.

MÉNDEZ, A., TARQUIS, A., SAA-REQUEJO, A., GUERRERO, F. & GASCÓ, G. 2013a. Influence of pyrolysis temperature on composted sewage sludge biochar priming effect in a loamy soil. Chemosphere, 93, 668-676.

MÉNDEZ, A., TARQUIS, A. M., SAA-REQUEJO, A., GUERRERO, F. & GASCÓ, G. 2013b. Influence of pyrolysis temperature on composted sewage sludge biochar priming effect in a loamy soil. Chemosphere, 93, 668-676.

MÉNDEZ, A., TERRADILLOS & GASCÓ, G. 2013c. Physicochemical and agronomic properties of biochar from sewage sludge pyrolysed at different temperatures. Journal of Analytical and Applied Pyrolysis, 102, 124-130.

MOHAN, D., PITTMAN JR, C. U., BRICKA, M., SMITH, F., YANCEY, B., MOHAMMAD, J., STEELE, P. H., ALEXANDRE-FRANCO, M. F., GÓMEZ-SERRANO, V. & GONG, H. 2007. Sorption of arsenic, cadmium, and lead by chars produced from fast pyrolysis of wood and bark during bio-oil production. Journal of colloid and interface science, 310, 57-73.

MOHAN, D. & SINGH, K. P. 2002. Single-and multi-component adsorption of cadmium and zinc using activated carbon derived from bagasse—an agricultural waste. Water research, 36, 2304-2318.

MOHANTY, S. K. & BOEHM, A. B. 2014. Escherichia coli removal in biochar-augmented biofilter: Effect of infiltration rate, initial bacterial concentration, biochar particle size, and presence of compost. Environmental science & technology, 48, 11535-11542.

MONJE-RAMIREZ, I. & DE VELASQUEZ, M. O. 2004. Removal and transformation of recalcitrant organic matter from stabilized saline landfill leachates by coagulation–ozonation coupling processes. Water research, 38, 2359-2367.

MOOSA, A. A., RIDHA, A. M. & HUSSIEN, N. A. 2016. Removal of Zinc Ions from Aqueous Solution by Bioadsorbents and CNTs. American Journal of Materials Science, 6, 105-114.

MORADI, O. & ZARE, K. 2013. Adsorption of ammonium ion by multi-walled carbon nanotube: kinetics and thermodynamic studies. Fullerenes, Nanotubes and Carbon Nanostructures, 21, 449-459.

MORENO-BARBOSA, J. J., LÓPEZ-VELANDIA, C., DEL PILAR MALDONADO, A., GIRALDO, L. & MORENO-PIRAJÁN, J. C. 2013. Removal of lead (II) and zinc (II) ions from aqueous solutions by adsorption onto activated carbon synthesized from watermelon shell and walnut shell. Adsorption, 19, 675-685.

MUBARAK, N., ALICIA, R., ABDULLAH, E., SAHU, J., HASLIJA, A. A. & TAN, J. 2013. Statistical optimization and kinetic studies on removal of Zn 2+ using functionalized carbon nanotubes and magnetic biochar. Journal of Environmental Chemical Engineering, 1, 486-495.

MUI, E. L., CHEUNG, W., VALIX, M. & MCKAY, G. 2010. Dye adsorption onto char from bamboo. Journal of hazardous materials, 177, 1001-1005.

MUKOME, F. N., ZHANG, X., SILVA, L. C., SIX, J. & PARIKH, S. J. 2013. Use of chemical and physical characteristics to investigate trends in biochar feedstocks. Journal of agricultural and food chemistry, 61, 2196-2204.

MUKHERJEE, A., ZIMMERMAN, A. & HARRIS, W. 2011. Surface chemistry variations among a series of laboratory-produced biochars. Geoderma, 163, 247-255.

MUKHERJEE, A. & ZIMMERMAN, A. R. 2013a. Organic carbon and nutrient release from a range of laboratory-produced biochars and biochar–soil mixtures. Geoderma, 193–194, 122-130.

MUKHERJEE, A. & ZIMMERMAN, A. R. 2013b. Organic carbon and nutrient release from a range of laboratory-produced biochars and biochar–soil mixtures. Geoderma, 193, 122-130.

NADEEM, M., MAHMOOD, A., SHAHID, S., SHAH, S., KHALID, A. & MCKAY, G. 2006. Sorption of lead from aqueous solution by chemically modified carbon adsorbents. Journal of Hazardous Materials, 138, 604-613.

NAMGAY, T., SINGH, B. & SINGH, B. P. 2010. Influence of biochar application to soil on the availability of As, Cd, Cu, Pb, and Zn to maize (Zea mays L.). Soil Research, 48, 638-647.

NASSER, R. A.-S. & AREF, I. M. 2014. Fuelwood Characteristics of Six Acacia Species Growing Wild in the Southwest of Saudi Arabia as Affected by Geographical Location.

NDOR, E., AMANA, S. & ASADU, C. 2015. Effect of biochar on soil properties and organic carbon sink in degraded soil of Southern Guinea Savanna Zone, Nigeria. Int. J. Plant Soil Sci, 4, 252-258.

NEVES, E. G., PETERSEN, J. B., BARTONE, R. N. & DA SILVA, C. A. 2003. Historical and socio-cultural origins of Amazonian dark earth. Amazonian dark earths. Springer.

NIGUSSIE, A., KISSI, E., MISGANAW, M. & AMBAW, G. 2012. Effect of biochar application on soil properties and nutrient uptake of lettuces (Lactuca sativa) grown in chromium polluted soils. American-Eurasian Journal of Agriculture and Environmental Science, 12, 369-376.

NOVAK, J. M., LIMA, I., XING, B., GASKIN, J. W., STEINER, C., DAS, K., AHMEDNA, M., REHRAH, D., WATTS, D. W. & BUSSCHER, W. J. 2009. Characterization of designer biochar produced at different temperatures and their effects on a loamy sand. Annals of Environmental Science, 3, 195-206.

NGUYEN, B. T. & LEHMANN, J. 2009. Black carbon decomposition under varying water regimes. Organic Geochemistry, 40, 846-853.

O'NEILL, B., GROSSMAN, J., TSAI, M., GOMES, J., LEHMANN, J., PETERSON, J., NEVES, E. & THIES, J. 2009. Bacterial community composition in Brazilian anthrosols and adjacent soils characterized using culturing and molecular identification. Microbial Ecology, 58, 23-35.

OGAWA, M. & OKIMORI, Y. 2010. Pioneering works in biochar research, Japan. Soil Research, 48, 489-500.

ONAY, O. 2007. Influence of pyrolysis temperature and heating rate on the production of bio-oil and char from safflower seed by pyrolysis, using a well-swept fixed-bed reactor. Fuel Processing Technology, 88, 523-531.

ORGANIZATION, W. H. 2004a. Back ground document for evelopment of WHO Guidelines for drinking water quality. PP.

ORGANIZATION, W. H. 2004b. Guidelines for drinking-water quality, World Health Organization.

ORUPOLD, K., TENNO, T. & HENRYSSON, T. 2000. Biological lagooning of phenols-containing oil shale ash heaps leachate. Water Research, 34, 4389-4396.

OTAL, E., VILCHES, L. F., LUNA, Y., POBLETE, R., GARCÍA-MAYA, J. M. & FERNÁNDEZ-PEREIRA, C. 2013. Ammonium ion adsorption and settleability improvement achieved in a synthetic zeolite-amended activated sludge. Chinese Journal of Chemical Engineering, 21, 1062-1068.

ÖZTÜRK, N. & BEKTAŞ, T. E. 2004. Nitrate removal from aqueous solution by adsorption onto various materials. Journal of hazardous materials, 112, 155-162.

PAETHANOM, A. & YOSHIKAWA, K. 2012. Influence of pyrolysis temperature on rice husk char characteristics and its tar adsorption capability. Energies, 5, 4941-4951.

PARK, J.-H., OK, Y. S., KIM, S.-H., CHO, J.-S., HEO, J.-S., DELAUNE, R. D. & SEO, D.-C. 2016. Competitive adsorption of heavy metals onto sesame straw biochar in aqueous solutions. Chemosphere, 142, 77-83.

PARK, J. H., CHOPPALA, G. K., BOLAN, N. S., CHUNG, J. W. & CHUASAVATHI, T. 2011. Biochar reduces the bioavailability and phytotoxicity of heavy metals. Plant and soil, 348, 439.

PELLERA, F.-M., GIANNIS, A., KALDERIS, D., ANASTASIADOU, K., STEGMANN, R., WANG, J.-Y. & GIDARAKOS, E. 2012. Adsorption of Cu (II) ions from aqueous solutions on biochars prepared from agricultural by-products. Journal of Environmental Management, 96, 35-42.

PUGA, A. P., MELO, L. C. A., DE ABREU, C. A., COSCIONE, A. R. & PAZ-FERREIRO, J. 2016. Leaching and fractionation of heavy metals in mining soils amended with biochar. Soil and Tillage Research, 164, 25-33.

QIAO, S., MATSUMOTO, N., SHINOHARA, T., NISHIYAMA, T., FUJII, T., BHATTI, Z. & FURUKAWA, K. 2010. High-rate partial nitrification performance of high ammonium containing wastewater under low temperatures. Bioresource technology, 101, 111-117.

QIU, Y., ZHENG, Z., ZHOU, Z. & SHENG, G. D. 2009. Effectiveness and mechanisms of dye adsorption on a straw-based biochar. Bioresour Technol, 100, 5348-51.

QURESI-II, T. I., KIMB, H.-T. & YOUNG-JU, K. 2002. UV-Catalytic Treatment of Municipal Solid-Waste Landfill Leachate with Hydrogen Peroxide and Ozone Oxidation. TOG, 146, 5.

RADNIA, H., GHOREYSHI, A. A. & YOUNESI, H. 2011. Isotherm and kinetics of Fe (II) adsorption onto chitosan in a batch process. Iranica Journal of Energy and Environment, 2, 250-257.

RAJKOVICH, S., ENDERS, A., HANLEY, K., HYLAND, C., ZIMMERMAN, A. R. & LEHMANN, J. 2012. Corn growth and nitrogen nutrition after additions of biochars with varying properties to a temperate soil. Biology and Fertility of Soils, 48, 271-284.

REGMI, P., MOSCOSO, J. L. G., KUMAR, S., CAO, X., MAO, J. & SCHAFRAN, G. 2012. Removal of copper and cadmium from aqueous solution using switchgrass biochar produced via hydrothermal carbonization process. Journal of environmental management, 109, 61-69.

RENOU, S., GIVAUDAN, J., POULAIN, S., DIRASSOUYAN, F. & MOULIN, P. 2008. Landfill leachate treatment: review and opportunity. Journal of hazardous materials, 150, 468-493.

RILLIG, M. C. & THIES, J. E. 2012. Characteristics of biochar: biological properties. Biochar for environmental management. Routledge.

ROUQUEROL, J., AVNIR, D., FAIRBRIDGE, C., EVERETT, D., HAYNES, J., PERNICONE, N., RAMSAY, J., SING, K. & UNGER, K. 1994. Recommendations for the characterization of porous solids (Technical Report). Pure and Applied Chemistry, 66, 1739-1758.

SABBAH, I., BARANSI, K., MASSALHA, N., DAWAS, A., SAADI, I. & NEJIDAT, A. 2013. Efficient ammonia removal from wastewater by a microbial biofilm in tuff-based intermittent biofilters. Ecological engineering, 53, 354-360.

SALEH, M. E., MAHMOUD, A. H. & RASHAD, M. 2012. Peanut biochar as a stable adsorbent for removing N [H. sub. 4]-N from wastewater: a preliminary study. Advances in environmental biology, 2170-2177.

SAMPER, E., RODRÍGUEZ, M., DE LA RUBIA, M. & PRATS, D. 2009. Removal of metal ions at low concentration by micellar-enhanced ultrafiltration (MEUF) using sodium dodecyl

sulfate (SDS) and linear alkylbenzene sulfonate (LAS). Separation and purification technology, 65, 337-342.

SARKHOT, D., GHEZZEHEI, T. & BERHE, A. 2013. Effectiveness of biochar for sorption of ammonium and phosphate from dairy effluent. Journal of environmental quality, 42, 1545-1554.

SCHMIDT, M. W. & NOACK, A. G. 2000. Black carbon in soils and sediments: analysis, distribution, implications, and current challenges. Global biogeochemical cycles, 14, 777-793.

SCHROEDER, J., CROOT, P., VON DEWITZ, B., WALLER, U. & HANEL, R. 2011. Potential and limitations of ozone for the removal of ammonia, nitrite, and yellow substances in marine recirculating aquaculture systems. Aquacultural engineering, 45, 35-41.

SEPTIEN, S., VALIN, S., DUPONT, C., PEYROT, M. & SALVADOR, S. 2012. Effect of particle size and temperature on woody biomass fast pyrolysis at high temperature (1000–1400 C). Fuel, 97, 202-210.

SEPTIEN, S., VALIN, S., PEYROT, M., SPINDLER, B. & SALVADOR, S. 2013. Influence of steam on gasification of millimetric wood particles in a drop tube reactor: Experiments and modelling. Fuel, 103, 1080-1089.

SHAHEEN, S. M., EISSA, F. I., GHANEM, K. M., EL-DIN, H. M. G. & AL ANANY, F. S. 2013. Heavy metals removal from aqueous solutions and wastewaters by using various byproducts. Journal of environmental management, 128, 514-521.

SHARMA, R. K., WOOTEN, J. B., BALIGA, V. L., LIN, X., GEOFFREY CHAN, W. & HAJALIGOL, M. R. 2004. Characterization of chars from pyrolysis of lignin. Fuel, 83, 1469-1482.

SHARMA, R. K., WOOTEN, J. B., BALIGA, V. L., MARTOGLIO-SMITH, P. A. & HAJALIGOL, M. R. 2002. Characterization of char from the pyrolysis of tobacco. Journal of agricultural and food chemistry, 50, 771-783.

SHEHZAD, A., BASHIR, M. J., SETHUPATHI, S. & LIM, J.-W. 2016. An insight into the remediation of highly contaminated landfill leachate using sea mango based activated bio-char: optimization, isothermal and kinetic studies. Desalination and Water Treatment, 57, 22244-22257.

SHEN, Y., ZHAO, P. & SHAO, Q. 2014. Porous silica and carbon derived materials from rice husk pyrolysis char. Microporous and Mesoporous Materials, 188, 46-76.

SMITH, N. J. 1980. ANTHROSOLS AND HUMAN CARRYING CAPACITY IN AMAZONIA∗. Annals of the Association of American Geographers, 70, 553-566.

SOHI, S., LOPEZ-CAPEL, E., KRULL, E. & BOL, R. 2009. Biochar, climate change and soil: A review to guide future research. CSIRO Land and Water Science Report, 5, 17-31.

SOHI, S. P., KRULL, E., LOPEZ-CAPEL, E. & BOL, R. 2010. Chapter 2 - A Review of Biochar and Its Use and Function in Soil. Advances in Agronomy. Academic Press.

SONG, W. & GUO, M. 2012. Quality variations of poultry litter biochar generated at different pyrolysis temperatures. Journal of analytical and applied pyrolysis, 94, 138-145.

SONG, Y., WANG, F., BIAN, Y., KENGARA, F. O., JIA, M., XIE, Z. & JIANG, X. 2012. Bioavailability assessment of hexachlorobenzene in soil as affected by wheat straw biochar. Journal of hazardous materials, 217, 391-397.

SPOKAS, K. A. 2010. Review of the stability of biochar in soils: predictability of O: C molar ratios. Carbon Management, 1, 289-303.

SPOKAS, K. A., CANTRELL, K. B., NOVAK, J. M., ARCHER, D. W., IPPOLITO, J. A., COLLINS, H. P., BOATENG, A. A., LIMA, I. M., LAMB, M. C. & MCALOON, A. J. 2012a. Biochar: a synthesis of its agronomic impact beyond carbon sequestration. Journal of environmental quality, 41, 973-989.

SPOKAS, K. A., NOVAK, J. M. & VENTEREA, R. T. 2012b. Biochar's role as an alternative N-fertilizer: ammonia capture. Plant and soil, 350, 35-42.

SPRYNSKYY, M., LEBEDYNETS, M., ZBYTNIEWSKI, R., NAMIEŚNIK, J. & BUSZEWSKI, B. 2005. Ammonium removal from aqueous solution by natural zeolite, Transcarpathian mordenite, kinetics, equilibrium and column tests. Separation and Purification Technology, 46, 155-160.

SRIVASTAVA, N. & MAJUMDER, C. 2008. Novel biofiltration methods for the treatment of heavy metals from industrial wastewater. Journal of hazardous materials, 151, 1-8.

STANDARD, A. 2009. Standard test method for chemical analysis of wood charcoal. American Society for Testing and Materials, Conshohocken, PA.

STEENSEN, M. 1997. Chemical oxidation for the treatment of leachate-process comparison and results from full-scale plants. Water Science and Technology, 35, 249-256.

STUART, B. H. 2004. Spectral analysis. Infrared spectroscopy: fundamentals and applications, 45-70.

SUN, Y., GAO, B., YAO, Y., FANG, J., ZHANG, M., ZHOU, Y., CHEN, H. & YANG, L. 2014. Effects of feedstock type, production method, and pyrolysis temperature on biochar and hydrochar properties. Chemical Engineering Journal, 240, 574-578.

TAGHIZADEH-TOOSI, A., CLOUGH, T. J., SHERLOCK, R. R. & CONDRON, L. M. 2012. A wood based low-temperature biochar captures NH3-N generated from ruminant urine-N, retaining its bioavailability. Plant and Soil, 353, 73-84.

TAKAYA, C., FLETCHER, L., SINGH, S., ANYIKUDE, K. & ROSS, A. 2016. Phosphate and ammonium sorption capacity of biochar and hydrochar from different wastes. Chemosphere, 145, 518-527.

TANAKA, J. & MATSUMURA, M. 2003. Application of ozone treatment for ammonia removal in spent brine. Advances in Environmental Research, 7, 835-845.

TATARKOVÁ, V., HILLER, E. & VACULÍK, M. 2013. Impact of wheat straw biochar addition to soil on the sorption, leaching, dissipation of the herbicide (4-chloro-2-methylphenoxy)

acetic acid and the growth of sunflower (Helianthus annuus L.). Ecotoxicology and environmental safety, 92, 215-221.

TATSI, A., ZOUBOULIS, A., MATIS, K. & SAMARAS, P. 2003. Coagulation–flocculation pretreatment of sanitary landfill leachates. Chemosphere, 53, 737-744.

THIES, J. E. & RILLIG, M. C. 2009. Characteristics of biochar: biological properties. Biochar for environmental management: Science and technology, 85-105.

THORNTON, A., PEARCE, P. & PARSONS, S. 2007. Ammonium removal from digested sludge liquors using ion exchange. Water research, 41, 433-439.

TRENKEL, M. E. 2010. Slow-and controlled-release and stabilized fertilizers: An option for enhancing nutrient use efficiency in agriculture, IFA, International fertilizer industry association.

UCHIMIYA, M., WARTELLE, L. H., KLASSON, K. T., FORTIER, C. A. & LIMA, I. M. 2011. Influence of pyrolysis temperature on biochar property and function as a heavy metal sorbent in soil. Journal of Agricultural and Food Chemistry, 59, 2501-2510.

UYGUR, A. & KARGI, F. 2004. Biological nutrient removal from pre-treated landfill leachate in a sequencing batch reactor. Journal of environmental management, 71, 9-14.

UZOMA, K., INOUE, M., ANDRY, H., FUJIMAKI, H., ZAHOOR, A. & NISHIHARA, E. 2011. Effect of cow manure biochar on maize productivity under sandy soil condition. Soil use and management, 27, 205-212.

VAN ZWIETEN, L., KIMBER, S., MORRIS, S., CHAN, K., DOWNIE, A., RUST, J., JOSEPH, S. & COWIE, A. 2010. Effects of biochar from slow pyrolysis of papermill waste on agronomic performance and soil fertility. Plant and soil, 327, 235-246.

VU, T. M., DOAN, D. P., VAN, H. T., NGUYEN, T. V., VIGNESWARAN, S. & NGO, H. H. 2017. Removing ammonium from water using modified corncob-biochar. Science of the Total Environment, 579, 612-619.

WANG, B., LEHMANN, J., HANLEY, K., HESTRIN, R. & ENDERS, A. 2015a. Adsorption and desorption of ammonium by maple wood biochar as a function of oxidation and pH. Chemosphere, 138, 120-126.

WANG, D., ZHANG, W. & ZHOU, D. 2013a. Antagonistic effects of humic acid and iron oxyhydroxide grain-coating on biochar nanoparticle transport in saturated sand. Environmental science & technology, 47, 5154-5161.

WANG, Y., HU, Y., ZHAO, X., WANG, S. & XING, G. 2013b. Comparisons of biochar properties from wood material and crop residues at different temperatures and residence times. Energy & fuels, 27, 5890-5899.

WANG, Y., LU, J., WU, J., LIU, Q., ZHANG, H. & JIN, S. 2015b. Adsorptive Removal of Fluoroquinolone Antibiotics Using Bamboo Biochar. Sustainability, 7, 12947-12957.

WANG, Z., GUO, H., SHEN, F., YANG, G., ZHANG, Y., ZENG, Y., WANG, L., XIAO, H. & DENG, S. 2015c. Biochar produced from oak sawdust by Lanthanum (La)-involved pyrolysis for adsorption of ammonium (NH_4^+), nitrate (NO_3^-), and phosphate (PO_4^{3-}). Chemosphere, 119, 646-653.

WAQAS, M., KHAN, S., QING, H., REID, B. J. & CHAO, C. 2014. The effects of sewage sludge and sewage sludge biochar on PAHs and potentially toxic element bioaccumulation in Cucumis sativa L. Chemosphere, 105, 53-61.

WEBER, W. J. & MORRIS, J. C. 1963. Kinetics of adsorption on carbon from solution. Journal of the Sanitary Engineering Division, 89, 31-60.

WIEDNER, K. & GLASER, B. 2015. Traditional use of biochar. Biochar for Environmental Management: Science, Technology and Implementation, 15.

WORCH, E. 2012. Adsorption technology in water treatment: fundamentals, processes, and modeling, Walter de Gruyter.

XU, X., CAO, X. & ZHAO, L. 2013a. Comparison of rice husk-and dairy manure-derived biochars for simultaneously removing heavy metals from aqueous solutions: role of mineral components in biochars. Chemosphere, 92, 955-961.

XU, X., CAO, X., ZHAO, L., WANG, H., YU, H. & GAO, B. 2013b. Removal of Cu, Zn, and Cd from aqueous solutions by the dairy manure-derived biochar. Environmental Science and Pollution Research, 20, 358-368.

YAKKALA, K., YU, M.-R., ROH, H., YANG, J.-K. & CHANG, Y.-Y. 2013. Buffalo weed (Ambrosia trifida L. var. trifida) biochar for cadmium (II) and lead (II) adsorption in single and mixed system. Desalination and Water Treatment, 51, 7732-7745.

YAMATO, M., OKIMORI, Y., WIBOWO, I. F., ANSHORI, S. & OGAWA, M. 2006. Effects of the application of charred bark of Acacia mangium on the yield of maize, cowpea and peanut, and soil chemical properties in South Sumatra, Indonesia. Soil science & plant nutrition, 52, 489-495.

YANG, F., ZHAO, L., GAO, B., XU, X. & CAO, X. 2016a. The Interfacial Behavior between Biochar and Soil Minerals and Its Effect on Biochar Stability. Environmental science & technology, 50, 2264-2271.

YANG, L., LIAO, F., HUANG, M., YANG, L. & LI, Y. 2015. Biochar improves sugarcane seedling root and soil properties under a pot experiment. Sugar Tech, 17, 36-40.

YANG, X., LIU, J., MCGROUTHER, K., HUANG, H., LU, K., GUO, X., HE, L., LIN, X., CHE, L. & YE, Z. 2016b. Effect of biochar on the extractability of heavy metals (Cd, Cu, Pb, and Zn) and enzyme activity in soil. Environmental Science and Pollution Research, 23, 974-984.

YANG, Y., LIN, X., WEI, B., ZHAO, Y. & WANG, J. 2014. Evaluation of adsorption potential of bamboo biochar for metal-complex dye: equilibrium, kinetics and artificial neural network modeling. International Journal of Environmental Science and Technology, 11, 1093-1100.

YAO, Y., GAO, B., INYANG, M., ZIMMERMAN, A. R., CAO, X., PULLAMMANAPPALLIL, P. & YANG, L. 2011. Biochar derived from anaerobically digested sugar beet tailings: characterization and phosphate removal potential. Bioresource technology, 102, 6273-6278.

YAO, Y., GAO, B., ZHANG, M., INYANG, M. & ZIMMERMAN, A. R. 2012. Effect of biochar amendment on sorption and leaching of nitrate, ammonium, and phosphate in a sandy soil. Chemosphere, 89, 1467-1471.

YARGICOGLU, E. N., SADASIVAM, B. Y., REDDY, K. R. & SPOKAS, K. 2015. Physical and chemical characterization of waste wood derived biochars. Waste Management, 36, 256-268.

YU, O.-Y., RAICHLE, B. & SINK, S. 2013. Impact of biochar on the water holding capacity of loamy sand soil. International Journal of Energy and Environmental Engineering, 4, 44.

YU, Q., XIA, D., LI, H., KE, L., WANG, Y., WANG, H., ZHENG, Y. & LI, Q. 2016. Effectiveness and mechanisms of ammonium adsorption on Biochars derived from biogas residues. RSC Advances, 6, 88373-88381.

YUAN, H., LU, T., ZHAO, D., HUANG, H., NORIYUKI, K. & CHEN, Y. 2013. Influence of temperature on product distribution and biochar properties by municipal sludge pyrolysis. Journal of Material Cycles and Waste Management, 15, 357-361.

YUAN, J.-H., XU, R.-K. & ZHANG, H. 2011. The forms of alkalis in the biochar produced from crop residues at different temperatures. Bioresource Technology, 102, 3488-3497.

YUAN, J. H. & XU, R. K. 2011. The amelioration effects of low temperature biochar generated from nine crop residues on an acidic Ultisol. Soil Use and Management, 27, 110-115.

ZACKRISSON, O., NILSSON, M.-C. & WARDLE, D. A. 1996. Key ecological function of charcoal from wildfire in the Boreal forest. Oikos, 10-19.

ZENG, Z., LI, T.-Q., ZHAO, F.-L., HE, Z.-L., ZHAO, H.-P., YANG, X.-E., WANG, H.-L., ZHAO, J. & RAFIQ, M. T. 2013. Sorption of ammonium and phosphate from aqueous solution by

biochar derived from phytoremediation plants. Journal of Zhejiang University Science B, 14, 1152-1161.

ZHANG, H., CHEN, L., LU, M., LI, J. & HAN, L. 2016. A novel film–pore–surface diffusion model to explain the enhanced enzyme adsorption of corn stover pretreated by ultrafine grinding. Biotechnology for biofuels, 9, 181.

ZHANG, M. & GAO, B. 2013. Removal of arsenic, methylene blue, and phosphate by biochar/AlOOH nanocomposite. Chemical engineering journal, 226, 286-292.

ZHANG, M., GAO, B., VARNOOSFADERANI, S., HEBARD, A., YAO, Y. & INYANG, M. 2013. Preparation and characterization of a novel magnetic biochar for arsenic removal. Bioresource technology, 130, 457-462.

ZHANG, Y., LI, Z. & MAHMOOD, I. B. 2014. Recovery of NH 4+ by corn cob produced biochars and its potential application as soil conditioner. Frontiers of Environmental Science & Engineering, 8, 825-834.

ZHENG, H., WANG, Z., DENG, X., ZHAO, J., LUO, Y., NOVAK, J., HERBERT, S. & XING, B. 2013. Characteristics and nutrient values of biochars produced from giant reed at different temperatures. Bioresource Technology, 130, 463-471.

ZHENG, R.-L., CAI, C., LIANG, J.-H., HUANG, Q., CHEN, Z., HUANG, Y.-Z., ARP, H. P. H. & SUN, G.-X. 2012. The effects of biochars from rice residue on the formation of iron plaque and the accumulation of Cd, Zn, Pb, As in rice (Oryza sativa L.) seedlings. Chemosphere, 89, 856-862.

ZHENG, W., GUO, M., CHOW, T., BENNETT, D. N. & RAJAGOPALAN, N. 2010. Sorption properties of greenwaste biochar for two triazine pesticides. Journal of Hazardous Materials, 181, 121-126.

ZHOU, M. & CHEN, M. 2001. Reactions of silicon dioxide with ammonia molecules: formation and characterization of the SiO2–NH3 complex and the H2NSiOOH molecule. Chemical Physics Letters, 349, 64-70.

ZHOU, Z., YUAN, J. & HU, M. 2015. Adsorption of ammonium from aqueous solutions on environmentally friendly barbecue bamboo charcoal: characteristics and kinetic and thermodynamic studies. Environmental Progress & Sustainable Energy, 34, 655-662.

ZHU, K., FU, H., ZHANG, J., LV, X., TANG, J. & XU, X. 2012. Studies on removal of NH 4+-N from aqueous solution by using the activated carbons derived from rice husk. Biomass and bioenergy, 43, 18-25.

ZIELIŃSKA, A. & OLESZCZUK, P. 2015. Evaluation of sewage sludge and slow pyrolyzed sewage sludge-derived biochar for adsorption of phenanthrene and pyrene. Bioresource technology, 192, 618-626.

ZIMMERMAN, A. R. 2010. Abiotic and microbial oxidation of laboratory-produced black carbon (biochar). Environmental science & technology, 44, 1295-1301.

ZORNOZA, R., MORENO-BARRIGA, F., ACOSTA, J., MUÑOZ, M. & FAZ, A. 2016. Stability, nutrient availability and hydrophobicity of biochars derived from manure, crop residues, and municipal solid waste for their use as soil amendments. Chemosphere, 144, 122-130.

ZOUBOULIS, A. I., JUN, W. & KATSOYIANNIS, I. A. 2003. Removal of humic acids by flotation. Colloids and Surfaces A: Physicochemical and Engineering Aspects, 231, 181-193.

Chapter 7. Conclusion

7.1 General conclusion.

Biochar has been receiving attention as a green soil amendment and environmental adsorbent. Various kinds of biomass were studied as potential materials for biochar production. In this case, agricultural residue (rice husk) and forestry wastes (wood chips and bamboo) were used to create the biochars which demonstrated various characterizations and several potential benefits. For example, biochars produced from wood and bamboo biomass had low ash content, but high BET surface area, high carbon content, and sophisticated morphology (hollow structure for wood BC and comb-like structure for bamboo BC). Meanwhile, rice husk BC demonstrated low BET surface area corresponding to smooth morphology and low carbon content, but high ash content and CEC value. The FTIR results indicated that the surface functional groups such as carboxyl and hydroxyl groups or CO_3^{2-} group were observed for all the three biochars, but PO_4^{3-} and SiO_2 groups were only showed for rice husk and wood BCs. The hollow structure may serve a good inhabitant for microorganism, water holding capacity and relate to adsorption by intraparticle diffusion, while high CEC plays an important role in adsorption via cation exchange. Particularly, the functional groups act as negative sites which attracts cations to form surface complex. The differences in physicochemical properties brought the various adsorption capacity and mechanisms among the biochars. The adsorption mechanisms for the cations were illustrated in the **Figure 1** of this section. In fact, although bamboo and wood BCs had higher the BET surface area than that of rice husk BC, the adsorption capacity of the biochar for single NH_4^+-N ion in aqueous artificial solution was in order of rice husk > bamboo BC > wood BC. In addition, data analysis by the isotherm and kinetic models indicated that chemical process

198

(surface functional groups, CEC, and intraparticle diffusion) governed the adsorption rather than physical adsorption, and the adsorption was taken place on heterogeneous surface by multilayer. Particularly, the NH_4^+-N adsorption of the three biochars was strongly based on the initial adsorbant concentration. In addition, the different morphology structure of biochar resulted to the various times for the equilibrium adsorption among them.
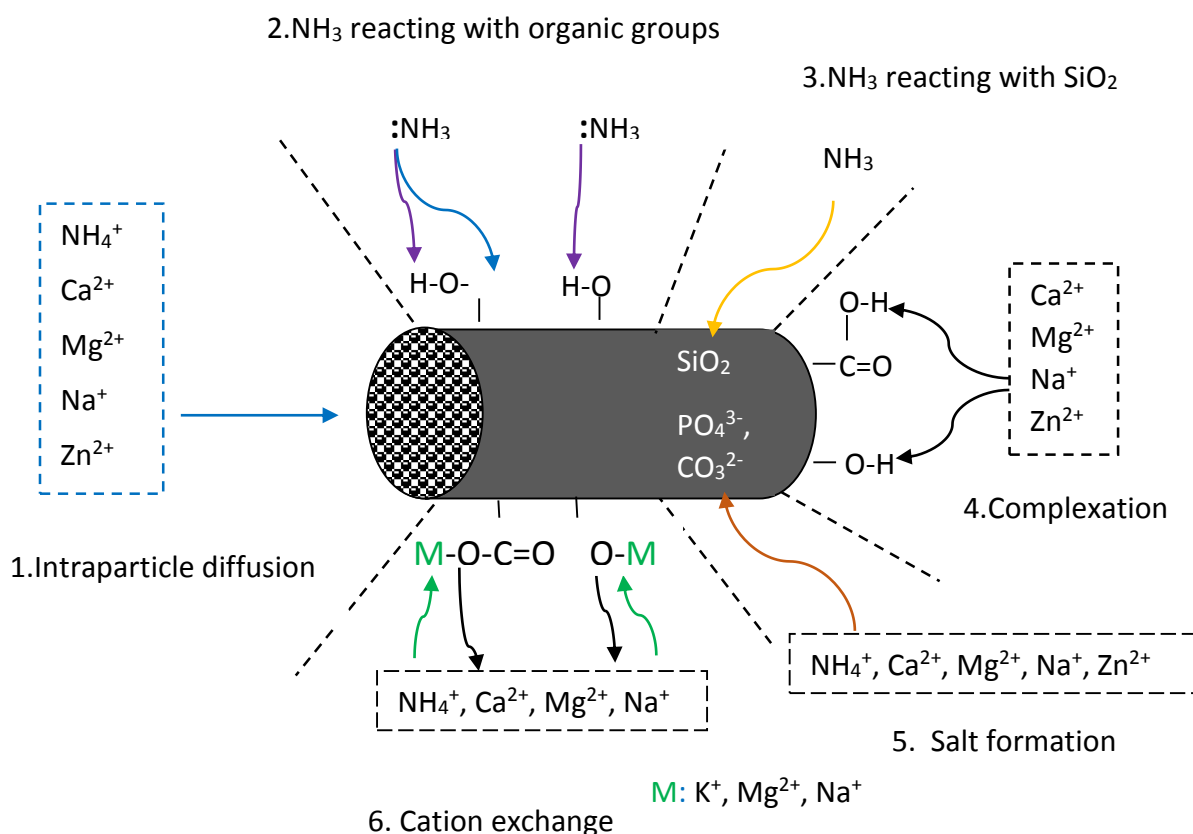

Figure1. Shematic of the geometry of the cations (NH_4^+ and Zn^{2+}) adsorbed onto a biochar particle.

In contrast, the adsorption for Zn^{2+} by the adsorbents was different with NH_4^+-N, with the order as bamboo BC > rice husk BC ≥ wood BC, and only the adsorption capacity of bamboo strongly increased with increasing initial concentrations of Zn^{2+}. In addition, the similar equilibrium adsorption was observed for the three biochar, which was taken place after one hour. However, the adsorption of the adsorbates onto the three biochars was also governed

by the chemical processes occurring on heterogeneous surface by multilayer the organic groups (carboxyl and hydroxyl groups) form complexation and chelation, and precipitate with inorganic groups (CO_3^{2-}, PO_4^{2-}) mainly controlled the adsorption rather than by ion exchange.

Although, the three biochars had good adsorption for ammonium (NH_4^+-N), the adsorption was only assessed single biochar with artificial solution having single adsorbate and lower concentration than the real wastewater like the landfill leachate (NH_4^+-N up to 1790.18 ± 2.53 mg/L). Therefore, the adsorption capacity of the three biochars and their mixture was evaluated for the multi pollutants in the leachate by equilibrium and filter experiments. The results indicated that although having adsorption completion of the other cations (Ca^{2+}, Mg^{2+}, Na^+), the NH_4^+-N adsorption was increased up to 44.06 mg/g for rice husk BC, 40.41 mg/g for bamboo BC, and 38.90 mg/g for wood BC. Particularly, their binary and ternary mixtures also showed good NH_4^+-N adsorption with in range of 39.98 – 43.10 mg/g. Interestingly, the other cations like Ca^{2+}, Mg^{2+}, and Na^+ in the leachate was also adsorbed by several biochars, which completed with the NH_4^+-N adsorption. In contrast, K^+ ion on the biochars surface mainly participated in the cation exchange for the NH_4^+-N adsorption, and the CEC contributed not to exceed 11% of the total NH_4^+-N adsorption. Hence, the results in this study indicated that all the three biochars and their mixture are prospective products for nutrient capture and environmental alleviation for wastewater having high ammonia concentration. Meanwhile, bamboo BC are good product using for reduction of heavy metal pollution like Zn.

7.2 Suggestions for future research

- The biochars need to be tested with real contaminated solutions containing various heavy metals in order to assess the effect of adsorption competition. The landfill leachate likely had numerous metals present, but testing this was beyond the scope of the current thesis due to time limitations.

- Desorption experiments should also be set up to evaluate the retention ability of the biochars for NH_4^+-N, which could give important data for designing slow release fertilizer or controlled release fertilizer. A balance would need to be struck between strong retention to reduce loss during heavy rainfall events, for example, and too strong retention that might prevent the re-release of the ammonium back into the soil / plants as needed.

- The various particle sizes of biochar should be tested for adsorption, which helps to identify suitable particles for use purposes. Additionally, the sequence of the layers, and the ratios of the different layers in the column experiments could be varied to optimize the removal of cations that compete with ammonium adsorption initially, for example, or to tip the balance further away from cation exchange towards other mechanisms that favor ammonium (or other required nutrient / pollutant) absorption.

- The *ex-situ* experiments need to set up in the field to evaluate the effects over the long term, and to optimize the recirculation versus continuous flow, and the optimal rate of percolation of the leachate through the biochar to reach the maximum adsorption capacity.